OXYLIPINS AND THEIR INVOLVEMENT IN PLANT RESPONSE TO BIOTIC AND ABIOTIC STRESS

Dissertation
zur Erlangung des akademischen Grades
doctor rerum naturalium

vorgelegt dem Rat der Biologisch-Pharmazeutischen Fakultät der
Friedrich-Schiller-Universität Jena

von Apothekerin
Birgit Schulze

geboren am 10.12.1975 in Bayreuth

Referees:

1. Prof. Dr. Wilhelm Boland	Max-Planck-Institut für chemische Ökologie, Jena
2. Prof. Dr. Jochen Lehmann	Institut für pharmazeutische Chemie Friedrich-Schiller-Universität, Jena
3. Prof. Dr. Dierk Scheel	Leibnitz-Institut für Pflanzen Biochemie, Halle

Date of oral examination: 20. September 2005

Date of public defense: 18. October 2005

Table of contents

1 General introduction 1
1.1 Hormones regulating plant defense reactions 1
1.1.1 Jasmonates: Signals mediating response to wounding and herbivory 2
1.1.2 Oxylipins: Multiple signals in plant stress responses 7
1.1.3 Salicylic acid: Induction of plant defense against pathogens 12
1.1.4 Ethylene: Modulation of plant stress responses 13
1.2 Cross-talk: Signaling network for multiple responses 15
2 Goals of this study 18
3 Analysis of labile oxylipins extracted from plant material 20
3.1 Introduction: Oxylipin monitoring 20
3.2 Results and discussion 21
3.2.1 Development of a method for comprehensive extraction of oxylipins from plant material 21
3.2.2 Analysis of labile oxylipins from plant material as PFB-oximes 25
3.2.2.1 Oxylipin identification 27
3.2.2.2 Stabilization of jasmonic acid epimers as their PFB-oximes 40
3.2.2.3 Searching for oxylipins in Lima bean leaves 41
3.2.2.4 Oxylipin quantification 43
3.3 Conclusions 48
4 The role of oxylipins in plant-insect interactions 50
4.1 Introduction: Signals shared by plants and insects 50
4.2 Results and discussion 52
4.2.1 Plant responses to mechanical wounding and caterpillar feeding 52
4.2.2 Spatial distribution of oxylipins in caterpillar damaged leaves 56
4.2.3 Oxylipins in the insect's gut 58
4.3 Conclusions 64
5 Plant stress response to chemical elicitation 66
5.1 Response of *Arabidopsis thaliana* to treatment with alamethicin 66
5.1.1 Introduction: Alamethicin induced plant stress responses 66
5.1.2 Results and discussion 69
5.1.2.1 Phytohormone levels 69
5.1.2.2 Defense gene expression 71
5.1.3 Conclusions 72
5.2 Heavy metal ions as elicitors of plant defense reactions 73
5.2.1 Introduction: Biotic and abiotic stress response in plants, a search for common signals 73
5.2.2 Results and discussion 75
5.2.2.1 Heavy metal ions induce volatile production 75
5.2.2.2 Heavy metal ions induce salicylic acid biosynthesis 77
5.2.2.3 Heavy metal ions induce ethylene emission 79
5.2.2.4 Oxylipin levels after heavy metal ion treatment 80
5.2.3 Conclusions 82

6 General conclusions and outlook 84
7 Abstract 88
8 Zusammenfassung 93
9 Materials and methods 98
9.1 Cultivation of plants and rearing of caterpillars 98
9.2 General methods and chemicals 99
9.2.1 Instruments 99
9.2.2 Chemicals 100
9.2.3 Oxylipins and phytohormone standards 100
9.2.4 Synthesis of oxylipins 101
9.2.5 Derivatization techniques for GC-MS analysis 103
9.3 Analysis of plant volatiles 104
9.3.1 Closed-loop-stripping 104
9.3.2 zNose 105
9.4 Phytohormone analysis 105
9.4.1 Ethylene 105
9.4.2 Salicylic acid 106
9.4.3 Oxylipins 106
9.5 Stress induction experiments 109
9.5.1 Mechanical wounding 109
9.5.2 Caterpillar feeding 109
9.5.3 Incubation of *A. thaliana* with alamethicin 110
9.5.4 Incubation of *P. lunatus* with chemical elicitors and inhibitors for volatile analysis 110
9.5.5 Incubation of *P. lunatus* with $CuSO_4$ 110
9.6 Collection of caterpillar regurgitant and frass 111
9.7 Isomerization of OPDA to *iso*-OPDA 111
9.8 Regression analysis and statistics 112
10 References 113
11 Acknowledgements 134
12 Curriculum vitae 137
13 Supplementary material 141
13.1 NMR-spectra 141
13.2 IR-spectra 145
13.3 MS-spectra 147
13.4 Data sheets 176

This thesis is supplemented with a CD containing a NIST-searchable MS-library of oxylipins and their derivatives.

Abbreviations

[$^2H_2$]-JA	[9,10-$^2H_2$]-dihydrojasmonic acid
[$^2H_2$]-*iso*-OPDA	[15,16-$^2H_2$]-tetrahydrodicranenone B
9-HPOTE	9-hydroperoxy-10,12,15-octadecatrienoic acid
9-HOTE	9-hydroxy-10,12,15-octadecatrienoic acid
9-KOTE	9-oxo-10,12,15-octadecatrienoic acid
12,13-epoxy-11-HODE	12,13-epoxy-11-hydroxy-9,15-octadecadienoic acid
13-HPOTE	13-hydroperoxy-9,11,15-octadecatrienoic acid
13-HOTE	13-hydroxy-9,11,15-octadecatrienoic acid
13-KOTE	13-oxo-9,11,15-octadecatrienoic acid
α-ketol	13-hydroxy-12-oxo-9,15-octadecadienoic acid
ALA	alamethicin
AOC	allene oxide cyclase
AOS	allene oxide synthase
CI	chemical ionization
CIP-rules	rules for the assignment of stereochemistry developed by R. S. Cahn, Sir C. Ingold, and V. Prelog
DMSO	dimethylsulfoxide
EI	electron impact
ET	ethylene
eV	electron volt
frw	fresh weight
FT-IR	fourier transform infrared
GC	gas chromatography
GC-MS	gas chromatograph coupled to a mass spectrometer
γ-ketol	9-hydroxy-12-oxo-10,15-octadecadienoic acid
GLC	gas liquid chromatography
GOX	glucose oxidase
HPLC	high performance liquid chromatography
HR-MS	high resolution mass spectrometry
ISR	induced systemic resistance
iso-OPDA	tetrahydrodicranenone B
JA	jasmonic acid
JAMe	methyl jasmonate
LOX	lipoxygenase
M	molecular mass
m/z	mass to charge ratio
$M^{\bullet+}$	molecular ion
MeSA	methyl salicylate
MS	mass spectrometry; mass spectrum
MSTFA	*N*-methyl-*N*-trimethylsilyl-trifluoroacetamide

NCI	negative chemical ionization
NMR	nuclear magnetic resonance
OPC-8:0	3-oxo-2-[2´(*Z*)-pentenyl]-cyclopentane-1-octanoic acid
OPDA	12-oxophytodienoic acid
OPR	12-oxophytodienoate reductase
OTMS	*O*-trimethylsilyl
PDGF	platelet-derived growth factor
PFB	*O*-(2,3,4,5,6-pentafluorobenzyl)
PFBBr	*O*-(2,3,4,5,6-pentafluorobenzyl)bromide
PFB-ester	*O*-(2,3,4,5,6-pentafluorobenzyl)ester
PFBHA	*O*-(2,3,4,5,6-pentafluorobenzyl)hydroxylamine hydrochloride
PFBO	C_6F_5-CH_2O-fragment
PFB-oxime	*O*-(2,3,4,5,6-pentafluorobenzyl)oxime
PI	protease inhibitor
PIOX	pathogen-induced-oxygenase
PPB_1	phytoprostane B_1
PPF_1	phytoprostane F_1
PUFA	polyunsaturated fatty acid
ROS	reactive oxygen species
RT	room temperature
SA	salicylic acid
SAR	systemic acquired resistance
SIM	selected ion monitoring
SPE	solid phase extraction
std	(internal) standard
TIC	total ion current
TMS	trimethylsilyl

Abbreviations of genes and mutants

CUC2	cup-shaped cotyledons 2
coi1	coronatine insensitive 1
def1	defenseless 1
jar	jasmonic acid methylester resistant
NAC	*Petunia* NAM and *Arabidopsis* ATAF1/2 and CUC2
NAM	no apical meristem
npr1	nonexpressor of PR 1
PR	pathogenesis related
VSP	vegetative storage protein
pdf1.2	plant defensin 1.2
rns1	S-like RNase 1

Abbreviations used in statistics

a	intercept
b	slope
Δ	increment
n	number of values
R^2	a measure of the amount of variation accounted for by a regression line of correlation
SEM	standard error of the mean

Abbreviations for NMR assignment

br	broad
d	dublett
δ	chemical resonance shift
m	multiplett
“t”	pseudo-triplett
q	quartett
s	singulett
t	triplett

1 GENERAL INTRODUCTION

1.1 Hormones regulating plant defense reactions

In our daily life plants are often regarded as objects rather than sensible organisms. However, as sessile life forms, they have to cope with various threats from their environment and respond in a coordinated way. Especially the defense against attacking herbivores and pathogens is crucial for their survival. Plant defense reactions can be distinguished into constitutive, i.e. permanently expressed, and inducible mechanisms. Induced defenses are triggered only after the contact of the plant with the aggressor [1]. Moreover, plant defenses can act directly and/or indirectly. Direct defenses comprise

- mechanical barriers such as thorns, hairs or waxes [2],
- the accumulation of deterrent or toxic secondary metabolites [3] and
- digestion inhibitory compounds like polyphenolics [4] or protease inhibitors (PI) [5].

During indirect defense, plants use organisms from a higher trophic level as allies [6,7]. A well studied example for this type of defense is the attraction of carnivorous insects or ichneumon flies by volatiles emitted from infested plants [8,9] (Figure 1). These insects reduce the feeding pressure on the plant by predation of the herbivore or parasitism of the feeding caterpillar larvae. The induction of plant volatile emission has been reported for chewing insects such as caterpillars [10,11] as well as for piercing-sucking herbivores e.g. mites, bedbugs and aphids [12,13].

Moreover, it has been confirmed that plants specifically recognize various insects, obviously being able to differentiate between various types of herbivory [14]. Thus, plants are capable to distinguish between related herbivore species [15] and their developmental stage [16], which enables plants to attract specific carnivores according to their needs. These examples implicate that plant use a complex network of signaling cascades to guarantee adequate reaction against various threats.

Early recognition mechanisms often consist of physicochemical or receptor-mediated cues which are received by the outer membranes of the damaged cell layers [17-19]. The primary signal reception is followed by other signals by a. shift of membrane potentials [19,20], calcium influx [21,22], the generation of reactive oxygen species (ROS) [23,24], as well as induction of protein phosphorylation cascades, e.g. mitogen activated protein (MAP) kinase cascades [25,26].

Next, these first signals trigger the accumulation of phytohormones, which are generally regarded as master switches in the coordination of plant responses. Key players in this network of defense regulation are the phytohormones jasmonic acid (JA; **1**), salicylic acid (SA; **2**) and ethylene (ET; **3**). These hormones are specifically upregulated and orchestrate the plant's response to various stresses [27,28].

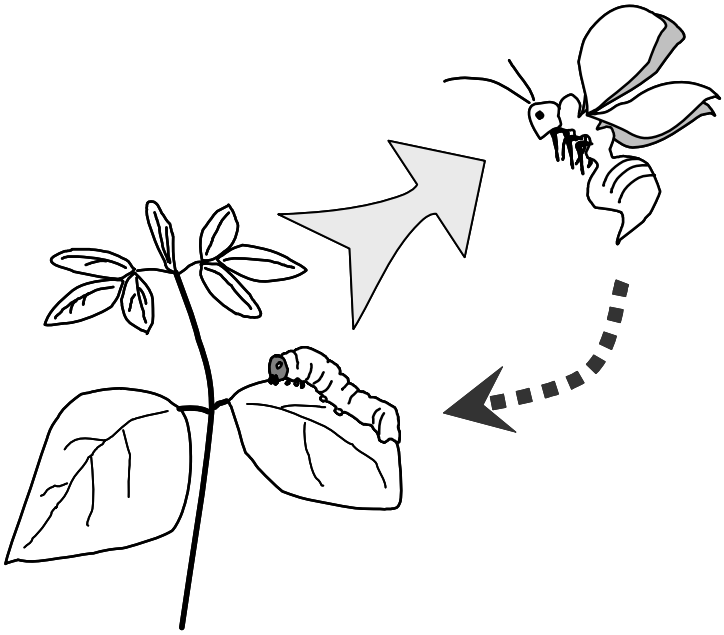

Figure 1 Indirect defense: The feeding caterpillar elicits plant volatile production. These chemicals attract predators or ichneumon flies, which reduce the feeding pressure on the plant.

1.1.1 Jasmonates: Signals mediating response to wounding and herbivory

Jasmonic acid (JA; **1**) which has initially been described as a growth inhibiting compound [29], has now been recognized to play a crucial role in mediating various physiological processes in plants. For example it influences seed germination [30], flower formation [31] and fertility [32], or regulation of photosynthesis [33]. Furthermore, JA (**1**) is involved in storage and mobilization of carbon and nitrogen e.g. by activation of genes encoding vegetative storage proteins (VSPs) [34] and influencing carbon transport and allocation [35]. Besides the control of plant developmental processes a highly noted function of JA (**1**) is the regulation of plant defense reactions against various stress factors from the environment. **1** induces defense reactions against both abiotic stress such as ozone [36] and salt stress [37] or biotic stress such as wounding [38] and herbivory [39,40]. The vital role of JA (**1**) in mediating plant defense was demonstrated recently by silencing JA-biosynthesis in

Nicotiana attenuata. Feeding herbivores exhibited increased performance on JA-deficient plants, both under controlled greenhouse conditions [41] and in natural field sites [42]. Additionally, the field experiments highlighted the importance of the indirect defense system mediated by volatile emission.

JA-biosynthesis (Figure 2) was first studied by Vick and Zimmerman in the early 1980s [43] (see Müller (1997) [44], Beale and Ward (1998) [45] and Schaller *et al.* (2005) [46] for review).

α-Linolenic acid (C18:3 *n*-3; **4**) derived from membrane phospholipids that are cleaved by phospholipases upon stress induction serves as a precursor for JA-generation [47,48]. The free fatty acid is oxidized to (13*S*)-hydroperoxy-9,11,15-octadecatrienoic acid (13-HPOTE, **5**) by a 13-lipoxygenase (13-LOX). Plant lipoxygenases are non-heme iron-containing fatty acid dioxygenases, which catalyze the oxidation of polyunsaturated fatty acids (PUFAs) carrying an activated 1,4-pentadienyl segment [49,50]. The allene oxide synthase (AOS) then converts **5** to an unstable allene oxide intermediate, (13*S*)-12,13-epoxy-9,11,15-octadecatrienoic acid (**6**) [51,52]. **6** undergoes cyclization to 12-oxophytodienoic acid (OPDA; **7**) under control of the allene oxide cyclase (AOC) [53]. OPDA (**7**) is formed in the chloroplasts [54], whereas the later enzymes for the formation of JA (**1**) are located in the cytoplasm and peroxysomes [55]. Therefore, **7** is transported into the cytoplasm where its cyclopentenone ring is reduced by a 12-oxopytodienoate reductase (OPR) [56] resulting in the formation of 3-oxo-2-[2´(*Z*)-pentenyl]-cyclopentane-1-octanoic acid (OPC-8:0; **8**). In the peroxysomes, stepwise β-oxidation of OPC-8:0 (**8**) finally leads to *cis*-configured (+)-7-*iso*-jasmonic acid (*cis*-JA; *cis*-**1**) [57,58].

cis-**1** is rapidly epimerized to the *trans*-configured (-)-jasmonic acid (*trans*-JA; *trans*-**1**), which is the thermodynamically more stable isomer. Whether epimerization of *cis*- to *trans*-JA (**1**) is a spontaneous process, or enzymes promote this reaction is still not known. Since *cis*-**1** is the biologically more active isomer [59,60], isomerization may be the first step to inactivate JA (**1**) after having fulfilled its role as signaling compound.

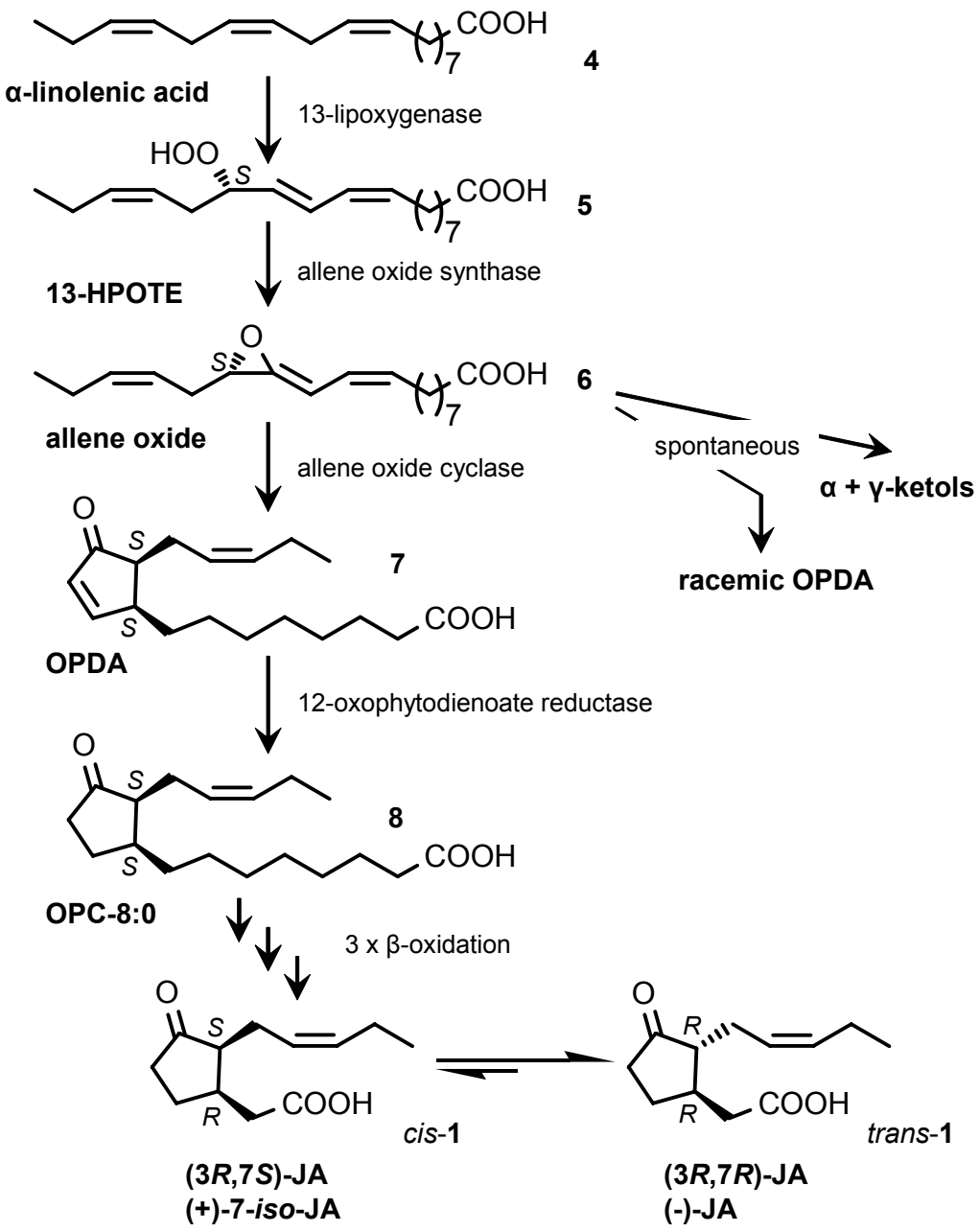

Figure 2 Biosynthesis of jasmonic acid (**1**).

However, not only the end product of the JA-biosynthesis is regarded as biologically active, also the precursors of **1** seem to have their own physiological function. Especially OPDA (**7**), has now been established as a JA-independent signaling compound [61,62]. It even exceeds the amount of JA (**1**) in leaf material of various plants both, at resting level and during wound response [63,64]. OPDA (**7**) was shown to be more active in inducing production of secondary defense metabolites (phytoalexins) in soybean (*Glycine max*) than JA (**1**) [65]. Moreover, OPDA (**7**) is highly potent in mediating mechanotransduction [66]. In the Lima bean (*Phaseolus lunatus*), early intermediates of jasmonate biosynthesis (α-linolenic acid (**4**)

and OPDA (**7**)) elicit the biosynthesis of volatiles of diterpenoid origin, whereas JA (**1**) predominately induces the synthesis of mono- and sesquiterpenes [67]. In general, the triggering of the OPDA-signal resembles that of JA (**1**), but distinctive cellular responses are observed, suggesting a differential activation of defense reactions.

In contrast to the well characterized actions of JA (**1**) and OPDA (**7**), their cellular receptor or target is still unknown. Investigations with radioactively labeled analogs of JA (**1**) and OPDA (**7**) are currently in progress.

As indicated in Figure 2, the JA-biosynthesis pathway is rather flexible since its enzymes can lead to the formation of various products. The key compound of the biosynthetic pathway is the unstable allene oxide intermediate **6**. If not under the control of the AOC, **6** can spontaneously undergo various reactions. It may cyclize resulting in formation of racemic OPDA (**7**), or hydrolyze, leading to the formation of 13-hydroxy-12-oxo-9,15-octadecadienoic acid (α-ketol; **9**) and 9-hydroxy-12-oxo-10,15-octadecadienoic acid (γ-ketol; **10**) [68]. **9** and **10** were demonstrated to be involved in flower formation [69,70]. Additionally, most enzymes of the JA-biosynthesis pathway were found not to be strictly specific for α-linolenic acid (**4**), but can also accept linoleic acid (C18:2 *n*-6) as substrate. This is supported by the isolation of 9,10-dihydro-JA from fungi and plant material [71,72]. In analogy to the formation of 9,10-dihydro-JA, 15,16-dihydro-OPDA was synthesized from an enzyme preparation of *Linum usitatissimum* after addition of linoleic acid [73]. Additionally, C-16 fatty acids are also utilized by the enzymes of the JA-biosynthesis pathway; consequently, dinor-OPDA has been isolated from plant material [74].

There is not only considerable variety and flexibility in the biosynthetic route leading to JA (**1**), additionally, **1** is further metabolized by diverse pathways (Figure 3). Methylation to methyl jasmonate (MeJA; **11**) [75] and transformation to *cis*-jasmone (**12**) [76] may be a way of disposing both volatile metabolites through the leaf surface; however the significance of this mechanism is still unclear [77]. Other metabolizing pathways [78] include the hydroxylation at C-11 or C-12 producing compounds such as tuberonic acid (**13**), reduction of the C-6 keto group, to form cucurbic acid (**14**), *O*-glucosylation of hydroxylated derivatives e.g. **15** [79], and conjugation of JA (**1**) or its derivatives with amino acids such as **16**. Recently, a sulfotransferase conjugating 12-hydroxyjasmonic acid (**13**) to its sulfate **17** has been isolated [80].

For many metabolites of JA (**1**) own physiological properties have been described. The volatile MeJA (**11**) is supposed to be involved in plant to plant communication [81,82], whereas tuberonic acid (**13**) [83] and cucurbic acid (**14**) [29] seem to induce tuber formation and act as growth inhibitors respectively.

JA-amino acid conjugates have long been discovered in flowers and pollen [84,85]. Despite the general assumption that conjugation to amino acids represents a deactivation step, the

conjugates of JA (**1**) are suggested to represent the actual receptor binding signal. Especially the JA-isoleucine conjugate (**16**) has been described as biologically active in respect to volatile production and defense gene expression [86,87]. Supporting this hypothesis, Staswick and Tiryaki (2004) [88] showed that **16** could overcome the block in JA-signaling of the *Arabidopsis thaliana* mutant *jar-1-1*[1] [89,90], albeit free JA (**1**) could not. This suggests that JA-amino acid conjugation may serve as an activation step, rather than deactivation of JA (**1**).

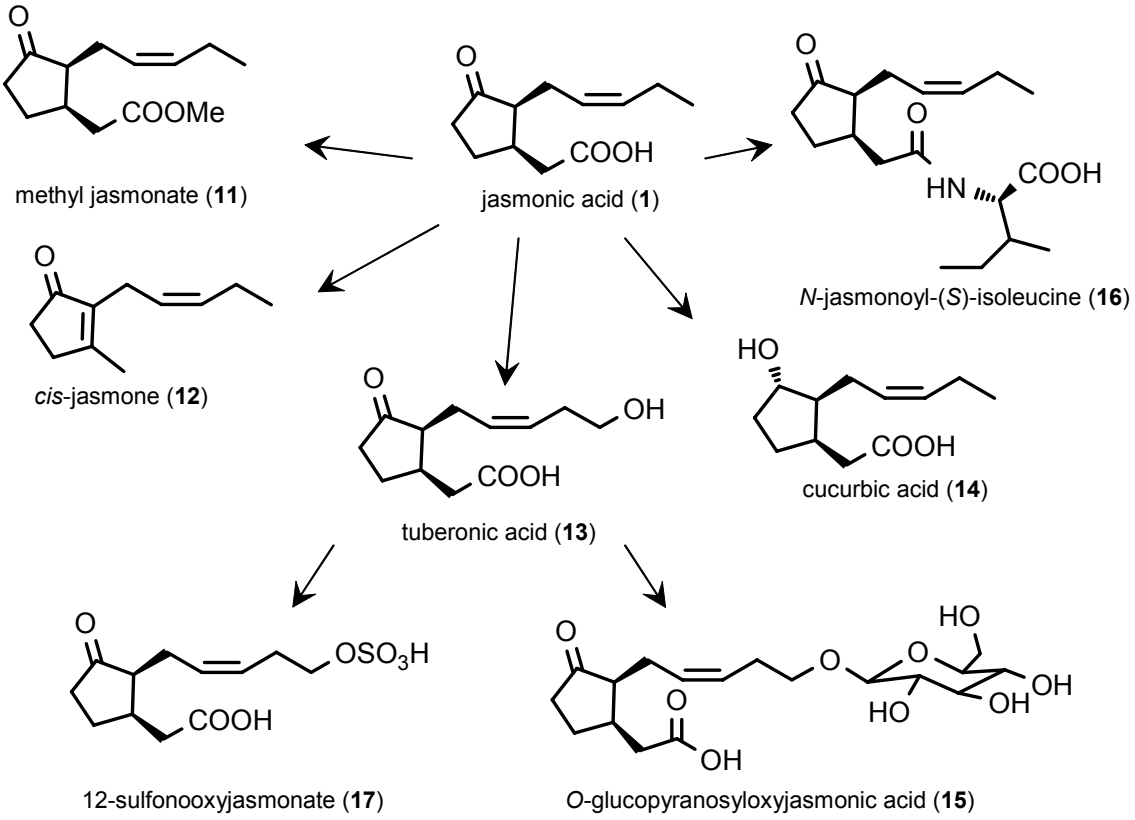

Figure 3 Metabolic pathways of jasmonic acid (**1**).

[1] The *jar* mutant is deficient in its response to exogenously applied JA (**1**).

1.1.2 Oxylipins: Multiple signals in plant stress responses

Besides JA (**1**) and its early precursor OPDA (**7**) the role of other fatty acid derived signaling compounds in plant defense reactions attracts more and more attention [91]. The formation of fatty acid hydroperoxides is the first step leading to the structurally highly diverse group of oxidized fatty acid metabolites (oxylipins). The activated bisallylic hydrogens of polyunsaturated fatty acids are prone to oxidation by either enzymatically catalyzed or non-enzymatic lipid peroxidation processes [92]. While reactions taking place under the control of an enzyme lead to stereochemically defined products, non-enzymatically formed oxylipins occur in racemic mixtures. By investigation of the stereochemistry e.g. of hydroxyl groups both mechanisms can be distinguished [93,94].

Linoleic acid and linolenic acid (**4**) serve as the major substrates of plant lipoxygenases, which catalyze their oxidation to either 9- or 13-hydroxyperoxides, or a mixture of both, depending on the enzyme [49,50,95]. Additionally, P450-like enzymes can introduce hydroxyl groups at the ω-position of the fatty acid backbone [96], while the α-position is oxidized by the cyclooxygenase-like α-dioxygenase [97]. This enzyme is commonly known as pathogen-induced-oxygenase (PIOX), as it is induced during disease response [98,99]. Moreover, enzymes of the lipoxygenase pathway were shown to convert *N*-acylethanolamines *in vitro* and *in vivo* to the respective oxylipins [100,101].
With excess of highly reactive hydroperoxides LOX enzymes are degraded. This leads to liberation of iron ions that may catalyze non-enzymatic lipid peroxidation causing a switch from enzyme controlled plant signaling processes to the generation of highly reactive and toxic compounds, finally leading to apoptosis [102]. Furthermore, reactive oxygen species (ROS) such as the superoxide anion ($O_2^{\bullet -}$), hydrogen peroxide (H_2O_2), and the hydroxyl radical ($^{\bullet}OH$) that are commonly generated under stress conditions possess strong oxidizing activities that can attack all types of biomolecules [103]. Besides intracellular sources of reactive oxygen species that include mitochondria, chloroplasts, and peroxisomes, the inducible production and accumulation of reactive oxygen species in plants as a defense response to pathogen attack is well documented and known as the so-called “oxidative burst” [24,104,105]. Reactive oxygen species that have been detected in plant pathogen interactions are $O_2^{\bullet -}$ ($^{\bullet}O_2H$), H_2O_2, and $^{\bullet}OH$ [24]. However, the enzymatic origin of these inducible reactive oxygen species is still under discussion. A variety of potential sources have been described in different plant species, including apoplastic amine-, diamine-, and polyamine-oxidase-type enzymes [106], a cell wall localized peroxidase that directly forms hydrogenperoxide [107], and a plasma membrane bound NADPH-oxidase [108]. The latter enzyme represents the most intense studied mechanism for generation of reactive oxygen species [24]. The product of this NADPH oxidase activity is very likely $O_2^{\bullet -}$ [109], which is

converted to the more stable H_2O_2 and O_2 spontaneously or by action of a superoxide dismutase; H_2O_2 is then subsequently converted to H_2O and O_2 by catalases. In the case of herbivory, the origin of ROS is not that clear. However, insect feeding causes wounding and thus the production of ROS in damaged tissues [110,111]. As shown for soybean, herbivory by *Helicoverpa zea* larvae induced a shift in the oxidative status of the plant causing an increase in $O_2^{\bullet-}$ and $^{\bullet}OH$ radical formation [112]. In a more direct way, insect salivary gland-derived enzymes such as the hydrogen peroxide generating glucose oxidase (GOX), converting glucose and O_2 to glucuronic acid and H_2O_2, might contribute to the increase in the concentration of ROS at the site of herbivore attack [113]. Thus both, the products of lipoxygenase activity as well as the products of non-enzymatic reactions described above can form fatty acid hydroperoxides and lead to the generation of a large number of structurally diverse oxylipins, as demonstrated for 13-HPOTE (**5**) in Figure 4. Corresponding oxylipins originate from 9-hydroperoxy-10,12,15-octadecatrienoic acid (9-HPOTE) [114] and other fatty acid hydroperoxides.

The complex branching of the oxylipin pathway was comprehensively reviewed amongst others by Blée (1998) [115], Grechkin (1998) [116] and Feussner and Wasternack (2002) [117]. Enzymatic oxylipin pathways are classified into three main processes (see Figure 4):

- the allene oxide synthase pathway, leading to JA (**1**), OPDA (**7**), and related jasmonates such as the α- and γ-ketols (**9** and **10**),
- hydroperoxide lyases, generating short chain cleavage products of the fatty acid backbone, e.g. 13-oxo-9,11-tridecadienoic acid (**18**),
- the peroxygenase pathway, leading to the formation of multifunctional alcohols and epoxides, e.g. 13-hydroxy-9,11,15-octadecatrienoic acid (13-HOTE; **19**) and 12,13-epoxy-11-hydroxy-9,15-octadecadienoic acid (12,13-epoxy-11-HODE; **20**).

Less characterized routes are

- the formation of keto fatty acids, e.g. 13-oxo-9,11,15-octadecatrienoic acid (**21**), by LOX-enzymes [118],
- the synthesis of divinyl ethers such as etherolenic acid (**22**) [119,120] or
- the non-enzymatic formation of cyclopentanoid phytoprostanes, e.g. phytoprostane B_1 type 1 (**23**) [121,122].

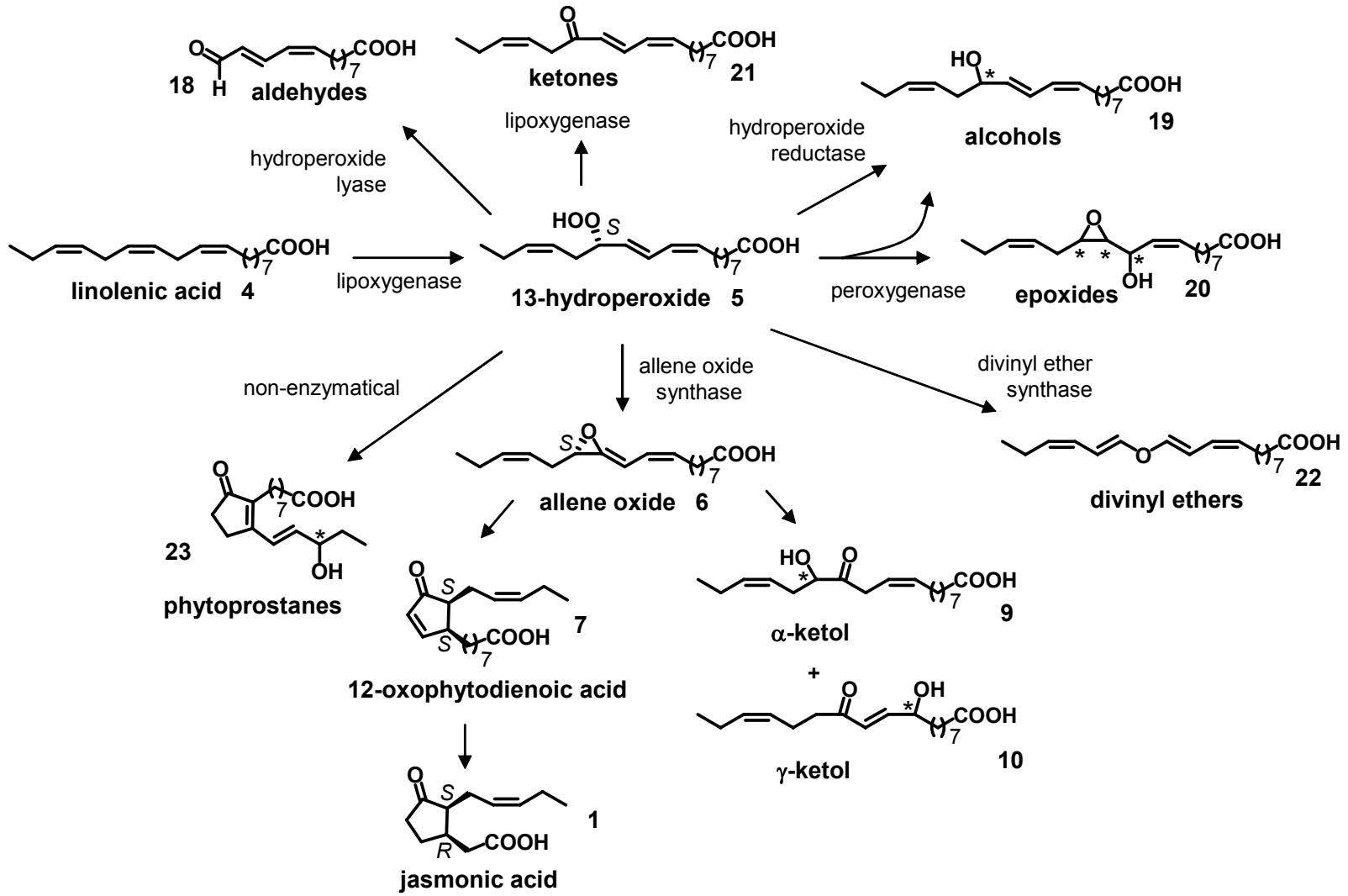

Figure 4 Oxylipins generated from 13-HPOTE (**5**) exemplify the variety of signaling pathways of linolenic acid (**4**) in plants. A similar spectrum of diverse products originates from 9-HPOTE and other fatty acid hydroperoxides.

The cyclopentanoid oxylipins JA (**1**), OPDA (**2**), and the phytoprostanes vividly highlight the parallels between the plant and mammalian fatty acid derived signaling compounds, in particular, as non-enzymatical cyclization of arachidonic acid has also been reported [123] (Figure 5).

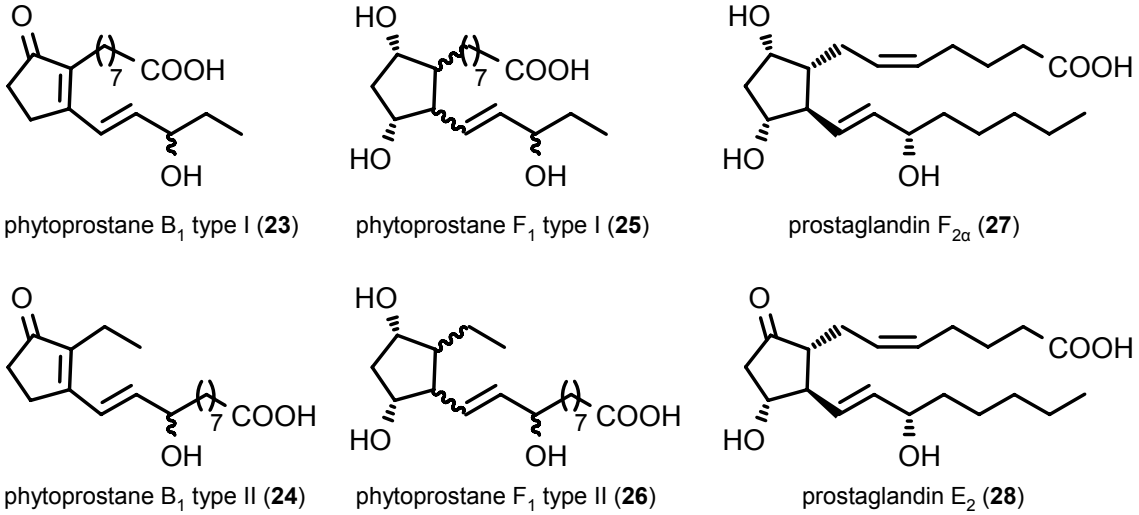

Figure 5 Phytoprostanes compared to the structurally related mammalian prostaglandins.

Biological activity has been demonstrated for hydroperoxide lyase products such as traumatin (**29**) [124], mucondialdehyde [125], and aldehydes e.g. 2-hexenal and hexanal, all of which exhibit antimicrobial activities [126,127]. 9-Oxononanoic acid (**30**) was found during aging of *S. tuberosum* tubers, however its physiological role is still not known [128]. Additionally, fatty acid derived aldehydes were demonstrated to mediate defense against aphids in tomato plants (*Lycopersicon esculentum*) [129]. Volatile compounds including 3-hexenyl acetate (**31**) serve as important attractants for host plant finding of female lepidopterans [130] but also predatory insects [9,131] and mediate plant-plant communication [132-134].

12-Hydroxy-9-dodecenoic acid was reported to activate protein phosphorylation more efficiently than JA (**1**) [135]. Other metabolites such as divinyl ethers [136,137] and the non-enzymatically formed phytoprostanes trigger disease response, accumulation of phytoalexins and detoxification processes [138,139].

However, in most cases the knowledge of the function of the diverse oxylipins in plant signaling processes is very limited and no general concept of their biological role has been established. Genetically modified plants, deficient in a specific biosynthetic pathway or unable to perceive a certain signal, are used to identify the importance of oxylipins in plant

physiology. For example in tomato plants, the compatible[2] interaction of the pathogen *Xanthomonas campestris* with its host was reduced in the *def1* mutant[3] [140] and in plants lacking the allene oxide cyclase enzyme. However, JA (**1**) and OPDA (**7**) appeared not to be involved in the regulation of this plant-susceptibility [141]. Furthermore, some wound-induced genes are apparently regulated independently from JA (**1**), as they were still expressed in *allene oxide cyclase antisense* plants [142]. Moreover, Royo *et al.* (1999) [143] reported that silencing of a specific 13-LOX isoenzyme of potato (*Solanum tuberosum*) plants resulted in a decrease of proteinase inhibitors (PI) and an increased performance of feeding insects. Interestingly, this gene silencing had no effect on JA-biosynthesis itself. As a consequence, other LOX derived compounds should be responsible for the alteration of the PI-levels. In fact, exogenously applied OPDA (**7**) triggered phytoalexine biosynthesis and accumulation in soybean, although during pathogen elicitor-treatment no increase of OPDA (**7**) has been detected [65]. This result indicates that the biological activity of externally applied compounds does not necessarily correspond to their physiological role in the activation of a particular defense response. Thus, independent signaling pathways may exist leading to the same result or the added oxylipin is structurally related to other still unknown oxylipins which are involved in this signaling processes. Moreover, it has been suggested, that Michael addition acceptors, such as electrophilic α,β-unsaturated systems play an important role as JA-independent plant signals [144]. Therefore, unsaturated fatty acid ketones and cyclopentenones are interesting candidates for oxylipin signaling in plants [91,145,146].

The involvement of multiple signals in the induction of plant defense may allow a fine tuning towards the needs of the plant in specific situations. Considering the possible role of the great variety of oxylipins produced enzymatically and non-enzymatically, the control mechanisms of plant defense might turn out to be by far more complex. Thereby high flexibility and specificity is given for the plant's reaction towards threats from the environment. Furthermore, for many of the reactive oxylipins an inherent toxic potential - as has been demonstrated for similar compounds in mammalian cells [147-149] - should be considered in the investigations of plant defense reactions. For example conjugated unsaturated aldehydes have been reported to act as cytotoxic agents in the defense system of marine diatoms against their plankton predators [150,151]. Similar action of reactive compounds can be imagined in plant-insect interactions.

---

[2] An interaction between a susceptible host plant and a pathogen that results in unrestricted parasitism of the plant.

[3] The *def1* mutant does not accumulate JA (**1**) in response to wounding; the precise nature of its mutation has not been determined yet.

1.1.3 Salicylic acid: Induction of plant defense against pathogens

Next to the fatty acid derived signals other low molecular weight compounds are involved in orchestrating the adaptable plant response to their environment. Besides its function in plant developmental processes, the phenolic compound salicylic acid (SA; **2**) plays a pivotal role in defense reactions, especially against pathogens [152]. SA (**2**) triggers pathogenesis-related (*PR*) gene activation and is involved in the induction of hypersensitive cell death that protects plants against biotrophic[4] pathogens. Additionally, **2** is required for the activation of systemic acquired resistance (SAR). SAR is a form of immunity that gives plants the ability to gain resistance against subsequent infections after encountering infection with certain pathogens [153,154]. For reviews on SA (**2**) see Klessig and Malamy (1994) [152] and Durner *et al.* (1997) [155].

SA (**2**) is biosynthesized from phenylalanine (**32**) via the phenylpropanoid pathway (Figure 6); however details concerning its biosynthesis are still unclear. The first step includes the phenylalanine ammonia-lyase (PAL)-catalyzed conversion of phenylalanine to *trans*-cinnamic acid (**33**). In tobacco it is assumed, that **33** is converted to benzoic acid (**38**) via β-oxidation, with the latter being *ortho*-hydroxylated to salicylic acid (**2**) [156]. Alternative routes, suggesting the involvement of benzaldehyde or *ortho*-coumaric acid seem to play only a minor role [156]. Free SA (**2**) is rapidly metabolized to its 2-*O*-β-glucoside from which it can be by released again on demand [152]. Similarly to JA (**1**), SA (**2**) is converted into its methyl ester (**39**) and serves as a volatile signal in plant-insect interactions [157] but also in plant-plant communication [158].

The mechanism of action of SA (**2**) is still discussed, since a cellular receptor has not yet been identified. Indeed, the activity of SA (**2**) seems to be interwoven with the oxidative burst which is required for hypersensitive response and pathogen resistance [24,104]. This hypothesis is supported by the identification of a soluble SA-binding protein, which is related to catalases [159,160] and suggests that SA (**2**) might act via modulation of enzyme activity and generation of ROS [161].

[4] Pathogens requiring living cells for reproduction.

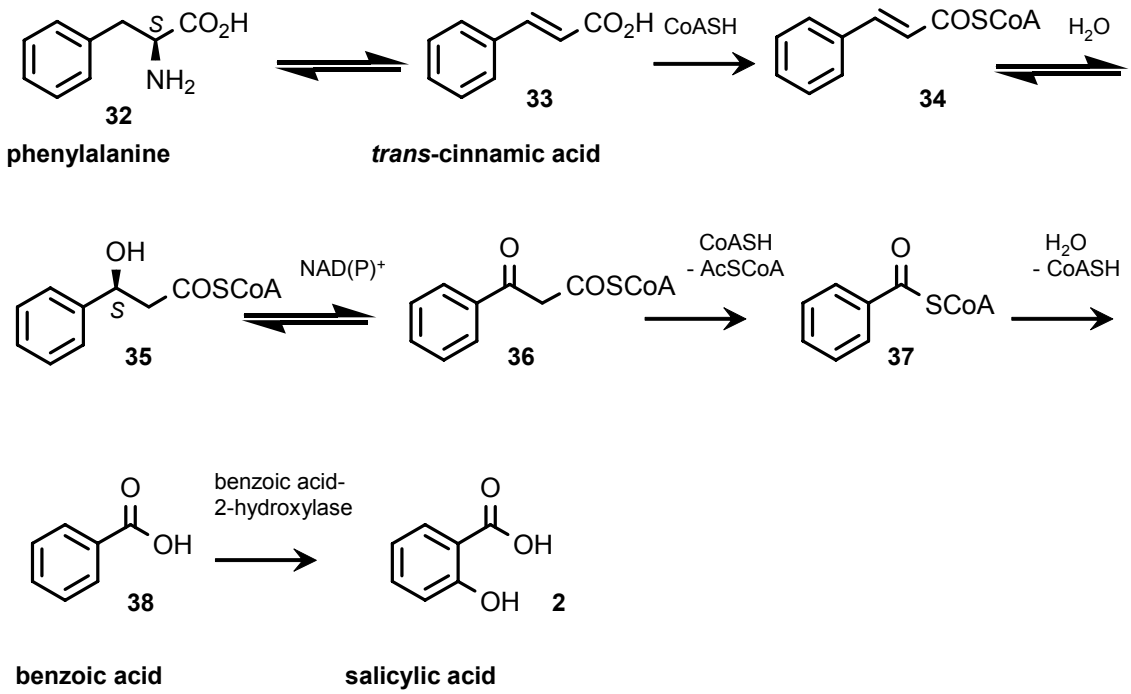

Figure 6 Proposed biosynthesis of salicylic acid (**2**).

1.1.4 Ethylene: Modulation of plant stress responses

Ethylene (ET; **3**) can be regarded as a versatile phytohormone involved in various processes during plant development, including seed germination, growth regulation, fruit ripening and senescence [162]. As a stress hormone, its production is triggered by wounding, herbivory, and pathogenesis, but also by abiotic stresses such as drought or heavy metal exposure [163]. During defense responses ET (**3**) regulates the expression of certain *PR*-genes, however its major function during stress response appears to be the coordinative regulation of JA-biosynthesis and JA-induced responses. ET (**3**) interacts in complex signaling networks with JA (**1**) and SA (**2**), ensuring differentiated defense reactions upon multiple stress situations (see Chapter 1.2). As volatile phytohormone ET (**3**) is capable to mediate interplant communication and may serve as a “social” signal between plants. Tobacco plants which were deficient in their ET-reception were unable to recognize adjacent plants, while wild-type tobacco plants tend to stop growing when contacting their neighbors [164]. However, the importance of this behavior has not been proven under field conditions.

ET (**3**) is biosynthesized from 1-aminocyclopropane-1-carboxylic acid (ACC; **40**) (Figure 7) [162,165,166] that is derived from *S*-adenosyl-L-methionine (SAM; **41**), an intermediate of the methionine cycle. By converting ACC (**40**) to *N*-malonyl-1-aminocyclopropane-1-carboxylic acid (**42**) instead of **3**, plants can regulate ethylene production [166].

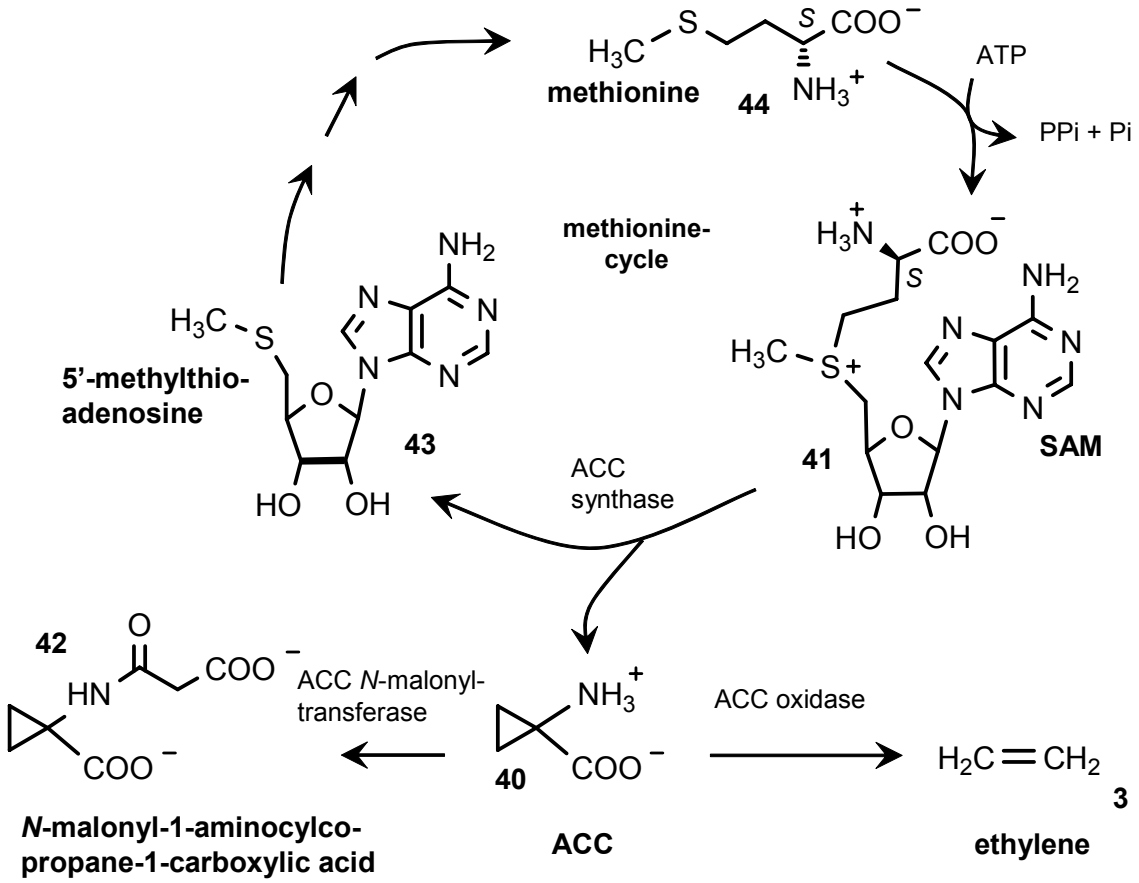

Figure 7 Biosynthesis of ethylene (**3**).

Unlike JA (**1**) and SA (**2**), ET-signal reception is well studied [167]. The ET-receptor consists of a two-component system known from bacteria [168,169]. The two components of the receptor comprise a sensor and a response regulator [170]. After receiving the signal, the receptor histidine kinase undergoes autophosphorylation and subsequently the phosphate group is transferred to the response regulator. Downstream signaling is assured by a phosphorylation cascade, mitogen activated protein (MAP) kinases and subsequent regulation of gene expression [162,170]. In a broad sense, the ethylene signal perception system resembles tyrosine kinase receptors and their signaling cascades of mammalian hormones such as insulin and the platelet-derived growth factor (PDGF) [171].

1.2 Cross-talk: Signaling network for multiple responses

To attain an integral and optimal response against different stress factors, signaling pathways interact with each other (cross-talk), either synergistically or antagonistically. Cross-talk interactions are of diverse nature and differ between plant species and the elicitors (e.g. pathogens or herbivores) investigated [172,173].

JA (**1**), SA (**2**), and ET (**3**), but also other phytohormones such as abscisic acid and indol-3-acetic acid are involved in the complex signaling network which has been comprehensively reviewed; see Felton and Korth (2000) [174], Rojo *et al.* [175] and Pozo *et al.* (2005) [176] (Figure 8).

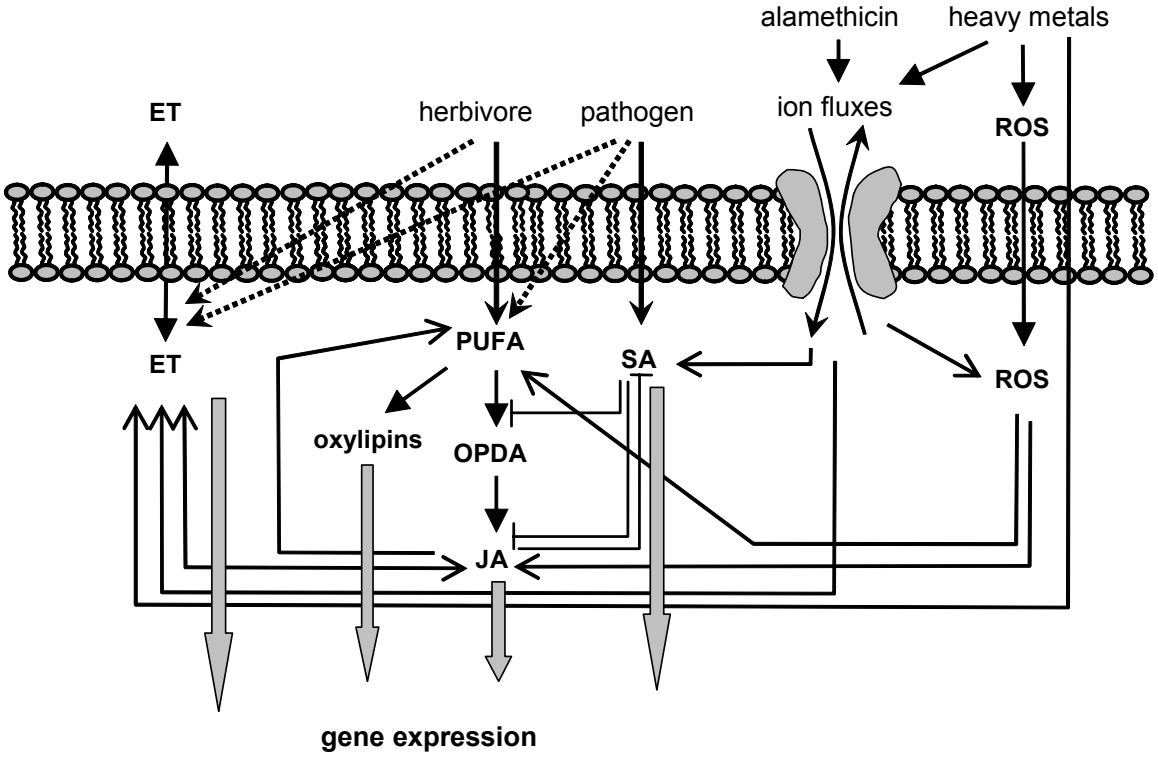

Figure 8 Hypothetical cross talk between the different phytohormone pathways. Biotic and abiotic elicitors, which will be described in this thesis, trigger various signal cascades. In *P. lunatus* the JA (**1**) biosynthesis is inhibited by SA (**2**), while JA (**1**) and ET (**3**) interact synergistically. Herbivores and pathogens mainly induce the JA (**1**) and the SA (**2**) signaling pathway respectively, the peptaibol alamethicin as well as heavy metal ions upregulate all three phytohormones. Closed arrows display signal perception and biosynthesis pathways; open arrows show positive interactions, blunted lines indicate negative regulation.

Many studies support the hypothesis that SA (**2**), which mediates defense response against pathogens, inhibits the JA-biosynthesis, which is involved in wound response as well as resistance against herbivory. Thus enhanced production of SA (**2**) or external application of SA-analogs such as acetylsalicylic acid or 2,6-dichloroisonicotinic acid can interfere with the biosynthetic pathway of JA (**1**) [177-179]. This interaction can be observed by an increased performance of feeding insects on plants with high levels of endogenous SA (**2**), or by exogenously applying **2**, or SA-analogs [180-182]. SA (**2**) and analogs do not directly inhibit the allene oxide synthase (AOS) or allene oxide cyclase (AOC) [183,184], but seem to influence the JA-response on the transcriptional level thereby decreasing AOS transcripts [183] or by inhibiting the transport of OPDA (**7**) from the chloroplast into the cytosol, making it inaccessible for β-oxidation [185]. Many examples from various plants have demonstrated this inhibition of JA-action by simultaneous activation of the SA-pathway [173,186,187].

However, defense against pathogens is not restricted to SA-signaling but can also be mediated by JA (**1**) and ET (**3**) [176,188]. The SA (**2**) mediated systemic acquired resistance (SAR) has to be distinguished from rhizobacteria-mediated induced systemic resistance (ISR) [189]. For ISR two mechanisms have been described: the SA-dependent and the SA-independent pathway. The SA-independent pathway is relying on JA (**1**) and ET (**3**) sensing [190]. Both resistance pathways seem to interact synergistically [191]. Conversely, Niki *et al.* (1998), found inhibitory effects of SA (**2**) and JA (**1**) during the activation of *PR* genes related to either of those phytohormones [192]. While SA (**2**) seems to play a protective role against biotrophic pathogens, JA (**1**) is rather involved in defense against necrotrophic[5] pathogens [193]. In contrast, Nickstadt *et al.* (2004) [194] found a jasmonate signaling mutant to be more resistant against biotrophic as well as necrotrophic pathogens. Additionally, in potato plants OPDA (**7**) seems to be involved in resistance against pathogens, besides SA (**2**)[195].

ET (**3**) constitutes an additional signal in this complex interaction of plant defense responses. ET (**3**) can either correlate positively or negatively with both SA (**2**) and JA (**1**) signaling [196]. In most cases **3** acts in concert with JA (**1**) and defense related gene activation [197-199], but it is also reported to suppress JA-induced nicotine accumulation in *Nicotiana attenuata* [200], albeit not the induction of volatile emission [201]. It has been shown that the negative interaction between ET (**3**) and JA (**1**) can be utilized by the plant to differentially regulate local and systemic responses [196]. During the volatile production of *P. lunatus*, an inhibitory cross-talk between SA (**2**) and JA (**1**) signaling pathways has been observed [186,202], whereas a synergistic effect of ET (**3**) on JA (**1**) mediated volatile production has

[5] Pathogens that kill the infected cell and feed on dead tissue.

been described [203]. Moreover, the production of ET (**3**) could be triggered by herbivore induced volatiles of neighboring plants under greenhouse conditions [204].

Especially the interaction between the JA- and the SA-pathway does not only affect the level of these phytohormones, but modifies the flux of precursors through the metabolic oxylipin network and shifts the distribution of individual oxylipins. Supporting this hypothesis, Weichert *et al.* (1999) found an accumulation of reductase pathway metabolites after treatment of barley (*Hordeum vulgare*) with SA (**2**) [205]. In *N. attenuata*, silencing of the LOX-gene responsible for the first steps in JA-biosynthesis, resulted in reduced resistance to herbivores, but also increased upregulation of α-dioxygenase genes [41]. Additionally, substrate competition between the AOS and the hydroperoxide lyase pathway had been demonstrated by gene silencing experiments [206]. This flux-control of free fatty acids through the oxylipin pathways can be easily shifted in cross-talk situations and becomes visible in characteristic plant reactions [186,207].

2 GOALS OF THIS STUDY

As mentioned in the introduction, plants perceive information from their environment relying on a complex network of signaling pathways that are subtly interconnected [17,144] and guarantee adequate reaction to various stresses such as herbivore feeding or abiotic stress. Lipids comprising the major component of cell membranes are the first sites to experience threats from the environment. Hence, fatty acids are ideal candidates for the formation of multiple and diverse signaling molecules, the so called oxylipins, by enzymatic and non-enzymatic oxidation processes [115,122].

Although the diversity of lipid peroxidation products is known for a long time [115], especially from studies about their involvement in mammalian diseases [148,208,209], in the field of plant science their biological role is still often unknown. Partly this lack of information about oxylipins in plants originates from the concentration on the octadecanoid pathway with JA (**1**) and OPDA (**7**) being recognized as crucial signals in plant defense reactions [62]. However, recently the interest in alternative oxylipin signaling pathways rises as observations that require additional signals accumulate [91,143].

Although a broad array of analytical separation techniques, such as HPLC and GC and their hyphenations with detection methods such as MS and NMR have been rapidly developed, the identification and quantification of highly active signaling compounds in complex matrices remains an analytical challenge. Nevertheless the analysis of the diversity and interdependency of signals upregulated in plants during various stresses are a prerequisite for a thorough understanding of plant stress reactions on the molecular level.

This work is designated to contribute to the understanding of oxylipins as active signals during plant-herbivore interactions and during abiotic stress, focusing on the following goals:

- In order to address the role of oxylipins and the integration of signaling pathways in plant defense reactions, a rapid and reliable method for identification and quantification of oxylipins from the plant matrix should be developed. The main focus should lie on the octadecanoids and reactive oxylipins carrying oxo-groups and α,β-unsaturated systems, as these are believed to play a key role as signaling compounds [145,146].
- It was aimed to identify novel oxylipins in leaf material of *Phaseolus lunatus* and investigate their upregulation during various stresses. A careful comparison of signaling compounds induced by simple mechanical wounding and herbivore damage would allow assessing the role of specific cues for elicitation of oxylipin signals in plant-herbivore interactions.

- To evaluate the relevance of fatty acid oxidation products as cross-kingdom signals, their distribution should not only be monitored in the herbivore damaged leaves, but also in the caterpillar's oral secretions and frass.
- In cooperation with Prof. Christiane Gatz, an attempt to combine metabolic profiling of signaling compounds with analysis of gene expression was planned, in order to gain more detailed insight in plant defense reactions from different viewpoints. As model system the genetically amenable and intensely studied *Arabidopsis thaliana* was chosen. The phytohormone profile of *A. thaliana* should be analyzed after treatment with the established elicitor alamethicin to evaluate the role of these signaling compounds in the regulation of defense gene expression.
- In addition to biotic stress, the influence of abiotic stress factors in plant defense reactions should be studied within the scope of the Graduate Research School "Analysis of the Functioning and Regeneration of Degraded Ecosystems" (GRK 266). It was planned to investigate the impact of heavy metal ion stress on plants. In this respect I aimed to compare common features of heavy metal ion stress and alamethicin induction in *P. lunatus*.

3 ANALYSIS OF LABILE OXYLIPINS EXTRACTED FROM PLANT MATERIAL

3.1 Introduction: Oxylipin monitoring

Although an entire range of oxylipins seems to be involved in plant defense reactions (see Chapter 1.1.2), previous analytical approaches mainly focused on the analysis of jasmonates such as JA (**1**) and OPDA (**7**) [64,210]. Since concentration on this very narrow range of compounds does not allow understanding of the complexity of the signal transduction pathways involved in plant defense reactions, I aimed to develop a versatile and reliable analytical method to monitor putative signaling compounds in plants after exposure to varying stress conditions. The ability to profile both new and established compounds is a prerequisite for a thorough investigation of physiological processes in plants. However, a comprehensive profiling of oxylipins is hampered by the limited stability of many of these highly functionalized compounds. Particularly sensitive are unsaturated ketones, conjugated unsaturated aldehydes and higher functionalized derivatives of polyunsaturated fatty acids. Moreover, the preservation of the original stereochemistry of JA (**1**) is yet another complication that has not been satisfactorily solved.

So far, different procedures for the extraction and derivatization of phytohormones have been reported, most of them rely on mass spectrometric detection after derivatization of the analytes to their methyl esters [64,186,211] or HPLC analysis using UV-detection [145,205,212]. Pentafluorobenzyl esters were used owing to the enhanced sensitivity which can be achieved by electron capture-negative chemical ionization mass spectrometry (NCI-MS) [63,210]. Various methods exist that describe so-called oxylipin-profiling [213,214]. In most cases, however, only certain products or product classes of oxylipins were addressed and rearrangement or breakdown of unstable oxylipins was widely ignored. Additionally, many reports concerning the type and kinetics of the formation of higher oxidized oxylipins only described the conversion of externally added linolenic acid (**4**) or defined hydroperoxy fatty acids by plant material or by isolated enzyme fractions and not the *in vivo* formation of these oxylipins [69,215,216]. More recent methods have been developed that allow the simultaneous monitoring of different phytohormones including JA (**1**), SA (**2**), abscisic acid or volatile compounds from complex biological matrices but fail to address higher oxidized oxylipins [64,217-219]. Rather sensitive compounds carrying, for example, an α,β-unsaturated carbonyl segment represent a large and heterogeneous group of signaling molecules that are supposed to act independently of JA (**1**) [91,145]. Such compounds are prone to undergo Michael addition reactions in the presence of cellular nucleophiles, such as glutathione and free thio-groups of amino acids and proteins [148,220], as well as with DNA

[221,222], and are likely to react during the workup process. Thus, so far none of the methods commonly used in plant science targeted the role of the diverse group of highly functionalized and reactive oxylipins as a whole with the potential to identify new signal compounds. Since some of these compounds were found to act in a phytohormone-like manner [91,146], the need to understand their contribution to the complex network of plant defense reactions is obvious. With a new approach for the analysis of labile oxylipins I provide a methodology for monitoring diverse plant signaling compounds in order to broaden the view on the signaling networks involved in plant defense reactions.

3.2 Results and discussion

3.2.1 Development of a method for comprehensive extraction of oxylipins from plant material

During method development, various techniques and workup strategies were evaluated in order to obtain an extraction procedure specific for fatty acid metabolites. Potent signaling molecules such as JA (**1**) are often active in nanomolar concentrations. Analyzing these trace-compounds in plant matrices is a challenge for every analytical approach. During my studies I focused on GC-MS analytics which combines the advantage of high separation efficiency of the GC with the potential of tentative structure assignment through interpretation of the MS-fragmentation patterns. Structure proposals of unknown compounds can be unambiguously verified by comparison of their retention time and MS-fragmentation pattern with synthetic standards.

Before GC-MS analysis of the compounds, they have to be extracted from the plant material. Hence, the leaf material is homogenized using an organic solvent in order to prevent enzyme activity during the workup. For the extraction of phytohormones and oxylipins from the plant material suitable solvent systems were evaluated. In 1959 Bligh and Dyer published a method for total lipid extraction using a monophasic system of chloroform, methanol and water [223,224]. This method extracts the total lipid content; however, I was mainly interested in free fatty acids and oxylipins. In fact, the method of Bligh and Dyer yielded too many and too much of unwanted lipids. Especially, phospholipids extracted with this protocol tended to block the NH_2-groups of the aminopropyl solid phase extraction (SPE)-cartridges used in the following purification step. Therefore alternative extraction procedures using diethylether [186,225] or binary solvent mixtures such as hexane:2-propanol 3:2 (v:v) [226] were evaluated. However, to analyze the broad spectrum of chemically diverse oxylipins, pre-separation into polar and less polar compound classes by liquid/liquid extraction improved the following purification steps significantly. Furthermore, the separation in polar

and less polar oxylipins enhanced recovery rates because overloading of the SPE-cartridges was prevented. Additionally, GC-separation and detection of the analytes was ameliorated, as less overlap of compounds during GC-MS analysis occurred. Therefore, partitioning of less polar compounds, (fatty acids, JA (**1**), OPDA (**7**), and aldehydes) and higher oxidized compounds (ketols and hydroxy-fatty acids) by subsequent extraction with hexane and CH_2Cl_2, was fundamental and resulted in better sensitivity and reliability of the analytical method.

The exhaustive extraction of fatty acids still leads to the accumulation of large amounts of unwanted unpolar accompanying substances from the plant material, such as chlorophyll and sterols. As my aim was to identify novel signaling compounds in plants I concentrated on oxylipins carrying an acidic moiety. This is justified by the fact that most known phytohormones (abscisic acid, indole-3-acetic acid, jasmonic acid (**1**), gibberellins) exhibit a carboxylic acid function. Purification of acidic compounds, like fatty acids and phytohormones carrying a free carboxylic acid moiety from unpolar compounds is therefore a crucial step and can be achieved by SPE. Different types of SPE-cartridges are available using various functionalities for separation of compounds such as reversed phase C-18 beads or ion exchange phases. As ion exchange chromatography is the most selective technique to purify acids, aminopropyl (NH_2)-cartridges were used for separation of free acids from uncharged compounds (Figure 9). Thus, acid and non-acidic compounds can be separated. Simple aldehydes or ketones are not retained on the cartridge and could possibly be analyzed from the eluant.

After this pre-separation, methylation of the free acids with diazomethane makes the sample suitable for GC-MS analysis. However, methylation is only possible at a late step of phytohormone extraction, and does not stabilize labile compounds carrying reactive functional groups. Furthermore, the interpretation of mass spectra of the obtained methyl esters is often not characteristic for compound classes and makes assignment of tentative structures difficult.

Selectivity and sensitivity can be enhanced by using selected ion monitoring (SIM); however, in this detection mode the spectral information evidencing compound identity is largely lost [186]. An elegant way to enhance sensitivity is the use of electron capture-negative chemical ionization (NCI) [227]. This form of ionization is achieved by creation of an electron plasma in the ion source of the MS by introducing a reactant gas, e.g. methane or methanol. Compared to electron impact (EI) ionization, the fragmentation is reduced, and more intense signals at higher molecular weight are generated. Moreover, NCI detection is selective for compounds carrying fluorine, phenolic or nitroaromatic moieties as they are prone to act as acceptors in electron transfer. Introducing these functional groups by derivatization renders the analytes suitable for NCI-MS [227].

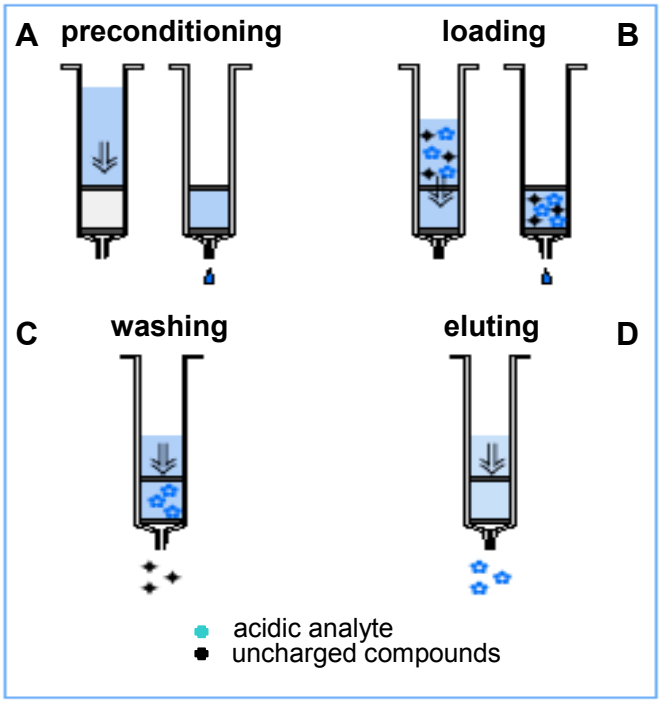

Figure 9 Principle of ion exchange solid phase extraction (SPE). A: Preconditioning of the cartridge with organic solvents; B: loading of the sample, acidic compounds will bind to the bead; C: washing of the cartridge to elute neutral compounds; D: elution of the analyte with acidified organic solvent.

Free acid moieties can be derivatized with pentafluorobenzyl bromide (PFBBr). This method has already been successfully used in plant science for the detection of JA (**1**) and OPDA (**7**) [63,210]. The PFB-moiety is ideal for NCI-MS measurements, providing the advantage of high sensitivity, combined with low background noise. Using PFBBr was therefore the first attempt to establish NCI for sensitive detection of the phytohormones JA (**1**), OPDA (**7**) and SA (**2**). PFB-esters of phytohormones exhibit characteristic mass fragments with high intensities (Figure 10). The NCI-mass spectrum is dominated by the $[M - 181]^{\bullet -}$ fragment, derived from the cleavage of the pentafluorobenzyl moiety (Figure 11).

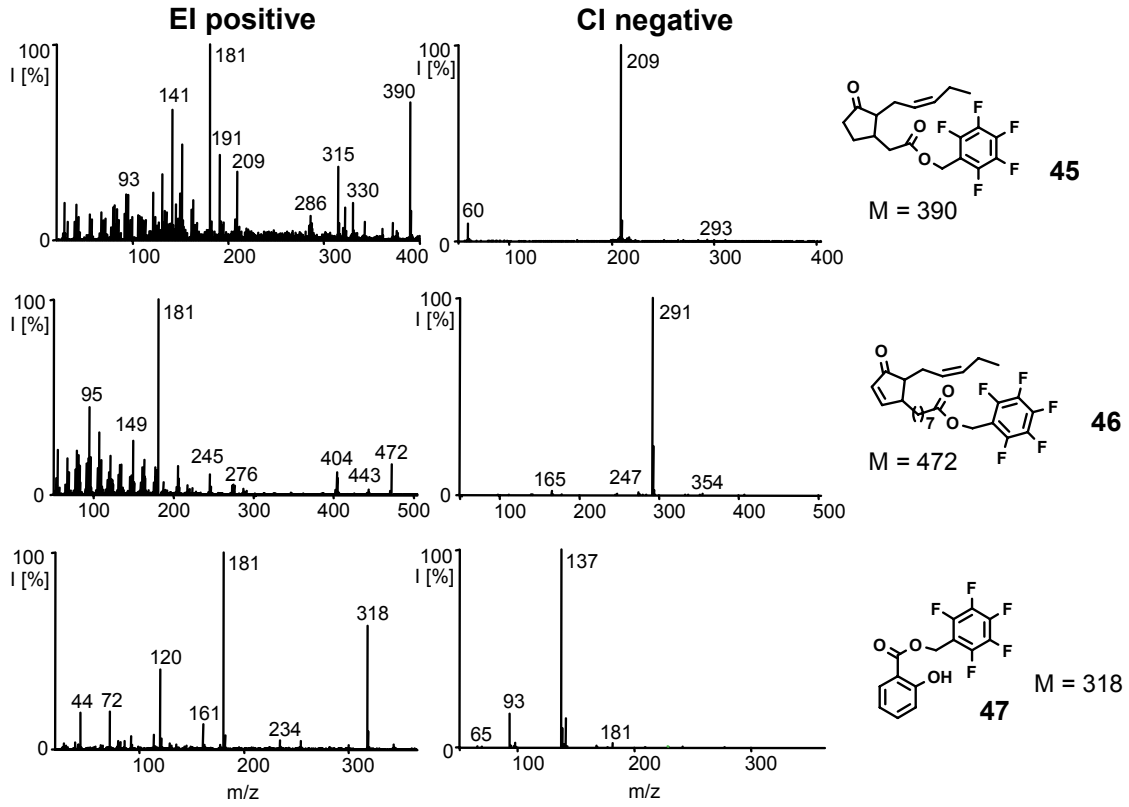

Figure 10 EI- and NCI-mass spectra of the PFB-esters of JA **45**, OPDA **46**, and SA **47**. The NCI-MS spectrum is dominated by the $[M - 181]^{\bullet -}$ fragment (Figure 10).

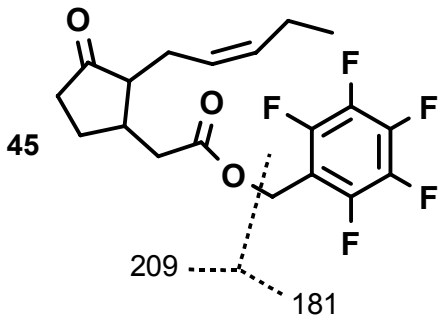

Figure 11 Formation of the $[M - 181]^{\bullet -}$ fragment in NCI-MS by cleavage of the pentafluorobenzyl moiety.

Although generation of a single base peak is ideal for quantification, PFBBr-derivatization turned out to be unsuitable, because the ester formation did not provide the necessary stabilization of labile compounds during sample preparation. This resulted in unacceptable high variability between individual samples of identical treatments. Hence, a derivatization step right at the beginning of the extraction procedure in order to stabilize labile compounds was crucial for the reliability and reproducibility of the analysis.

Therefore, pentafluorobenzyl hydroxylamine (PFBHA) was chosen to react with oxo-groups resulting in the formation of oximes, which thereby are protected from further reaction [228-231]. In contrast to previous methods using PFBHA for the analysis of aldehydic compounds form plant material [232], the reagent was added directly at the beginning of the workup procedure. Due to this *in situ* derivatization, fatty acid derived oxo-derivatives are immediately converted into corresponding stable pentafluorobenzyl-oximes (PFB-oximes) preventing degradation and isomerization. With a similar approach, Wichard *et al.* (2005) were able to stabilize reactive α,β,γ,δ-unsaturated aldehydes out of phytoplankton with preservation of the original stereochemistry [233].

Additional derivatization of hydroxyl-groups with *N*-methyl-trimethylsilyl-trifluoroacetamide (MSTFA) to trimethylsilyl(TMS)-ethers made the highly polar oxylipins suitable for GC-separation and at the same time provided further information for structure elucidation. TMS-ethers generate characteristic m/z 73 fragments and induce α-cleavages next to the OTMS-group (see Table 1, Chapter 3.2.2.1 for a detailed list of common mass fragments).

3.2.2 Analysis of labile oxylipins from plant material as PFB-oximes

The novel extraction protocol developed for the analysis of oxylipins from plant material is based on the *in situ* formation of stable PFB-oximes allowing a simultaneous profiling of stable and unstable oxo-derivatives, which could not be addressed by previous methods. The *in situ* formation of PFB-oximes is rapid and proceeds quantitatively in aqueous and organic media thereby preventing further isomerization during sample preparation [228,229,234]. PFB-derivatives of less oxidized oxylipins can be efficiently extracted with unpolar solvents such as hexane, while compounds bearing additional polar substituents require dichloromethane for extraction [235]. Consecutive extraction with both solvents allows a simple pre-separation of the complex oxylipins into two classes (Figure 2). Further enrichment of the PFB-derivatives is achieved by passing the analytes through aminopropyl SPE-cartridges (Chromabond NH_2) to bind the acidic oxylipins. Bound PFB-derivatives were eluted with diethyl ether:formic acid (98:2, v:v) and esterified with diazomethane. Hydroxyl groups in the analytes were converted into TMS-ethers by treatment with MSTFA. The TMS-derivatives of *O*-functionalyzed PFB-oximes are fairly stable and can be stored for more than two months at 4 °C without significant changes [235].

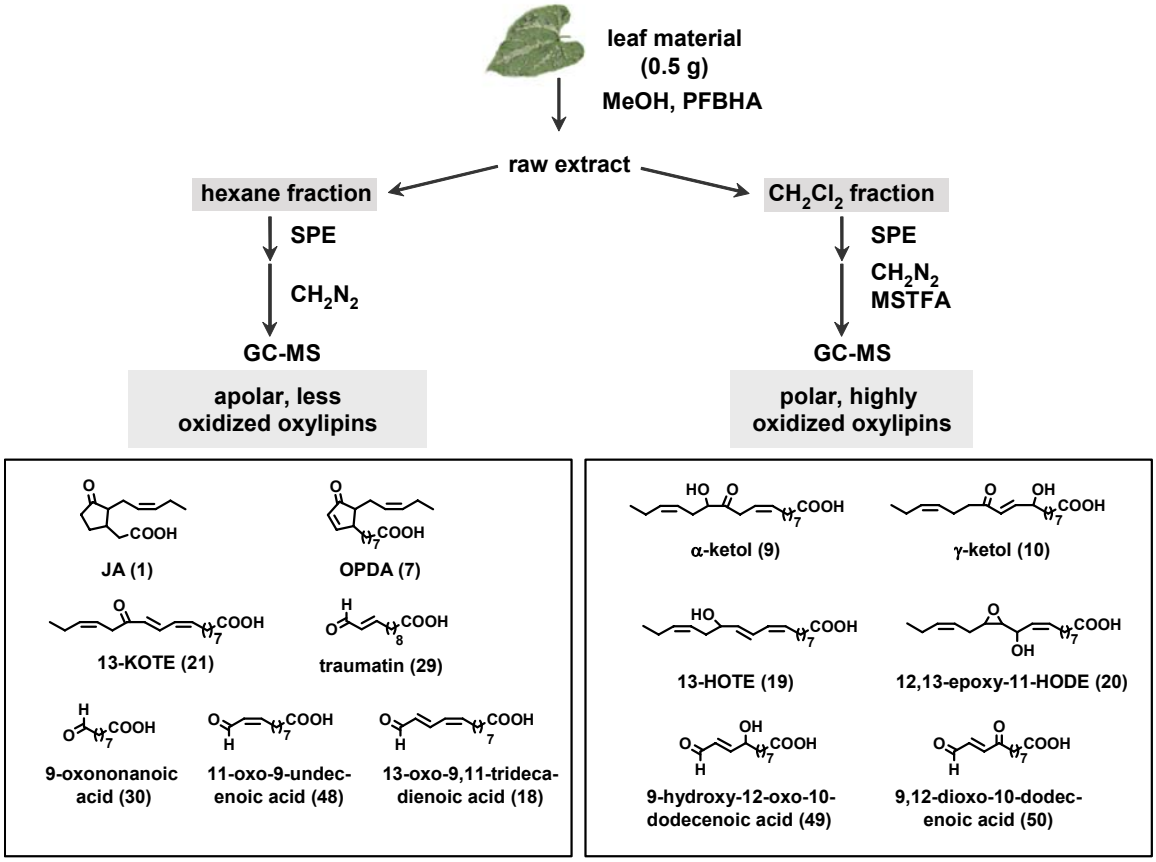

Figure 12 Scheme of the extraction procedure. The structures illustrate identified oxylipins from *P. lunatus* leaves in the corresponding extract fraction.[6]

Derivatization with PFBHA does not only prevent addition of nucleophiles to the reactive Michael acceptors, but also inhibits isomerization of the *de novo* synthesized *cis*-JA (*cis*-**1**) to the thermodynamically more stable *trans*-**1**. This indeed had not been achieved by most other extraction protocols focusing on JA-analysis. As *cis*-**1** rapidly isomerizes during the extraction, especially when encountering acidic pH-extremes [236], most methods so far analyze JA (**1**) as its more stable *trans*-isomer. Transformation of the oxo-group into a PFB-oxime prevents this isomerization by inhibiting enolization and thus isomerization at position C7. This provides the unique possibility to follow the time course of *cis*-**1** during stress responses of plants. Müller *et al.* (1994) [210] used a similar approach, stabilizing *cis*-JA (*cis*-**1**) as dithioketal. However, this derivatization technique was not applied at the beginning of the workup procedure and although pH extremes were avoided, isomerization of *cis*-**1** during extraction cannot be excluded.

[6] For sake of clarity, the fully derivatized oxylipins (PFBHA, CH_2N_2 and MSTFA) are depicted as their underivatized precursors.

3.2.2.1 Oxylipin identification

Application of the above described analytical protocol for the analysis of oxylipins from 0.5 g fresh weight (frw) of Lima bean leaves revealed, besides the well known phytohormones JA (**1**) and OPDA (**7**), a number of additional functionalized octadecanoids and fatty acid oxidation products (Figure 12). Compounds were identified by comparison of their mass spectra and retention time with authentic references. 9-Hydroxy-12-oxo-10-dodecenoic acid (**49**) and 9,12-dioxo-10-dodecenoic acid (**50**) were identified by comparing their characteristic mass spectra with literature [237,238]. The structure of **49** was verified by isolating it as product of α-linolenic acid (**4**) autoxidation experiments (Dr. Mesmin Mekem Sonwa, personal communication).

The three-step derivatization sequence with PFBHA, diazomethane and MSTFA resulted in a specific modification of the analytes that easily can be recognized from its mass spectrum. Approaches for the identification of PFB-derivatives of lipid peroxidation products have been published in detail [239-241]. A collection of characteristic fragments used for identification of unknown compounds is given in Table 1 and Table 2.

Table 1 Typical masses and fragments of oxylipins and PFB-oximes in EI-MS.

m/z	Chemical formula	Literature
M-15	$[M\text{-}CH_3]^{\bullet+}$	Hesse *et al.* (2002) [242]
M-31	$[M\text{-}OCH_3]^{\bullet+}$	Hesse *et al.* (2002) [242]
M-29	$[M\text{-}COH]^{\bullet+}$ or $[M\text{-}CH_2CH_3]^{\bullet+}$	Hesse *et al.* (2002) [242]
M-59	$[M\text{-}COOCH_3]^{\bullet+}$	Hesse *et al.* (2002) [242]
73	$[Si(CH_3)_3]^{\bullet+}$ ($[TMS]^{\bullet+}$)	Hesse *et al.* (2002) [242]
89	$[OTMS]^{\bullet+}$	Hesse *et al.* (2002) [242]
90	$[HOTMS]^{\bullet+}$	Hesse *et al.* (2002) [242]
104	$[CH_3OTMS]^{\bullet+}$	Hesse *et al.* (2002) [242]
181	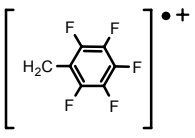	Hsu *et al.* (1999) [240]
239 saturated aldehydes	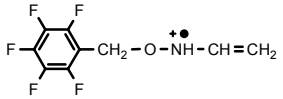	Spiteller *et al.* (1999) [241]
250 α-unsaturated aldehydes	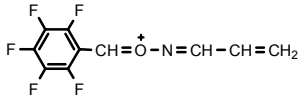	Spiteller *et al.* (1999) [241]
326 α-hydroxy aldehydes	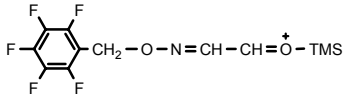	Loidl-Stahlhofen *et al.* (1995) [231]

In the positive EI-MS mode the mass spectra of all oxylipins carrying an oxo-group, exhibit a characteristic ion at m/z 181, which is due to the pentafluorobenzyl(PFB)-fragment $[C_6F_5CH_2]^{\bullet+}$ of the oximes. Besides the generally intense PFB-ion at m/z 181 the spectra often display the ion $[M - 181]^{\bullet+}$ resulting from the loss of the pentafluorobenzyl-group and the ion $[M - 197]^{\bullet+}$ that originates from the loss of the entire $C_6F_5CH_2O$-fragment (PFBO-fragment). If present, both fragment ions are rather intensive. Compounds possessing additional hydroxyl-groups are also easily recognized owing to the presence of two characteristic ions, namely the PFB-ion at m/z 181 and a fragment ion at m/z 73, which is characteristic for trimethylsilylated substituents (TMS-group). The characteristic ions can be used for ion searches displaying only the accordingly functionalized compounds (Figure 13).

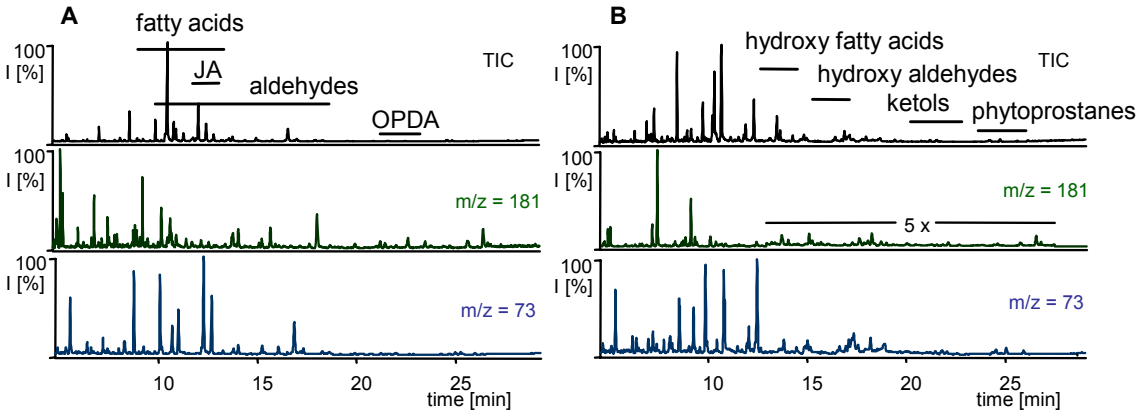

Figure 13 GL-chromatograms of A: the hexane extract and B: the CH_2Cl_2 extract of Lima bean leaves treated with PFBHA, CH_2N_2 and MSTFA. The ion traces of m/z 181 and m/z 73 illustrate how PFB-oximes and TMS-derivatives can be visualized in the chromatogram. Elution regions for important derivatized oxylipins and oxylipin classes are indicated by lines.[7]

In NCI-MS mode, PFB-oximes can readily be identified by the loss of HF leading to generally intense $[M - 20]^{\bullet-}$ ions (Table 2). The loss of the PFB-radical results in a $[M - 181]^{\bullet-}$ ion which in the case of acylic compounds is often the most abundant fragment. If TMS-ethers are present, the simultaneous loss of the $C_6F_5CH_2/C_6F_5CH_2O$ moieties along with TMS-OH generates the most prominent fragments. Unlike positive EI-MS, where PFB-oximes can be easily recognized because of their intense pentafluorobenzyl-cation at m/z 181, in the negative CI-MS mode the corresponding diagnostic ions are m/z 167 $[C_6F_5]^{\bullet-}$ and m/z 197

[7] For sake of clarity, the fully derivatized oxylipins (PFBHA, CH_2N_2 and MSTFA) are denominated as their underivatized precursors.

$[C_6F_5CH_2O]^{\bullet-}$ respectively (Table 2). Detailed information on the fragmentation of PFB-oximes during NCI-MS has been published by Hsu *et al.* (1999) [240].

Table 2 Typical masses and fragments of oxylipins and PFB-oximes in NCI-MS.

m/z	Chemical formula	Literature
M-20	$[M\text{-}HF]^{\bullet-}$	Hsu *et al.* (1999) [240]
M-47	$[M\text{-}HF\text{-}HCN]^{\bullet-}$	Hsu *et al.* (1999) [240]
M-50	$[M\text{-}HF\text{-}NO]^{\bullet-}$	Hsu *et al.* 1999 [240]
M-90	$[M\text{-}HOTMS]^{\bullet-}$	Hesse *et al.* (1984) [242]
167	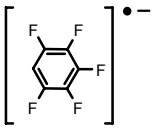	Hsu *et al.* (1999) [240]
196	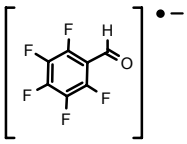	Hsu *et al.* (1999) [240]
197	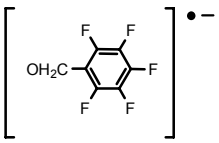	Hsu *et al.* (1999) [240]

In summary, from the combination of positive EI- and negative CI-mass spectra of the PFB-derivatives many structures can be proposed and reliably identified by comparison with reference compounds without the need for time consuming isolation and purification.

An overview on the EI- and NCI- mass spectra of selected PFBHA derivatized oxylipins is presented in Figure 14. A summary of the mass spectra of all oxylipins investigated is given in the supplementary material. Moreover I generated a searchable oxylipin database which can be found on the included CD.

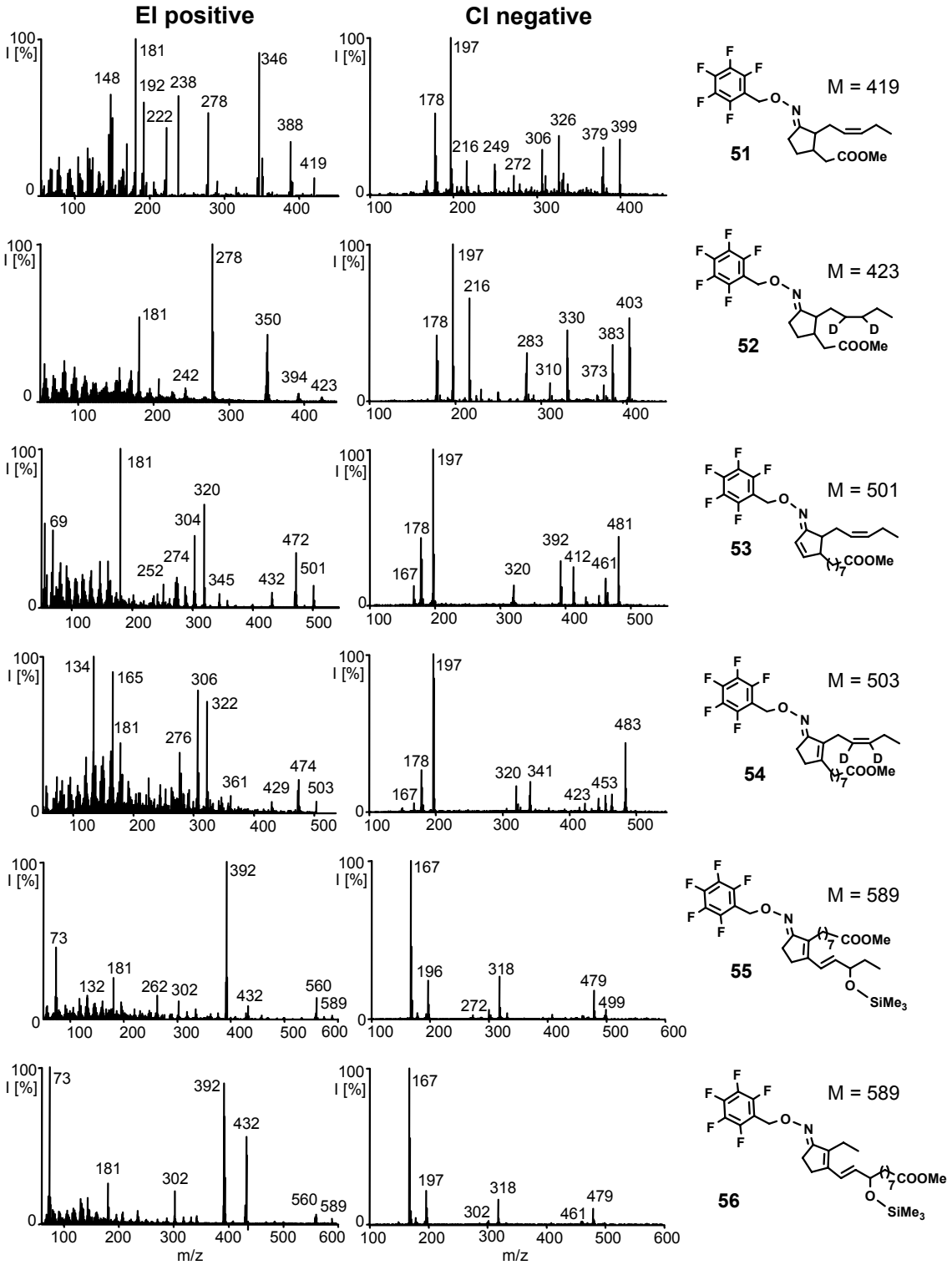

Figure 14-1 Mass spectra of derivatized oxylipins and standards used for quantification.

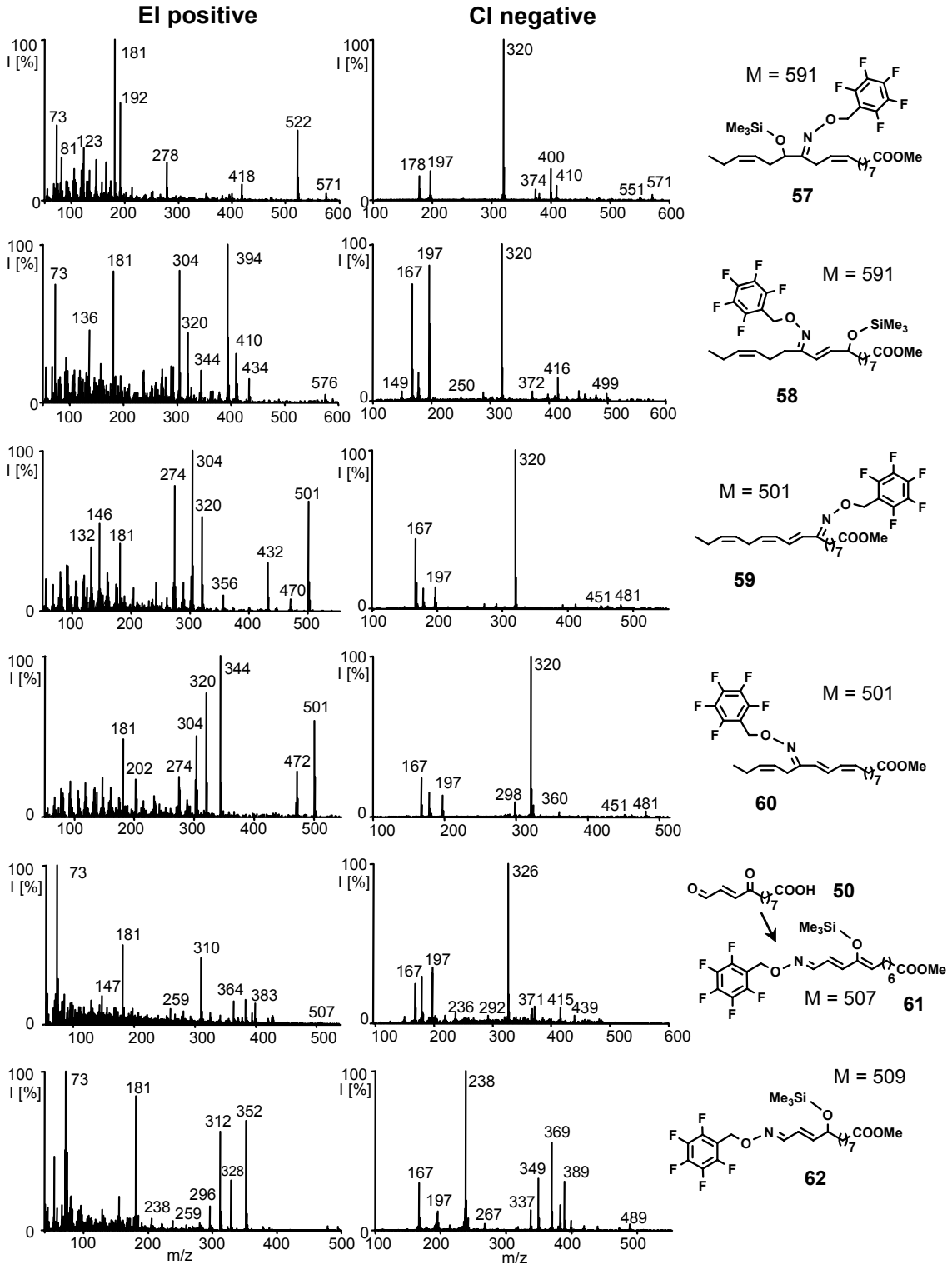

Figure 14-2 Mass spectra of derivatized oxylipins and standards used for quantification. 9,12-Dioxo-10-dodecenoic acid (**50**) is rearranging to **61** [237,238].

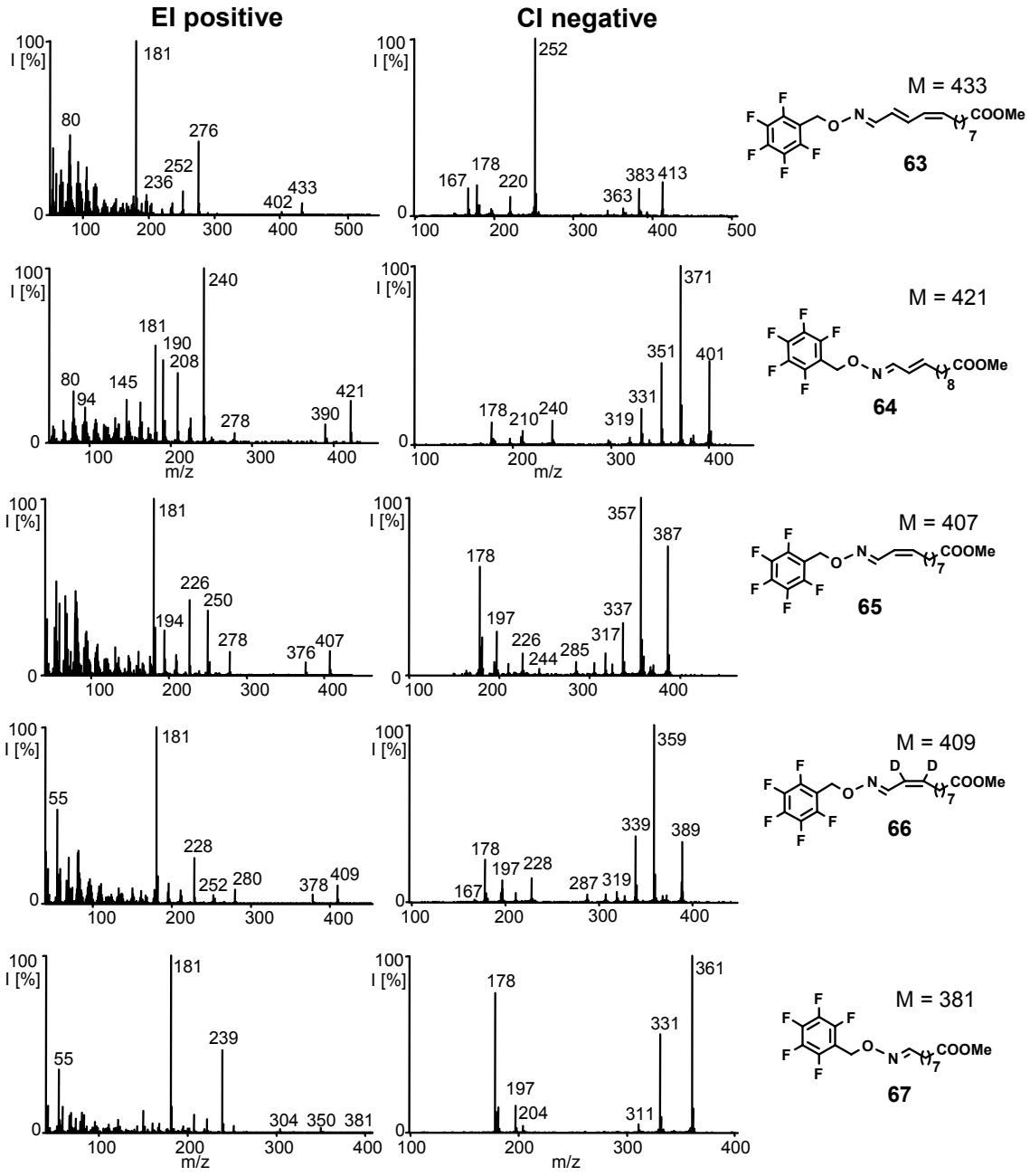

Figure 14-3 Mass spectra of derivatized oxylipins and standards used for quantification.

The typical MS-fragmentation patterns of various structures permit the establishment of certain rules, which point towards characteristic chemical properties. Thus, in EI-MS, the comparison of the typical MS-fragmentation of the cyclopentanoid oxylipins shows similarities which can be used for their identification.

Cyclopentanoid PFB-oximes

For example, higher mass fragments of the PFB-oximes of jasmonic acid methyl ester **51** (Figure 14 and Figure 15) are governed by elimination of $^{\bullet}OCH_3$ (m/z 388) and $^{\bullet}CH_2COOMe$ (m/z 346), while the fragments at m/z 238 and m/z 222 result from elimination of the PFB-radical or the PFBO-moiety. The fragment at m/z 350 results from the loss of the side chain at position C7, while the ion at m/z 278 is indicative for the loss of both side chains of the pentanone ring and is, thus, common for methyl jasmonate and its deuterated analog (Figure 14).

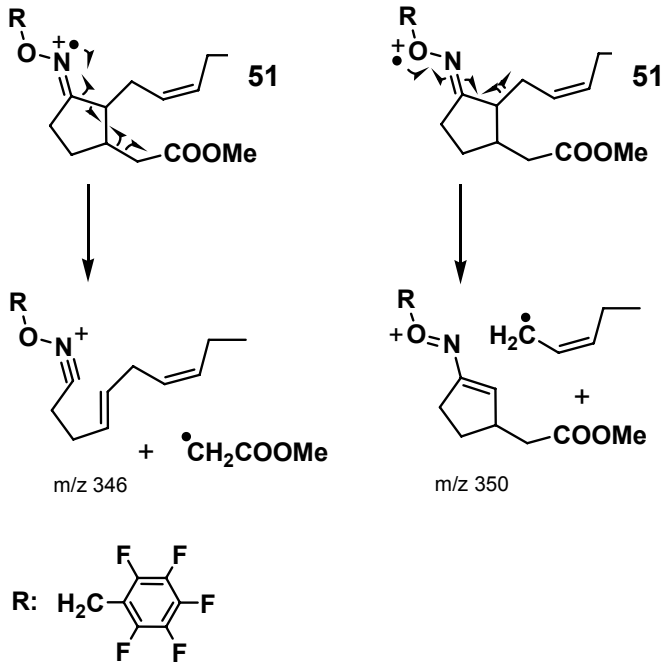

Figure 15 Formation of the fragments m/z 346 and m/z 350 from the PFB-oxime of JA methyl ester **51**. Similar rearrangements can be found for other cyclopentanoid oxylipins.

Similar cleavage patterns govern the mass spectrum of the PFB-oxime of OPDA methyl ester **53** (Figure 14). Elimination of the pentenyl side chain generates m/z 432 and a loss of a $^{\bullet}CH_2CH_3$ radical leads to the fragment at m/z 472. The fragments at m/z 320 and m/z 304 result from the loss of the PFB-radical or the PFBO-moiety, respectively. Fragmentation of the PFB-oxime of the deuterated OPDA analog ([15,16-$^2H_2$]-tetrahydrodicranenone B; [$^2H_2$]-*iso*-OPDA; **54**) follows the same general pattern leading to e.g. to a M - 181 ion. Additionally **54** exhibits diagnostically valuable fragments at m/z 165 (307 - 142) and m/z 134 (276 - 142) due to the position of the double bond between both alkyl side chains which

allows a McLafferty type rearrangement leading to the loss of methyl 6-heptenoate (M 142) from m/z 307 (Figure 16).

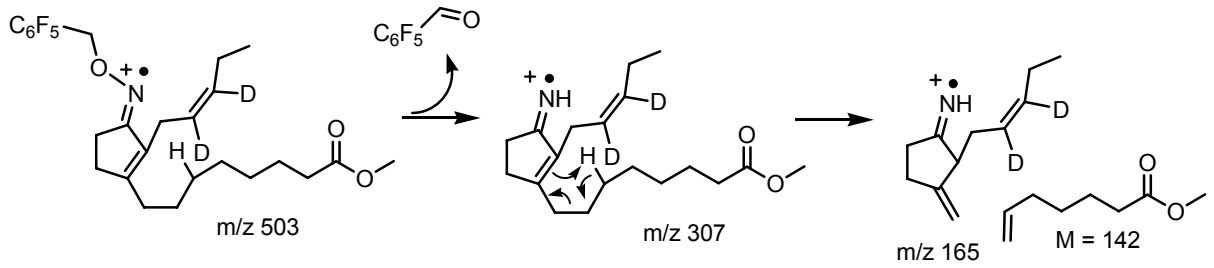

Figure 16 McLafferty type rearrangement leading to the loss of methyl 6-heptenoate.

The fragmentation of the PFB-oxime of phytoprostane PPB_1 type II methyl ester **56** leads to the ion m/z 432 (M - $^{\bullet}(CH_2)_7COOMe$). Since the elimination of small radicals is energetically disfavored, the corresponding ion m/z 560 (M - $^{\bullet}CH_2CH_3$) of the derivative of phytoprostane PPB_1 type I **55** is only of low intensity. Elimination of the PFBO-moiety yields m/z 392 for both compounds **55** and **56** (Figure 14).

Acyclic PFB-oximes

The derivatives of α- and γ-ketols (**57** and **58**) carrying an OTMS-group, exhibit intense ions which result from α-cleavage next to the OTMS-group at m/z 522 (M - $^{\bullet}C_5H_9$) and m/z 434 (M - $^{\bullet}(CH_2)_7COOMe$) respectively. In both cases a cation is formed that is stabilized by a neighboring double bond and the OTMS-group.

PFB-oximes of polyunsaturated linear oxo-derivatives yield another series of intense diagnostic ions by fragmentative cyclization to substituted pyridinium ions as described by Spiteller *et al.* (1999) [241]. This is demonstrated by the fragment at m/z 344 of the PFB-oxime of 13-KOTE **60** as shown in Figure 17 and the fragment at m/z 432 of the derivative of 9-KOTE **59**. PFB-aldoximes of 13-oxo-9,11-tridecadienoic acid methyl ester **63**, for example, display the same cleavage pattern yielding m/z 276. PFB-oximes **63** and **64** rearrange analogously to m/z 278, although this ion occurs in lower intensities.

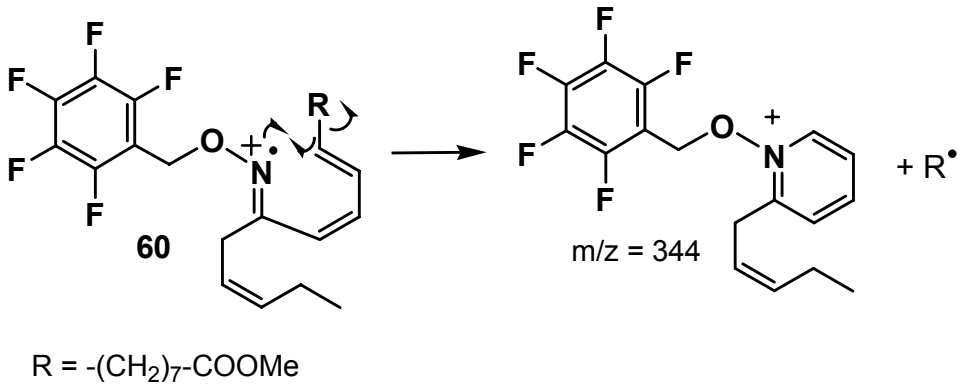

Figure 17 Formation of the pyridinium ion m/z 344 from the PFB-oxime of 13-KOTE **60**.

Unsaturated and saturated aldehydes can be distinguished by their characteristic McLafferty fragments [243]. For example the PFB-oxime of 11-oxo-9-undecenoic acid methyl ester **65** exhibits the McLafferty fragment at m/z 250, typical for PFB-aldoximes carrying an α-unsaturation [241] (Table 1). While, the PFB-oxime of 9-oxononanoic acid methyl ester **67** displays an intense McLafferty fragment at m/z 239 resulting from the elimination of 6-heptenoic acid methyl ester. This fragment can be regarded as an indicator for saturated PFB-aldoximes [241] (Table 1).

The derivatization as PFB-oximes has only one disadvantage, which is the formation of *E*- and *Z*-isomers of the oxime moiety. In most cases, these isomers are separated on the GC-column resulting in a splitting of the signal into two peaks for most compounds. In the literature the stereochemistry of PFB-oximes is often still denominated according to the older *syn*- and *anti*-nomenclature. The assignment of *syn* and *anti* results form the position of the free electron pair at the nitrogen (Figure 18) [240]. Today, the *E*- and *Z*- nomenclature, following the CIP-rules for assignment of priorities, should be preferred and is used in this work.

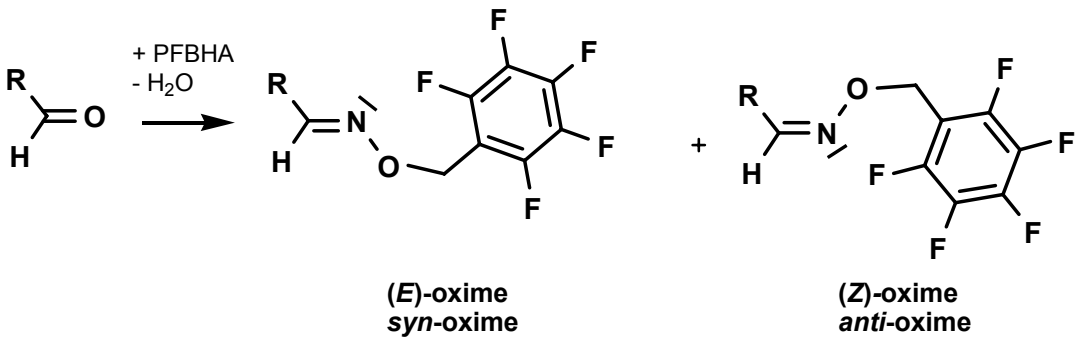

Figure 18 Formation of (*E*) (*syn*)- and (*Z*) (*anti*)-oximes with PFBHA.

Typically the (*Z*)-isomer elutes earlier than the (*E*)-isomer from the GLC-column, which can be explained by the steric structure as in most cases compounds are separated according to their boiling point and interaction with the liquid film coating of the GLC-column. This effect leads to a doubling of peak number per compound. However, due to the characteristic fragmentation, it is possible to assign the individual isomers to each peak. This can be nicely exemplified in the case of the 10-(pentafluorobenzyloxy)imino-9-trimethylsilyloxy-octadecanoic acid methyl ester (**68**) and 9-(pentafluorobenzyloxy)imino-10-trimethylsilyloxy-octadecanoic acid methyl ester (**69**) with each isomer exhibiting a characteristic positive EI-mass spectrum. Due to the (*E*)- and (*Z*)-orientation of the isomer, as well as the position of the OTMS- and the PFB-group, only the formation of a specific cleavage product is favored (Figure 19 and Figure 20). For example, the (Z)-oxime of methyl 10-(pentafluoro-benzyloxy)imino-9-trimethylsilyloxyoctadecanoate ((*Z*)-oxime **68**) generates a McLafferty product at m/z 497 by elimination of 1-heptene (Figure 20). This ion is absent in the (*E*)-isomer ((*E*)-oxime **68**). Instead, (*E*)-oxime **68** eliminates the polar segment of the fatty acid backbone as 7-octenoic acid methyl ester (M = 156) and yields an intense McLafferty fragment at m/z 439. The pair of (*E*)- and (*Z*)-oximes of the regioisomer methyl 9-(pentafluorobenzyloxy)imino-10-trimethylsilyloxyoctadecanoate (**69**) exhibit a different set of McLafferty rearrangement products. The (*Z*)-isomer produces a fragment at m/z 453 and the (*E*)-isomer a corresponding fragment at m/z 483 demonstrating the high diagnostic value of these fragments for structural assignments (Figure 20). After the McLafferty rearrangement **68** and **69** undergo further fragmentation e.g. by loss of the m/z 181 of m/z 197 fragments yielding characteristic ions for each isomer.

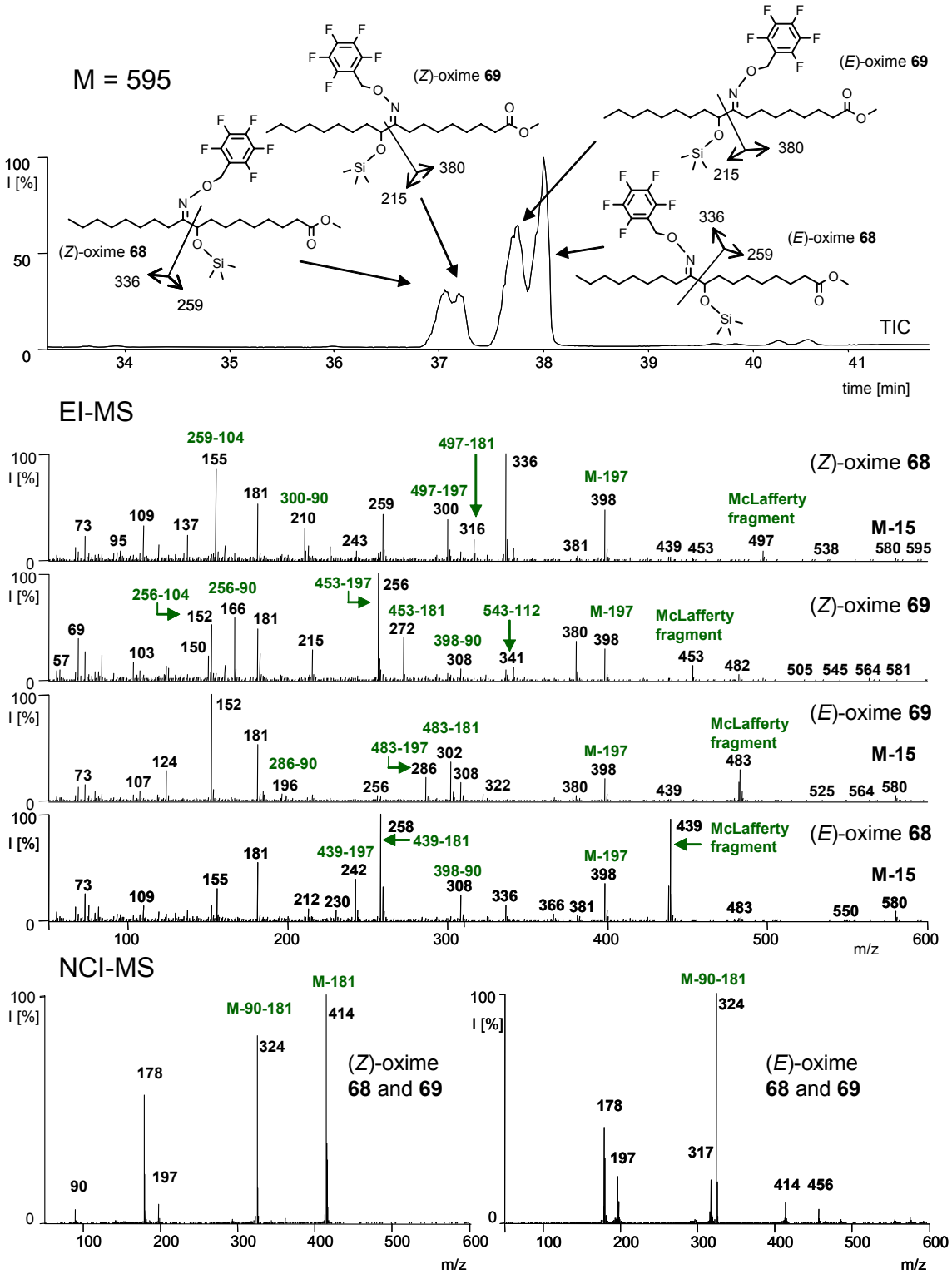

Figure 19 Separation of methyl 10-(pentafluorobenzyloxy)imino-9-trimethylsilyloxy-octadecanoate (**68**) and methyl 9-(pentafluorobenzyloxy)imino-10-trimethyl-silyloxyoctadecanoate (**69**) on a Restek RTX-200 column. Isomers can be assigned by their differing fragmentation pattern in the positive EI-mass spectrum (for explanation see Figure 20). Additional information to assign the (*E*)- and (*Z*)-isomers is obtained from their NCI-mass spectrum.

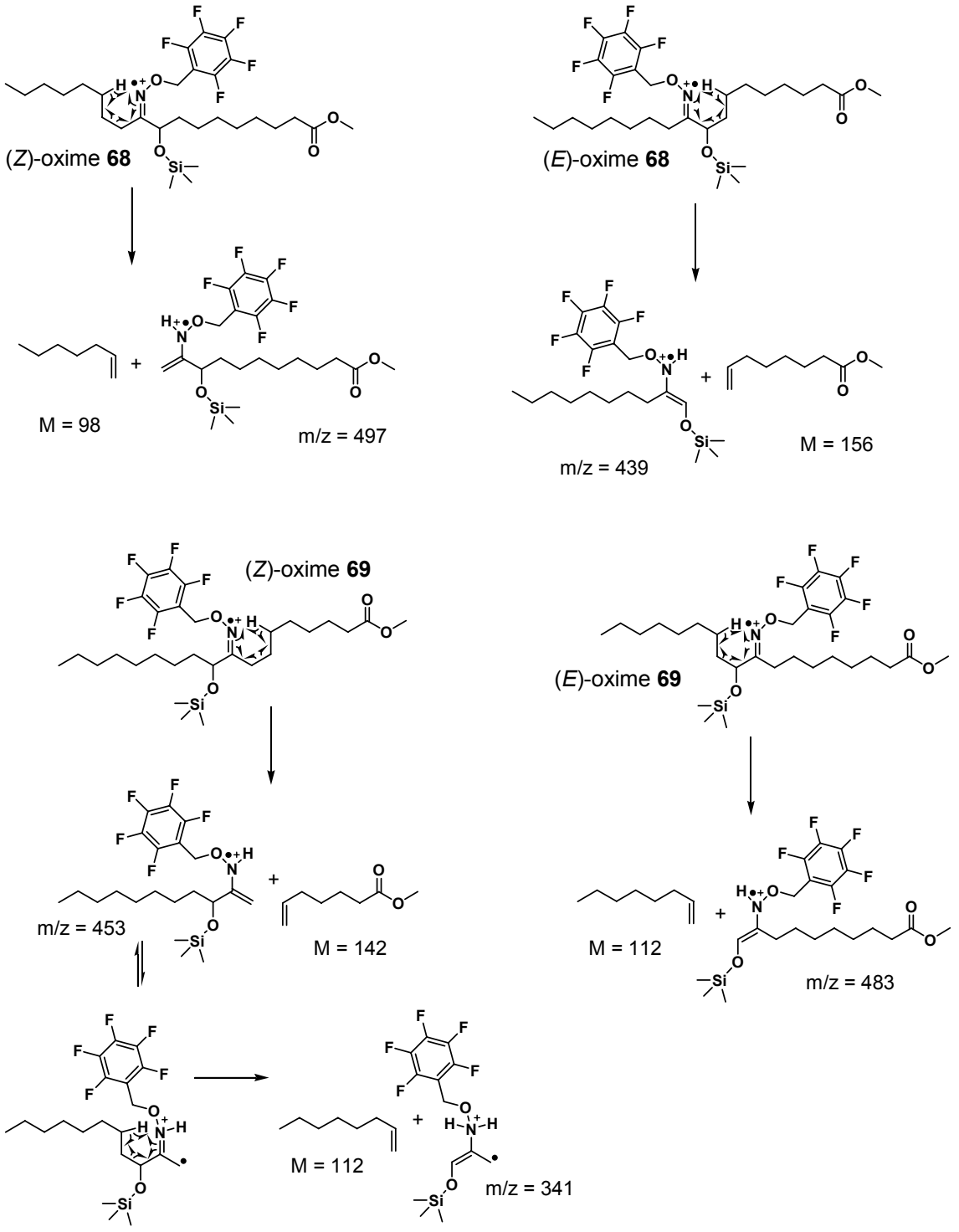

Figure 20 MS-fragmentation of methyl 10-(pentafluorobenzyloxy)imino-9-trimethylsilyloxy-octa-decanoate (**68**) and methyl 9-(pentafluorobenzyloxy)imino-10-trimethyl-silyloxyocta-decanoate (**69**).

In the case of the aldoximes **65** and **63**, the difference between the two oxime isomers is visible due to the varying intensities of fragments in NCI-MS, while the EI-MS spectra are highly similar for all isomers (Figure 21) [240]. The tentative assignment of isomers to the corresponding peak is possible by considering the influence of the steric structure on the retention time and the differences in peak heights of the NCI-MS spectrum.

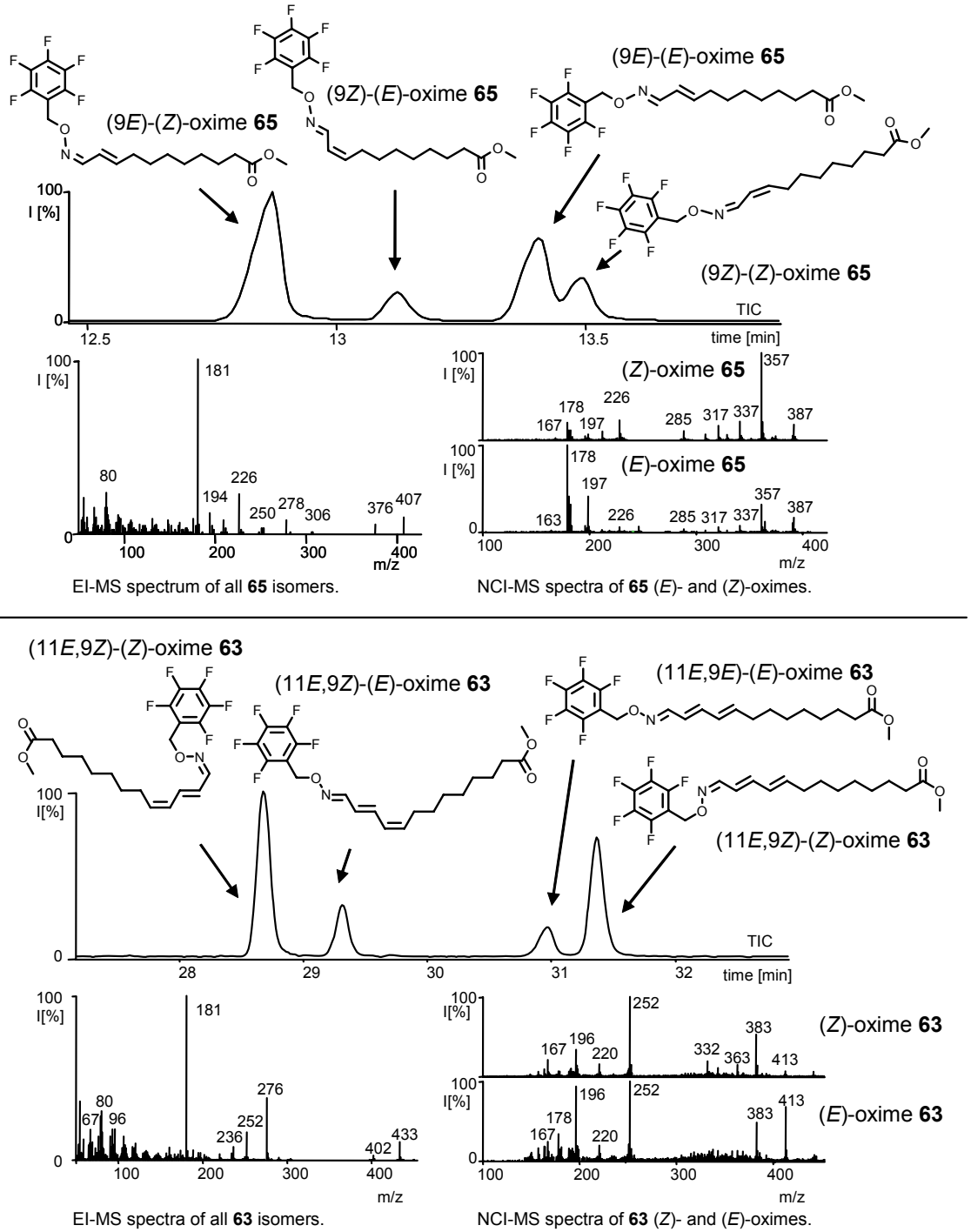

Figure 21 Separation of PFB-oximes of 11-oxo-9-undecenoic acid **65** and 13-oxo-9,11-tridecadienoic acid **63** on an Alltech EC-5 column. Isomers can be assigned by differing ion intensities of their NCI-MS fragmentation patterns.

3.2.2.2 Stabilization of jasmonic acid epimers as their PFB-oximes

The derivatization with PFBHA provides a valuable tool for the separation of *cis*-JA (*cis*-**1**) and *trans*-JA (*trans*-**1**) which allows a differentiated monitoring of both epimers. Also the JA-oxime can be observed as two geometric (*E*)- and (*Z*)-isomers, which are separated on the GC-column. In the case of PFB-oxime of JA methyl ester, *trans*-**51** forms both, (*E*)- and (*Z*)-isomers, whereas due to steric hindrance for *cis*-**51** only the (*E*)-isomer is observed (Figure 22 and Figure 23).

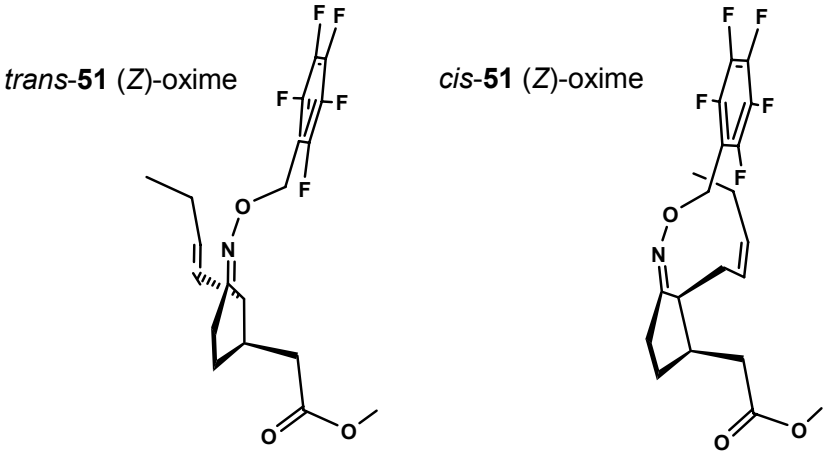

Figure 22 Stick model of the (*Z*)-PFB-oximes of *trans*-JA methyl ester (*trans*-**51**) and *cis*-JA methyl ester (*cis*-**51**). Due to steric hindrance of the side chains, the formation of the (*Z*)-oxime of *cis*-**51** is disfavored.

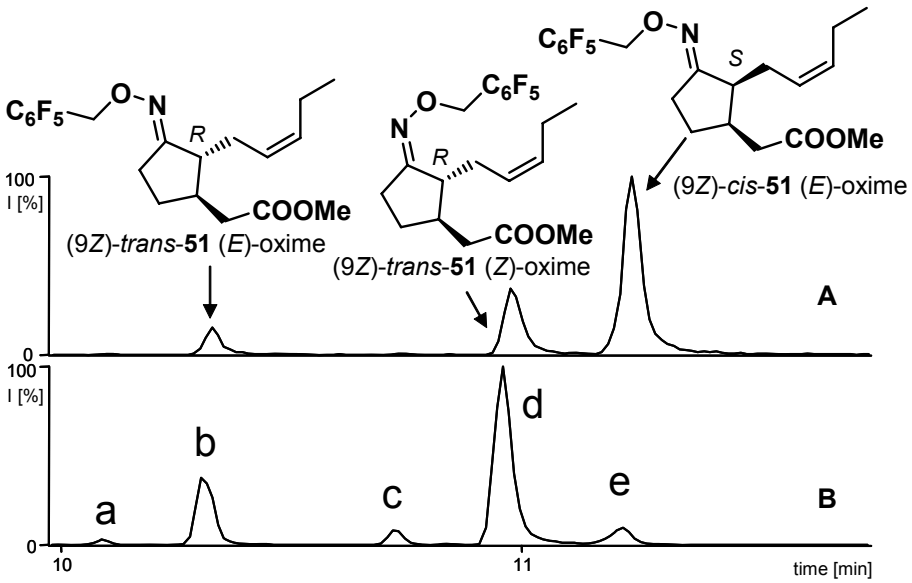

Figure 23 Separation of (*E*)- and (*Z*)-oximes of *trans*- and *cis*-JA methyl ester **51** by GL-chromatography. A: Sample enriched with *cis*-**51**; B: isomers of **51** at their thermodynamical equilibrium. In pure samples, also the side chain (9*E*)- and (9*Z*)-isomers can be observed. a: (9*E*)-*trans*-**51** (*E*)-oxime; b: (9*Z*)-*trans*-**51** (*E*)-oxime; c: (9*E*)-*trans*-**51** (*Z*)-oxime; d: (9*Z*)-*trans*-**51** (*Z*)-oxime; e: (9*Z*)-*cis*-**51** (*E*)-oxime.

3.2.2.3 Searching for oxylipins in Lima bean leaves

Using the information of MS-fragmentation patterns, the plant extract was screened for various oxylipins. Structure verification was achieved by comparison with reference compounds. Next to the phytohormones JA (**1**) and OPDA (**7**) also the hydrolysis products of the allene oxide intermediate **6** of the JA-biosynthesis, α- and γ-ketol (**9** and **10**) were identified in plant material (Table 3). Moreover highly reactive oxylipins like the Michael acceptor 13-KOTE (**21**) and α,β-unsaturated (**29** and **48**) or even α,β,γ,δ-unsaturated aldehydes (**18**) were observed. Additionally, bifunctional electrophiles such as 9-hydroxy-12-oxo-10-dodecenoic acid (**49**) and dioxododecenoic acid (**50**) were identified from 0.5 g Lima bean leaf material.

However, many oxylipins which were searched for in the Lima bean leaves after various stress treatments were not detected: These include 9-HOTE (**70**), 9-KOTE (**71**), trihydroxy-fatty acids (**72** and **73**), 10,11-epoxy-9-hydroxy-12,15-octadecadienoic acid (**74**), 12,13-epoxy-9-hydroxy-10,15-octadecadienoic acid (**75**), and the phytoprostanes **23** - **26**. This might indicate that lipid oxidation in *P. lunatus* is under the control of enzymes leading to a more defined product spectrum than non-enzymatic lipid peroxidation processes, at least under the stress situations investigated. This hypothesis is further supported by the observation that hydroxy fatty acids are the major products of non-enzymatically induced lipid peroxidation [244]. Alternatively, it is reasonable to assume that in the complex plant matrix highly reactive oxylipins rapidly undergo further metabolism or reaction with cell constituents and, hence, escape detection. Furthermore, compounds under the detection limit of this method could not be covered. This seems to be the case for the phytoprostanes F_1 type I and II (**25** and **26**) which could be detected after extraction and purification from larger amounts (2 g frw) of wounded Lima bean leaf material (Dr. Jian-Wen Tan, personal communication).

Table 3 Detection of oxylipins in leaf material (0.5 g frw) of *P. lunatus*.
[a] **25** and **26** were not detected with the protocol described, but by an alternative method.

Oxylipin Name	Structure	Occurrence in leaves of *P. lunatus*
JA (**1**)	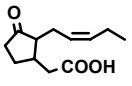 **1**	+
OPDA (**7**)	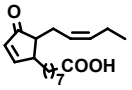 **7**	+
PPB_1 type I (**23**)	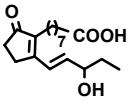 **23**	-
PPB_1 type II (**24**)	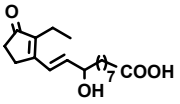 **24**	-
PPF_1 type I (**25**)	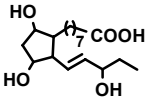 **25**	(+)[a]
PPF_1 type II (**26**)	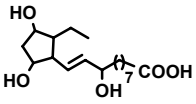 **26**	(+)[a]
α-Ketol (**9**)	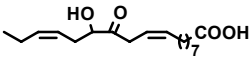 **9**	+
γ-Ketol (**10**)	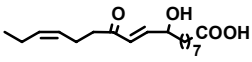 **10**	+
9-HOTE (**70**)	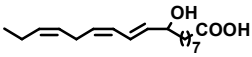 **70**	-
13-HOTE (**19**)	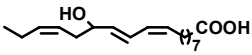 **19**	+
9-KOTE (**71**)	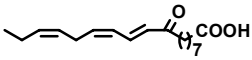 **71**	-
13-KOTE (**21**)	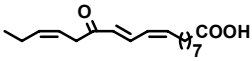 **21**	+
9-Hydroxy-12-oxo-10-dodecenoic acid (**49**)	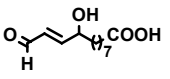 **49**	+
9,12-Dioxo-10-dodecenoic acid (**50**)	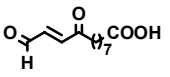 **50**	+
13-Oxo-9,11-tridecadienoic acid (**18**)	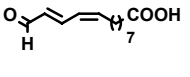 **18**	+
Traumatin (**29**)	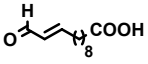 **29**	+
11-Oxo-9-undecenoic acid (**48**)	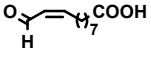 **48**	+

Oxylipin Name	Structure	Occurrence in leaves of *P. lunatus*
9-Oxononanoic acid (**30**)	 **30**	+
10,11-Epoxy-9-hydroxy-12,15-octadecadienoic acid (**74**)	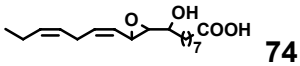 **74**	-
12,13-Epoxy-9-hydroxy-10,15-octadecadienoic acid (**75**)	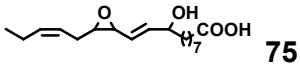 **75**	-
12,13-Epoxy-11-hydroxy-9,15-octadecadienoic acid (**20**)	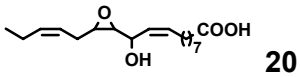 **20**	+
9,10,11-Trihydroxy-12,15-octadecadienoic acid (**72**)	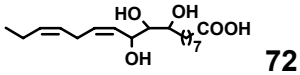 **72**	-
9,12,13-Trihydroxy-10,15-octadecadienoic acid (**73**)	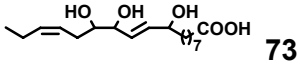 **73**	-

3.2.2.4 Oxylipin quantification

In order to assess the influences of abiotic and biotic stress factors on signaling processes of plants, the kinetics and distribution of the various signaling compounds involved in the induction of plant defense reactions is needed. Quantitative information about the temporal pattern and spatial distribution of signals provides insights in signaling networks and the interdependency of signal pathways. Furthermore, accumulation of oxylipins after various stresses provides evidence for the involvement of newly identified oxylipins in plant defense reactions.

Calibration curves

For quantification of oxylipins internal standards with identical chemical properties are fundamental. Quantification and thus evaluation of recovery and linearity of the method was only possible for compounds for which an internal standard was available. Additionally, the background of the typical m/z 197 fragment of PFB-oximes in NCI-MS is too high to be used as quantification ion. Instead, characteristic fragment ions of the PFB-oximes of each compound were chosen:

- m/z 399 for JA **51** and m/z 403 for [$^2H_2$]-JA **52** (both [M - HF]$^{\bullet-}$),
- m/z 481 for OPDA **53** and m/z 483 for [$^2H_2$]-*iso*-OPDA **54** (both [M - HF]$^{\bullet-}$),
- m/z 357 [M – HF - NO]$^{\bullet-}$ for 11-oxo-9-undecenoic acid **65**, m/z 359 [M - HF - NO]$^{\bullet-}$ for [9,10-$^2H_2$]-11-oxo-9-undecenoic acid **66** and
- m/z = 252 [M - 181]$^{\bullet-}$ for 13-oxo-9,12-tridecadienoic acid **63**

For creating calibration curves compounds were added to leaf material and the workup procedure was followed. The area ratio of the analyte to the corresponding standard (std) was plotted against the amount of added compound (Figure 24). Using Origin 7, the slope and the intercept of the plotted curve were calculated. The linear relationship between the added analyte and the resulting peak area ratio of analyte to standard was calculated by regression analysis.

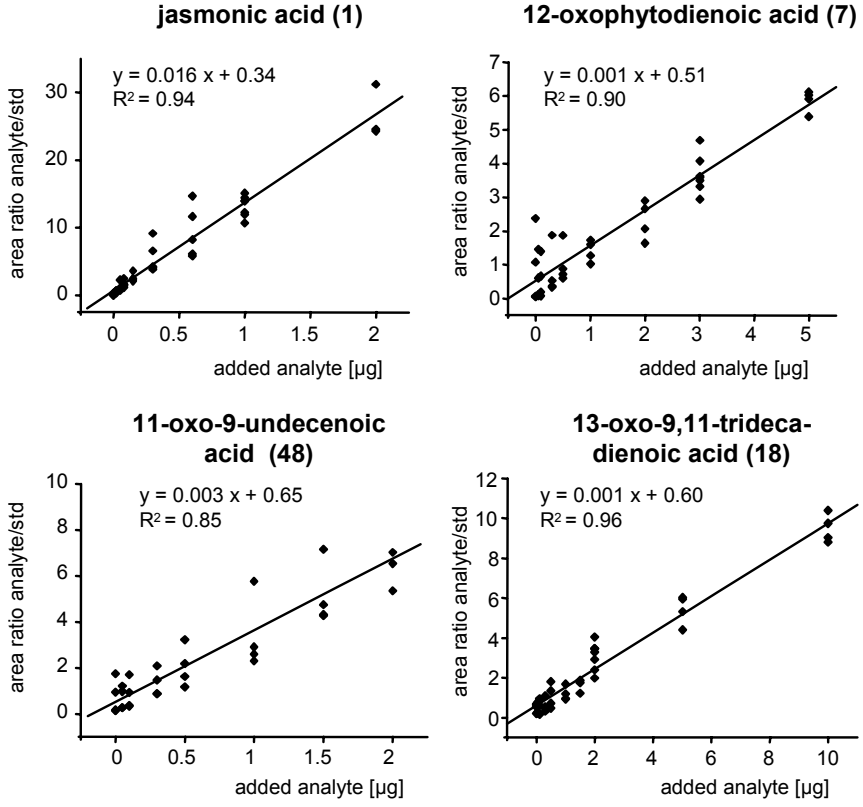

Figure 24 Calibration curves for JA (**1**), OPDA (**7**), 11-oxo-9-undecenoic acid (**48**), and 13-oxo-9,11-tridecadienoic acid (**18**); n = 4.

Resting levels of analytes in the Lima bean leaves were calculated from the intercept of the regression curve with the x-axis (see Chapter 9.8). In parallel, resting levels were verified for each compound during experiments (Table 4).

The analytical method is not restricted to *P. lunatus*, but also applicable to other plant species. Hence, additionally resting levels of *A. thaliana* and *Medicago truncatula* which were taken form control plants from independent experiments are displayed in Table 4. Compared to literature data, the resting levels found for *P. lunatus* are in line with values previously described [186]. Resting levels of JA (**1**) in *A. thaliana* are markedly high compared to literature, whereas levels of OPDA (**7**) were quite low [55,64,74]. This can be explained from different growth conditions, as the values listed in Table 4 are taken from

hydroponically grown plants (see Chapter 5.1). Also the values for JA (**1**) levels of *M. truncatula* are in line with previously published data [245].

Table 4 Resting levels of oxylipins in various plants. Values are given in ng / g frw (±SEM); n = 4.

	JA (1)	**OPDA (7)**	**11-Oxo-9-undec-enoic acid (48)**	**13-Oxo-9,11-trideca-dienoic acid (18)**
P. lunatus	43 (±34)	987 (±127)	393 (±85)	836 (±197)
A. thaliana	100 (±18)	349 (±64)	not determined	not determined
M. truncatula	52 (±12)	75 (±19)	85 (±5)	2979 (±780)

Recovery rate

For the compounds analyzed, the newly developed extraction and derivatization protocol showed a high recovery rate and linearity. As depicted in Figure 25, recovery was linear in the range from 0.02 to 2 µg added analyte for JA (**1**) and 11-oxo-9-undecenoic acid (**48**), 0.05 to 5 µg added analyte for OPDA (**7**), and 0.05 to 10 µg added analyte for 13-oxo-9,11-tridecadienoic acid (**18**). Slopes of the linear regressions demonstrate a recovery, between 85 % for JA (**1**) and 11-oxo-9-undecenoic acid (**48**), 90 % for OPDA (**7**) and 130 % for 13-oxo-9,11-tridecadienoic acid (**18**). The regression coefficient (R^2) illustrates the accuracy and reproducibility of the measurements. The relative lower performance of the recovery rate of **18** may originate from the slightly different chemical properties of the standard ([$^2H_2$]-11-oxo-9-undecenoic acid) and the analyte, which becomes also obvious by their differences in the MS-fragmentation generating different base peaks.

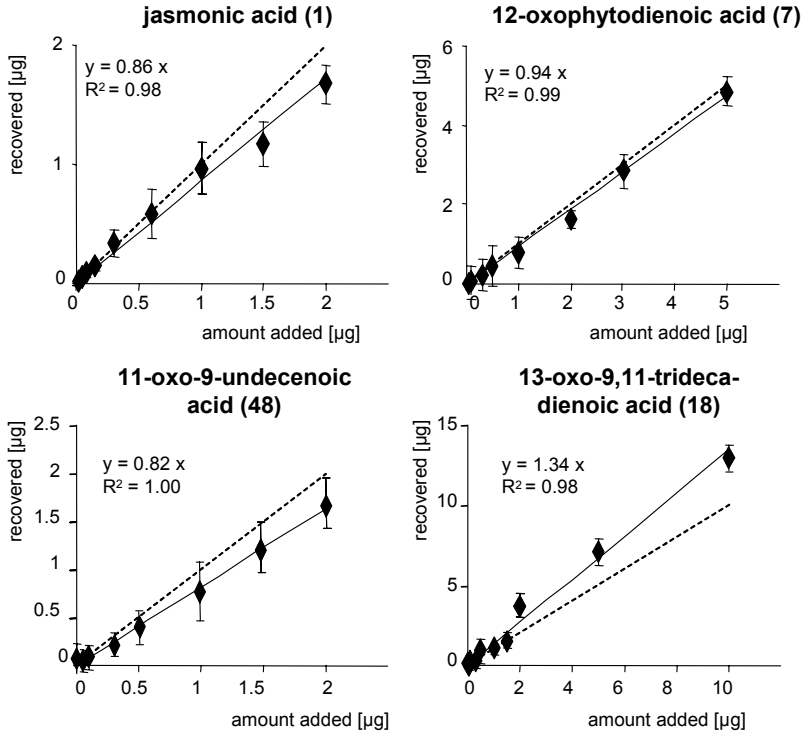

Figure 25 Recovery rates of the oxylipins quantified. The dashed line represents the bisecting line. Error bars indicate SEM; n = 4.

Detection limits

The detection limit of pure derivatized compounds was 1 pg per injected µl for the PFB-oxime of JA methyl ester (**51**), OPDA methyl ester (**53**) and methyl 11-oxo-9-undecenoate (**65**) and 20 pg for the PFB-oxime of methyl 13-oxo-9,12-tridecadienoate (**63**) at a signal to noise ratio of 10. Naturally, the detection limit of the analytes from plant tissue is higher because of the background of the plant matrix. Still, all compounds could be well detected at their resting level from 0.5 g Lima bean leaf material (Table 5).

Table 5 Detection of oxylipins from 0.5 g Lima bean leaf at the given peak noise ratios.

Oxylipin (PFB-oxime)	Resting level [ng/g frw]	Amount injected [ng μl^{-1}] per 0.5 g frw extracted	Peak to noise ratio
JA (**51**)	43	≈ 0.7	≈ 7
OPDA (**53**)	987	≈ 16	< 25
11-Oxo-9-undec-enoic acid (**65**)	393	≈ 7	< 25
13-Oxo-9,11-trideca-dienoic acid (**63**)	836	≈ 14	< 50

Estimating the abundance of higher oxidized oxylipins

For estimation of the abundance of higher oxidized oxylipins present in the CH_2Cl_2 fraction, the mixture of 9-hydroxy-10-oxooctadecanoic acid (**76**) and 10-hydroxy-9-oxooctadecanoic acid (**77**) was used as an internal standard. The abundance of higher oxidized oxylipins such as ketols and hydroxylated fatty acid aldehydes was estimated by calculating the area ratio of the compound and the added internal standard. However, the molecules behave differently during ionization, as can be seen by the varying base peaks of structurally similar compounds (Figure 14). Therefore, the peak-area-ratio does not necessarily directly represent a value to calculate the amount of oxylipin analyzed. Moreover, the CI-ionization efficiency depends on the instrument conditions, making comparison between different experiments difficult. Thus, a factor was calculated based on the intensities of the fragment ion used for quantification. This correction factor was applied to the peak area and took values between 1 and 0.5, depending on whether the 100 % base peak or a less intense ion was used for quantification. In addition, the standards (**76** and **77**) partitioned between the hexane phase and the CH_2Cl_2 phase in a ratio of 1:3, which introduced another unstable parameter. A similar distribution between both organic phases could only be observed for some free fatty acids, but not for the other oxylipins of interest.

3.3 Conclusions

A method for the exhaustive extraction of the chemically highly diverse group of oxylipins from plant material was developed. The main focus lay on JA (**1**), OPDA (**7**), and higher oxidized unsaturated fatty acids carrying reactive oxo-groups. Owing to the presence of PFBHA in the extraction medium, oxo-derivatives are immediately converted into corresponding stable PFB-oximes, which are suitable for NCI-GC-MS analysis. This allows the detection of trace amounts without the need of tedious and time consuming HPLC pre-purification of the plant extract [211,232]. The detection of PFB-oximes with NCI-MS enhances the sensitivity similar to PFB-esters used earlier for the quantification of JA (**1**) and OPDA (**7**) [63,210]. PFB-oxime formation has previously been applied for the analysis of short chain aldehydes and oxo-compounds from biological matrices [228,229,231,246], but has not yet been used to assess the role of highly oxidized fatty acid derivatives in plant defense. NCI-mass spectrometry of perfluorinated compounds achieves a 100-fold higher sensitivity over EI-ionization, due to mild ionization and low background. Furthermore, NCI-mass spectrometry provides sensitivity along with spectral information, ensuring structural assignment of known metabolites in contrast to e.g. HPLC-UV-analysis or single ion monitoring-MS methods. Moreover, the combined EI-MS and NCI-MS analysis offers enough information to propose structures of previously undiscribed oxylipins from plant material. For example, I was able to identify 9-hydroxy-12-oxo-10-dodecenoic acid (**49**), 9,12-dioxo-10-dodecenoic acid (**50**), and various unsaturated fatty acid aldehydes (**18**, **29** and **48**) for the first time in stressed and unstressed Lima bean leaves. Moreover, the stabilization of *cis*-JA (*cis*-**1**) gives the unique possibility to analyze the time course of *de novo* biosynthesis and following epimerization of JA (**1**) upon various stresses.

The formation of (*E*)- and (*Z*)-isomers of the PFB-oximes is certainly a disadvantage of this method, because most of these isomers are separated on the GLC column. This leads to a doubling of peaks per molecule and results in a higher complexity of the chromatogram. Together with (*E*)-and (*Z*)-isomers of double bonds, this can lead to many peaks for one compound. On the other hand the characteristic double peaks of PFB-oximes are an additional indication for the identification of novel compounds.

For quantitative measurements the recovery, reproducibility, and linearity was verified by addition of oxylipins to plant material and proved to be high for all compounds tested (Figure 25); however, it is crucial to reference the analyte to a chemically identical internal standard. Since this was not possible for all oxylipins observed, quantification is only demonstrated for JA (**1**), OPDA (**7**), 11-oxo-9-undecenoic acid (**48**), and 13-oxo-9,11-tridecadienoic acid (**18**). Quantification of other oxylipins is principally possible if internal standards are available, e.g. by synthesizing them from isotopically labeled linolenic acid (**4**).

The sensitivity of the method is in the range of previously described extraction methods [64]. PFB-esters [210] exhibit similar high sensitivity in NCI-MS measurements like PFB-oximes, but lack the stabilizing properties of PFB-oximes that are crucial for the reliable quantification of labile and reactive oxylipins.

Due to the high sensitivity downscaling of sample size as described by Müller *et al.* (2002) [64] is possible and thus provides a tool to investigate e.g. the spatial distribution of oxylipin patterns throughout a single plant leaf (see Chapter 4.2.2).

In summary, this versatile method is ideally suited to address the actual oxylipin status of organisms, since it allows the characterization of yet unidentified oxylipins and at the same time monitoring of known plant hormones, and assessment of their kinetics and spatial distribution. Using *P. lunatus* and *A. thaliana* as model plants, this new method was employed to analyze the fingerprint of the actually released fatty acids along with their oxygenated metabolites and greatly facilitated the structural identification of a number of unstable and/or complexly modified oxylipins previously not found in stressed leaves. Applications of the method to gain insights in various aspects of plant defense mechanisms will be presented in the following chapters.

4 THE ROLE OF OXYLIPINS IN PLANT-INSECT INTERACTIONS

4.1 Introduction: Signals shared by plants and insects

The involvement of higher trophic levels in plant-herbivore interactions requires an evolutionary optimized communication pathway between both kingdoms [8] (see General introduction, Figure 1). The recognition of attacking herbivores is a prerequisite for the success of inducible defense mechanisms. Since the plant is not immediately protected after the onset of this defense system, early recognition of the threat is essential [247,248]. On the other hand, defensive reactions may consume the plant's energy resources, and thus result in costs that have to be compensated by the benefits of the defense reaction [8,249].

The insect's oral secretions (salivary secretion and regurgitant) are one of the first cues which come in contact with the damaged plant cells. It has been demonstrated that various substances from the insect's oral secretion induce plant defense reactions. These elicitors can be either proteins or small molecules. For instance, a β-glucosidase from *Pieris brassicae* regurgitant has been shown to elicit volatile emission of cabbage (*Brassica sp.*) attracting the parasitic wasp *Cotesia glomerata* [250]. Whereas a polygalacturonase from the salivary secretion of lygus bugs (Miridae) seems to be responsible for causing extensive tissue damage in alfalfa (*Medicago sativa*) [251]. Highly noted is the tritrophic interaction between maize plants (*Zea mays*), beet armyworm larvae (*Spodoptera exigua*) and their parasitoids *Cotesia marginiventris* and *Microplitis croceipes* [10]. Here, the interaction is mediated via the semiochemical volicitin (*N*-(17-hydroxylinolenoyl)-L-glutamine) [252,253]. Since the first report of this signal molecule, various related *N*-acylglutamines of similar structure have been reported to be produced by lepidopteran larvae [254,255]. Whether these fatty acid amino acid conjugates are synthesized by the caterpillar itself or by commensal gut bacteria is still under discussion [255-258], although recently an enzyme capable of formation of *N*-acylglutamine conjugates from a gut bacterium was isolated and characterized [259,260].

However, herbivores are not committed to the plant's defense system and have evolved strategies to overcome the plant's defensive arsenal. Mechanisms for detoxification of plant secondary compounds such as cyanogenic glucosides [261], glucosinolates [262-264], or alkaloids like nicotine [265] have been intensively studied. Here again, evidence is emerging that the insect's oral secretions are important mediators in detoxifying the plant's defense metabolites. Thus, it has been found that high amounts of glycine are secreted into the gut lumen of specialized lepidopteran larvae [266]. This free amino acid seems to protect the larvae against the denaturing activity of phenolics that can occur in high amounts in plant

leaves [267]. Phenolic compounds are chemically highly active, and are prone to condense with themselves, generating condensed polyphenolics, additionally, they can react with amino acid residues of proteins, causing denaturation of digestive enzymes [4]. High amounts of free amino acids such as lysine or glycine may prevent protein denaturation by covalently binding to the phenolic compounds [268-270]. Moreover, the insect's oral secretion serves not only to detoxify plant defense compounds, but also to suppress plant defense reactions. It has lately been shown, that the enzyme glucose oxidase (GOX), is able to suppress defense reactions in solanaceous plants, i.e. the production of nicotine in tobacco (*Nicotiana tobaccum*) [271-273]. The secretion of GOX seems to correlate with the activated defense status of the attacked plant and thus is produced on demand [274].

In many cases, P450-dependent enzymes and other metabolizing enzymes are involved in the detoxification of plant secondary compounds [275,276]. In fact, specialist herbivores have not only developed the ability to overcome plant toxins but are also able to accumulate these in order to use them for their own defense against generalist predators. This type of specialization has been vividly described in the case of pyrrolizidine alkaloids which are utilized by various lepidopterans, making them unattractive for their predators [277-279]. Similar adaptations have been reported for the tobacco hornworm (*Manduca sexta*) to the allelochemical[8] nicotine [265,280,281] and the Blister beetles (Meloidae) to palasonine [282]. As a result, this co-evolution of defense and adaptation has led to an arms race bringing forth new strategies of defense and counter defense [283].

To develop an effective strategy for counter defense, feeding insects have to recognize defensive plant compounds to activate their detoxification system. In analogy to the plant's induced defense, the insect is best protected, when using early cues to recognize the upregulation of plant toxins. Li *et al.* (2002) have found that typical plant hormones such as SA (**2**) and JA (**1**) can be sensed by the insect and trigger upregulation of P450-enzymes [284]. This ability of insects to recognize the levels of phytohormones allows them to accommodate their metabolism early against forthcoming plant toxins.

The complex interactions between plants and their invertebrate herbivores suggest an effective recognition system between kingdoms. When comprehensively comparing signaling molecules and receptors shared by plants and animals, it becomes obvious that different organisms often utilize common signals, which enable them to recognize each others status. For example plants produce glutamate, a signaling compound widely present in animals. In fact, recent analyses have located a putative glutamate receptor in the genome of *A. thaliana*, suggesting that plants use glutamate as a signaling compound as well [285,286].

[8] Allelochemicals are toxic or deterrent compounds produced by one species in order to affect a receiving susceptible species.

Conversely, plant auxins are also found in phloem-feeding insects such as aphids, which introduce these molecules into the plant upon feeding, manipulating the plant's metabolism to release nutrients [287]. Moreover, gall-forming insects secret cytokines or related compounds to induce initiation of galls [288,289]. This list of examples can be extended to a whole set of shared signaling molecules and receptors [290,291].

Fatty acid derived metabolites are perfect candidates for mediating trophic interactions, as they are ubiquitous in cell membranes, and thus mediate the contact of a cell to its environment. From the point of evolution it might be speculated that free-radical non-enzymatic lipid peroxidation stands at the beginning of the utilization of fatty acid oxidation products as signaling compounds. As enhanced production of ROS is typical for cell damage, rising levels of oxylipins can easily be used for recognition and reaction upon various stresses. In fact Müller and co-workers isolated prostaglandin like non-enzymatically formed phytoprostanes from plant material, which have been discussed as evolutionary old signals [292]. Indeed, prostaglandins, which are synthesized in the insects' midgut [293] can be recognized by the plant, probably by utilizing the phytoprostane signaling cascade and can induce plant defense [294]. Additionally, plants are able to perceive other fatty acid signals such as free linolenic acid (**4**) [67] and arachidonic acid [295]. The evolvement of enzymes which channel early hydroperoxides into defined oxylipins, leads to the diverse picture of signaling cascades we can observe in plants (see Chapter 1.1.2).

Many of the above discussed examples infer that oxylipins are ideal candidates to act as cross-kingdom signals during plant-insect interactions while various defense strategies between plants and herbivores take place at the actual feeding site of the insect.

4.2 Results and discussion

4.2.1 Plant responses to mechanical wounding and caterpillar feeding

During plant-insect interactions fatty acid derived compounds can either serve as signals acting in concert with the classical phytohormones JA (**1**) and OPDA (**7**) [146] or may represent toxins themselves, as has been demonstrated for example for α,β,γ,δ-unsaturated aldehydes [150,151] or hydroxylated aldehydes [220]. In order to separate general signals from herbivore specific cues in the Lima bean, simple mechanical wounding was compared to feeding damage of the Mediterranean climbing cutworm (*Spodoptera littoralis*). Lima bean plants were mechanically wounded with a pattern wheel and leaf material harvested in time intervals until 10 h after wounding, which allows monitoring the formation and decline of oxylipins after a single stress event. In contrast, the feeding of an insect represents a

combination of continuous mechanical damage with the introduction of specific elicitors into the leaf material; both parameters seem to be equally important factors [296].

After mechanical wounding, the total amount of JA (**1**) increased more than 20-fold with a maximum after 120 min. Additionally, due to the *de novo* biosynthesis of **1** the ratio of *trans*-**1** to *cis*-**1** is shifted in favor of the *cis*-**1** isomer (Figure 26). While at resting level, the *trans*-**1** isomer dominated with about 80 %, which is slightly less than the thermodynamic equilibrium of JA (**1**), 40 min after wounding the *cis*-**1** level rose to 80 % of total JA (**1**) content. This high level of *cis*-JA (*cis*-**1**) slowly declined, while the overall JA (**1**) content also decreased (Figure 27). This result is in line with the observation of elevated levels of *cis*-**1** in plant cell cultures elicited with yeast elicitor, as has been previously reported by Müller *et al.* (1994) [210] stabilizing *cis*-JA (*cis*-**1**) as its dithioketal. Four hours after wounding the amount of total JA (**1**) was back to the resting level, while the *cis*-JA (*cis*-**1**) amount was still high and required up to ten hours until the reaching the initial *cis/trans*-ratio. This indicates the upregulation of JA-deactivation mechanisms, while the *de novo* biosynthesis of JA (**1**) was still high (Figure 26).

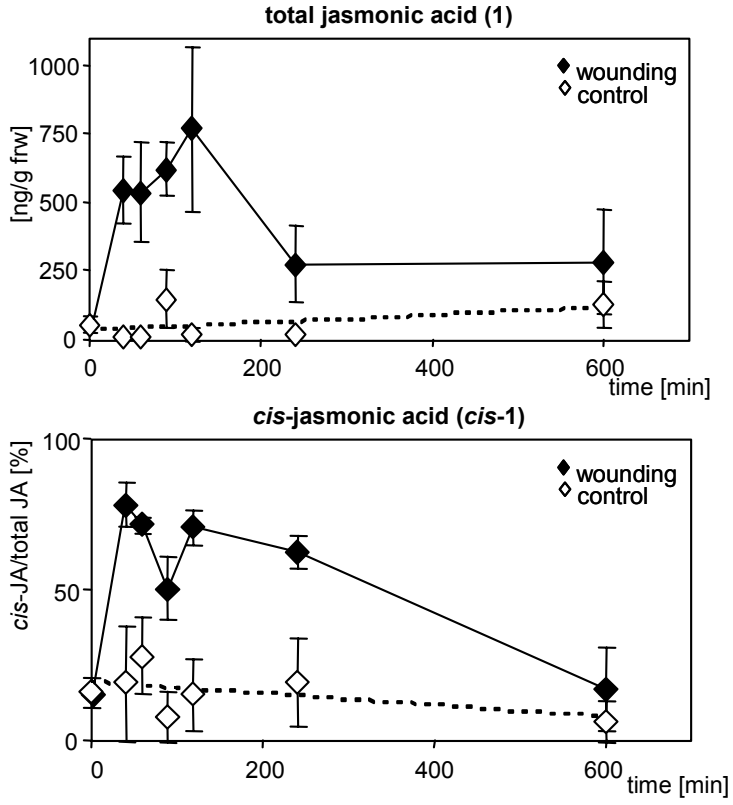

Figure 26 Time course of JA (**1**) formation in *P. lunatus* leaves after a single wounding event. Maximum concentration of total-JA (**1**) was reached after 120 min. The relative amount of *cis*-**1** increased shortly after wounding due to *de novo* synthesis of **1**. *cis*-**1** declined, as the overall amount of **1** decreased. Error bars indicate the 95 % confidence interval; n = 4. For clarity the values are plotted with trend lines (moving average for JA and linear regression for controls).

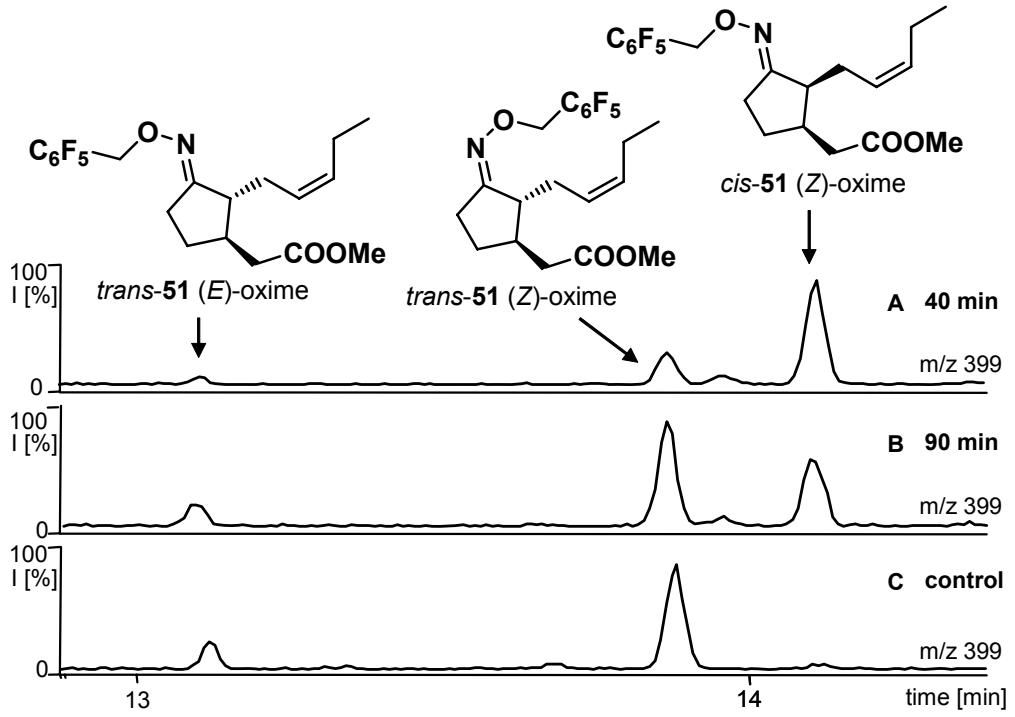

Figure 27 GL-chromatogram of the PFB-oximes of JA methyl ester (**51**) from Lima bean leaves after a single wounding event. The dynamic formation of *cis*-**51** is depicted by selected ion-chromatograms of m/z = 399 (for the $[M - 20]^{\bullet -}$) at 40 min (A) and 90 min (B) after mechanical wounding in comparison to a control leaf (C).

To evaluate the possible involvement of oxylipins in plant defense reactions, the oxylipin profile after caterpillar feeding was compared to simple mechanical wounding (Figure 28).

After wounding, the oxylipin formation followed a similar time course as shown for JA (**1**) in Figure 26. Data points for mechanical wounding presented in Figure 28 were taken from the maximum of induction between 90 and 120 min after wounding of the Lima bean leaf. In order to collect enough caterpillar damaged leaf material, plants which were treated with *S. littoralis* larvae were harvested after 24 h and plant material adjacent to the caterpillar's feeding site was collected.

Both wounding and caterpillar damage enhanced the level of JA (**1**), demonstrating the involvement of **1** in both stress situations. In contrast, OPDA-levels were not elevated after mechanical wounding, whereas there was a near four fold increase of **7** after feeding of *S. littoralis* larvae. Also 11-oxo-9-undecenoic acid (**48**) and 13-oxo-9,11-tridecadienoic acid (**18**) accumulated after caterpillar feeding, but not after wounding. The α-ketol (**9**) and γ-ketol (**10**) behaved differently in the both stress situations; while levels of **9** did not rise, although a slight trend towards higher amount in the stressed leaves is visible, the level of **10** was elevated in both cases. The formation of 9-hydroxy-12-oxo-10-dodecenoic acid (**49**) again was induced by both caterpillar feeding and wounding, while levels of 13-KOTE (**21**) and

12,13-epoxy-11-HODE (**20**) were not elevated neither by caterpillar feeding, nor by mechanical wounding.

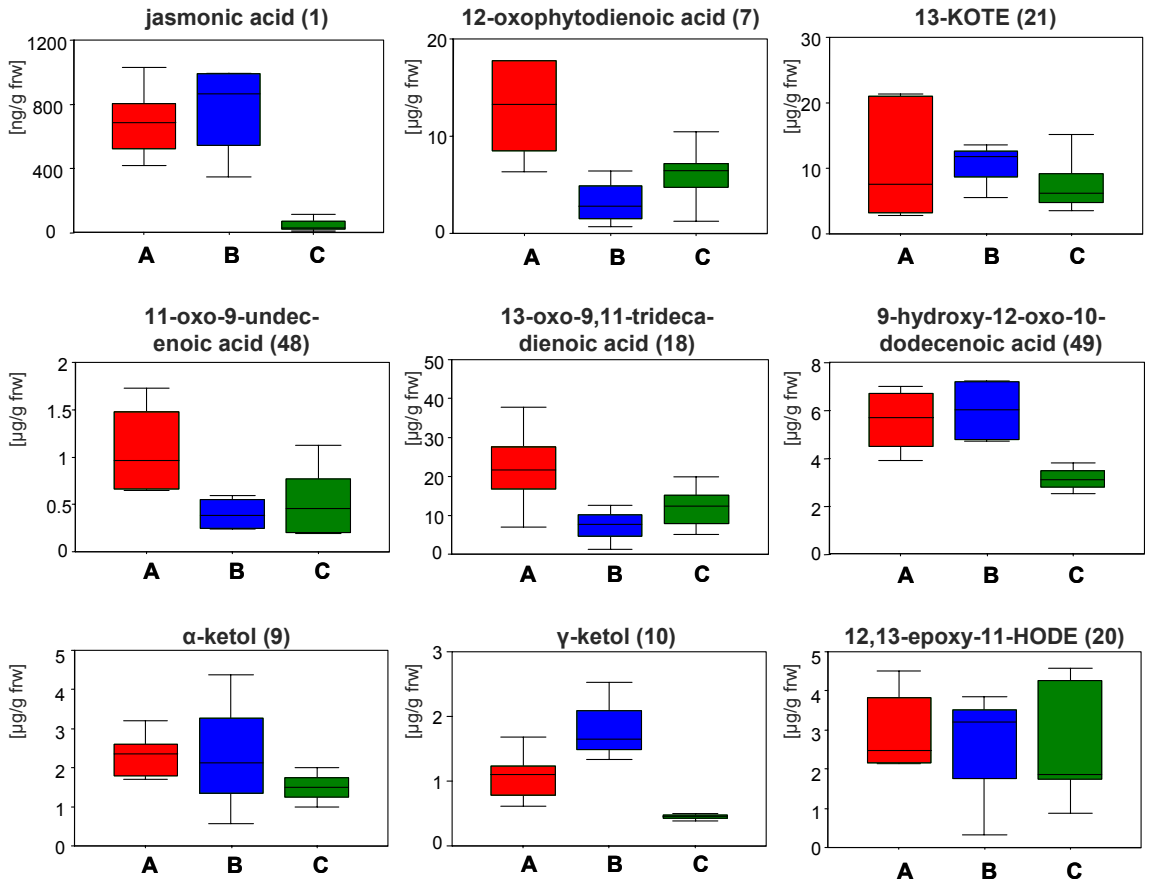

Figure 28 Amount of oxylipins after caterpillar feeding and a single wounding event. A, red: *S. littoralis* feeding (n = 6); B, blue: mechanical wounding (n = 4); C, green: control (n = 4). The depiction of the data as box-whisker-plots allows illustration of the data distribution. Boxes indicate the interquartile range of the data, intersected by the median; whiskers indicate minimum and maximum of the data.

The comparison of mechanically damaged and herbivore infested Lima bean plants infers that the plant is indeed able to distinguish between both stress situations. The differential formation of oxylipins in mechanically wounded respectively herbivore infested leaves suggests an active and controlled synthesis of putative signaling compounds in response to varying threads.

4.2.2 Spatial distribution of oxylipins in caterpillar damaged leaves

To evaluate translocation of the oxylipin signals in the plant during caterpillar feeding, the spatial distribution of oxylipin levels throughout a Lima bean plantlet was analyzed. After 24 h insect feeding on the primary leaves, samples were taken in different distances from the feeding site, from neighboring leaves, and from the upper, secondary leaves (Figure 29).

Figure 29 Samples of damaged leaf material were taken after 24 h of *S. littoralis* feeding. Red: 0 - 10 mm from feeding area; dark orange: 10 - 20 mm from feeding area; light orange: neighboring leaf; yellow: secondary systemic leaves.

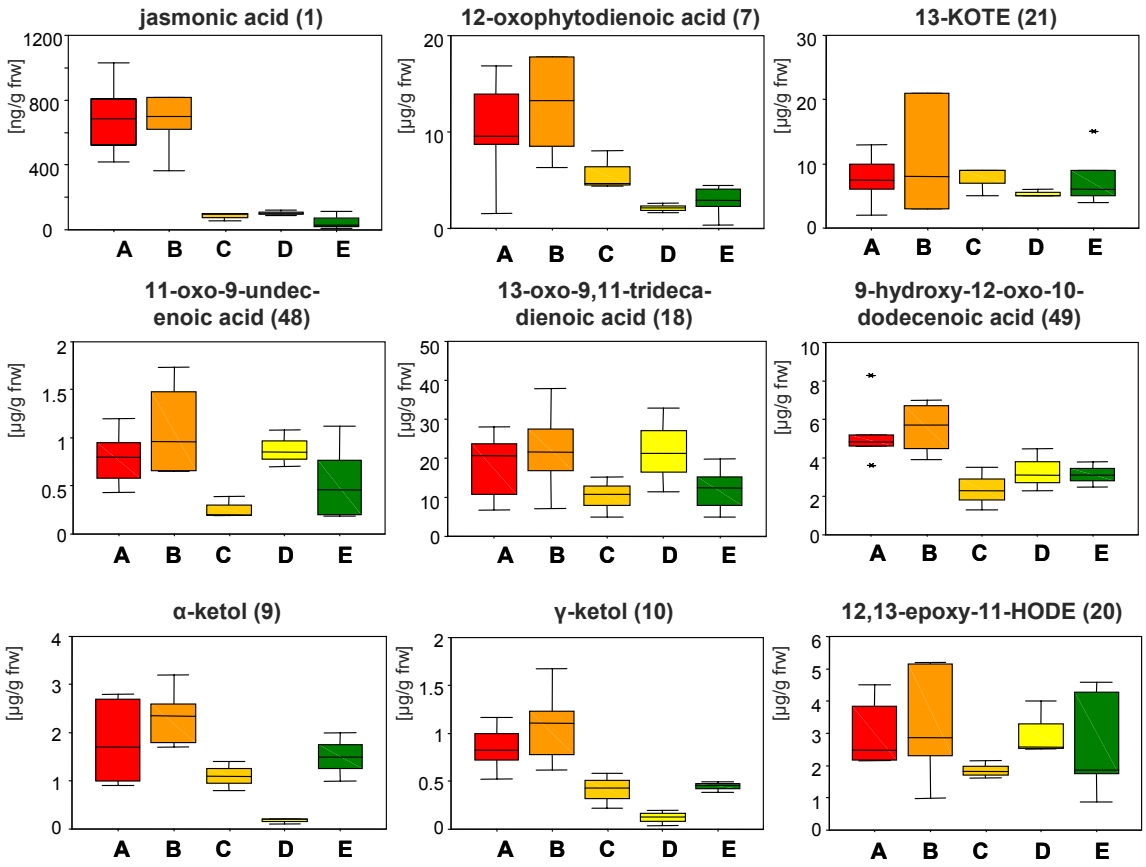

Figure 30 Spatial distribution of oxylipins after 24 h feeding of *S. littoralis* larvae. A, red: 0 - 10 mm from feeding area (n = 6); B, dark orange: 10 - 20 mm from feeding area (n = 6); C, light orange: neighboring primary leaf (n = 3); D, yellow: systemic secondary leaf (n = 3); E, green: control, primary leaves of undamaged plantlet (n = 4). The depiction of the data as box-whisker-plots allows illustration of the data distribution. Boxes indicate the interquartile range of the data, intersected by the median; whiskers indicate minimum and maximum of the data; * indicates outliers.

During the feeding process of a caterpillar a clear spatial gradient of oxylipin induction was detectable (Figure 30). Oxylipin levels were highest directly at the feeding site, but also in areas up to 20 mm inside the leaf elevated amounts of phytohormones and oxylipins were observed. Especially JA (**1**) was induced locally; levels increased 20-fold from 40 ng / g frw to an average of 800 ng / g frw, with a maximum level at the feeding site and no induction of JA (**1**) in the neighboring and systemic leaves. The local response in *P. lunatus*, is consistent with other reports and the general view, that the JA-signal is not translocated in the plant [185,297]. However, the JA-signal was at least transported to the neighboring areas 10 - 20 mm adjacent of the actual feeding site of the insect. Conversely OPDA (**7**) increased 5-fold compared to the resting level and a definite increase was also observed in the

neighboring leaf (C, light orange), but not in the upper systemic leaves (D, yellow) which suggests that to some extent the induction of OPDA-synthesis, or transport to the neighboring leaf occurred.

While the amount of 11-oxo-9-undecenoic acid (**48**) was induced compared to the control, the changes in levels of 13-oxo-9,11-tridecadienoic acid (**18**) were less pronounced and because variance was high, only a slight trend to increased values can be assumed between leaf material adjacent to the feeding area (B, dark orange) compared to the control (E, green). The formation of 9-hydroxy-12-oxo-10-dodecenoic acid (**49**) instead was strongly induced at the biting zone of the lepidopteran larvae. This indicates that unsaturated conjugated aldehydes might play a role during plant herbivore interactions, in particular as they have been described as bioactive compounds [150,151] and act against pathogens and aphids [127,129]. Interestingly, for **48** and **18** a trend towards higher levels in systemic leaves, compared to the control was obvious. Whether this phenomenon can be interpreted as a systemic signal, or whether the amounts of **18** and **48** are generally higher in secondary leaves, can not be deduced from this experiment, since only primary leaves were collected as controls. Supporting this hypothesis Vancanneyt *et al.* (2001) found hydroperoxide lyase gene expression being higher in younger than in older leaves of potato plants [129].

Additionally, the ketols **9** and **10** accumulated locally after feeding of insects. While α-ketol (**9**) only showed slightly elevated levels in the caterpillar damaged leaf material, γ-ketol (**10**) levels were conspicuously high. Furthermore, the very low amounts of ketols in the systemic secondary leaves are striking; here the amount of **9** and **10** even dropped below the levels of undamaged primary leaves. This indicates that these compounds may play an additional role in plant physiology. Indeed, ketols seem to be involved in plant development, as they were shown to activate flower formation [69]; however, a function related to leaf developmental stages has not been reported.

Other oxylipins, such as 13-KOTE (**21**) and 12,13-epoxy-11-HODE (**20**), were not induced significantly by herbivore feeding.

4.2.3 Oxylipins in the insect's gut

Various defense and counter defense strategies take place both at the actual feeding site of the insect and in the insect's gut. Hence, the occurrence of oxylipins in the insect's gut was elucidated. Here oxylipins may either act as toxic or deterrent compounds themselves, or serve the caterpillar as signaling molecules to avoid toxic plant-allelochemicals as has been described for JA (**1**) and SA (**2**) [284]. The presence or absence of oxylipins may give insight into the metabolism of bioactive compounds by the caterpillar. The massive increase of phytohormones such as JA (**1**) directly at the biting zone of the feeding insect suggests that the insect is likely to directly encounter these chemicals during the feeding process.

Together with the rapidly ingested leaf material, the caterpillar takes up phytohormones and oxylipins.

To evaluate the occurrence of oxylipins in the caterpillar's gut, *S. littoralis* larvae were fed with Lima bean leaves and digested leaf material was obtained by collecting the caterpillar's regurgitant. Many caterpillars release droplets of regurgitated foregut content as a defense reaction [298]. By touching the larvae with soft tweezers this reaction can be provoked and the regurgitant can be easily collected in glass capillaries.

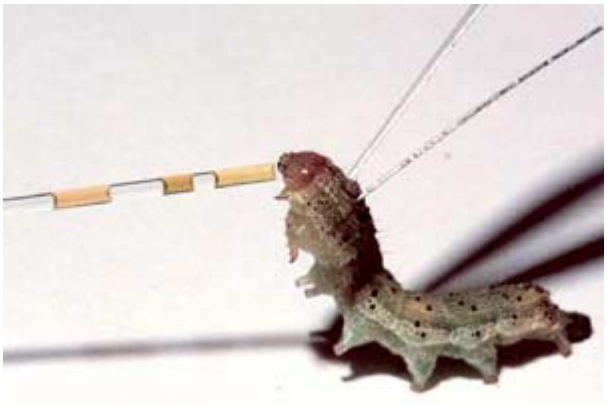

Figure 31 Collection of caterpillar regurgitant (*Spodoptera frugiperda*) with a glass capillary.[9]

When placing the caterpillars, which were usually reared on light yellow artificial diet on the green Lima bean leaves, the process of food ingestion can be observed, as the green plant material in the gut can be seen through the caterpillar's skin. Thus it can be estimated, that the leaf material in the fore gut of the insect larva was taken up within the last few hours.

Analysis of the plant material digested by *S. littoralis* larvae revealed that the oxylipin signature differed from that of the attacked plant (Table 6). First of all, the abundance of free fatty acids was pronounced in the regurgitant and the frass compared to the leaf material. The occurrence of JA (**1**) in regurgitant and frass was ambiguous. While during one experiment fairly high amounts of JA (**1**) could be detected, this result could not be reproduced. This variation could result from a rapid metabolism of JA (**1**) in the digestive tract of the caterpillar. In case of OPDA (**7**) I was indeed able to observe such a metabolic activity by the insect. In ingested leaf material OPDA (**7**) was found to be converted into tetrahydrodicranenone B (*iso*-OPDA; **78**) (Figure 32). This rearrangement seems to be quantitative, as no traces of **7** were detectable.

[9] Photograph by Dr. Sabine Thiessen.

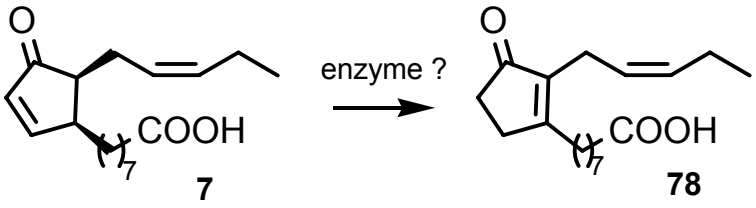

Figure 32 Isomerization of OPDA (**7**) to *iso*-OPDA (**78**) in the caterpillar's gut.

The isomerization of **7** to **78** was suggested by a shift of the m/z 481 $[M - 20]^{\bullet -}$ peak of the OPDA-PFB-oxime **53** to the same retention time of $[^2H_2]$-*iso*-OPDA-PFB-oxime **54** when comparing the leaf extract to the derivatized regurgitant (Figure 33).

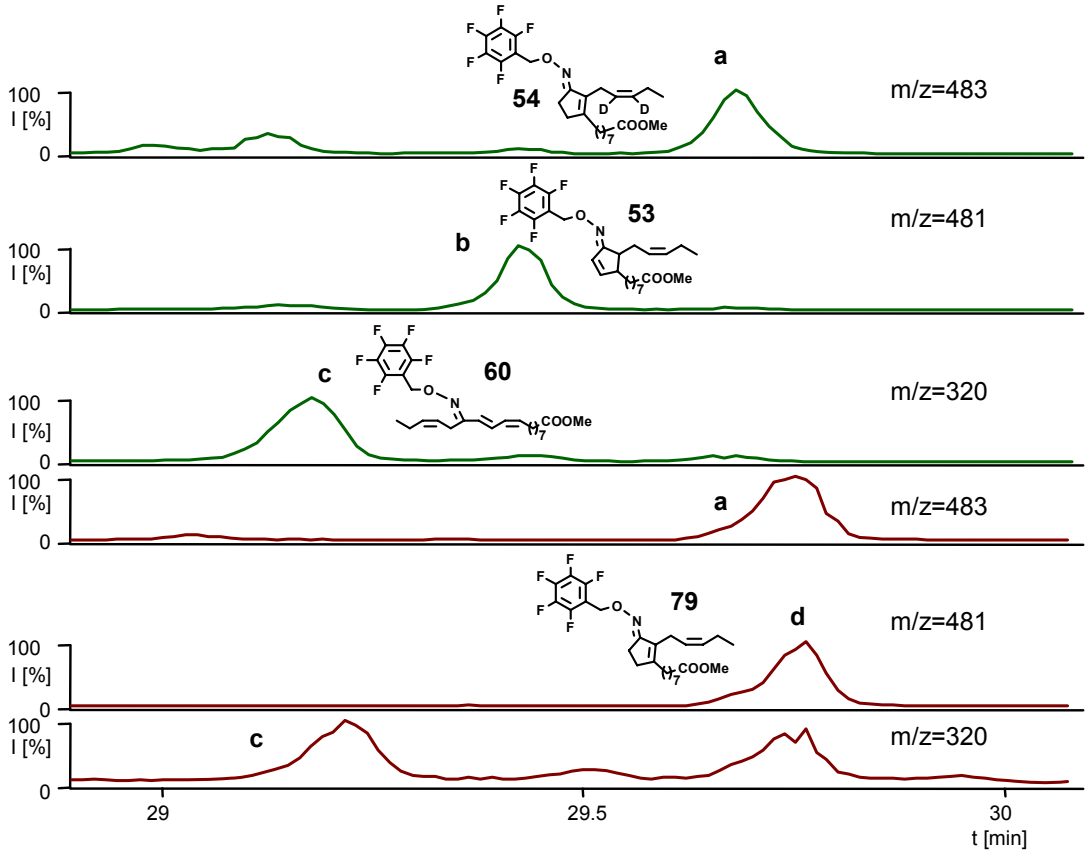

Figure 33 Shifting of the m/z 481 signal of OPDA-PFB-oxime **53** $[M - 20]^{\bullet -}$ in the caterpillar's regurgitant. Green: chromatogram from leaf material; red: chromatogram from *S. littoralis* regurgitant. a: $[^2H_2]$-*iso*-OPDA-PFB-oxime **54**; b: OPDA-PFB-oxime **53**; c: 13-KOTE-PFB-oxime **60**; d: *iso*-OPDA-PFB-oxime **79**. The conversion of OPDA (**7**) to *iso*-OPDA (**78**) can be deduced from the shift of the m/z 481 peak relative to the m/z 483 (**54**) and m/z 320 (**60**) peaks.

Additional confirmation for the identity of *iso*-OPDA (**78**) can be deduced from the mass spectrum of its PFB-oxime, which follows the fragmentation pattern of the PFB-oxime of [$^2H_2$]-*iso*-OPDA **54**, rather than that of OPDA-PFB-oxime **53** (Figure 34). Comparing the NCI-mass spectrum of **78** and **54**, most ions of **78** are shifted by two mass units, which is due to the lack of the deuterium labeling. Prominent are the ions $[M - 20]^{\bullet-}$ ($[M - HF]^{\bullet-}$), $[M - 50]^{\bullet-}$ ($[M - HF - NO]^{\bullet-}$) and the m/z 339 (m/z 341) ion ($[M - 20 - 142]^{\bullet-}$). The fragment at m/z 339 for **78** and m/z 341 for **54** are characteristic for *iso*-OPDA derivatives. Only the position of the double bond between the side chains of the pentenone ring allows a McLafferty type rearrangement resulting in the loss of methyl 6-heptanoate (M = 142) in analogy to the similar fragmentation in the positive EI-MS as already shown in Figure 16 (Chapter 3.2.2.1). However, the amounts of oxylipins in the regurgitant samples were too low to be detectable in EI-MS. Therefore, complementary data from the fragmentation pattern of the *iso*-OPDA-PFB-oxime **78** under positive EI-conditions could not be obtained so far.

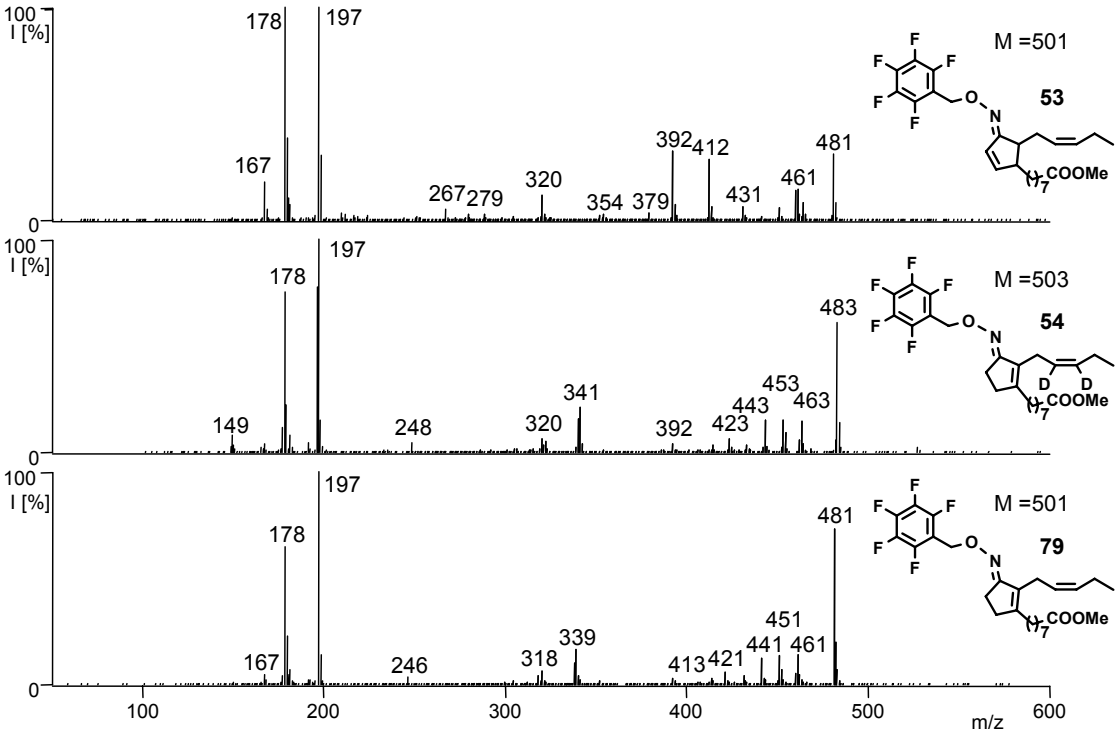

Figure 34 NCI-mass spectra of the PFB-oximes of OPDA **53**, [$^2H_2$]-*iso*-OPDA **54**, and *iso*-OPDA **79**.

To evaluate a possible non-enzymatic isomerization of **7** to the more stable *iso*-OPDA isomer (**78**) [45], OPDA (**7**) was incubated in various buffers of different pH values (pH 3, pH 5, pH 7, and pH 10) for 4 h and 10 h at RT. The formation of *iso*-OPDA (**78**) may be catalyzed by the alkaline medium (about pH 10 [299]) in the insect's foregut (Figure 35). In this experiment, no isomerization of **7** to *iso*-OPDA (**78**) occurred, although an epimerization from the *cis*-OPDA (*cis*-**7**) to *trans*-OPDA (*trans*-**7**) was detected. These results suggest the involvement of an enzyme that catalyzes the quantitative isomerization of **7** to *iso*-OPDA (**78**) in the insect's gut.

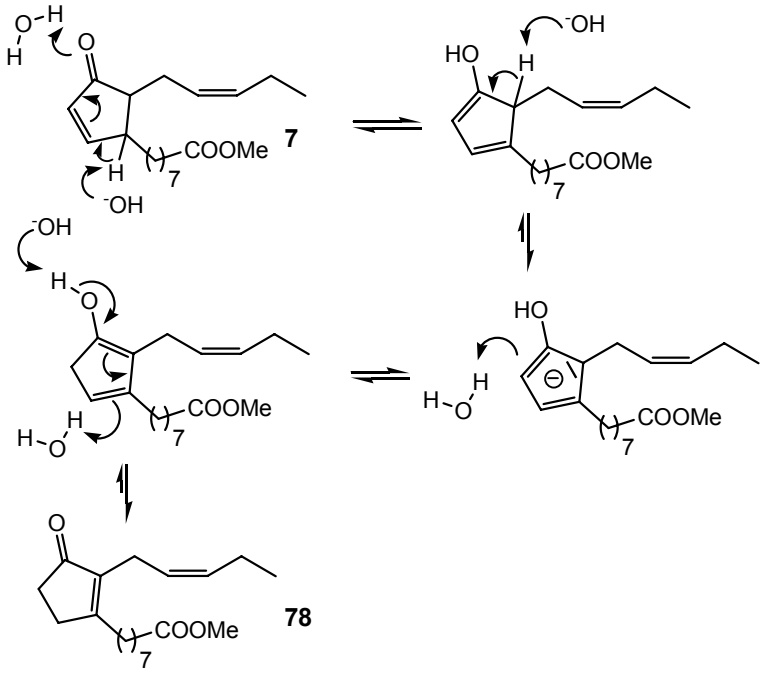

Figure 35 Proposed mechanism for the isomerization of OPDA (**7**) to *iso*-OPDA (**78**) in alkaline medium.

Also other oxo-compounds seem to be metabolized by the insect. While α-ketol (**9**) was found in leaves, regurgitant and frass, γ-ketol (**10**) was not detected in the ingested leaf material. Interesting is the high quantity of 13-KOTE (**21**) in the frass, although **21** was present in fairly low amounts in the regurgitant. One possible reason for this might be that the Michael acceptor system of **21** reacts rapidly with proteins or other biomolecules in the insect's gut, whereas in frass probably non-enzymatically formed 13-KOTE (**21**) can accumulate.

All short chain fatty acid aldehydes (**18**, **29**, **30**, **48**, **49**, **50**) were detectable in leaf material, in the insect's gut and in frass (Table 6), although in some cases superimposition with GLC-peaks of compounds from the gut matrix made identification difficult. Interestingly, 13-oxo-

9,11-tridecadienoic acid (**18**), occurred in the leaf material mainly as the (*Z*)-isomer and was isomerized in the insect's gut to larger proportions of the (*E*)-isomer. Moreover, 12,13-epoxy-11-HODE (**20**) was highly abundant in the leaf material, as well as in regurgitant and frass.

Table 6 Oxylipins in Lima bean plant leaves, regurgitant and frass of *S. littoralis* larvae after 24 h feeding on Lima bean leaves. Occurrence of oxylipins in regurgitant and frass was deduced from 4 independent analyses. In regurgitant and frass, variance was high and in most cases, compounds could only be detected by NCI-MS, the occurrence of compounds marked with "+" is reliable.

Oxylipin		*P. lunatus*	*S. littoralis*	
Name	**Structure**	**Leaf**	**Regurgitant**	**Frass**
JA (**1**)	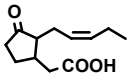 **1**	+	- (+)	- (+)
OPDA (**7**)	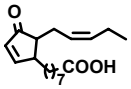 **7**	+	-	-
iso-OPDA (**78**)	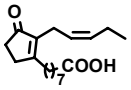 **78**	-	+	+
α-Ketol (**9**)	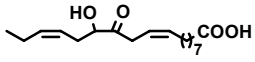 **9**	+	+	+
γ-Ketol (**10**)	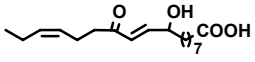 **10**	+	-	-
13-HOTE (**19**)	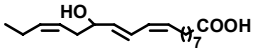 **19**	+	+	-
13-KOTE (**21**)	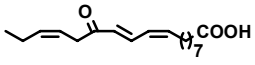 **21**	+	+	+
9-Hydroxy-12-oxo-10-dodecenoic acid (**49**)	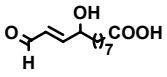 **49**	+	+	+
9,12-Dioxo-10-dodecenoic acid (**50**)	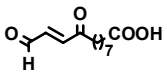 **50**	+	-	-
9-Oxononanoic acid (**30**)	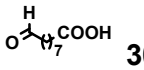 **30**	+	+	+
11-Oxo-9-undecenoic acid (**48**)	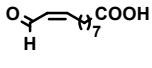 **48**	+	+	+
Traumatin (**29**)	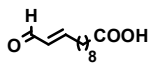 **29**	+	+	+
13-Oxo-9,11-tridecadienoic acid (**18**)	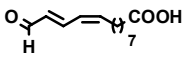 **18**	+	+	+
11-Hydroxy-12,13-epoxy-9,15-octadecadienoic acid (**20**)	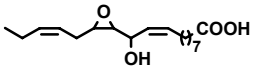 **20**	+	+	+

4.3 Conclusions

Plants are able to distinguish between a single mechanical wounding event and feeding damage. This enables the plant not only to optimize their defense strategies against herbivores, but also to save costs due to translocation of resources into defense metabolites [249]. Differences between mechanical wounding and herbivory can be deduced from the distinct upregulation of signaling pathways.

Generally, more different types of oxylipins were produced during caterpillar feeding than after a single wounding event. Most obvious was the lack of OPDA-accumulation after mechanical wounding, while JA-levels increased in both stress situations. But also the amounts of 11-oxo-9-undecenoic acid (**48**) and 13-oxo-9,11-tridecaenoic acid (**18**) were not pronounced by simple mechanical wounding. Furthermore, amounts of oxylipins were generally higher in caterpillar damaged leaves than after a single mechanical wounding event. Apart from chemical cues from the insect's salivary secretion [10] also the intensity and duration of the attack [296] seems to be important for the discrimination between harmless mechanical wounding and herbivory.

The analysis of the spatial distribution of oxylipin accumulation in the plant leaf infers that oxylipins are almost exclusively produced directly in the attacked leaf region as it is the case for the JA-signal. Although it was impossible to analyze single cell layers, the increase of oxylipins directly in the wounded cells may be some orders of magnitude higher as in the 10 mm thick leaf slices analyzed.

However, oxylipins are not necessarily only signals mediating plant responses, also the herbivore itself is likely to use these as cues. The feeding insect encounters high amounts of oxylipins at the feeding site; moreover, only recently it has been shown that enzymes from the lipoxygenase family can act also on bound fatty acids such as monolinoleoyl-glycerol [300]. Furthermore, Stelmach *et al.* (2001) [301] and Hisamatsu *et al.* (2003, 2005) [302,303] reported OPDA (**7**) and dinor-OPDA containing monogalactosyl-diacylglycerides from *A. thaliana*, whereas Ohashi *et al.* (2005) described a monogalactosyl-monoacylglyceride containing OPDA (**7**) [304]. The bound OPDA (**7**) can be released from these lipids by specific lipases. Therefore, it would not be surprising if unspecific lipases, as digestive enzymes in the insect's gut are capable to hydrolyze such lipids [305]. Consequently, insects will even encounter higher levels of free oxylipins as occur in the damaged plant leaves.

My experiments clearly show that together with the plant material high amounts of oxylipins are taken up by feeding insects and processed in their digestive system. Here, reactive oxylipins and phytohormones can act themselves as toxins [148,151,209,220] but at the same time might serve the caterpillar as cues for activating its metabolic potential to detoxify and breakdown plant secondary defense metabolites [284]. For the feeding insect it is

important to rapidly metabolize toxic compounds or to deactivate signals. Hence, additional metabolism needs to take place in the insect's gut to modify the original composition of plant-derived oxylipins. These modified oxylipins may be reintroduced into the plant leaf through the contact with the insect's oral secretions. Consequently, the plant may utilize the modified oxylipin pattern as a cue for recognizing (specific) herbivores or the herbivore might interfere with the plant's defense signaling cascade by blocking receptors with modified but inactive compounds.

In the case of the stress signal OPDA (**7**) that was observed in high levels at the insect wounded biting site I was able to directly observe the fascinating and powerful potential of the modification of plant signaling compounds in the insect's gut. In the gut OPDA (**7**) is not present, but seems to be quantitatively isomerized to *iso*-OPDA (**78**). My preliminary experiments suggest that this reaction is catalyzed by an enzymatic activity in the gut. However, further experiments are needed to investigate whether the formation of *iso*-OPDA (**78**) might be catalyzed by a pH shift from the more neutral to slightly acidic pH in the leaf material [306] to the high pH (about 10) in the insect's foregut [299] or by an enzyme.

Moreover, JA (**1**) and γ-ketol (**10**), which are upregulated in leaf material after caterpillar feeding were not found in the regurgitant suggesting their rapid uptake or conversion to so far unknown metabolites. The relative low amount of 13-KOTE (**21**) in the insect's regurgitant suggests that this Michael acceptor is quickly metabolized by the insect or reacts with biomolecules in the gut and thus might inhibit the insect's digestive enzymes [145,148,222]. Similar activity has been described for phenolic compounds, which exhibit protein denaturation activities [4,270]. These oxylipins are good candidates for mediating plant-insect recognition, as compounds which are rapidly taken up by the insects and quickly modified in their gut should be considered as potentially biologically active.

In summary, it has been confirmed that the diverse family of oxylipins plays an active role during plant-insect interactions. Besides the importance of oxylipins for plant signaling processes their role as toxins and cues for the feeding insects as well as their potential as cross-kingdom signals is obvious.

5 PLANT STRESS RESPONSE TO CHEMICAL ELICITATION

5.1 Response of *Arabidopsis thaliana* to treatment with alamethicin

5.1.1 Introduction: Alamethicin induced plant stress responses

Exogenously applied chemicals can be utilized in bioassays in order to deduce their involvement in plant defense, or to specifically trigger signaling pathways. The Lima bean is an ideal model plant for these assays, as it responds to different compounds or treatments with the emission of very characteristic volatile patterns [307-309]. After herbivory *P. lunatus* emits a volatile blend which attracts carnivorous predators [310] (Figure 36). A similar plant reaction can be evoked by treatment with JA (**1**), the main phytohormone responsible for the plant's response to herbivory (Chapter 1.1.1). However, a careful comparison between the volatile bouquet emitted by Lima bean plants treated with **1** or subjected to herbivore feeding reveals clear differences (Figure 36). Herbivory induces more sesquiterpenoid homoterpenes such as 4,8-dimethyl-1,3,7-nonatriene (DMNT; **80**) and 4,8,12-trimethyl-1,3,7,11-tridecatetraene (TMTT; **81**) compared to JA-treatment. In contrast, JA (**1**) elicits mainly the production of monoterpenoids and only low amounts of methyl salicylate (MeSA; **39**) and TMTT (**81**). Interestingly, exactly these three compounds are emitted by the plant after incubation with the peptaibol alamethicin[10] (ALA) (Figure 36). Peptaibols are peptides, which form transient channels in membranes [311], causing early signals such as ion flux and membrane depolarization [312]. By Engelberth *et al.* (2000) ALA was established as a powerful elicitor of plant volatile production of the Lima bean [313].

[10] Alamethicin is a mixture of highly homologous proteins, isolated from the widespread soil fungus *Trichoderma viride*.

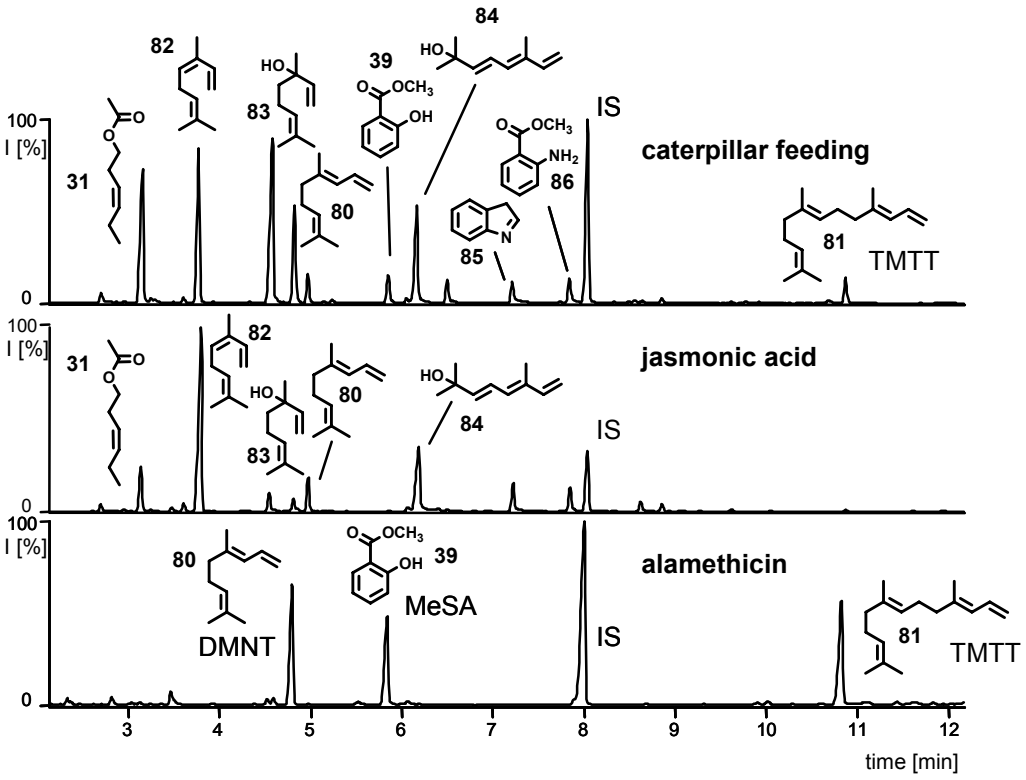

Figure 36 GL-chromatogram of volatiles emitted by *P. lunatus* 24 h after application of various elicitors: caterpillar feeding (*S. littoralis* larvae); jasmonic acid: (**1**; 1 mM); alamethicin (10 µg / ml). Identification of compounds: (3*Z*)-hexenylacetate (**31**); β-ocimene (**82**); linalool (**83**); 4,8-dimethyl-1,3,7-nonatriene (DMNT; **80**) ; methyl salicylate (MeSA; **39**); 2,6-dimethyl-3,5,7-octatrien-2-ol (**84**); indole (**85**); methyl anthranilate (**86**); 4,8,12-trimethyl-1,3,7,11-tridecatetraene (TMTT; **81**); IS, internal standard: 1-bromodecane.

As ALA induces exactly these volatiles, which are not triggered by JA (**1**), it had been hypothesized that ALA upregulates an alternative signaling pathway [186]. Phytohormone analysis of *P. lunatus* treated with ALA revealed that the JA- and the SA-pathway, as well as ET-emission was induced [186]. These findings suggest that the specific volatile blend was the result of JA-SA-signaling cross-talk (see Chapter 1.2). In *P. lunatus* ALA-induced volatile production can be inhibited by aristolochic acid (**87**) and phenidone (**88**) (Figure 37). **87** is a potent inhibitor of phospholipase A_2 and prevents the release of fatty acids from their membrane lipids [314,315], whereas the pyrazoline derivative phenidone inhibits the fatty acid oxygenating lipoxygenases (LOX) [316]. These findings imply the involvement of an oxylipin signal during this stress response [67,186].

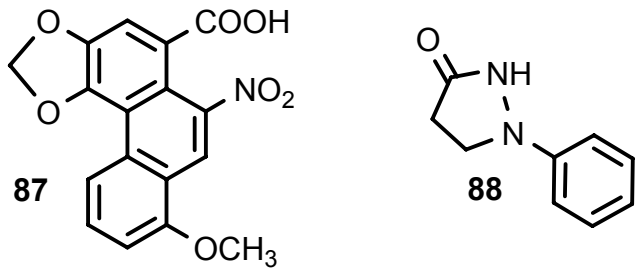

Figure 37 Aristolochic acid (**87**) and phenidone (**88**), inhibitors of the oxylipin biosynthesis in *P. lunatus*.

Despite its differential response towards various elicitors, a disadvantage of *P. lunatus* is that its genome has not been elucidated yet. This makes it unsuitable for analysis of gene expression, a powerful tool to analyze the signaling network triggering various plant reactions. Silencing of genes responsible for phytohormone biosynthesis as well as overexpression of the involved proteins are important for unraveling signal interactions in plant physiology [317]. Therefore, *Arabidopsis thaliana*, the genetically best studied plant was chosen to investigate its reactions to ALA-treatment. In cooperation with Prof. Christiane Gatz and Marco Herde (Albrecht-von-Haller-Institut für Pflanzenwissenschaften der Universität Göttingen, Göttingen) the impact of ALA on phytohormone levels and the expression of various defense related genes in *A. thaliana* were investigated.

In previous studies, a variety of mutants of *A. thaliana*, deficient in their JA-biosynthesis or response to JA (**1**) have been isolated. Most important are the mutant *coi1* (coronatine[11] insensitive), which is not responding to the jasmonate signals [32] and the mutant *npr1* (nonexpressor of *PR* genes) that is defective in SA-signaling and unable to establish systemic acquired resistance (SAR; see Chapter 1.1.3) [318,319]. Investigations of phytohormone signaling in *A. thaliana* have shown that resistance against herbivory (*S. littoralis*) is influenced by a negative interaction between the SA- and the JA-pathway. In this study, *coi1* mutants were more susceptible to herbivory, whereas *npr1* mutants showed enhanced resistance. Exogenous SA-application to the *npr1* mutant reduced its resistance to the herbivore, confirming cross-talk between **2** and **1** [182].

Indeed, Cui *et al.* (2002, 2005) [320,321] suggest that signaling networks in *A. thaliana* are of more complex nature. Their investigations of the interaction between SA-regulated resistance to the pathogen *Pseudomonas syringae* and the JA-dependent defense against the cabbage looper (*Trichoplusia ni*) are in line with the JA-SA-cross-talk hypothesis [320]. Conversely, infection with an avirulent strain of *P. syringae*, increased resistance to

[11] Coronatine is a fungal elicitor, mimicking JA-action.

herbivory, although infection with this strain resulted in the accumulation of high levels of SA (**2**) in the plant [321]. These findings point to a SA-independent systemic signal triggered by the avirulent pathogen.

5.1.2 Results and discussion

5.1.2.1 Phytohormone levels

Arabidopsis thaliana was grown hydroponically and elicited with ALA via the growth medium. To follow the time course of the upregulation of various phytohormones, plant leaves were harvested after certain intervals until 12 h after induction. According to the observations in the Lima bean [186], ALA-treatment induced both SA- and JA-production in *A. thaliana*. The level of SA (**2**) increased in similar kinetics and to a comparable extent as in *P. lunatus* (Figure 38), for data on *P. lunatus* see Engelberth *et al.* (2001) [186].

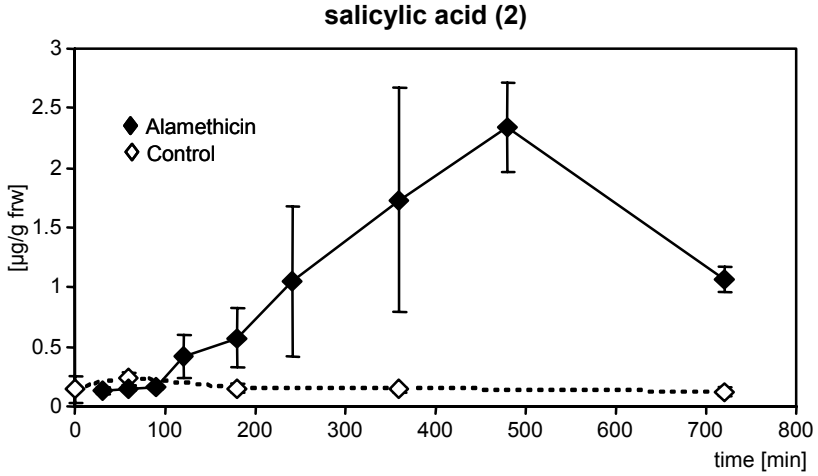

Figure 38 SA-levels in *A. thaliana* after elicitation with alamethicin. Error bars (may be hidden by the symbols) indicate the 95 % confidence interval; n = 5.

However, unlike in *P. lunatus*, after ALA-treatment of *A. thaliana* the increase of intracellular SA (**2**) did not impede the accumulation of JA (**1**). The JA-levels in *A. thaliana* increased more transient and reached high rates despite high levels of SA (**2**). Moreover, already the JA-resting level of the hydroponically grown *A. thaliana* was higher than those reported for soil grown plants [55,218], this may indicate that plants were already stressed due to the culturing technique.

After ALA-treatment, OPDA-levels did not change over the time of observation, although a slight increase at 90 and 360 min was detected (Figure 39). In general, OPDA-levels were three times lower in *A. thaliana* than in *P. lunatus* (see Table 4, Chapter 3.2.2.4).

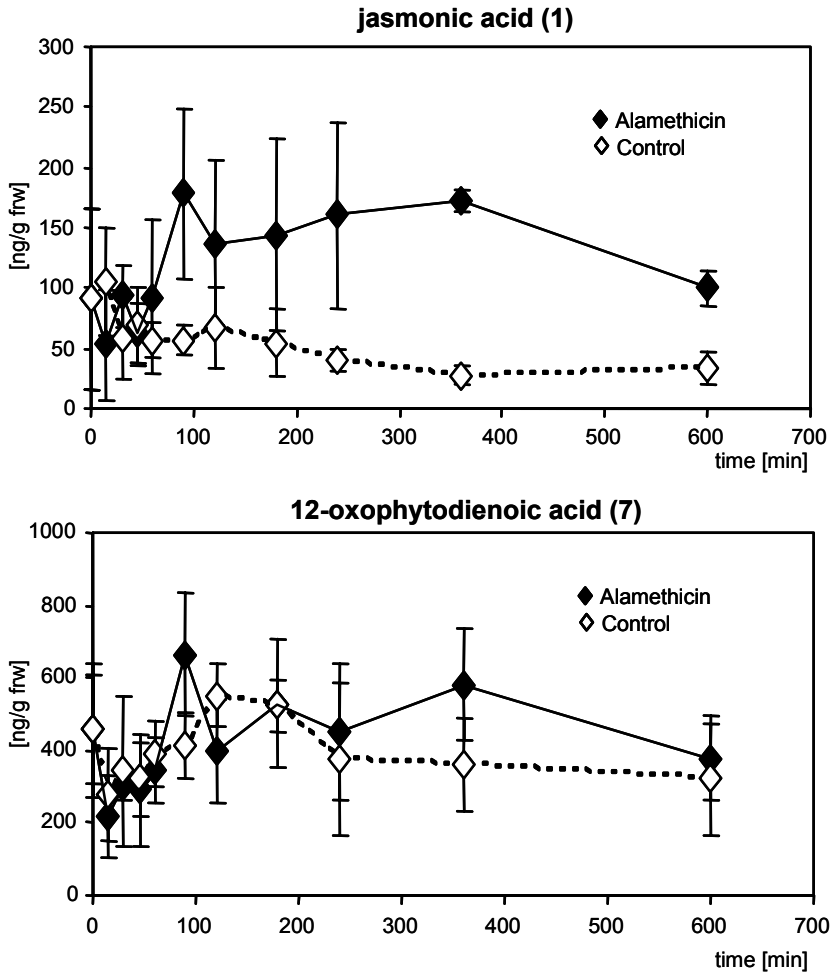

Figure 39 JA- and OPDA-levels in *A. thaliana* after elicitation with alamethicin. Error bars indicate the 95 % confidence interval; n = 3.

Although the SA-JA-cross-talk was not obvious regarding the kinetics of total JA (**1**), investigations of the *de novo* biosynthesis of *cis*-JA-levels revealed a marked change in the *de novo* biosynthesis of JA (**1**). In contrast to *P. lunatus* (see Chapter 4.2.1), the resting levels of *cis*-**1** were extremely high (about 50 % *cis*-**1** to total-**1**), pointing to a high turnover rate of JA (**1**), combined with high rates of *de novo* biosynthesis (Figure 38). Shortly after accumulation of SA (**2**), the *cis*-JA-amounts rapidly decreased. This observation implies that although the accumulation of intracellular JA (**1**) was not blocked by SA (**2**), the *de novo* biosynthesis indeed was. However, it can only be speculated about the origin of the JA-enrichment in *A. thaliana* after ALA-treatment. *De novo* formation is not necessarily the only source for intracellular accumulation of JA (**1**). For example, **1** could be cleaved from its amino acid conjugates which have been described to be readily formed and could act as a source for fast mobilization of **1** after elicitation [87].

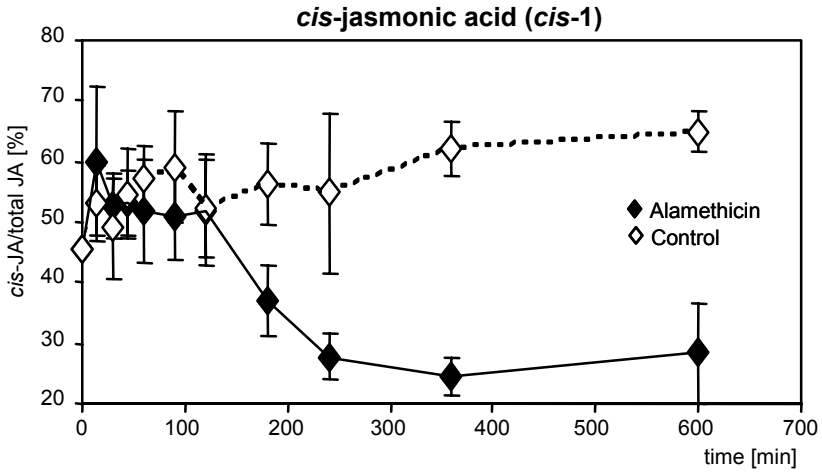

Figure 40 Ratio of *cis*-JA (*cis*-**1**) to total JA (**1**) in *A. thaliana* after alamethicin elicitation. Error bars indicate the 95 % confidence interval; n = 3.

5.1.2.2 Defense gene expression

The expression of *A. thaliana* transcription factors and defense related genes [322] during ALA-induction was studied by Prof. Christiane Gatz and Marco Herde. ALA induced SA-related transcription factors, whereas JA-inducible factors were not upregulated (Marco Herde, personal communication). Typical JA-dependent marker genes [323] which were investigated are the vegetative storage proteins (VSPs, see Chapter 1.1.1), pdf1.2 (plant defensin 1.2) and rns1 (S-like RNase 1). VSPs play an important nutritional role during plant development and stress response. In *Arabidopsis*, VSPs are upregulated during mechanical wounding and herbivory [324]. Plant defensins are peptides which exhibit antimicrobial activity. Although defensins are pathogenesis-induced proteins [325], they are in part regulated independently from SA (**2**) [326]. Similarly, RNS1 is wound-induced, albeit systemic activation of RNases seems to be controlled by a JA-independent pathway [327].
In this context transcription factors belonging to the so called NAC-family[12] [328,329] are of great interest. They are specific for plants and were found to be involved in diverse processes, such as plant development, defense, and abiotic stress adaptation; however, the complex regulation and function of NAC-transcription factors is not completely understood yet [329]. In *Arabidopsis*, a transcription factor (At1g52890) a member of the NAC-family was upregulated after ALA-induction (Marco Herde, personal communication). This factor has been described as *coi1* dependent, but not JA-inducible, pointing to the involvement of another octadecanoid [330]. Additionally, terpene synthase genes were induced by ALA-

[12] NAC stands for *Petunia* NAM and *Arabidopsis* ATAF1/2 and CUC2.

treatment, which correlates with the strong volatile emission observed after ALA-treatment for both *P. lunatus* [186] and *A. thaliana* [331-333].

However, the evaluation of gene expression is not completed yet. Further analysis and experiments will enhance insight into the complex signaling pathways during phytohormone cross-talk.

5.1.3 Conclusions

As the effect of ALA on the physiology of the Lima bean is already well understood [186,313], this powerful elicitor was used for experiments with *A. thaliana*, a genetically well documented plant, providing the opportunity to study molecular aspects of phytohormone signaling.

Phytohormone analysis indicated that in fact, JA-SA cross-talk occurred in *A. thaliana* after treatment with ALA, although less pronounced than in *P. lunatus*. Inhibition of the *de novo* biosynthesis of *cis*-JA (*cis*-**1**), points towards a block in the octadecanoid pathway by SA (**2**). The finding of an decrease in JA-biosynthesis, although JA (1) accumulated, vividly highlights the importance of stabilizing labile compounds and the preservation of their original stereochemistry. Without a separate analysis of *cis*-**1** and *trans*-**1**, this important information would have been lost. The responsible mechanism or pool for the transient increase of JA (**1**) is not known yet. However, as *cis*-JA (*cis*-**1**) is generally believed to be the more active isomer [59,60], JA-signaling should be reduced during increase of SA (**2**). This was verified by the analysis of gene expression were ALA induced SA-related transcription factors. Moreover, the upregulation of the NAC-transcription factor At1g52890 infers the involvement of an oxylipin signal. These results are in line with the inhibition of the typical ALA-induced volatile spectrum by aristolochic acid (**87**) and phenidone (**88**) in *P. lunatus*. However, the interpretation of gene expression is hampered, because many genes of interest were often already upregulated in the control group of the hydroponically grown plants, compared to plants grown in pot soil (Marco Herde personal communication).

Further investigations of the response of *A. thaliana* to defined stress conditions such as ALA-treatment along with the use of well described mutants, will provide us with more insight into the complex signaling network of plants.

5.2 Heavy metal ions as elicitors of plant defense reactions

5.2.1 Introduction: Biotic and abiotic stress response in plants, a search for common signals

Plant stress responses, such as the accumulation of secondary metabolites or the production of volatile compounds, are often regarded as specifically directed against biotic threats. However, also abiotic stress factors such as heavy metal ions can elicit similar responses. Many examples have been described, for heavy metal salts eliciting plants to synthesize and accumulate secondary stress metabolites, which are typically induced during pathogen or herbivore attack. For example, glyceollins, isoflavonoid phytoalexins involved in the interaction between soybean (*Glycine max*) and the phytopathogenic oomycete *Phytophthora sojae* [334], were induced by mercury ($HgCl_2$)-treatment [335]. Up to now, there is no convincing explanation for this finding or for any other of the examples given in a recent survey by Mithöfer *et al.* (2004) [207].

Similarly, heavy metal ion treatment of *P. lunatus* caused the emission of a volatile spectrum resembling that after induction with ALA (Figure 41) [336]. As a consequence, in *P. lunatus*, heavy metal stress should lead to a similar cross-talk situation involving fatty acid derived signals and SA (**2**) as it has been described for ALA-treatment [186]. The parallels between elicitation with ALA and heavy metal stress were suggestive, but needed confirmation. Moreover, the upregulation of endogenous SA (**2**) should make plants more susceptible to herbivory, which would represent an additional cost, next to the direct toxicity of metal ions, for plants growing on heavy metal polluted sites.

Within the scope of the Graduate Research School “Analysis of the Functioning and Regeneration of Degraded Ecosystems” (GRK 266) the plant’s reaction to heavy metal stress was studied. The Graduate Research School combined long term observations on heavily degraded aquatic and terrestrial ecosystems to elucidate common principles of ecosystem regeneration [337]. The terrestrial field site “Steudnitz” is located in the Central Saale Valley, 13 km north of Jena, Thuringia, Germany. It is a calcareous slope, covering an area of 4.8 ha. Between 1960 and 1990, phosphate fertilizer production resulted in alkaline dust deposition and contamination of the field site that lay downwind of the factory [338]. As a consequence, the soil pH raised to values of up to 10, and levels of phosphate, sodium, calcium, cadmium, and fluoride were exceedingly high [339]. Due to this pollution, the lower part of the slope, close to the factory, was a mosaic of bare ground and patches of the salt-tolerant grass *Puccinellia distans*. The upper part of the slope was occupied by species-poor *Elytrigia repens* grassland [338]. A nine year period of intense study concerning various

factors influencing regeneration and ecosystem functioning was carried out at different distances from the former factory and thus varying levels of degradation.

The goal of my studies within the framework of the Graduate Research School was to evaluate plant responses to heavy metal stress, in particular considering the elicitation of volatile production and upregulation of phytohormone levels by heavy metal salts [186,336]. Owing to the work of Engelberth *et al.* (2001) [186] and Koch (2001) [340] on the reaction of the Lima bean to ALA-treatment, *P. lunatus* was chosen as a model plant to study phytohormone upregulation and oxylipin formation after exposure to heavy metal ions. The confirmation of the hypothesis of SA-upregulation in heavy metal ion stressed plants is a precondition giving way to future studies testing the impact of this plant response in ecological field studies. In this context, oxylipins may not only play an important role during plant-herbivore interactions, but also mediate responses after encountering abiotic stress. Moreover, the intriguing similarity between reactions upon different stresses calls for an evaluation of the shared principles.

5.2.2 Results and discussion

5.2.2.1 Heavy metal ions induce volatile production

A series of heavy metal salts were tested in concentrations between 10 -1000 µM for their ability to induce volatile emission in *P. lunatus*. Therefore plantlets were detached and placed in individual vials containing a heavy metal salt solution. All heavy metal ion elicitors induced a volatile blend resembling that emitted after elicitation with ALA (Figure 41) which clearly differs from the volatile pattern observed after herbivory or JA-treatment (Figure 36, Chapter 5.1.1).

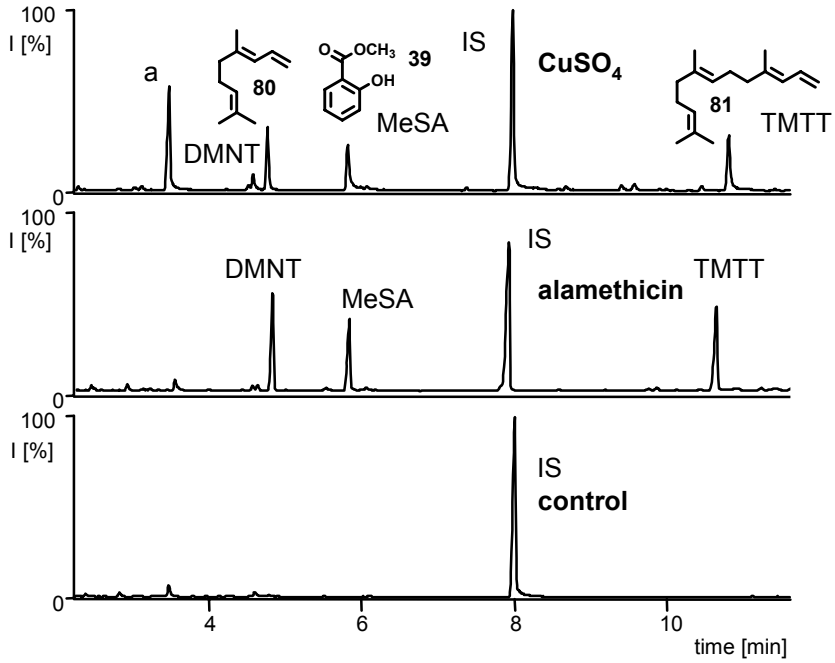

Figure 41 Volatile production of detached *P. lunatus* plantlets treated with various stressors. Elicitors were: $CuSO_4$ (700 µM); alamethicin (10 µg / ml); control: H_2O. Volatiles emitted: DMNT (**80**); MeSA (**39**); TMTT (**81**); a: 2-ethylhexanol (contamination); IS, internal standard: 1-bromodecane.

The most active elicitors were Cu^{2+}- and Hg^{2+}-ions, which reproducibly induced volatile production in a range of 300 µM to 1000 µM (Table 7). Fe^{2+}- and Cr^{6+}-ions turned out to be weak elicitors, i.e. volatile production of *P. lunatus* was not always reproducible in individual experiments. Al^{3+}-, Zn^{2+}-, Ni^{2+}-, Fe^{3+}-, Mn^{2+}-, and Sn^{2+}-ions did not induce volatile emission (Table 7). To some extend, the lesser activity of Al^{3+}- and Fe^{3+}-ions might be caused by their precipitation as hydroxides. Also Cd^{2+}-ions, the major heavy metal pollutant at the Steudnitz field site, were only active in this bioassay in high concentrations (Table 7). Therefore, $CuSO_4$ (700 µM) was used for further experiments as Cu^{2+}-ions were strong and reliable inducers of the volatile biosynthesis of the Lima bean.

Table 7 Heavy metal salts tested as elicitors of volatile emission of Lima bean. Shown is the concentration range of reproducible induction of volatile emission. Volatile induction experiments were repeated at least 3 times for every salt and concentration. For every experiment control plants were detached and placed in vials with tap water.

salt	volatile emission	salt	volatile emission
$AlCl_3$	-	$CuSO_4$	500-1000 µM
K_2CrO_4	800 µM	$ZnSO_4$	-
$MnSO_4$	-	$CdCl_2$	1000 µM
$(NH_4)_2Fe(SO_4)_2$	800-1000 µM	$SnCl_2$	-
$FeCl_3$	-	$HgCl_2$	500-1000 µM
$NiCl_2$	-		

In *P. lunatuns* the volatile production induced by ALA follows a diurnal rhythm [248]. In analogy, kinetic measurements with a zNose[13] revealed that also the volatile production after heavy metal treatment was rhythmic and light dependent (Figure 42).

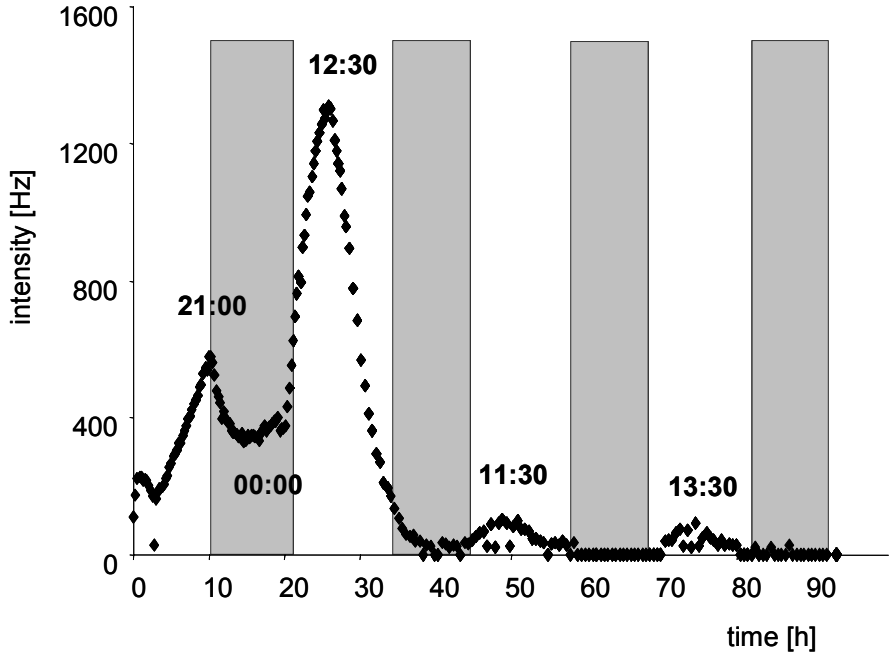

Figure 42 Rhythmic emission of terpenoids, displayed for TMTT (**81**) after $CuSO_4$-treatment (700 µM) of *P. lunatus*. The gray bars indicate dark periods. Samples were taken every 10 min. Maximum and minimum emission of volatiles is labeled with the time of day. Depicted is a representative experiment out of three replicates.

[13] A sensitive portable GC equipped with a piezoelectric quartz crystal as a detector. This instrument is capable to analyze volatile compounds every 2-3 min.

The comparison between the volatile patterns (Figure 36 and Figure 41) emitted after treatment with JA (**1**) or $CuSO_4$, implicates that JA (**1**) cannot be the phytohormone responsible for triggering the emission of DMNT (**80**), MeSA (**39**) and TMTT (**81**). Similarly to ALA-treatment, heavy metal ion induced volatile biosynthesis was inhibited after preincubation of the plantlets with aristolochic acid (**87**) (Figure 43). Pretreatment with phenidone (**88**) was not successful, because this compound formed complexes with the Cu^{2+}-ions, which resulted in precipitation of the inhibitor. The observed inhibition of volatile biosynthesis by aristolochic acid (**87**) indicates that a fatty acid derived signal accounts for the induction of volatile biosynthesis.

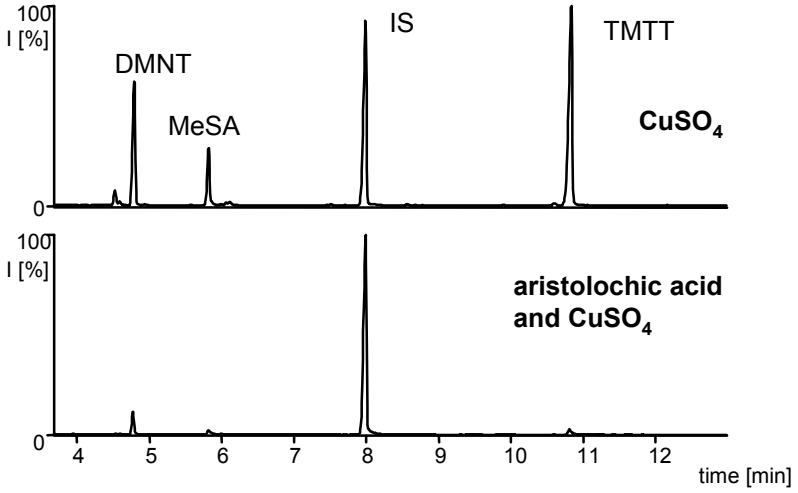

Figure 43 Inhibition of volatile production of *P. lunatus* with aristolochic acid (**87**; 300 µM). Elicitor: $CuSO_4$ (700 µM).

5.2.2.2 Heavy metal ions induce salicylic acid biosynthesis

Encouraged by the obvious parallels between the activity of ALA and heavy metal salts in the induction volatile biosynthesis, SA-levels after treatment with $CuSO_4$ were analyzed. Indeed, increasing SA-levels were found in Lima bean leaves treated with Cu^{2+}-ions (Figure 44). The accumulation of **2** started about 200 min after elicitation and depended on the concentration of $CuSO_4$ applied (Figure 45). Accordingly, the volatile production correlated with the increase of SA (**2**), as $CuSO_4$ concentrations below 300 µM did not induce volatile biosynthesis, and concentrations above 700 µM were as strong elicitors of volatile biosynthesis as ALA. Consistently, treatment with $CdCl_2$, which did not induce volatile bioysynthesis, also did not result in an increase of SA (**2**).

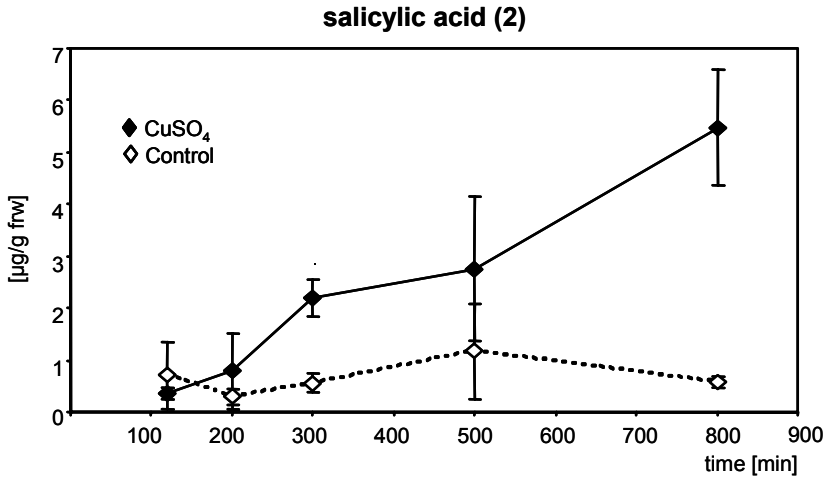

Figure 44 Increase of SA (**2**) after treatment of *P. lunatus* with $CuSO_4$ (700 µM); control: H_2O; error bars indicate 95 % confidence interval; n = 4.

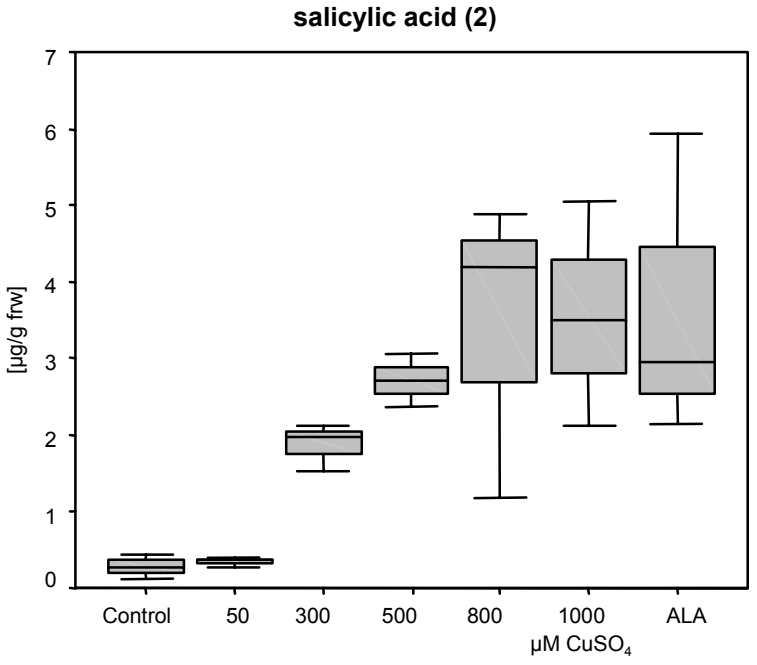

Figure 45 Increase of SA (**2**) in *P. lunatus* after treatment with different concentrations of $CuSO_4$. Values were taken after 500 min incubation time. Control: H_2O; ALA: alamethicin (10 µg ml^{-1}); n = 3.

5.2.2.3 Heavy metal ions induce ethylene emission

To complete the survey on parallels between ALA-treatment and heavy metal stress in *P. lunatus*, the induction of ethylene emission by heavy metal salts was investigated. ET-emission was analyzed in cooperation with Prof. Dr. Frank Kühnemann (Institut für Angewandte Physik der Universität Bonn, Bonn) with the help of photo acoustic laser spectroscopy. [313,341]. ALA and JA (**1**) are strong elicitors of the ET-biosynthesis [307,313]. As expected, Cu^{2+}-ions but interestingly also Cd^{2+}-ions were powerfully inducing ET-biosynthesis. Like the terpenoid biosynthesis, ET-emission was underlying a rhythm, although its light dependence was not as pronounced compared to the biosynthesis of terpenoids (Figure 42). ET-emission of *P. lunatus* after treatment with heavy metal ions was high compared to that after ALA treatment [313].

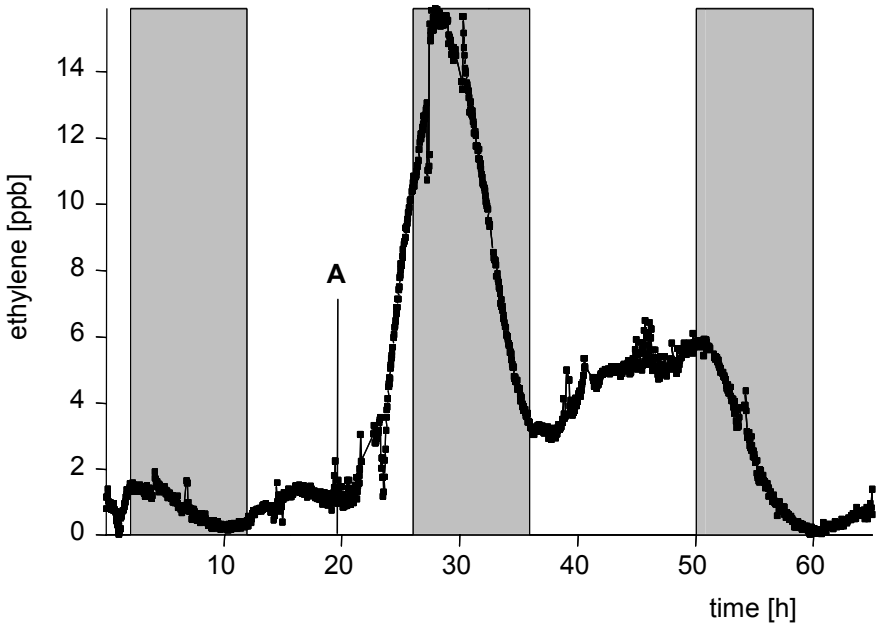

Figure 46 Ethylene biosynthesis of *P. lunatus* after application of 700 µM $CuSO_4$-solution. A: time of application of $CuSO_4$. The experiment depicted is a representative sample out of two replicates.

5.2.2.4 Oxylipin levels after heavy metal ion treatment

The results concerning the volatile biosynthesis of *P. lunatus* after treatment with heavy metals, and the intriguing similarities between $CuSO_4$ and ALA induced plant response infer that a fatty acid derived signal is involved in triggering these reactions. Since SA (**2**), inhibits the octadecanoid pathway (Chapter 5.1) the flux of fatty acid derived precursors can be shifted to other oxylipin pathways. The analysis of oxylipin levels in heavy metal treated plants should provide a way to identify this signal, as it was assumed that oxylipin levels rise during accumulation of intracellular SA (**2**) [186]. To assess this hypothesis, detached Lima bean plantlets were placed in 700 µM $CuSO_4$ and harvested in time intervals after the beginning of the treatment until 9 h of induction.

The accumulation of SA (**2**) after $CuSO_4$-treatment of Lima bean plants resulted in a similar cross-talk situation as observed after ALA-application [186]. A pronounced increase in OPDA (**7**) after elicitation (Figure 47), but no induction of JA (**1**) supports the inhibition of the JA-, but not OPDA-biosynthesis by SA (**2**) [186]. However, levels of all oxylipins studied were only elevated in the first 90 min after induction, indicating that the plant's response to heavy metal salt application is a fast process. After $CuSO_4$-treatment the biosynthesis of 11-oxo-9-undecenoic acid (**49**) and 13-oxo-9,11-tridecadienoic acid (**19**) was induced. Levels of α-ketol (**9**), γ-ketol (**10**), and 9-hydroxy-12-oxo-10-dodecenoic acid (**49**) were slightly increasing shortly after elicitation. Similar to wounding and caterpillar feeding (see Chapter 4.2.1), the level of 13-KOTE (**22**) was not elevated after $CuSO_4$-treatment. An accumulation of a specific class of oxylipins during the time of SA-increase was however not observed (Figure 47). Consequently, it can not be clearly assigned so far, which oxylipin accounts for the induction of the typical volatile spectrum after $CuSO_4$- or ALA-treatment. However, the pattern of oxylipin induction varied from that of mechanical wounding and caterpillar feeding (see Chapter 4.2.1). Together with the findings of volatile production, SA-accumulation and ET-biosynthesis, the results clearly indicate that heavy metals, besides their direct toxicity interfere with the complex defense system of higher plants.

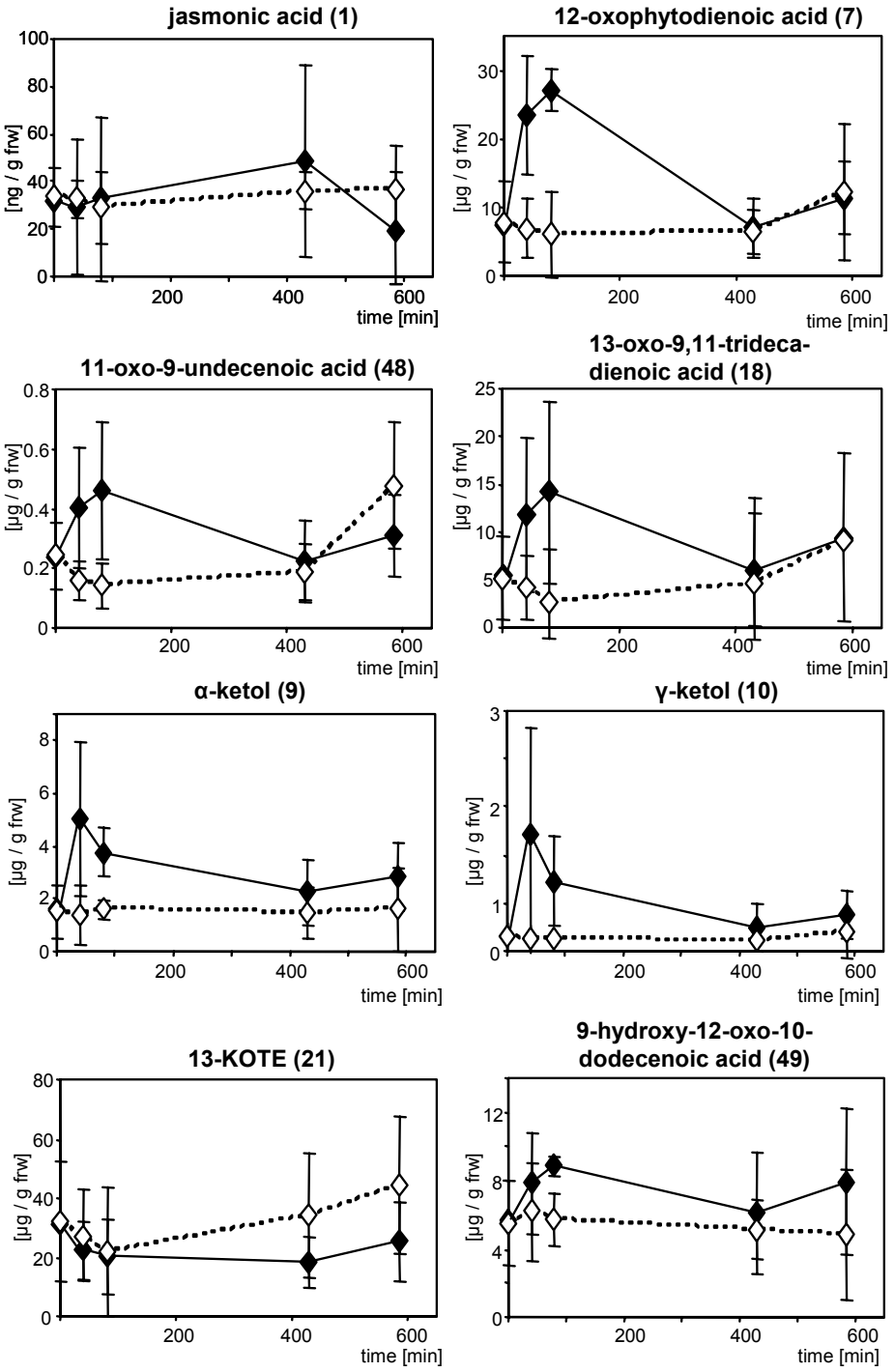

Figure 47 Induction of oxylipins after $CuSO_4$-treatment of *P. lunatus*. ♦ $CuSO_4$ (700 µM); ◊ control (H_2O). Differences in oxylipin levels can be read from the error bars displaying the 95 % confidence interval; n = 4.

5.2.3 Conclusions

It could be demonstrated that ALA and $CuSO_4$, two structurally unrelated compounds, share common features in the eliciting of stress response in *P. lunatus*. Due to the induction of the pathogen-related SA-pathway, plants which encounter heavy metal stress ought to be more susceptible to herbivory. The hypothesis concerning heavy metal ions as inducers of SA-biosynthesis which inhibits of the octadecanoid pathway, are in line with findings of Dr. Matthias Held, a Graduate Research School member, studying herbivory rates on a pollution gradient at the Steudnitz field site. Indeed, he was able to observe higher herbivory rates and an altered spectrum of secondary phenolic metabolites in *Arthemisia vulgaris* plants on sites with higher pollution [342]. However, the main pollutant at the Steudnitz site, Cd^{2+}-ions, were not active in my bioassays on volatile production, although they induced ET-emission in *P. lunatus*. This indicates that Cd^{2+}-ions may induce similar effects in other plants as described for the impact of Cu^{2+}-ions on *P. lunatus*. For instance, induction of lipid peroxidation in *Phaseolus vulgaris* after $Cd(NO_3)_2$ and $ZnSO_4$ treatment [343] as well as accumulation of malonedialdehyde after incubation of *Amaranthus* seedlings with $PbCl_2$ and $CdCl_2$ has been reported [344].

Moreover, the striking similarities between abiotic and biotic stress on the induction of secondary metabolites call for a search for common principles. Although pathogen infection, herbivore attack, or even heavy metal ion exposure, are quite different forms of stress, plants show a common response: an induced accumulation of secondary metabolites. For this finding, an underlying mechanism is proposed that is as simple as efficient. The common feature is the ROS-mediated or/and enzyme-catalyzed formation of fatty acid hydroperoxides. The presence of these compounds is a prerequisite and the initial point for the non-enzymatic or enzyme-catalyzed generation of numerous oxylipins (Figure 4, Chapter 1.1.2).

The oxidative burst is a well described phenomenon that is associated with wounding, pathogen infection or abiotic stress leading to an extensive local accumulation of fatty acid hydroperoxides (see Chapter 1.1.2). The exposure of plants to certain heavy metal ions shifts the balance of free radical turnover towards an accumulation of H_2O_2. In the presence of redox active transition metals such as Cu^{+}- and Fe^{2+}-ions, H_2O_2 can be converted to the highly reactive hydroxyl radical ($^{\bullet}OH$) in the metal-catalyzed Fenton reaction [345]. The oxidized metal ions undergo a reduction in a subsequent reaction with the superoxide radical ($O_2^{\bullet-}$) (Scheme 1). An alternative mechanism of $^{\bullet}OH$ formation directly from H_2O_2 and $O_2^{\bullet-}$ is the metal-independent Haber-Weiss reaction (Scheme 1) [346].

The $^{\bullet}OH$ radical is one of the most reactive species known [345]. Because of its ability to initiate radical chain reactions it is suspected to induce irreversible chemical modifications of various cellular components, with unsaturated lipids comprising activated bisallylic methylene

moieties being susceptible targets for radical attack [347]. Other ROS that are involved in lipid peroxidation is the protonated form of $O_2^{\bullet-}$ and the hydroperoxyl radical ($^{\bullet}O_2H$). An additional mechanism causing an accumulation of ROS, is the inhibition of antioxidative enzymes such as glutathione reductase [105], catalase, and superoxide dismutase by heavy metal ions [344].

Fenton reaction:

$$H_2O_2 + Fe^{2+} / Cu^{+} \rightarrow {}^{\bullet}OH + OH^{-} + Fe^{3+} / Cu^{2+}$$

$$^{\bullet}O_2^{-} + Fe^{3+} / Cu^{2+} \rightarrow Fe^{2+} / Cu^{+} + O_2$$

Haber-Weiss reaction:

$$H_2O_2 + {}^{\bullet}O_2^{-} \rightarrow {}^{\bullet}OH + OH^{-} + O_2$$

Scheme 1 Chemical reactions involved in hydroxyl radical ($^{\bullet}OH$) generation.

Consequently, Müller and co-workers showed in a remarkable series of studies that in plants a free radical-catalyzed oxidation of linolenic acid (**4**) alone yielded a high number of phytoprostanes, which may act as signaling compounds [138,348]. Interestingly, F_1-phytoprostane levels have been induced in the presence of heavy metal ions (Cu^{2+}) and wounding [348]. Additionally, it has been reported that high levels of H_2O_2 stimulate SA-biosynthesis [349,350]. Conversely, SA (**2**) itself is discussed to induce lipid peroxidation and subsequent formation of lipid peroxidation products. SA (**2**) has been shown to bind to and inhibit the catalase enzyme in tobacco and thus enhance the formation of H_2O_2 [159,160]. Although this catalase-inhibiting function has not been verified, H_2O_2 is still being discussed as a second messenger of SA (**2**) [351] and has been demonstrated to act synergistically with **2** in pant-pathogen defense [352]. Also the high ET-inducing activity of heavy metal ions is consistent with high levels of ROS and lipid peroxidation products. Lipid hydroperoxides have been shown to convert ACC into ET (**3**) independent from the native enzyme responsible for this transformation [353]. **3** itself may be a ROS inducing factor reciprocally, as ET (**3**) has been shown to enhance H_2O_2 formation and trigger induced programmed cell death in tomato cell cultures, possibly through blocking of ROS-inactivating enzymes [354]. Hence, ROS and the accumulation of fatty acid hydroperoxides play a central role in linking the formation and action of various phytohormones. This hypothesis of ROS release and subsequent formation of unsaturated fatty acid derived signals provides a reasonable explanation for the similarities in heavy metal ions stress and certain biotic stress responses in plants.

6 GENERAL CONCLUSIONS AND OUTLOOK

The development of a method for the comprehensive extraction and sensitive analysis of oxylipins from complex biological matrices was a prerequisite to study of their role as signaling compounds in biological processes.

In situ derivatization of oxylipins possessing oxo-groups with PFBHA to the corresponding PFB-oximes at the beginning of the workup procedure stabilizes structurally sensitive compounds. Thus reactive molecules e.g. Michael acceptors such as α,β-unsaturated aldehydes are prevented from further reactions with biomolecules from the plant matrix. This warrants genuine and reliable profiles of the oxylipins involved in plant stress responses. Additionally, the original stereochemistry of compounds that tend to isomerize during sample preparation can be preserved. The efficiency of this protection of the stereochemistry is most vividly demonstrated by the monitoring of *cis*-JA (*cis*-**1**) in plants treated with different elicitors (Chapter 4.2.1 and Chapter 5.1.2.1).

Since most oxylipins are either not commercially available or only in minute amounts, a future task includes the synthesis of oxylipins or labeled standards to improve the quantification protocol for highly oxidized oxylipins. The synthesis of oxylipins will also provide compounds for feeding studies and bioassays which are needed to further evaluate the role of newly identified oxylipins in signaling cascades.

Besides oxylipin profiling, the developed protocol bears the potential to additionally include acidic plant metabolites such as salicylic acid and abscisic acid in the measurements for a more complete coverage of signaling pathways involved in plant defense reactions.

My experiments addressing the response of *P. lunatus* to various stresses clearly show that in addition to the classical phytohormones JA (**1**) and OPDA (**7**) the formation of oxylipins is induced e.g. α- and γ-ketols (**9** and **10**) and α,β-unsaturated aldehydes (**18**, **48** and **49**) were upregulated during biotic and abiotic stress. The comparison of the results from mechanical wounding, caterpillar feeding, and heavy metal ion induced stress, infers that oxylipins are differentially involved in various signaling processes. An active and controlled mechanism can be anticipated, because the oxylipin pattern clearly differs in dependence of the respective stressor (Table 8). With the observation of defined oxylipin patterns as a reaction to different stress factors, a major challenge will be the understanding how this flexibility in the oxylipin signature is regulated.

Table 8 Differential induction of oxylipins in *P. lunatus* after mechanical wounding, caterpillar feeding and $CuSO_4$ treatment.

Oxylipin		Treatment		
Name	**Structure**	**Mechanical wounding**	**Herbivory**	**$CuSO_4$**
JA (**1**)	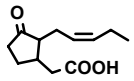 **1**	+	+	-
OPDA (**7**)	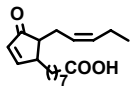 **7**	-	+	+
α-Ketol (**9**)	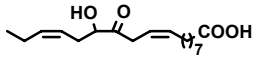 **9**	+/-	+/-	+
γ-Ketol (**10**)	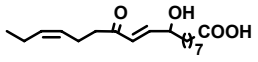 **10**	+	+	+
13-KOTE (**21**)	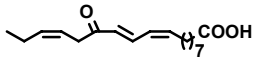 **21**	-	-	-
9-Hydroxy-12-oxo-10-dodecenoic acid (**49**)	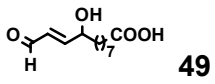 **49**	+	+	-
11-Oxo-9-undecenoic acid (**48**)	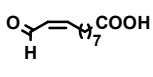 **48**	-	+	+
13-Oxo-9,11-tridecadienoic acid (**18**)	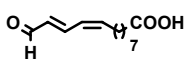 **18**	-	+	-
12,13-Epoxy-11-HODE (**20**)	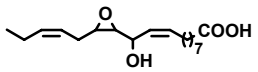 **20**	-	-	-

In this context it is of high interest to investigate the distinct local response of oxylipin induction during caterpillar feeding. The spatial analysis of the oxylipin pattern throughout an attacked plant will provide further details about the signaling fluxes of plants to organize efficient defense reactions. With my experiments I already demonstrated that there are major differences in the oxylipin/plant hormone distribution in an attacked leaf. It will be necessary to adapt the methodology to be able to monitor the reactions in just a few cell layers which will provide a much better view of the plant's defense mechanisms than analyzing whole leaf samples with a huge background from the less affected tissue.

Most fascinating is the monitoring of oxylipins not only in the damaged plant material, but also in the insect's gut (Chapter 4.3). Oxylipins are ingested by the insects, especially as they are formed directly in the plant material that is damaged. The metabolism of oxylipins by the caterpillar can be deduced from the presence and absence of compounds in the damaged leaf and the caterpillar's regurgitant (Chapter 4.2.3). Interestingly, compounds like JA (**1**) and γ-ketol (**10**), which were upregulated in the plant leaf, occurred only in very low amounts in the caterpillar's regurgitant. Moreover, the rearrangement of OPDA (**7**) to

iso-OPDA (**78**) points towards an additional metabolism in the insect's gut. Understanding the role of oxylipins as cross-kingdom signals is still at infancy. However, the mutualistic interaction of plants and insects, as it has been evolved since the early emergence of life, calls for an elaborate signaling and recognition system of both organisms. A further analysis of oxylipins occurring in both plant and the insects digestive system and the enzymes involved will contribute to elucidate this complex interaction.

P. lunatus is a perfect tool for the analysis of signaling cascades, as it responds very distinct to its environment with easy to follow reactions, i.e. the dynamic emission of various volatile compounds [308,309]. A disadvantage of this model plant is the lack of genetic information and thus the availability of mutants and the possibility to investigate gene regulation after certain stresses. The transfer of the analysis of oxylipins on a genetically modifiable plant like *A. thaliana* has been started and needs to be deepened. First results concerning the comparability of the reaction of *A. thaliana* and *P. lunatus* upon treatment with ALA confirm that both plants react similar (Chapter 5.1). However, the reaction of *A. thaliana* on ALA induction is less pronounced and especially the analysis of gene regulation needs further assessment.
Molecular biological analysis in addition to physiological studies will be useful to position oxylipin signals in their transduction pathways and to understand how these signals are perceived and mediated to downstream responses. Transcriptional profiling techniques such as DNA-arrays will allow studying the expression of defense genes in response to oxylipins. The specific knock-out of certain genes and enzymes involved in the formation of oxylipins and the subsequent analysis of not only the plants' performance, but also the spectrum of oxylipins formed upon blocking of a pathway is required for the deeper understanding of oxylipins as phytohormone like compounds.
However, although the understanding of function and regulation of specific genes has been improving in the last decades, the investigation of the signaling compounds themselves can not be substituted by a simple observation of up or down regulation of transcripts. Molecular biological analysis can only be comprehensively understood when actual signaling cascades are revealed, and the information combined.

Moreover, not only biotic factors, also abiotic stress can induce pronounced changes in phytohormone and oxylipin levels (Chapter 5.2). The similarities of the reaction of *P. lunatus* to heavy metals compared to biotic stress or to pathogen derived elicitors are striking. Both, $CuSO_4$ and ALA, induced volatile emission, and the biosynthesis of SA (**2**), and ET (**3**) to a similar extend. The experiments with inhibitors of the biosynthesis of fatty acid metabolism confirmed that an oxylipin signal is involved in triggering this typical stress response of plants

after heavy metal treatment. However, a single oxylipin being involved in stress signaling was not identified so far. Despite this, the striking similarities between biotic and abiotic stress implicate the involvement of a common signal. Non-enzymatic oxidation of polyunsaturated fatty acids by reactive oxygen species is possibly a mechanism to generate similar signaling compounds during various types of stress.

7 ABSTRACT

Plants reply with coordinated reactions against threats from their environment such as wounding, herbivory or abiotic stress factors. In order to guarantee adequate and specific answers against various challenges, plants rely on a complex network of signaling compounds. However, up to now our knowledge of the signal cascades involved is very limited. Especially the role of oxidized lipids (oxylipins) in signaling processes of plants is not fully understood, as most methods for the analysis of plant signaling compounds focused on jasmonates such as jasmonic acid (JA; **1**) and 12-oxophytodienoic acid (OPDA; **7**) [64,210]. However, new findings implicate the involvement of other fatty acid derived compounds in plant signaling [91].

Monitoring the oxylipin profile of plants

In order to assess the role of these less studied oxylipins along with known phytohormones in plant responses to biotic and abiotic stress factors, a rapid and reliable GC-MS based method for the analysis of plant signaling compounds was established. In contrast to known detection methods of phytohormones, the reactivity and lability of oxylipins was considered.

The key step of my method involves the *in situ* derivatization of oxo-moieties with pentafluorobenzyl hydroxylamine (PFBHA) to stable oximes already during the extraction of the leaf material. Thereby, reactive aldehydes and ketones such as compounds carrying an α,β-unsaturated carbonylic moiety are stabilized and a loss of labile molecules during sample preparation is prevented. Simple pre-separation of the crude lipid extract in a hexane phase containing less polar compounds and a CH_2Cl_2 phase containing highly oxidized polar lipids, improved the following workup and the detection by GC-MS significantly (Figure 48). Compounds containing acid moieties were selectively purified by solid phase extraction (SPE) using aminopropyl cartridges.

To make the oxylipins GC-volatile the samples were methylated and free hydroxyl groups were subsequently trimethylsilylated. The high separation efficiency of the gas liquid chromatography allows comprehensive analysis of the oxylipin profile. Owing to this derivatization technique the detection of diverse compound classes is simplified by the option to screen for characteristic fragments by ion trace search. Alongside the monitoring of known phytohormones, identification of novel putative signaling compounds is possible without the need for time consuming purification and isolation.

With just two fast purification steps the workup procedure is suitable for high sample throughput as needed for a detailed analysis of plant signaling compounds e.g. for kinetic measurements. The crucial sensitivity for quantification of oxo-acids is achieved by the PFB-

derivatization in combination with negative-chemical ionization mass spectrometry (NCI-MS), which is about 100-times more sensitive than EI-MS methods.

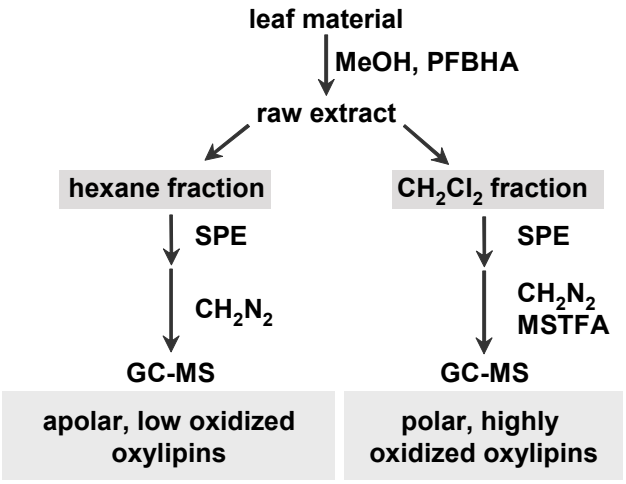

Figure 48 Sample preparation for the analysis of oxylipins from plants

Identification of new oxylipins in the Lima bean

The oxylipin profile of the Lima bean (*Phaseolus lunatus*) was intensively studied with the described method. Thereby a series of aldehydic fatty acids such as 9-hydroxy-12-oxo-10-dodecenoic acid (**49**) and 9,12-dioxo-10-dodecenoic acid (**50**), and other oxo-compounds were identified in Lima bean leaves for the first time (Figure 49).

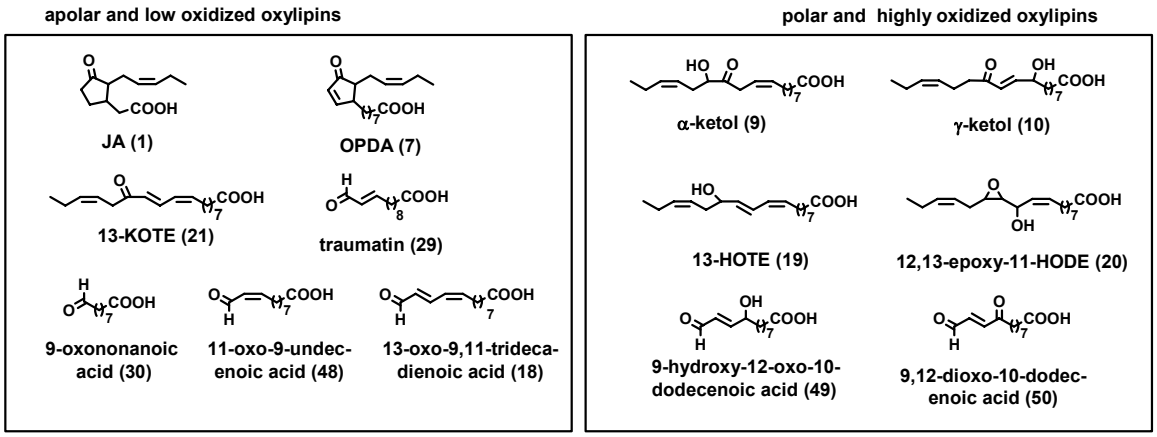

Figure 49 Oxylipins identified in the Lima bean (*Phaseolus lunatus*).

Remarkably, several common lipid peroxidation products e.g. hydroxy fatty acids were not found in the Lima bean extracts, even after different treatments to provoke plant stress. This indicates that lipid peroxidation processes in the induced Lima bean leaves are mainly controlled by enzymatic processes limiting the variety of different oxylipins.

Quantification of oxylipin signatures after biotic and abiotic stress

For a more thorough understanding of the physiological role of oxylipins in the plant responses to biotic and abiotic stress factors, I applied the developed method for quantitative measurements of the kinetics and spatial distribution of oxylipin formation.

Comparison between mechanical wounding and caterpillar feeding

The Lima bean reacted to a single mechanical wounding event with the *de novo* biosynthesis of *cis*-JA (*cis*-**1**). This production was followed by a slow isomerization from *cis*-**1** to *trans*-**1** until a resting level was reached. The kinetic investigation of the *de novo* biosynthesis of *cis*-**1** is only possible when the samples are *in situ* derivatized with PFBHA during extraction as this prevents *cis* → *trans* isomerization of JA (**1**) during sample preparation.

The comparison between mechanical wounding and caterpillar feeding reveals striking differences in the oxylipin patterns: Whereas JA-biosynthesis was induced in both cases, OPDA (**7**) accumulated only after caterpillar feeding presumably by the insect's specific elicitors. Also the formation of 11-oxo-9-undecenoic acid (**48**) and 13-oxo-9,11-tridecadienoic acid (**18**) was characteristic for caterpillar feeding. In general, higher amounts of oxylipins were induced by caterpillar feeding than by mechanical wounding. The highest levels of oxylipins were observed directly at the biting zone of the insect.

Oxylipin profile in the gut of lepidopteran larvae

Oxylipins were also detected in the gut of lepidopteran larvae (*Spodoptera littoralis*). Interestingly, the oxylipin profile of the gut content was significantly different to that of the Lima bean leaves. For example JA (**1**) and OPDA (**7**) were absent in the caterpillar's regurgitant. Moreover I was able to observe the occurrence of tetrahydrodicranenone B (*iso*-OPDA; **78**) in the regurgitant, indicating an active metabolism of oxylipins in the caterpillar's gut (Figure 50). Initial experiments on the formation of *iso*-OPDA (**78**) in the insect's gut point towards an enzymatically catalyzed isomerization of OPDA (**7**) to *iso*-OPDA (**78**). Future work will show whether the identified oxylipins serve the caterpillar as signal compounds [284] or whether modified oxylipins from the gut are reintroduced into leaves during feeding and induce or suppress plant defense reactions.

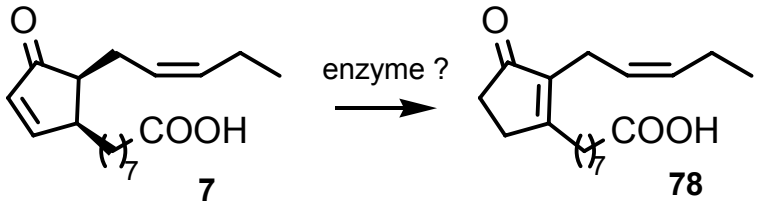

7 **78**

Figure 50 Isomerization of OPDA (**7**) to *iso*-OPDA (**78**) in the gut of *S. littoralis* larvae.

Stress induction by the peptaibol alamethicin

In cooperation with Prof. Christiane Gatz and Marco Herde a combined phytohormone profiling and transcript analysis with DNA-arrays of *Arabidopsis thaliana* was established, in order to address the plant's reaction to stress from different viewpoints. For the experiments the well characterized elicitor alamethicin was chosen. In analogy to the Lima bean, in *A. thaliana* an induction of salicylate (SA; **2**) was observed after ALA-treatment. This led to the interference of **2** with the biosynthesis of JA (**1**).

Although *A. thaliana* showed high levels of total JA (**1**) throughout the period of SA-increase the separate analysis of *cis*- und *trans*-JA (**1**) clearly indicated the block of the octadecanoid pathway. Only the separation into *cis*- and *trans*-**1** benefiting from the *in situ* stabilization of *cis*-JA (*cis*-**1**) by PFB-derivatization enabled me to demonstrate this interaction. This proves the importance to trap labile signaling compounds during the workup procedure.

The investigations of the expression of transcription factors by Prof. Christiane Gatz and Marco Herde back the findings of a block of the JA-biosynthesis as the expression of SA-regulated genes was observed, whereas JA-dependent factors were not induced.

Heavy metal ion stress

Besides biotic elicitors, abiotic factors influence the phytohormone levels of plants. Within the framework of the Research School on Function and Regeneration of Degraded Ecosystems (GRK 266) the plant's reaction to heavy metal ion exposure was investigated.

Using the Lima bean as model system an induction of volatile emission, and the biosynthesis of SA (**2**) and ethylene (ET; **3**) after heavy metal ion exposure in particular Cu^{2+}-ions (700 mM) was observed. The reaction of *Phaseolus lunatus* to heavy metal ions resembles in many aspects its response to the peptaibol alamethicin.

The inhibition of the volatile production by aristolochic acid (**87**), an inhibitor of phospholipases, proves the involvement of a fatty acid derived compound in the signal transduction of the Lima bean after heavy metal treatment. Although the quantitative analysis of the oxylipin profile revealed an intrinsic pattern after Cu^{2+}-ion treatment, it was so far not possible to assign a specific oxylipin responsible for the induction of plant volatile

biosynthesis after heavy metal treatment. Nevertheless, I was able to evidence the involvement of enzymatical and non-enzymatical lipid peroxidation as a common feature triggering the plants responses to biotic as well as abiotic stress.

8 ZUSAMMENFASSUNG

Pflanzen koordinieren ihre Reaktionen auf Bedrohungen aus ihrer Umwelt, z. B. gegen Herbivore oder abiotische Stressfaktoren, mit Hilfe eines komplexen Netzwerkes von Signalmolekülen. Unser Verständnis der beteiligten Signalkaskaden ist jedoch immer noch sehr begrenzt, da sich die meisten Untersuchungen pflanzlicher Signalmoleküle hauptsächlich auf die bekannten Phytohormone Jasmonsäure (JA; **1**) und 12-Oxo-phytodiensäure (OPDA; **7**) konzentrieren [64,210]. Neue Befunde legen jedoch die Beteiligung weiterer oxidierter Fettsäureprodukte (Oxylipine) bei diesen Signalprozessen nahe [91].

Analyse des Oxylipinprofils von Pflanzen

Mit dem Ziel neben den bekannten Phytohormonen auch strukturell labile Oxylipine bei pflanzlichen Reaktionen auf biotische oder abiotische Stressfaktoren zu studieren, wurde eine schnelle und zuverlässige GC-MS-basierte Methode entwickelt. Im Gegensatz zu anderen Nachweisverfahren für Phytohormone wurde die Reaktivität und Instabilität vieler Oxylipine berücksichtigt.

Der Schlüsselschritt der vorgestellten Methode liegt in der *in situ* Derivatisierung von Oxogruppen mit Pentafluorbenzylhydroxylamin (PFBHA) zu stabilen Oximen bereits während der Extraktion des Blattmaterials. Dadurch werden reaktive Oxylipine, wie α,β-ungesättigte Carbonylverbindungen, stabilisiert und der Verlust labiler Aldehyde und Ketone während der Probenaufarbeitung vermieden. Durch eine sequentielle Vorfraktionierung des methanolischen Rohextraktes in eine Hexanphase, die weniger polare Oxylipine enthält, und in eine CH_2Cl_2-Phase mit den höher oxidierten polaren Verbindungen, konnten die nachfolgenden Aufarbeitungsschritte und die anschließende Detektion per GC-MS optimiert werden (Abbildung 1). Aus beiden Fraktionen wurden mittels Festphasenextraktion (SPE) an Aminopropylkartuschen Verbindungen mit Säure-funktionalitäten selektiv angereichert. Für die GC-MS-Analytik wurden die Oxylipine methyliert und anschließend die freien Hydroxygruppen trimethylsilyliert. Die hohe Trennleistung der Kapillargaschromatographie erlaubt die vollständige Erfassung des komplexen Oxylipinprofils. Zusätzlich ermöglicht die Derivatisierungstechnik die Ionenspursuche nach charakteristischen Fragmenten unterschiedlicher Verbindungsklassen. Durch die Interpretation der Massenspektren ist es möglich, ohne zeitaufwändige Aufreinigung und Isolierung des Analyten, Strukturvorschläge für neue potentielle Signalmoleküle zu erstellen.

Mit nur zwei schnellen Aufreinigungsschritten eignet sich dieses Verfahren für einen hohen Probendurchsatz wie er für eine detaillierte Analyse pflanzlicher Signalprozesse, z. B. durch kinetische Studien, unerlässlich ist.

Die zur Quantifizierung notwendige Empfindlichkeit bietet die PFB-Derivatisierung in Kombination mit negativ-chemischer Ionisations-Massenspektrometrie (NCI-MS), wodurch im Gegensatz zu EI-MS Methoden ein 100-mal empfindlicherer Nachweis der PFB-Derivate möglich wird.

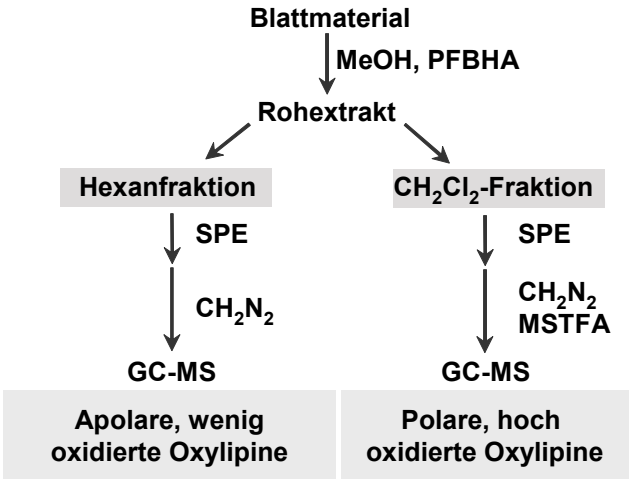

Abbildung 1 Probenvorbereitung zur Analyse des Oxylipinprofils von Pflanzen.

Nachweis neuer Oxylipine in *Phaseolus lunatus*

Das Oxylipinprofil der Limabohne (*Phaseolus lunatus*) wurde mit der beschriebenen Methode untersucht. Dabei konnten eine Reihe von Aldehydsäuren, wie z. B. 9-Hydroxy-12-oxo-10-dodecensäure (**49**), 9,12-Dioxo-10-dodecensäure (**50**) sowie weitere Oxo-verbindungen erstmals in der Limabohne nachgewiesen werden (Abbildung 2). Bemerkenswert ist, dass sich in der Limabohne nach unterschiedlicher Stressinduktion eine Reihe typischer Lipidperoxidationsprodukte, wie Hydroxyfettsäuren, nicht nachweisen ließen. Diese Beobachtung deutet darauf hin, dass in der Limabohne Lipidperoxidationsprozesse in erster Linie durch Enzyme kontrolliert werden und daher nur eine begrenzte Anzahl von Oxylipinen gebildet wird.

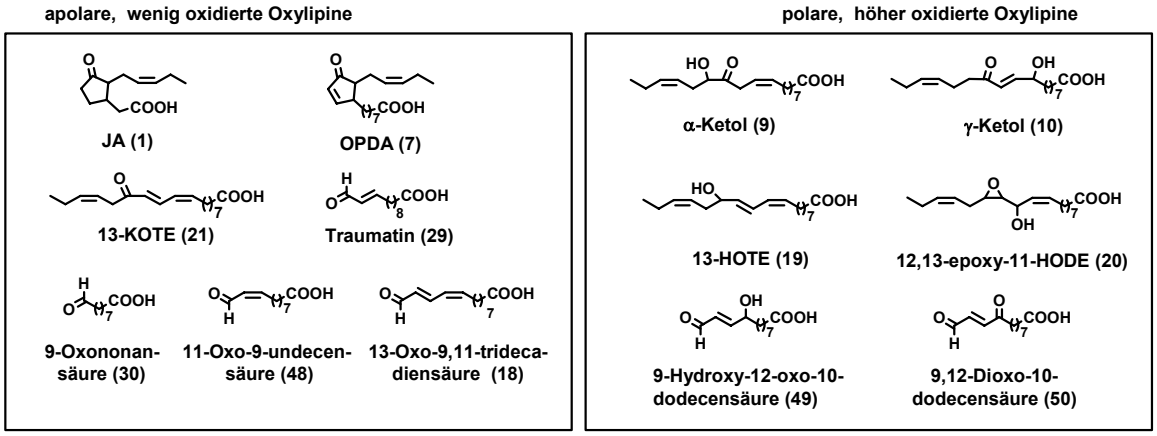

Abbildung 2 Identifizierte Oxylipine aus *Phaseolus lunatus*.

Quantifizierung von Oxylipinen nach biotischem und abiotischem Stress

Für ein tiefergreifendes Verständnis der physiologischen Rolle von Oxylipinen in pflanzlichen Signalprozessen wurde die entwickelte Methodik für kinetische Messungen und zur Bestimmung der Verteilung von Oxylipinen in unterschiedlichen Bereichen der Pflanze angewendet.

Vergleich zwischen mechanischer Verletzung und Raupenfraß

In der Limabohne kam es nach einmaliger mechanischer Verletzung zur *de novo* Biosynthese von *cis*-JA (*cis*-**1**). Danach isomerisierte *cis*-**1** langsam zu *trans*-**1** bis ein Basalniveau erreicht wurde. Die Beobachtung des *cis*/*trans*-Verhältnisses wurde erst durch die *in situ* PFB-Derivatisierung der Proben möglich, da diese eine *cis* → *trans* Isomerisierung von JA (**1**) während der Aufarbeitung verhindert. Dies erlaubt die Quantifizierung der *de novo* Biosynthese von *cis*-**1** und ihrer zeitabhängigen Deaktivierung zu *trans*-**1**.

Der Vergleich zwischen mechanischer Verletzung und Raupenfraß zeigte deutliche Unterschiede im Oxylipinmuster. Während JA (**1**) in beiden Fällen akkumulierte, wurde die Biosynthese von OPDA (**7**) nur bei Raupenfraß, wahrscheinlich durch raupenspezifische Elizitoren, induziert. Die Bildung von 11-Oxo-9-undecensäure (**48**) und 13-Oxo-9,11-tridecadiensäure (**18**) war ebenfalls charakteristisch für Raupenfraß. Im Allgemeinen wurden durch Raupenfraß höhere Gehalte an Oxylipinen induziert als durch mechanische Verletzung. Die höchsten Konzentrationen an Oxylipinen wurden direkt an der Fraßstelle der Schädlinge gemessen.

Oxylipinprofil im Raupendarm

Auch im Darm von *Spodoptera littoralis* treten Oxylipine auf. Interessanterweise unterschied sich das Oxylipinprofil des Raupenregurgitats signifikant von dem der geschädigten Pflanzen. So fehlten z. B. JA (**1**) und OPDA (**7**) im Raupenregurgitat, andererseits ließ sich Tetrahydrodicranenon B (*iso*-OPDA; **78**) nachweisen, was einen aktiven Metabolismus von Oxylipinen im Raupendarm nahe legt (Abbildung 3). Erste Untersuchungen zur Bildung von **78** im Raupendarm deuten auf eine enzymatisch katalysierte Isomerisierung von OPDA (**7**) zu *iso*-OPDA (**78**) hin. Zukünftige Experimente werden zeigen, ob die identifizierten Oxylipine als Signalstoffe für die Raupe dienen [284] oder die im Darm modifizierten Oxylipine beim Fraßprozess wieder in das Blatt gelangen und dort Reaktionen auslösen oder Signalprozesse unterdrücken.

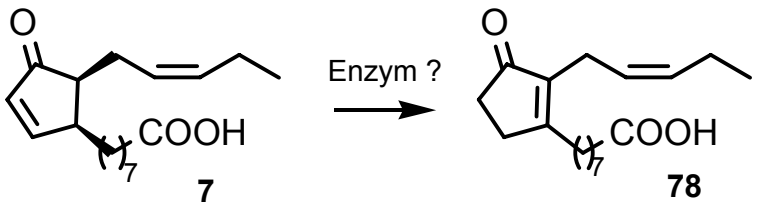

7 **78**

Abbildung 3 Isomerisierung von OPDA (**7**) zu *iso*-OPDA (**78**) im Darm von *S. littoralis.*

Stressinduktion durch den Kanalbildner Alamethicin

Um pflanzliche Reaktionen auf Stress umfassend analysieren zu können, wurde in Zusammenarbeit mit Prof. Christiane Gatz und Marco Herde die Phytohormonanalytik mit Transkriptanalysen mittels DNA-chips von *Arabidopsis thaliana* kombiniert. Für die Untersuchung wurde Alamethicin als Elizitor gewählt, da dieser schon an der Limabohne intensiv untersucht worden war. Analog zur Limabohne induzierte Alamethicin in *A. thaliana* die Biosynthese von Salicylsäure (SA, **2**). Dies führte zu einer Inhibierung der Biosynthese von JA (**1**). Obwohl in *A. thaliana* auch während des Anstiegs von SA (**2**) hohe Gehalte an JA (**1**) erreicht wurden, konnte durch die separate Untersuchung von *cis*- und *trans*-JA (**1**) die Blockade des Octadecanoidweges aufgezeigt werden. Dies belegt, wie wichtig es ist labile Oxylipine während der Aufarbeitung zu stabilisieren, da nur die Trennung von *cis*- und *trans*-JA (**1**) den Einfluss von SA (**2**) auf die JA-Biosynthese verdeutlichte. Parallel wurde von Prof. Christiane Gatz und Marco Herde die Expression von Transkriptionsfaktoren untersucht. Ihre Resultate deuten auf eine Expression von SA-regulierten Genen hin, während JA-abhängige Faktoren nicht induziert wurden; dies bestätigt die Hypothese der Blockade der JA-Biosynthese durch SA (**2**) bei *A. thaliana*.

Stress durch Schwermetallionen

Neben biotischen Elizitoren beeinflussen auch abiotische Stressfaktoren den Phytohormonhaushalt von Pflanzen. Im Rahmen des Graduiertenkollegs zur Regenerations- und Funktionsanalyse degenerierter Ökosysteme (GRK 266) wurden pflanzliche Reaktionen auf Schwermetallbelastung untersucht.

In Modellversuchen mit *P. lunatus* wurde eine Induktion von Duftemission und der Biosynthese von SA (**2**) und Ethylen (ET; **3**) durch Schwermetallionen, insbesondere durch Cu^{2+}-Ionen (700 µM), beobachtet. Die Stressantwort von *P. lunatus* auf Schwermetallionen ähnelt dabei ihrer Reaktion auf den Kanalbildner Alamethicin.

Die Inhibierung der Duftproduktion durch Aristolochiasäure (**87**), einem Phospholipase-inhibitor, belegt die Beteiligung eines fettsäureabgeleiteten Signals bei der Reaktion der Limabohne auf Schwermetallionen. Zwar ergab die Quantifizierung von Oxylipinen nach Cu^{2+}-Ionenbehandlung ein charakteristisches Oxylipinmuster, jedoch wurde bisher noch keine Verbindung identifiziert, die als Signal nach Schwermetallbelastung wirkt. Es konnte aber gezeigt werden, dass sowohl enzymatisch als auch nichtenzymatisch gebildete Fettsäureoxidationsprodukte eine Schlüsselrolle bei diesen sehr ähnlichen pflanzlichen Reaktionen auf biotischen und abiotischen Stress spielen.

9 MATERIALS AND METHODS

9.1 Cultivation of plants and rearing of caterpillars

Plant material

Lima bean (*Phaseolus lunatus* L. cv. Ferry Morse var. Jackson Wonder Bush) plants were grown in sterilized pot soil under greenhouse conditions at 21 - 23 °C, 50 - 60 % humidity, and a light regime of 14 h light (approximately 300 µE m^{-2} s^{-1}) and 10 h darkness. Experiments were conducted with 12- to 14-day-old plantlets with fully developed primary leaves.

Arabidopsis thaliana was grown hydroponically on non sterile rock wool under short day conditions (9.30 h light, approximately 200 µE m^{-2} s^{-1}) at 22 °C, 50 % humidity. Stone wool was used to carry the seeds and was in contact with a 10 l tank, containing Hoagland solution [355]. Six week old plants were used for the experiments.

Medicago truncatula seeds were allowed to germinate in the dark for 4 days, and then the seedlings were grown under greenhouse conditions at 18 - 23 °C with a light period from 7:00 to 21:00. Humidity was kept at 60 - 70 %.

Caterpillar rearing

Spodoptera littoralis larvae were hatched from eggs and reared on agar-based artificial diet. Plastic cabinets with the diet and larvae were kept at 23 - 25 °C under a regime of 16 h illumination and a dark period of 8 h.

The artificial diet was prepared from 500 g of ground white beans, which were soaked over night in 1200 ml water. 9 g vitamin C, 9 g paraben, 4 g formalin, 75 g agar boiled in 1000 ml water were added (modified after Bergomaz and Broppé (1986) [356]). Experiments were conducted with 2^{nd} - 3^{rd} instar larvae.

9.2 General methods and chemicals

9.2.1 Instruments

Fourier Transform Infrared Spectroscopy (FT-IR)

IR-spectra were recorded with a Bruker Equinox 55 FT-IR using an IRscope II microscope (Bruker BioSpin GmbH, Rheinstetten, Germany).

Nucleic Magnetic Resonance Spectroscopy (NMR)

NMR-spectra were recorded with a Bruker Avance DRX 500 or Bruker AV 400 (Bruker BioSpin GmbH, Rheinstetten, Germany).

Chemical shifts δ are given in ppm and coupling constants *J* in Hz. The solvent signal was used for calibration: ^{1}H-NMR: $CDCl_3$ δ = 7.26 ppm, ^{13}C-NMR $CDCl_3$ δ = 77.16 ppm; ^{1}H-NMR: CD_3OD δ = 3.31 ppm, ^{13}C-NMR CD_3OD δ = 49.00 ppm.

Gas Chromatography-Mass Spectrometry (GC-MS)

EI-GC-MS: quadrupole instrument Finnigan Trace MS (Thermoelectron, Bremen, Germany): Ionization energy 70 eV; GC-column: Alltech EC-5 (15 m x 0.25 mm x 0.25 µm; Alltech, Unterhachingen, Germany); automatical injection: A200S (CTC-Analytics, Zwingen, Switzerland). Data were acquired under the control of the software package Finnigan Xcalibur version 1.1.

EI-GC-MS and NCI-GC-MS: ion trap instrument Finnigan GCQ (Thermoelectron, Bremen, Germany): Ionization energy 70 eV; CI-gas: methane; GC-columns: Alltech EC5 (30 m x 0.25 mm, 0.25 µm; Alltech, Unterhachingen, Germany) and Restek RTX-200 (30 m x 0.25 mm, 0.25 µm; Restek, Bad Homburg, Germany); automatical injection: A200SE (CTC-Analytics, Zwingen, Switzerland). Data were acquired using the software package Finnigan Xcalibur 1.0.

High resolution mass spectra were obtained using a Waters LCT Premier by directly injecting the sample.

Preparative HPLC

Preparative separation was achieved by a Gilson HPLC (Gilson international, Bad Camberg, Germany) equipped with a Gilson 115 UV detector and a Gilson 206 fraction collector. The instruments were controlled by the UniPoint 3.01 software.

9.2.2 Chemicals

All chemicals used were at least p.a. grade and purchased from Sigma-Aldrich (Taufkirchen, Germany). Selected chemicals were obtained from specified providers. Solvents and silica gel were purchased from VWR International GmbH (Darmstadt, Germany). *N*-methyl-trimethylsilyl-trifluoroacetamide (MSTFA) was obtained from Macherey-Nagel (Düren, Germany).

9.2.3 Oxylipins and phytohormone standards

Jasmonic acid (**1**) was obtained from its methyl ester (provided by Dr. R. Kaiser, Givaudan-Roure, Dübendorf, Switzerland) by saponification with K_2CO_3. Enriched *cis*-jasmonic acid (*cis*-**1**) (Bedoukian Research Inc., Danbury, USA) and a sample of pure *cis*-jasmonic acid (*cis*-**1**) (Larodan Fine Chemicals, Malmö, Sweden) were kindly provided by Prof. I. T. Baldwin (MPI-CO, Jena, Germany). 12-Oxophytodienoic acid (**7**) was donated by Prof. Dr. C. Wasternack (IPB, Halle, Germany). Phytoprostanes of the F_1 type (**25** and **26**) were a gift from Prof. Dr. Thierry Dunand (Université Montpellier, Montpellier, France).
13-Hydroxy-12-oxo-9,15-octadecadienoic acid (α-ketol; **9**), 9-hydroxy-12-oxo-10,15-octadecadienoic acid (γ-ketol; **10**), 12,13-epoxy-11-hydroxy-9,15-octadecadienoic acid methyl ester (12,13-epoxy-11-HODE; **20**) 10,11-epoxy-9-hydroxy-12,15-octadecadienoic acid (**74**), 12,13-epoxy-9-hydroxy-10,15-octadecadienoic acid (**75**), 9,10,11-trihydroxy-12,15-octadecadienoic acid (**72**), 9,12,13-trihydroxy-10,15-octadecadienoic acid (**73**) and traumatin (**29**) were purchased from Larodan Fine Chemicals (Malmö, Sweden).

[3,4,5,6-$^2H_4$]-salicylic acid was synthesized from [3,4,5,6-$^2H_4$]-salicylaldehyde [357] via oxidation [340]. [9,10-$^2H_2$]-dihydrojasmonic acid was obtained by hydrogenation of JA (**1**) with deuterium gas following a procedure of Koch *et al.* [67]. Both standards were already available in our group. Ryan Lauchli synthesized [15,16-$^2H_2$]-tetrahydrodicranenone B [358] as well as 11-oxo-9-undecenoic acid (**48**) and [9,10-$^2H_2$]-11-oxo-9-undecenoic acid. The latter were synthesized by *i*) alkylation of 8-bromooctanoic acid with the lithium salt of propinyl-THP, followed by *ii)* deprotection, *iii)* reduction of the triple bond with P2-Ni [359] and *iv)* oxidation of the allylic alcohol with MnO_2. 13-Oxo-9,11-tridecadienoic acid (**18**) was synthesized by Sven Adolph [360]. 9-Oxononanoic acid (**30**) was synthesized by Dieter Spiteller [361]. Phytoprostane B_1 type I and type II (**23** and **24**) were synthesized by Annika Schmidt after a modified approach of Lauchli *et al*. (2003) [358].

9.2.4 Synthesis of oxylipins

Synthesis of 9-KOTE (71)

1 kg of ripe tomato fruits was homogenized in 500 ml 0.1 M phosphate buffer pH 5.7. 1 g of α-linolenic acid (**4**) was emulsified in 30 ml of the same buffer containing 0.1 ml of Tween 20 with the help of ultrasound. The α-linolenic acid (**4**) was added to the tomato homogenate and stirred for 4 h while being continuously flushed by a flow of compressed air. The reaction was stopped by adding 20 ml of 0.2 N HCl, and the fatty acid hydroperoxide was extracted three times with 300 ml diethylether. After removal of the solvents, a crude yellow oil resulted (0.7 g; 70%). The hydroperoxides were redissolved in 10 ml CH_2Cl_2 and reduced with 100 µl $P(OCH_3)_3$ to their alcohols. The solvent and excess reagent was removed *in vacuo* and 9-HOTE (**70**) was purified on silica gel (Kieselgel 60, 230 - 400 mesh) using $CHCl_3$ as solvent (0.35 g yield: 50%).

9-HOTE (**70**) was oxidized to 9-KOTE (**71**) with the help of Bobbitt´s reagent (4-acetylamino-2,2,6,6-tetramethylpiperidine-1-oxoammonium perchlorate) [362]. 200 mg of 9-HOTE were dissolved in 10 ml CH_2Cl_2 containing 280 mg Bobbitt´s oxoammonium salt and 200 mg silica. After stirring the mixture for about 1 h, it was filtered through filter paper. After removal of solvent on a rotation evaporator, the mixture was purified by flash chromatography on silica using hexane/ethylacetate/acetic acid (1:1:0.1 % v:v:v) (yield 172 mg, 86 %).

FT-IR (cm^{-1}): 2500-3500, 2932, 2857, 1708, 1631, 1589, 1461, 1409, 1279, 976.

^{1}H-NMR: (500 MHz, $CDCl_3$): δ (ppm) 0.99 (t, *J* = 7.46, 3H, CH_3-18), 1.28-1.40 (m, 6H), 1.56-1.69 (m, 4H), 2.10 (“q”, *J* = 7.40, 2H, CH_2-17), 2.35 (t, *J* = 7.51, 2H, CH_2-8), 2.55 (t, *J* = 7.43, 2H, CH_2-2), 3.06 (t, *J* = 7.46, 2H, CH_2-14), 5.28-5.36 (m, 1H, CH_2-15), 5.44-5.52 (m, 1H, CH_2-16), 5.82-5.90 (m, 1H, CH_2-13), 6.10-6.18 (m, 1H, CH_2-12), 6.18-6.22 (d, *J* = 15,30, 1H, CH_2-10), 7.46-7.46 (dd, *J* = 15,19, *J* = 11,70, 1H, CH_2-11).

^{13}C-NMR (125 MHz, $CDCl_3$): δ (ppm) 14.84, 21.32, 24.91, 25.29, 27.27, 29.55, 29.72, 29.75, 34.54, 41.69, 125.96, 127.56, 130.39, 134.03, 137.44, 140.86, 179.83, 201.70

HR-ESI-MS: $[M+Na]^+$ ($C_{18}H_{28}O_3Na$) observed: 315.1932, calc: 315.1936;
$[M+H]^+$ ($C_{18}H_{29}O_3$) observed: 293.2137, calc: 293.2117.

Synthesis of 13-KOTE (21)

0.5 g of α-linolenic acid (**4**) was emulsified in 300 ml of 0.1 M Tris-buffer pH 9 containing 0.1 ml of Tween 20 with the help of ultrasound. The α-linolenic acid (**4**) was incubated with 50 mg soybean lipoxygenase while stirring and continuously flushing with compressed air for 1 h. The reaction was stopped by adding 5 ml of 2 N HCl, and the fatty acid hydroperoxide was extracted three times with 100 ml diethyl ether. After removal of the solvents, a crude oil was obtained (450 mg; 90%). The hydroperoxide was redissolved in 10 ml MeOH and reduced with $NaBH_4$ (50 mg) for 2 h at 0 °C and 1 h at RT [95]. The fatty acid was extracted from the reaction mixture with diethylether. The solvent was removed and the 13-HOTE (**19**) purified on silica gel using CH_2Cl_2/methanol/acetic acid (12:1:0.1 % v:v:v) as solvent (yield: 175 mg, 31 %).

175 mg of 13-HOTE (**19**) was oxidized to 13-KOTE (**21**) with the help of Bobbitt´s reagent following the same procedure as described for 9-KOTE (**71**) (yield: 130 mg, 74 %). The product turned out to be a mixture of various oxo-fatty acid isomers. An attempt was made to separate these by preparative HPLC.

HPLC conditions:

Column: Grom Sil 120 ODS-5ST (particle size 5 µm; 250 mm x 10 mm; Grom Chromatography GmbH, Rottenburg-Hailfingen); Solvents: H_2O + 0.1 % formic acid (A) and acetonitrile (B). Flow rate: 6.25 ml / min. Gradient: start with 35 % B, in 15 min to 60 % B, in 4 min to 65 % B, hold for 4 min, in 7 min to 100 % B, hold for 2 min. Detection: UV at 234 nm.

The separation was not satisfactory and only a small fraction of a mixture of 9-KOTE (**71**) and 13-KOTE (**21**) was obtained (14 mg, 10 %). However, by comparison with the pure 9-KOTE (**71**) sample together with literature data of 13-KOTE (**21**) the obtained mixture was sufficient to confirm the identity of 13-KOTE (**21**) in plant material with GC-MS.

FT-IR (cm^{-1}): 2500-3500, 3014, 2930, 2856, 1708, 1587, 1000-1461.

^{1}H-NMR (500 MHz, $CDCl_3$): 0.99 (t, *J* = 7.48, 3H), 1.15-1.4 (m, 8H), 1.50-1.62 (m, 2H), 2.00-2.12 (m, 2H), 2.30-2.38 (m, 4H), 3.30 (d, *J* = 6.35, 2H), 5.43-5.65 (m, 2H), 5.81-5.96 (m, 1H), 6.07-6.24 (m, 2H), 7.48-7.55 (m, 1H).

HR-ESI-MS: $[M+Na]^+$ ($C_{18}H_{28}O_3Na$) observed: 315.1931, calc: 315.1936;
$[M+H]^+$ ($C_{18}H_{29}O_3$) observed: 293.2126, calc: 293.2117.

Synthesis of 9-hydroxy-10-oxostearic acid (76) and 10-hydroxy-9-oxostearic acid (77)

Both compounds were obtained by oxidizing *threo*-9,10-dihydroxystearic acid with Bobitt´s reagent [362]. About 100 mg of 9,10-dihydroxystearic were dissolved in 30 ml CH_2Cl_2 containing 200 mg Bobbitt´s oxoammonium salt and 200 mg silica. This resulted in unspecific oxidation of either the 9-hydroxy- or the 10-hydroxy-moiety. Formation of the dioxo-compound was not observed. After stirring the mixture for about 2 h, it was filtered through filter paper. The removal of solvent on a rotation evaporator yielded 94 mg (94 %) of crude oxidized fatty acid. The mixture was separated by flash chromatography on silica with petroleum ether/diethylether 1:2 (yield: 10 mg, 10 %), however, the regioisomers 9-hydroxy-10-oxostrearic acid (**76**) and 10-hydroxy-9-oxostreatic acid (**77**) were not separated and used as a mixture of both compounds.

FT-IR (cm^{-1}): 2400-3500, 3328, 3239, 2919, 2851, 1710, 899-1464.

^{1}H-NMR (500 MHz, $CDCl_3$): δ (ppm) 0.88 (t, *J* = 6.67, 6H, CH_3-18), 1.17-1.40 (m, 36H), 1.40-1.56 (m, 4H), 1.56-1.70 (m, 8H), 1.74-1.86 (m, 2H), 2.27-2.54 (m, 8H), 4.14-4.20 (m, 2H, CHOH 9, CHOH 10).

^{13}C-NMR (125 MHz, $CDCl_3$): δ (ppm) 14.75, 14.76, 23.31, 23.33, 24.21, 24.36, 25.28, 25.32, 25.45, 29.50, 29.58, 29.62, 29.68, 29.70, 29.78, 29.88, 29.89, 29.93, 29.99, 30.10, 30.15, 32.48, 32.53, 34.39, 34.48, 38.49, 38.58, 77.03, 77.12.

HR-ESI-MS: $[M+H]^+$ ($C_{18}H_{35}O_4$) observed: 315.2527, calc: 315.2535.

9.2.5 Derivatization techniques for GC-MS analysis

Methylation using diazomethane

Diazomethane was obtained by dropwise addition of an ethereal solution of diazald to 0.1 M KOH in presence of diethyleneglycol monoethylether at 70 °C. The generated ethereal solution of diazomethane was distilled and collected at -80 °C.

For methylation 1 ml of a diazomethane solution in diethylether were added to the sample. After 5 min excess of diazomethane and diethylether were removed in a gentle stream of nitrogen.

Generation of pentafluorobenzylesters

Samples (about 0.05 - 0.5 mg) were treated with 200 µl *N*,*N*-diisopropylethylamine (10 % in acetontrile, v:v) and 200 µl 2,3,4,5,6-pentafluorobenzyl bromide (PFBBr) (10 % in acetonitrile, v:v). Reaction took place for 30 min at RT, and then the solvent and excess reagent was removed under a stream of nitrogen [363]. Depending on the amount, the sample had to be diluted with diethyl ether of CH_2Cl_2 before GC-MS analysis.

Generation of pentafluorobenzyloximes

Samples were derivatized with excess of PFBHA (0.1 - 1 ml, 0.05 M in MeOH) for 2 h at RT. The solvent was removed with a stream of nitrogen; the samples were methylated and depending on their amount, were diluted before GC-MS analysis.

Trimethylsilylation

To derivatize free hydroxyl groups of highly functionalized oxylipins 10 - 50 µl *N*-methyl-trimethylsilyl-trifluoroacetamide (MSTFA) were added to the sample usually after methylation. The sample was incubated for 60 min at 40 °C. Depending on the amount, the sample had to be diluted with diethyl ether or CH_2Cl_2 before GC-MS analysis.

9.3 Analysis of plant volatiles

9.3.1 Closed-loop-stripping

Volatile collection

Lima bean plantlets were cut and placed in small vials containing 2 ml of water. For elicitation of volatile emission chemicals were dissolved in the water or *S. littoralis* larvae were placed on the leaves (see stress induction experiments, Chapter 9.5). To achieve high concentration of emitted volatiles in the headspace, the vials with the cut plantlets were enclosed in small (750 ml) desiccators. These were sealed with Teflon-stoppers and volatiles were collected with small pumps (Fürgut, Aitrach, Gemany) on charcoal filters (1.5 mg of charcoal, CLSA-filter; Le Ruisseau de Montbrun, Daumazan sur Arize, France), according to the „closed-loop-stripping“-method [364]. Volatiles were desorbed from the carbon traps with CH_2Cl_2 (2 x 20 µl) containing the internal standard 1-bromodecane (200 µg ml^{-1}). Volatiles were analyzed by GC-MS.

GC-MS conditions for volatile detection

Analysis was carried out on a Trace MS instrument. The instrument was equipped with an Alltech EC-5 capillary (15 m x 0.25 mm x 0.25 µm). Helium at a constant flow (1.5 ml min^{-1}) served as carrier gas. Samples (1 µl) were automatically injected with a split ratio of 1:10; the injector temperature was adjusted to 220 °C. Separation of compounds was achieved under programmed conditions (40 °C for 2 min, 10 °C min^{-1} to 200 °C, 30 °C min^{-1} to 280 °C, hold for 1 min). The transfer line was set to 270 °C. Filament emission current was 250 µA with an ion source temperature of 200 °C. Compounds were identified by retention time and matching against reference spectra.

9.3.2 zNose

For continuous monitoring of volatile emission from leaves of *P. lunatus*, a small portable GC (zNose, Electronic Sensor Technology, Newbury Park, CA, USA) was used [248]. The GC was equipped with a DB 5 stainless steel column (1 m x 0.25 µm x 0.25 mm) and a very sensitive surface acoustic wave quartz microbalance detector. After a 30 s collection time on absorption material (Tenax) the volatiles were separated in a 3 ml min^{-1} He flow from 40 °C to 175 °C in 5 °C min^{-1}. The inlet and the 4 port valve were heated to 180 °C and 160 °C respectively. Samples were taken every 10 min. Compounds were identified by retention time compared to synthetic standards.

9.4 Phytohormone analysis

9.4.1 Ethylene

Ethylene emission was determined in cooperation with Prof. Frank Kühnemann (Institut für Angewandte Physik der Universität Bonn). Emission of this volatile phytohormone was analyzed with the help of photoacoustic laser spectroscopy. [341,365]. The instrument consists of a CO_2-laser (9 - 11 µm wavelength) and a resonant photoacoustic cell which is in line with a flow-through system. The ethylene absorbs the emission frequency of the laser which is mechanically chopped and the molecules are exited to a higher vibration state. Collision with other molecules increases kinetic energy and thus leads to a higher temperature of the gas, which also leads to an increase in pressure of the closed photoacoustic cell. The periodical pressure changes of the cell can be recorded with a sensitive microphone. The instrument used by Prof. Frank Kühnemann is tuned to detect trace amounts of ET (**3**) as low as 6 picoliters per liter. For details see Voesenek *et al.* (1990) [365].

Lima bean plantlets were cut and placed into a vial containing 700 µM $CuSO_4$ or water for control plants. Samples and controls were positioned into separate chambers which were connected to two photoacoustic cells via a constant flow of catalytically purified air. ET-emission from elicited and control plants was monitored every 3 min.

9.4.2 Salicylic acid

For determination of SA (**2**) the protocol of Engelbert *et al.* (2001) [186] was followed. In brief, one gram of frozen plant material was ground with a high performance dispenser at 24000 rpm (Ultra-Turrax T 25, IKA-Werk, Germany) in a solution of acetone and 50 mM citric acid (70:30 v:v); [3,4,5,6-$^2H_4$]-SA (500 ng) was added as internal standard. The acetone was evaporated over night and samples were extracted three times with 10 ml diethylether. The pooled organic phases were purified by solid phase extraction on Chromabond NH_2 cartridges (0.5 g; Macherey-Nagel, Düren, Germany). After loading of the sample, the cartridges were washed with a solvent mixture of 2-propanol:CH_2Cl_2 (5 ml, 2:1, v:v) and eluted with diethyl ether:formic acid (10 ml, 98:2, v:v). The samples were taken to dryness in a stream of argon, and the residue was methylated with excess of an ethereal diazomethane solution.

GC-MS conditions for SA detection

Samples were analyzed with a Finnigan Trace MS. The instrument was equipped with an Alltech EC-5 capillary column (15 m x 0.25 mm x 0.25 µm). Helium at a constant flow (3 ml min^{-1}) served as carrier gas. Samples (1 µl) were automatically injected with a split ratio of 1:10; the injector temperature was adjusted to 260 °C. The transfer line was kept at 290 °C. Separation of compounds was achieved under programmed conditions from 80 °C (2 min) to 127 °C at 8 °C min^{-1} (hold 5 min) and 30 °C min^{-1} to 280 °C, maintained for 3 min prior to cooling. Mass spectra were taken at 70 eV (EI mode). Filament emission current was set to 250 µA with an ion source temperature of 200 °C. To enhance sensitivity, mass spectra were recorded in selected ion monitoring (SIM) by monitoring the base peak of MeSa (**39**) and [3,4,5,6-$^2H_4$]-MeSa fragments at m/z 120 and m/z 124 respectively.

9.4.3 Oxylipins

Analysis of oxylipins as pentafluorobenzyl esters

Leaf material was extracted after a modified protocol of Engelbert *et al*. (2001) [186]. Instead of using diazomethane for transesterification, samples were treated with 200 µl *N*,*N*-diisopropylethylamine (10 % in acetonitrile, v:v) and 200 µl 2,3,4,5,6-pentafluorobenzyl bromide (PFBBr) (10 % in acetonitrile, v:v). Reaction took place for 30 min at RT, then the

solvent and excess reagent was removed under a stream of nitrogen [363]. Samples were taken up in 50 µl diethyl ether and analyzed by GC-MS.

Analysis of oxylipins as pentafluorobenzyl oximes

Leaf material (ca. 0.5 g) was harvested, immediately frozen with liquid nitrogen and stored at -80 °C. For oxylipin analysis, the plant material was covered with 5 ml MeOH containing 0.05 % 2,6-di-*tert*-butyl-4-methylphenol (BHT) followed by addition of PFBHA (3 ml, 0.05 M in methanol). For quantification [$^2H_2$]-JA (150 ng), [$^2H_2$]-*iso*-OPDA (250 ng), [$^2H_2$]-11-oxoundec-9-enoic acid (250 ng), and 250 ng of the 9(10)-hydroxy-10(9)-oxooctadecanoic acid mixture (**76** and **77**) were added as internal standards. Next, the whole mixture was cooled on ice and homogenized for 5 min under an inert atmosphere (argon) with a high performance dispenser at 24000 rpm (Ultra-Turrax T 25, IKA-Werk, Germany). To complete the extraction and *in situ* derivatization the samples were vigorously shaken at RT for 2 h. Then, 4 ml diluted HCl (pH 3) was added to the raw methanol extract. The methanol/water phase was carefully extracted with hexane (3 x 10 ml) and after centrifugation the hexane layers were collected and combined (hexane fraction). 4 ml diluted HCl (pH 3) were added to the remaining polar phase to enhance phase separation and extraction was repeated with CH_2Cl_2 (2 x 10 ml). After separation of phases by centrifugation the dichloromethane extracts were combined (CH_2Cl_2 fraction).

Next, the combined hexane fractions were passed through Chromabond NH_2 cartridges (0.5 g; Macherey-Nagel, Düren, Germany). Prior to loading, the cartridges were preconditioned with MeOH (5 ml) and hexane (5 ml). After loading of the samples, the cartridges were washed with a binary solvent mixture of 2-propanol:CH_2Cl_2 (5 ml, 2:1, v:v) and eluted with diethyl ether:formic acid (10 ml, 98:2, v:v). The solvent was removed at RT by a stream of argon. For derivatization of the carboxyl groups, the samples were treated with an etheral solution of diazomethane (1 ml). After 2 min, excess of diazomethane and the solvent were removed by a stream of nitrogen; the residue was dissolved in dichloromethane (30 µl) and analyzed by GC-MS. For derivatization of hydroxyl groups of the oxylipins, 30 µl MSTFA were added and the sample was heated to 40 °C for 1 h, and analyzed without further dilution. Since relevant oxylipins in the hexane fraction did not contain hydroxyl groups, this derivatization step was not routinely applied to the hexane fraction.

The CH_2Cl_2 fractions, containing more polar oxylipins, were passed through preconditioned Chromabond NH_2 cartridges (1 g; Macherey-Nagel, Düren, Germany). Preconditioning was achieved by consecutive passage of methanol (5 ml) and dichloromethane (5 ml). After loading the analytes, the cartridges were washed with dichloromethane (5 ml) and eluted with a binary mixture of diethylether and formic acid (10 ml, 98:2, v:v). The solvent was evaporated by a stream of argon at RT and the residue treated with an etheral solution of

diazomethane (1 ml) for 5 min. After evaporation to dryness (nitrogen stream at RT) the residue was dissolved in MSTFA (30 µl) and exhaustive silylation was achieved at 40 °C in 1 h. The samples were analyzed by GC-MS without further dilution.

GC-MS conditions for oxylipin detection

Samples were analyzed with a Finnigan GCQ ion trap mass spectrometer. The instrument was run in the EI positive mode for identification of fatty acids and oxylipins. The negative chemical ionization mode (NCI) was used for the quantification of PFB-oximes. Alternatively, EI-MS analysis was performed on a Finnigan GC-Trace MS quadrupol mass spectrometer.

***Instrumental conditions (Finnigan GCQ)*:** The instrument was equipped with a nonpolar guard column (3 m; Supelco, Taufkirchen, Germany) linked to a RTX-200 capillary column (30 m x 0.25 mm x 0.25 µm). Helium at a constant rate of 40 cm s^{-1} served as carrier gas. Samples (1 µl) were automatically injected with a split ratio of 1:10; the injector temperature was adjusted to 290 °C. The transfer line was kept at 300 °C. Separation of compounds was achieved under programmed conditions from 100 °C to 210 °C at 10 °C min^{-1} and at 1 °C min^{-1} to 237 °C, followed by rapid heating 40 °C min^{-1} to 300 °C, maintained for 2 min prior to cooling. Mass spectra were taken at 70 eV. The filament emission current was set to 250 µA with a source temperature of 180 °C (same for EI and NCI mode). Methane (at 0.1 mbar pre-vacuum) served as the reagent gas for routine NCI analyses. Low levels of jasmonic acid were determined by using methanol as the reactant gas (0.1 mbar pre-vacuum) for chemical ionization. Methanol is a weaker reactant gas and generates more intense $[M - 20]^{\bullet -}$ fragments. Compounds were identified by their characteristic fragmentation patterns in combination with authentic reference compounds, others were tentatively assigned using the NIST98-library.

***Instrumental conditions (Finnigan Trace MS)*:** The instrument was equipped with an Alltech EC-5 capillary column (15 m x 0.25 mm x 0.25 µm). Helium at a constant flow (1.5 ml min^{-1}) served as carrier gas. Samples (1 µl) were automatically injected with a split ratio of 1:10; the injector temperature was adjusted to 290 °C. The transfer line was kept at 290 °C. Separation of compounds was achieved under programmed conditions from 100 °C to 190 °C at 10 °C min^{-1} and at 4 °C min^{-1} to 250 °C, followed by 15 °C min^{-1} to 300 °C, maintained for 3 min prior to cooling. Mass spectra were taken at 70 eV (EI mode). Filament emission current was set to 250 µA with an ion source temperature of 200 °C. Compounds were identified by their characteristic fragmentation pattern in combination with authentic reference compounds or tentatively assigned using the NIST98-library.

Calibration curves and recovery rates

Response factors and calibration curves were obtained by adding increasing amounts of pure JA (**1**), OPDA (**7**), 11-oxo-9-undecenoic acid (**48**) and 13-oxo-9,11-tridecadienoic acid (**18**) in the range of 20 - 10 000 ng to a solution of the respective internal standards in methanol. Compounds were derivatized with PFBHA (1 ml, 0.05 M in MeOH) for 2 h at RT and with diazomethane (1 ml) as described above. Mass spectroscopic analyses were performed using negative ion chemical ionization (NCI) with methane as reactant gas. Calibration curves were obtained by plotting the area ratio of the test compound and the internal standard ([$^2H_2$]-JA for JA, [$^2H_2$]-*iso*-OPDA for OPDA (**7**) and [$^2H_2$]-11-oxo-9-undecenoic acid for 11-oxo-9-undecenoic acid (**48**) and 13-oxo-9,11-tridecadienoic acid (**18**)) against the amount of added test compound.

Recovery rates were determined from standard addition experiments: The same amounts of analyte and internal standards as used for calibration were added to untreated Lima bean leaves (0.5 g) and carried through the extraction and derivatization procedure. Standard addition curves were calculated by plotting the area ratio of each compound and its internal standard against the amount of added test compound. From the intersection of the curve with the x-axis the resting level for the respective oxylipin of non-induced Lima bean leaves was obtained (Chapter 9.8). Recovery was calculated by comparison with the external standard curve. The calculated amount of JA (**1**), OPDA (**7**) and the two aldehydes (**48** and **18**) were corrected by the respective resting level of the untreated Lima bean leaves to give the recovered amount of the analyte.

9.5 Stress induction experiments

9.5.1 Mechanical wounding

Primary leaves of 12- to 14-days-old undamaged Lima bean plantlets were wounded with a pattern wheel, in a way that the entire primary leaf was punched. Damaged leaves were harvested 40, 60, 90 120, 240 and 600 min after wounding, weighed, and immediately frozen with liquid nitrogen and stored at -80 °C until they were used for phytohormone analysis.

9.5.2 Caterpillar feeding

2nd - 3rd instar *S. littoralis* larvae were placed on intact plantlets of *P. lunatus* (four on each plant). Plant material from the caterpillar-damaged leaves was harvested after 24 h. To distinguish between different regions of the damaged leaf, the leaf material around the feeding areas was cut with a razor blade generating up to 10 mm thick leaf stripes. Then again a 10 mm thick stripe was cut to receive leaf material further away from the feeding

area. The cutting with the razorblade was done as quickly as possible and the leaf stripes were immediately frozen, to avoid scrambling of the signal due to wound response. Additionally, the neighboring leaves and the systemic developing leaves were harvested. The plant material was weighed and immediately frozen in liquid nitrogen and stored at -80 °C until the samples were subjected to the workup procedure.

9.5.3 Incubation of *A. thaliana* with alamethicin

ALA was added to the hydroponic medium of *A. thaliana*, thus that the end concentration was 5 µg ml^{-1}. Plants were harvested in time intervals of 30, 60, 90 120, 180, 240, 360, 480, and 720 min after induction, weighed, and stored at -80 °C until phytohormone analysis. Control plants were kept in the hydroponic medium only.

9.5.4 Incubation of *P. lunatus* with chemical elicitors and inhibitors for volatile analysis

For induction of plant stress response with chemical elicitors, plantlets were cut with a razor blade and immediately transferred into vials containing a solution of the elicitor, allowing it to be taken up through the petiole.

ALA was dissolved in methanol at a concentration of 10 mg ml^{-1}. 10 µl of the stock solution were added to 10 ml of tap water resulting in a final concentration of 10 µg ml^{-1} ALA.
Heavy metal salts ($AlCl_3$, K_2CrO_4, $MnSO_4$, $(NH_4)_2Fe(SO_4)_2$, $FeCl_3$, $NiCl_2$, $CuSO_4$, $ZnSO_4$, $CdCl_2$, $SnCl_2$, $HgCl_2$) were applied in concentrations between 10 - 1000 mM in tap water.

For preincubation of Lima bean with inhibitors of volatile biosynthesis, plantlets were placed in vials containing the inhibitor and preincubated for 24 h. Then, the plants were placed in vials containing the elicitor ($CuSO_4$, 700 mM) together with the inhibitor and volatile collection was conducted during the following 24 h.
Phenidone (**88**) was applied as a 1 mM solution in tap water. Aristolochic acid (**87**) was dissolved in DMSO at a concentration of 1 mM. This stock solution was dissolved in 10 ml of tap water to achieve a final concentration of 0.3 mM aristolochic acid [186,315]. Control plants were kept in tap water (with the respective amount of MeOH or DMSO) for 2 x 24 h.

9.5.5 Incubation of *P. lunatus* with $CuSO_4$

For SA-analysis, Lima bean plantlets were cut with a razor blade and immediately transferred into vials containing 700 mM of $CuSO_4$. Plant leaves were harvested after 120, 200, 300, 500 and 800 min, weighed, and immediately frozen with liquid nitrogen and stored

at -80 °C until they were used for phytohormone analysis. Control plants were kept in vials containing H_2O only.

In an independent experiment, Lima bean plantlets were detached with a razor blade and immediately transferred into vials containing 750, 300, 500, 800 or 1000 mM of $CuSO_4$ or 10 µg ml^{-1} ALA. Plant leaves were harvested after 500 min, weighed, and immediately frozen with liquid nitrogen and stored at -80 °C until they were used for phytohormone analysis. Control plants were kept in vials containing H_2O only.

For oxylipin analysis Lima bean plantlets were cut with a razor blade and immediately transferred into vials containing 700 mM of $CuSO_4$. Plant leaves were harvested after 40, 80, 430 and 585 min, weighed, and immediately frozen with liquid nitrogen and stored at -80 °C until they were used for phytohormone analysis. Control plants were kept in vials containing H_2O only.

9.6 Collection of caterpillar regurgitant and frass

2^{nd}-3^{rd} instar larvae were allowed to feed on detached Lima bean plantlets, which were placed with their stalk in sealed plastic tubes to provide the plants with water. Regurgitant was collected after 24 h of feeding by holding the insect with a pair of light forceps and gently touching the mandibles with a small glass capillary. The volume of obtained regurgitant was measured with a volumetric pipette (usually about 300 - 700 µl) and immediately 1 ml of 0.05 M PFBHA in MeOH was added to the regurgitant to derivatize labile compounds. Frass from the caterpillars was collected from the bottom of rearing container. Only dark green frass (0.5 g), derived from plant material was collected and treated accordingly to the regurgitant. The samples were then subjected to the extraction and purification protocol for oxylipins (Chapter 9.4.3).

9.7 Isomerization of OPDA to *iso*-OPDA

OPDA (**7**) was incubated in citrate-phophate buffer (pH 3, 5, or 7) and Tris-HCl buffer (pH 8 or 10) for 4 h and for 10 h. The oxylipin was extracted from the acidified aqueous medium with CH_2Cl_2 and derivatized with PFBHA and diazomethane prior to GC-MS-analysis (Chapter 9.4.3).

9.8 Regression analysis and statistics

Regression analysis

The unknown amount of analyte in a sample of plant extract can be calculated by regression analysis. A calibration curve was recorded (see Chapter 9.4.3) and a linear relationship between the area ration of analyte and internal standard (y) with the amount of present analyte (x) was calculated using Origin 7 (Equation 1). Resting levels of analytes in the Lima bean leaves were estimated from the intercept of the regression curve, y = 0 representing the value of no additionally added analyte (
Equation 2).

$$y = a + b\,x$$

Equation 1 Linear relationship between the area ration of analyte and internal standard (y) and the amount of added analyte (x).

$$-x = a / b$$

Equation 2 Calculation of the resting level of the analyte in the plant matrix.

Each factor a and b is afflicted with an error, Δa and Δb which was calculated using Origin 7. The standard deviation of x (Δx) was calculated after Gauß [340,366] (Equation 3).

$$\Delta x = \left[\left(-\frac{(y-a)}{b^2} \cdot \Delta b \right)^2 + \left(\frac{1}{b} \cdot \Delta y \right)^2 + \left(-\frac{1}{b} \cdot \Delta a \right)^2 \right]^{\frac{1}{2}}$$

Equation 3 Gaussian calculation of the standard deviation of x.

When calculating the resting level from the standard addition curve (y = 0), the error can be estimated using Equation 4.

$$\Delta x = \left[\left(-\frac{1}{b} \cdot \Delta a \right)^2 + \left(\frac{a}{b^2} \cdot \Delta b \right)^2 \right]^{\frac{1}{2}}$$

Equation 4 Gaussian calculation of the standard deviation of the resting level.

Statistics

Due to small numbers of replicates of 3 to 6, statistical analysis of the data was assumed to be not meaningful. Differences between various treatments can be readily deduced from the box-plots, or by comparing the error bars representing the 95 % confidence interval of the data set.

10 REFERENCES

1. A.A. Agrawal, S. Tuzun, and E. Bent. **1999**. Induced plant defenses against pathogens and herbivores - Biochemistry, ecology and agriculture. APS Press, St. Paul, Minesota.
2. H. Schildknecht. **1981**. Irritant and defense substances of higher plants - a chemical herbarium. Angew. Chem.-Int. Edit. Engl. 20(2): 164-184.
3. U. Wittstock and J. Gershenzon. **2002**. Constitutive plant toxins and their role in defense against herbivores and pathogens. Curr. Opin. Plant Biol. 5(4): 300-307.
4. K. Konno, C. Hirayama, H. Yasui, and M. Nakamura. **1999**. Enzymatic activation of oleuropein: A protein crosslinker used as a chemical defense in the privet tree. Proc. Natl. Acad. Sci. USA 96(16): 9159-9164.
5. R.M. Broadway, S.S. Duffey, G. Pearce, and C.A. Ryan. **1986**. Plant proteinase inhibitors: a defense against herbivorous insects? Entomol. Exp. Appl. 41(1): 33-38.
6. R. Karban and I.T. Baldwin. **1997**. Induced responses to herbivory. Univ. of Chicago Press, Chicago.
7. G. Arimura, C. Kost, and W. Boland. **2005**. Herbivore-induced, indirect plant defences. Biochim. Biophys. Acta Mol. Cell Biol. Lipids. 1734(2): 91-111.
8. J. Takabayashi and M. Dicke. **1996**. Plant-carnivore mutualism through herbivore-induced carnivore attractants. Trends Plant Sci. 1(4): 109-113.
9. P.W. Paré and J.H. Tumlinson. **1999**. Plant volatiles as a defense against insect herbivores. Plant Physiol. 121(2): 325-331.
10. T.C.J. Turlings, P.J. McCall, H.T. Alborn, and J.H. Tumlinson. **1993**. An elicitor in caterpillar oral secretions that induces corn seedlings to emit chemical signals attractive to parasitic wasps. J. Chem. Ecol. 19(3): 411-425.
11. P.W. Paré and J.H. Tumlinson. **1997**. Induced synthesis of plant volatiles. Nature 385(6611): 30-31.
12. L.L. Walling. **2000**. The myriad plant responses to herbivores. J. Plant Growth Regul. 19(2): 195-216.
13. L. Williams, C. Rodriguez-Saona, P.W. Paré, and S.J. Crafts-Brandner. **2005**. The piercing-sucking herbivores *Lygus hesperus* and *Nezara viridula* induce volatile emissions in plants. Arch. Insect Biochem. Physiol. 58(2): 84-96.
14. T.C.J. Turlings, M. Bernasconi, R. Bertossa, F. Bigler, G. Caloz, and S. Dorn. **1998**. The induction of volatile emissions in maize by three herbivore species with different feeding habits: Possible consequences for their natural enemies. Biol. Control 11(2): 122-129.
15. C.M. De Moraes, W.J. Lewis, P.W. Paré, H.T. Alborn, and J.H. Tumlinson. **1998**. Herbivore-infested plants selectively attract parasitoids. Nature 393(6685): 570-573.
16. J. Takabayashi, S. Takahashi, M. Dicke, and M.A. Posthumus. **1995**. Developmental stage of herbivore *Pseudaletia separata* affects production of herbivore-induced synomone by corn plants. J. Chem. Ecol. 21(3): 273-287.
17. M.J. Chrispeels, L. Holuigue, R. Latorre, S. Luan, A. Orellana, H. Peña-Cortés, N.V. Raikhel, P.C. Ronald, and A. Trewavas. **1999**. Signal transduction networks and the biology of plant cells. Biol. Res. 32(1): 35-60.
18. C. Delessert, I.W. Wilson, D. Van der Straeten, E.S. Dennis, and R. Dolferus. **2004**. Spatial and temporal analysis of the local response to wounding in *Arabidopsis* leaves. Plant Mol.Biol. 55(2): 165-181.
19. M. Maffei, S. Bossi, D. Spiteller, A. Mithöfer, and W. Boland. **2004**. Effects of feeding *Spodoptera littoralis* on Lima bean leaves. I. Membrane potentials, intracellular calcium variations, oral secretions, and regurgitate components. Plant Physiol. 134(4): 1752-1762.

20. O. Herde, H. Peña Cortés, C. Wasternack, L. Willmitzer, and J. Fisahn. **1999**. Electric signaling and Pin2 gene expression on different abiotic stimuli depend on a distinct threshold level of endogenous abscisic acid in several abscisic acid-deficient tomato mutants. Plant Physiol. 119(1): 213-218.
21. S. Zimmermann, T. Ehrhardt, G. Plesch, and B. Müller-Röber. **1999**. Ion channels in plant signaling. Cell. Mol. Life Sci. 55(2): 183-203.
22. B. Blume, T. Nürnberger, N. Nass, and D. Scheel. **2000**. Receptor-mediated increase in cytoplasmic free calcium required for activation of pathogen defense in parsley. Plant Cell 12(8): 1425-1440.
23. T. Jabs, M. Tschöpe, C. Colling, K. Hahlbrock, and D. Scheel. **1997**. Elicitor-stimulated ion fluxes and O_2^- from the oxidative burst are essential components in triggering defense gene activation and phytoalexin synthesis in parsley. Proc. Natl. Acad. Sci. USA 94(9): 4800-4805.
24. D. Scheel. **2002**. Oxidative burst and the role of reactive oxygen species in plant-pathogen interaction. Pages 137-153 *in* D. Inzé and M. Van Montagu, editors. Oxidative stress in plants. Taylor & Francis, London.
25. W. Ligterink, T. Kroj, U. zur Nieden, H. Hirt, and D. Scheel. **1997**. Receptor-mediated activation of a MAP kinase in pathogen defense of plants. Science 276(5321): 2054-2057.
26. P.C. Morris. **2001**. MAP kinase signal transduction pathways in plants. New Phytol. 151(1): 67-89.
27. G.L. de Bruxelles and M.R. Roberts. **2001**. Signals regulating multiple responses to wounding and herbivores. Crit. Rev. Plant Sci. 20(5): 487-521.
28. J. Zhao, L.C. Davis, and R. Verpoorte. **2005**. Elicitor signal transduction leading to production of plant secondary metabolites. Biotechnol. Adv. 23(4): 283-333.
29. H. Fukui, K. Koshimizu, Y. Yamazaki, and S. Usuda. **1977**. Structures of plant growth inhibitors in seeds of *Cucurbita pepo* L. Agr. Biol. Chem. 41(1): 189-194.
30. R. Ranjan and S. Lewak. **1992**. Jasmonic acid promotes germination and lipase activity in nonstratified apple embryos. Physiol. Plant. 86(2): 335-339.
31. B. Hause, I. Stenzel, O. Miersch, H. Maucher, R. Kramell, J. Ziegler, and C. Wasternack. **2000**. Tissue-specific oxylipin signature of tomato flowers: allene oxide cyclase is highly expressed in distinct flower organs and vascular bundles. Plant J. 24(1): 113-126.
32. B.J.F. Feys, C.E. Benedetti, C.N. Penfold, and J.G. Turner. **1994**. *Arabidopsis* mutants selected for resistance to the phytotoxin coronatine are male-sterile, insensitive to methyl jasmonate, and resistant to a bacterial pathogen. Plant Cell 6(5): 751-759.
33. R.A. Creelman and J.E. Mullet. **1997**. Biosynthesis and action of jasmonates in plants. Annu. Rev. Plant Physiol. Plant Molec. Biol. 48: 355-381.
34. S. Berger, E. Bell, and J.E. Mullet. **1996**. Two methyl jasmonate-insensitive mutants show altered expression of AtVsp in response to methyl jasmonate and wounding. Plant Physiol. 111(2): 525-531.
35. B.A. Babst, R.A. Ferrieri, D.W. Gray, M. Lerdau, D.J. Schlyer, M. Schueller, M.R. Thorpe, and C.M. Orians. **2005**. Jasmonic acid induces rapid changes in carbon transport and partitioning in Populus. New Phytol. 167(1): 63-72.
36. M.V. Rao, H. Lee, R.A. Creelman, J.E. Mullet, and K.R. Davis. **2000**. Jasmonic acid signaling modulates ozone-induced hypersensitive cell death. Plant Cell 12(9): 1633-1646.
37. G. Abdala, O. Miersch, R. Kramell, A. Vigliocco, E. Agostini, G. Forchetti, and S. Alemano. **2003**. Jasmonate and octadecanoid occurrence in tomato hairy roots. Endogenous level changes in response to NaCl. Plant Growth Regul. 40(1): 21-27.

38. G.A. Howe. **2004**. Jasmonates as signals in the wound response. J. Plant Growth Regul. 23(3): 223-237.
39. J.S. Thaler. **1999**. Jasmonate-inducible plant defences cause increased parasitism of herbivores. Nature 399(6737): 686-688.
40. R. Halitschke and I.T. Baldwin. **2004**. Jasmonates and related compounds in plant-insect interactions. J. Plant Growth Regul. 23(3): 238-245.
41. R. Halitschke and I.T. Baldwin. **2003**. Antisense LOX expression increases herbivore performance by decreasing defense responses and inhibiting growth-related transcriptional reorganization in *Nicotiana attenuata.* Plant J. 36(6): 794-807.
42. A. Kessler, R. Halitschke, and I.T. Baldwin. **2004**. Silencing the jasmonate cascade: Induced plant defenses and insect populations. Science 305(5684): 665-668.
43. B.A. Vick and D.C. Zimmerman. **1984**. Biosynthesis of jasmonic acid by several plant species. Plant Physiol. 75(2): 458-461.
44. M.J. Mueller. **1997**. Enzymes involved in jasmonic acid biosynthesis. Physiol. Plant. 100(3): 653-663.
45. M.H. Beale and J.L. Ward. **1998**. Jasmonates: key players in the plant defence. Nat. Prod. Rep. 15(6): 533-548.
46. F. Schaller, A. Schaller, and A. Stintzi. **2005**. Biosynthesis and metabolism of jasmonates. J. Plant Growth Regul. 23(3): 179-199.
47. K.D. Chapman. **1998**. Phospholipase activity during plant growth and development and in response to environmental stress. Trends Plant Sci. 3(11): 419-426.
48. T. Munnik, R.F. Irvine, and A. Musgrave. **1998**. Phospholipid signalling in plants. Biochim. Biophys. Acta-Lipids Lipid Metab. 1389(3): 222-272.
49. S.T. Prigge, J.C. Boyington, M. Faig, K.S. Doctor, B.J. Gaffney, and L.M. Amzel. **1997**. Structure and mechanism of lipoxygenases. Biochimie 79(11): 629-636.
50. A.R. Brash. **1999**. Lipoxygenases: Occurrence, functions, catalysis, and acquisition of substrate. J. Biol. Chem. 274(34): 23679-23682.
51. A.R. Brash, S.W. Baertschi, C.D. Ingram, and T.M. Harris. **1988**. Isolation and characterization of natural allene oxides - unstable intermediates in the metabolism of lipid hydroperoxides. Proc. Natl. Acad. Sci. USA 85(10): 3382-3386.
52. D. Laudert, U. Pfannschmidt, F. Lottspeich, H. Holländer-Czytko, and E.W. Weiler. **1996**. Cloning, molecular and functional characterization of *Arabidopsis thaliana* allene oxide synthase (CYP 74), the first enzyme of the octadecanoid pathway to jasmonates. Plant Mol.Biol. 31(2): 323-335.
53. M. Hamberg. **1988**. Biosynthesis of 12-oxo-10,15(*Z*)-phytodienoic acid - Identification of an allene oxide cyclase. Biochem. Biophys. Res. Commun. 156(1): 543-550.
54. H. Weber. **2002**. Fatty acid-derived signals in plants. Trends Plant Sci. 7(5): 217-224.
55. F.L. Theodoulou, K. Job, S.P. Slocombe, S. Footitt, M. Holdsworth, A. Baker, T.R. Larson, and I.A. Graham. **2005**. Jasmonoic acid levels are reduced in COMATOSE ATP-binding cassette transporter mutants. Implications for transport of jasmonate precursors into peroxisomes. Plant Physiol. 137(3): 835-840.
56. F. Schaller and E.W. Weiler. **1997**. Molecular cloning and characterization of 12-oxophytodienoate reductase, an enzyme of the octadecanoid signaling pathway from *Arabidopsis thaliana* - Structural and functional relationship to Yeast Old Yellow Enzyme. J. Biol. Chem. 272(44): 28066-28072.
57. C.Y. Li, A.L. Schilmiller, G.H. Liu, G.I. Lee, S. Jayanty, C. Sageman, J. Vrebalov, J.J. Giovannoni, K. Yagi, Y. Kobayashi, and G.A. Howe. **2005**. Role of β-oxidation in jasmonate biosynthesis and systemic wound signaling in tomato. Plant Cell 17(3): 971-986.

58. K. Schneider, L. Kienow, E. Schmelzer, T. Colby, M. Bartsch, O. Miersch, C. Wasternack, E. Kombrink, and H.P. Stuible. **2005**. A new type of peroxisomal acyl-coenzyme A synthetase from *Arabidopsis thaliana* has the catalytic capacity to activate biosynthetic precursors of jasmonic acid. J. Biol. Chem. 280(14): 13962-13972.
59. Y. Koda, Y. Kikuta, T. Kitahara, T. Nishi, and K. Mori. **1992**. Comparisons of various biological-activities of stereoisomers of methyl jasmonate. Phytochemistry 31(4): 1111-1114.
60. L. Holbrook, P. Tung, K. Ward, D.M. Reid, S. Abrams, N. Lamb, J.W. Quail, and M.M. Moloney. **1997**. Importance of the chiral centers of jasmonic acid in the responses of plants. Plant Physiol. 114(2): 419-428.
61. S. Blechert, W. Brodschelm, S. Hölder, L. Kammerer, T.M. Kutchan, M.J. Mueller, Z.Q. Xia, and M.H. Zenk. **1995**. The octadecanoic pathway: Signal molecules for the regulation of secondary pathways. Proc. Natl. Acad. Sci. USA 92(10): 4099-4105.
62. C. Wasternack, O. Miersch, R. Kramell, B. Hause, J. Ward, M. Beale, W. Boland, B. Parthier, and I. Feussner. **1998**. Jasmonic acid: biosynthesis, signal transduction, gene expression. Fett-Lipid 100(4-5): 139-146.
63. S. Parchmann, H. Gundlach, and M.J. Mueller. **1997**. Induction of 12-oxo-phytodienoic acid in wounded plants and elicited plant cell cultures. Plant Physiol. 115(3): 1057-1064.
64. A. Müller, P. Düchting, and E.W. Weiler. **2002**. A multiplex GC-MS/MS technique for the sensitive and quantitative single-run analysis of acidic phytohormones and related compounds, and its application to *Arabidopsis thaliana*. Planta 216(1): 44-56.
65. J. Fliegmann, G. Schüler, W. Boland, J. Ebel, and A. Mithöfer. **2003**. The role of octadecanoids and functional mimics in soybean defense responses. Biol. Chem. 384(3): 437-446.
66. B.A. Stelmach, A. Müller, and E.W. Weiler. **1999**. 12-oxo-phytodienoic acid and indole-3-acetic acid in jasmonic acid-treated tendrils of *Bryonia dioica*. Phytochemistry 51(2): 187-192.
67. T. Koch, T. Krumm, V. Jung, J. Engelberth, and W. Boland. **1999**. Differential induction of plant volatile biosynthesis in the Lima bean by early and late intermediates of the octadecanoid-signaling pathway. Plant Physiol. 121(1): 153-162.
68. A.N. Grechkin, R.A. Kuramshin, E.Y. Safonova, S.K. Latypov, and A.V. Ilyasov. **1991**. Formation of ketols from linolenic acid 13-hydroperoxide via allene oxide. Evidence for two distinct mechanisms of allene oxide hydrolysis. Biochim. Biophys. Acta 1086(3): 317-325.
69. A.N. Grechkin, L.S. Mukhtarova, and M. Hamberg. **2000**. The lipoxygenase pathway in tulip (*Tulipa gesneriana*): detection of the ketol route. Biochem. J. 352: 501-509.
70. M. Yokoyama, S. Yamaguchi, S. Inomata, K. Komatsu, S. Yoshida, T. Iida, Y. Yokokawa, M. Yamaguchi, S. Kaihara, and A. Takimoto. **2000**. Stress-induced factor involved in flower formation of *Lemna* is an α-ketol derivative of linolenic acid. Plant Cell Physiol. 41(1): 110-113.
71. O. Miersch, A. Preiss, G. Sembdner, and K. Schreiber. **1987**. (+)-7-*iso*-jasmonic acid and related-compounds from *Botryodiplodia theobromae*. Phytochemistry 26(4): 1037-1039.
72. O. Miersch, G. Sembdner, and K. Schreiber. **1989**. Occurrence of jasmonic acid analogs in *Vicia faba*. Phytochemistry 28(2): 339-340.
73. H. Gundlach and M.H. Zenk. **1998**. Biological activity and biosynthesis of pentacyclic oxylipins: The linoleic acid pathway. Phytochemistry 47(4): 527-537.

74. H. Weber, B.A. Vick, and E.E. Farmer. **1997**. Dinor-oxo-phytodienoic acid: A new hexadecanoid signal in the jasmonate family. Proc. Natl. Acad. Sci. USA 94(19): 10473-10478.
75. H.S. Seo, J.T. Song, J.J. Cheong, Y.H. Lee, Y.W. Lee, I. Hwang, J.S. Lee, and Y.D. Choi. **2001**. Jasmonic acid carboxyl methyltransferase: A key enzyme for jasmonate-regulated plant responses. Proc. Natl. Acad. Sci. USA 98(8): 4788-4793.
76. T. Koch, K. Bandemer, and W. Boland. **1997**. Biosynthesis of *cis*-jasmone: a pathway for the inactivation and the disposal of the plant stress hormone jasmonic acid to the gas phase? Helv. Chim. Acta 80(3): 838-850.
77. C.C. von Dahl and I.T. Baldwin. **2004**. Methyl jasmonate and *cis*-jasmone do not dispose of the herbivore-induced jasmonate burst in *Nicotiana attenuata.* Physiol. Plant. 120(3): 474-481.
78. G. Sembdner and B. Parthier. **1993**. The biochemistry and the physiological and molecular actions of jasmonates. Annu. Rev. Plant Physiol. Plant Molec. Biol. 44: 569-589.
79. H. Matsuura and T. Yoshihara. **2003**. Metabolism of deuterium-labeled jasmonic acid and OPC 8:0 in the potato plant (*Solanum tuberosum* L.). Biosci. Biotech. Biochem. 67(9): 1903-1907.
80. S.K. Gidda, O. Miersch, A. Levitin, J. Schmidt, C. Wasternack, and L. Varin. **2003**. Biochemical and molecular characterization of a hydroxyjasmonate sulfotransferase from *Arabidopsis thaliana.* J. Biol. Chem. 278(20): 17895-17900.
81. E.E. Farmer and C.A. Ryan. **1990**. Interplant communication: Airborne methyl jasmonate induces synthesis of proteinase inhibitors in plant leaves. Proc. Natl. Acad. Sci. USA 87(19): 7713-7716.
82. R. Karban, I.T. Baldwin, K.J. Baxter, G. Laue, and G.W. Felton. **2000**. Communication between plants: induced resistance in wild tobacco plants following clipping of neighboring sagebrush. Oecologia 125(1): 66-71.
83. Y. Koda, Y. Kikuta, H. Tazaki, Y. Tsujino, S. Sakamura, and T. Yoshihara. **1991**. Potato tuber-inducing activities of jasmonic acid and related compounds. Phytochemistry 30(5): 1435-1438.
84. C. Brückner, R. Kramell, G. Schneider, H.D. Knöfel, G. Sembdner, and K. Schreiber. **1986**. *N*-[(-)-jasmonoyl]-*S*-tyrosine: a conjugate of jasmonic acid from *Vicia faba.* Phytochemistry 25(9): 2236-2237.
85. H.D. Knöfel and G. Sembdner. **1995**. Jasmonates from pine pollen. Phytochemistry 38(3): 569-571.
86. T. Krumm, K. Bandemer, and W. Boland. **1995**. Induction of volatile biosynthesis in the Lima bean (*Phaseolus lunatus*) by leucine- and isoleucine conjugates of 1-oxo- and 1-hydroxyindan-4-carboxylic acid: Evidence for amino acid conjugates of jasmonic acid as intermediates in the octadecanoid signalling pathway. FEBS Lett. 377(3): 523-529.
87. R. Kramell, O. Miersch, B. Hause, B. Ortel, B. Parthier, and C. Wasternack. **1997**. Amino acid conjugates of jasmonic acid induce jasmonate-responsive gene expression in barley (*Hordeum vulgare* L.) leaves. FEBS Lett. 414(2): 197-202.
88. P.E. Staswick and I. Tiryaki. **2004**. The oxylipin signal jasmonic acid is activated by an enzyme that conjugates it to isoleucine in *Arabidopsis.* Plant Cell 16(8): 2117-2127.
89. P.E. Staswick, W.P. Su, and S.H. Howell. **1992**. Methyl Jasmonate Inhibition of Root-Growth and Induction of a Leaf Protein Are Decreased in an Arabidopsis-Thaliana Mutant. Proc. Natl. Acad. Sci. USA 89(15): 6837-6840.
90. P.E. Staswick, I. Tiryaki, and M.L. Rowe. **2002**. Jasmonate response locus JAR1 and several related Arabidopsis genes encode enzymes of the firefly luciferase superfamily

that show activity on jasmonic, salicylic, and indole-3-acetic acids in an assay for adenylation. Plant Cell 14(6): 1405-1415.
91. A. Stintzi, H. Weber, P. Reymond, J. Browse, and E.E. Farmer. **2001**. Plant defense in the absence of jasmonic acid: The role of cyclopentenones. Proc. Natl. Acad. Sci. USA 98(22): 12837-12842.
92. H. Kitaguchi, K. Ohkubo, S. Ogo, and S. Fukuzumi. **2005**. Direct ESR detection of pentadienyl radicals and peroxyl radicals in lipid peroxidation: Mechanistic insight into regioselective oxygenation in lipoxygenases. J. Am. Chem. Soc. 127(18): 6605-6609.
93. A. Mlakar and G. Spiteller. **1996**. Distinction between enzymic and nonenzymic lipid peroxidation. J. Chromatogr. A 743(2): 293-300.
94. S. Berger, H. Weichert, A. Porzel, C. Wasternack, H. Kühn, and I. Feussner. **2001**. Enzymatic and non-enzymatic lipid peroxidation in leaf development. Biochim. Biophys. Acta Mol. Cell Biol. Lipids 1533(3): 266-276.
95. H.W. Gardner. **1989**. Soybean lipoxygenase-1 enzymically forms both (9*S*)-hydroperoxides and (13*S*)-hydroperoxides from linoleic acid by a pH-dependent mechanism. Biochim. Biophys. Acta 1001(3): 274-281.
96. F. Pinot, M. Skrabs, V. Compagnon, J.P. Salaün, I. Benveniste, L. Schreiber, and F. Durst. **2000**. ω-Hydroxylation of epoxy- and hydroxy-fatty acids by CYP94A1: possible involvement in plant defence. Biochem. Soc. Trans. 28: 867-870.
97. A. Saffert, J. Hartmann-Schreier, A. Schön, and P. Schreier. **2000**. A dual function α-dioxygenase-peroxidase and NAD^+ oxidoreductase active enzyme from germinating pea rationalizing α-oxidation of fatty acids in plants. Plant Physiol. 123(4): 1545-1551.
98. M. Hamberg, A. Sanz, and C. Castresana. **1999**. α-Oxidation of fatty acids in higher plants - Identification of a pathogen-inducible oxygenase (PIOX) as an α-dioxygenase and biosynthesis of 2-hydroperoxylinolenic acid. J. Biol. Chem. 274(35): 24503-24513.
99. M. Hamberg, A. Sanz, M.J. Rodriguez, A.P. Calvo, and C. Castresana. **2003**. Activation of the fatty acid α-dioxygenase pathway during bacterial infection of tobacco leaves - Formation of oxylipins protecting against cell death. J. Biol. Chem. 278(51): 51796-51805.
100. M. van der Stelt, M.A. Noordermeer, T. Kiss, G. van Zadelhoff, B. Merghart, G.A. Veldink, and J.F.G. Vliegenthart. **2000**. Formation of a new class of oxylipins from *N*-acyl(ethanol)amines by the lipoxygenase pathway. Eur. J. Biochem. 267(7): 2000-2007.
101. R. Shrestha, M.A. Noordermeer, M. Van der Stelt, G.A. Veldink, and K.D. Chapman. **2002**. *N*-acylethanolamines are metabolized by lipoxygenase and amidohydrolase in competing pathways during cottonseed inhibition. Plant Physiol. 130(1): 391-401.
102. C. Fuchs and G. Spiteller. **2000**. Iron release from the active site of lipoxygenase. Z.Naturforsch.(C) 55(7-8): 643-648.
103. P. Wojtaszek. **1997**. Oxidative burst: An early plant response to pathogen infection. Biochem. J. 322: 681-692.
104. P.S. Low and J.R. Merida. **1996**. The oxidative burst in plant defense - function and signal transduction. Physiol. Plantarum 96(3): 533-542.
105. A. Schützendübel and A. Polle. **2002**. Plant responses to abiotic stresses: heavy metal-induced oxidative stress and protection by mycorrhization. J. Exp. Bot. 53(372): 1351-1365.
106. A.C. Allan and R. Fluhr. **1997**. Two distinct sources of elicited reactive oxygen species in tobacco epidermal cells. Plant Cell 9(9): 1559-1572.
107. G.P. Bolwell and P. Wojtaszek. **1997**. Mechanisms for the generation of reactive oxygen species in plant defence - a broad perspective. Physiol. Mol. Plant Pathol. 51(6): 347-366.

108. C. Lamb and R.A. Dixon. **1997**. The oxidative burst in plant disease resistance. Annu. Rev. Plant Physiol. Plant Molec. Biol. 48: 251-275.
109. A.U. Khan and M. Kasha. **1994**. Singlet molecular oxygen in the Haber-Weiss reaction. Proc. Natl. Acad. Sci. USA 91(26): 12365-12367.
110. J.A. Gatehouse. **2002**. Plant resistance towards insect herbivores: a dynamic interaction. New Phytol. 156(2): 145-169.
111. F. Van Breusegem, E. Vranová, J.F. Dat, and D. Inzé. **2001**. The role of active oxygen species in plant signal transduction. Plant Sci. 161(3): 405-414.
112. J.L. Bi and G.W. Felton. **1995**. Foliar oxidative stress and insect herbivory: primary compounds, secondary metabolites, and reactive oxygen species as components of induced resistance. J. Chem. Ecol. 21(10): 1511-1530.
113. G.W. Felton and H. Eichenseer. **1999**. Herbivore saliva and its effects on plant defense against herbivores and pathogens. Pages 19-36 *in* A.A. Agrawal, S. Tuzun, and E. Bent, editors. Induced plant defenses against pathogens and herbivores - Biochemistry, ecology and agriculture. APS Press, St. Paul, Minesota.
114. G.A. Howe and A.L. Schilmiller. **2002**. Oxylipin metabolism in response to stress. Curr. Opin. Plant Biol. 5(3): 230-236.
115. E. Blée. **1998**. Phytooxylipins and plant defense reactions. Prog. Lipid. Res. 37(1): 33-72.
116. A. Grechkin. **1998**. Recent developments in biochemistry of the plant lipoxygenase pathway. Prog. Lipid. Res. 37(5): 317-352.
117. I. Feussner and C. Wasternack. **2002**. The lipoxygenase pathway. Annu. Rev. Plant Biol. 53: 275-297.
118. I. Feussner and C. Wasternack. **1998**. Lipoxygenase catalyzed oxygenation of lipids. Fett-Lipid 100(4-5): 146-152.
119. M. Hamberg. **2002**. Biosynthesis of new divinyl ether oxylipins in *Ranunculus* plants. Lipids 37(4): 427-433.
120. M. Hamberg. **2005**. Hidden stereospecificity in the biosynthesis of divinyl ether fatty acids. FEBS J. 272(3): 736-743.
121. M.J. Mueller. **1998**. Radically novel prostaglandins in animals and plants: the isoprostanes. Chem. Biol. 5(12): R323-R333.
122. I. Thoma, M. Krischke, C. Loeffler, and M.J. Mueller. **2004**. The isoprostanoid pathway in plants. Chem. Phys. Lipids. 128(1-2): 135-148.
123. J.D. Morrow, K.E. Hill, R.F. Burk, T.M. Nammour, K.F. Badr, and L.J. Roberts. **1990**. A series of prostaglandin F_2-like compounds are produced *in vivo* in humans by a non-cyclooxygenase, free radical-catalyzed mechanism. Proc. Natl. Acad. Sci. USA 87(23): 9383-9387.
124. D.C. Zimmerman and C.A. Coudron. **1979**. Identification of traumatin, a wound hormone, as 12-oxo-*trans*-10-dodecenoic acid. Plant Physiol. 63(3): 536-541.
125. S. Tahara, S. Kasai, M. Inoue, J. Kawabata, and J. Mizutani. **1994**. Identification of mucondialdehyde as a novel stress metabolite. Experientia 50(2): 137-141.
126. K.P.C. Croft, F. Juttner, and A.J. Slusarenko. **1993**. Volatile products of the lipoxygenase pathway evolved from *Phaseolus vulgaris* (L.) leaves inoculated with *Pseudomonas syringae* pv *phaseolicola*. Plant Physiol. 101(1): 13-24.
127. S.F. Vaughn and H.W. Gardner. **1993**. Lipoxygenase-derived aldehydes inhibit fungi pathogenic on soybean. J. Chem. Ecol. 19(10): 2337-2345.
128. M.L. Fauconnier, R. Welti, E. Blée, and M. Marlier. **2003**. Lipid and oxylipin profiles during aging and sprout development in potato tubers (*Solanum tuberosum* L.). Biochim. Biophys. Acta Mol. Cell Biol. Lipids 1633(2): 118-126.

129. G. Vancanneyt, C. Sanz, T. Farmaki, M. Paneque, F. Ortego, P. Castañera, and J.J. Sánchez-Serrano. **2001**. Hydroperoxide lyase depletion in transgenic potato plants leads to an increase in aphid performance. Proc. Natl. Acad. Sci. USA 98(14): 8139-8144.
130. D. Natale, L. Mattiacci, A. Hern, E. Pasqualini, and S. Dorn. **2003**. Response of female *Cydia molesta* (Lepidoptera:Tortricidae) to plant derived volatiles. Bull. Entomol. Res. 93(4): 335-342.
131. D.G. James. **2005**. Further field evaluation of synthetic herbivore-induced plant volatiles as attractants for beneficial insects. J. Chem. Ecol. 31(3): 481-495.
132. H.J. Zeringue. **1992**. Effects of C_6-C_{10} alkenals and alkanals on eliciting a defense response in the developing cotton boll. Phytochemistry 31(7): 2305-2308.
133. J. Engelberth, H.T. Alborn, E.A. Schmelz, and J.H. Tumlinson. **2004**. Airborne signals prime plants against insect herbivore attack. Proc. Natl. Acad. Sci. USA 101(6): 1781-1785.
134. M.A. Farag, M. Fokar, H.A. Zhang, R.D. Allen, and P.W. Paré. **2005**. (*Z*)-3-Hexenol induces defense genes and downstream metabolites in maize. Planta 220(6): 900-909.
135. F.G. Karimova, I.A. Tarchevsky, N.U. Mursalimova, and A.N. Grechkin. **1999**. Effect of 12-hydroxydodecenoic acid, a product of the lipoxygenase pathway, on plant protein phosphorylation. Russ. J. Plant Physiol. 46(1): 128-131.
136. H. Weber, A. Chételat, D. Caldelari, and E.E. Farmer. **1999**. Divinyl ether fatty acid synthesis in late blight-diseased potato leaves. Plant Cell 11(3): 485-493.
137. M. Stumpe, R. Kandzia, C. Göbel, S. Rosahl, and I. Feussner. **2001**. A pathogen-inducible divinyl ether synthase (*CYP74D*) from elicitor-treated potato suspension cells. FEBS Lett. 507(3): 371-376.
138. I. Thoma, C. Loeffler, A.K. Sinha, M. Gupta, M. Krischke, B. Steffan, T. Roitsch, and M.J. Mueller. **2003**. Cyclopentenone isoprostanes induced by reactive oxygen species trigger defense gene activation and phytoalexin accumulation in plants. Plant J. 34(3): 363-375.
139. C. Loeffler, S. Berger, A. Guy, T. Durand, G. Bringmann, M. Dreyer, U. von Rad, J. Durner, and M.J. Mueller. **2005**. B_1-phytoprostanes trigger plant defense and detoxification responses. Plant Physiol. 137(1): 328-340.
140. G.A. Howe, J. Lightner, J. Browse, and C.A. Ryan. **1996**. An octadecanoid pathway mutant (JL5) of tomato is compromised in signaling for defense against insect attack. Plant Cell 8(11): 2067-2077.
141. P.J. O'Donnell, E. Schmelz, A. Block, O. Miersch, C. Wasternack, J.B. Jones, and H.J. Klee. **2003**. Multiple hormones act sequentially to mediate a susceptible tomato pathogen defense response. Plant Physiol. 133(3): 1181-1189.
142. N. Groß, C. Wasternack, and M. Köck. **2004**. Wound-induced *RNaseLE* expression is jasmonate and systemin independent and occurs only locally in tomato (*Lycopersicon esculentum* cv. Lukullus). Phytochemistry 65(10): 1343-1350.
143. J. Royo, J. Léon, G. Vancanneyt, J.P. Albar, S. Rosahl, F. Ortego, P. Castañera, and J.J. Sánchez-Serrano. **1999**. Antisense-mediated depletion of a potato lipoxygenase reduces wound induction of proteinase inhibitors and increases weight gain of insect pests. Proc. Natl. Acad. Sci. USA 96(3): 1146-1151.
144. E.E. Farmer, E. Alméras, and V. Krishnamurthy. **2003**. Jasmonates and related oxylipins in plant responses to pathogenesis and herbivory. Curr. Opin. Plant Biol. 6(4): 372-378.
145. S. Vollenweider, H. Weber, S. Stolz, A. Chételat, and E.E. Farmer. **2000**. Fatty acid ketodienes and fatty acid ketotrienes: Michael addition acceptors that accumulate in wounded and diseased *Arabidopsis* leaves. Plant J. 24(4): 467-476.

146. E. Alméras, S. Stolz, S. Vollenweider, P. Reymond, L. Mène-Saffrané, and E.E. Farmer. **2003**. Reactive electrophile species activate defense gene expression in *Arabidopsis.* Plant J. 34(2): 202-216.
147. W. Palinski, M.E. Rosenfeld, S. Ylä-Herttuala, G.C. Gurtner, S.S. Socher, S.W. Butler, S. Parthasarathy, T.E. Carew, D. Steinberg, and J.L. Witztum. **1989**. Low density lipoprotein undergoes oxidative modification *in vivo.* Proc. Natl. Acad. Sci. USA 86(4): 1372-1376.
148. K. Uchida, S. Toyokuni, K. Nishikawa, S. Kawakishi, H. Oda, H. Hiai, and E.R. Stadtman. **1994**. Michael addition-type 4-hydroxy-2-nonenal adducts in modified low-density lipoproteins: markers for atherosclerosis. Biochemistry 33(41): 12487-12494.
149. D. Spiteller and G. Spiteller. **2000**. Oxidation of linoleic acid in low-density lipoprotein: An important event in atherogenesis. Angew. Chem.-Int. Edit. 39(3): 585-589.
150. A. Miralto, G. Barone, G. Romano, S.A. Poulet, A. Ianora, G.L. Russo, I. Buttino, G. Mazzarella, M. Laabir, M. Cabrini, and M.G. Giacobbe. **1999**. The insidious effect of diatoms on copepod reproduction. Nature 402(6758): 173-176.
151. S. Adolph, S. Bach, M. Blondel, A. Cueff, M. Moreau, G. Pohnert, S.A. Poulet, T. Wichard, and A. Zuccaro. **2004**. Cytotoxicity of diatom-derived oxylipins in organisms belonging to different phyla. J. Exp. Biol. 207(17): 2935-2946.
152. D.F. Klessig and J. Malamy. **1994**. The salicylic acid signal in plants. Plant Mol.Biol. 26(5): 1439-1458.
153. L. Sticher, B. Mauch-Mani, and J.P. Métraux. **1997**. Systemic acquired resistance. Annu. Rev. Phytopathol. 35: 235-270.
154. J.P. Métraux, C. Nawrath, and T. Genoud. **2002**. Systemic acquired resistance. Euphytica 124(2): 237-243.
155. J. Durner, J. Shah, and D.F. Klessig. **1997**. Salicylic acid and disease resistance in plants. Trends Plant Sci. 2(7): 266-274.
156. A.P. Jarvis, O. Schaaf, and N.J. Oldham. **2000**. 3-Hydroxy-3-phenylpropanoic acid is an intermediate in the biosynthesis of benzoic add and salicylic acid but benzaldehyde is not. Planta 212(1): 119-126.
157. J.G. de Boer and M. Dicke. **2004**. The role of methyl salicylate in prey searching behavior of the predatory mite *Phytoseiulus persimilis.* J. Chem. Ecol. 30(2): 255-271.
158. V. Shulaev, P. Silverman, and I. Raskin. **1997**. Airborne signalling by methyl salicylate in plant pathogen resistance. Nature 385(6618): 718-721.
159. Z.X. Chen and D.F. Klessig. **1991**. Identification of a soluble salicylic acid-binding protein that may function in signal transduction in the plant disease-resistance response. Proc. Natl. Acad. Sci. USA 88(18): 8179-8183.
160. Z.X. Chen, J. Malamy, J. Henning, U. Conrath, P. Sánchez-Casas, H. Silva, J. Ricigliano, and D.F. Klessig. **1995**. Induction, modification, and transduction of the salicylic acid signal in plant defense responses. Proc. Natl. Acad. Sci. USA 92(10): 4134-4137.
161. D.P. Singh, C.A. Moore, A. Gilliland, and J.P. Carr. **2004**. Activation of multiple antiviral defence mechanisms by salicylic acid. Mol. Plant Pathol. 5(1): 57-63.
162. P.R. Johnson and J.R. Ecker. **1998**. The ethylene gas signal transduction pathway: A molecular perspective. Annu. Rev. Genet. 32: 227-254.
163. J.R. Ecker. **1995**. The ethylene signal transduction pathway in plants. Science 268(5211): 667-675.
164. M. Knoester, L.C. van Loon, J. van den Heuvel, J. Hennig, J.F. Bol, and H.J.M. Linthorst. **1998**. Ethylene-insensitive tobacco lacks nonhost resistance against soil-borne fungi. Proc. Natl. Acad. Sci. USA 95(4): 1933-1937.

165. H. Kende. **1993**. Ethylene biosynthesis. Annu. Rev. Plant Physiol. Plant Molec. Biol. 44: 283-307.
166. K.L.C. Wang, H. Li, and J.R. Ecker. **2002**. Ethylene biosynthesis and signaling networks. Plant Cell 14(Supplement): S131-S151.
167. A.B. Bleecker and H. Kende. **2000**. Ethylene: A gaseous signal molecule in plants. Annu. Rev. Cell Dev. Biol. 16: 1-18.
168. J.S. Parkinson and E.C. Kofoid. **1992**. Communication modules in bacterial signaling proteins. Annu. Rev. Genet. 26: 71-112.
169. S.M. Wurgler-Murphy and H. Saito. **1997**. Two-component signal transducers and MAPK cascades. Trends Biochem.Sci. 22(5): 172-176.
170. C. Chang and E.M. Meyerowitz. **1995**. The ethylene hormone response in *Arabidopsis*: A eukaryotic two-component signaling system. Proc. Natl. Acad. Sci. USA 92(10): 4129-4133.
171. G. Löffler and P.E. Petrides. **2003**. Biochemie and Pathobiochemie. Springer, Berlin.
172. M.J. Stout, A.L. Fidantsef, S.S. Duffey, and R.M. Bostock. **1999**. Signal interactions in pathogen and insect attack: systemic plant-mediated interactions between pathogens and herbivores of the tomato, *Lycopersicon esculentum.* Physiol. Mol. Plant Pathol. 54(3-4): 115-130.
173. J.S. Thaler, R. Karban, D.E. Ullman, K. Boege, and R.M. Bostock. **2002**. Cross-talk between jasmonate and salicylate plant defense pathways: effects on several plant parasites. Oecologia 131(2): 227-235.
174. G.W. Felton and K.L. Korth. **2000**. Trade-offs between pathogen and herbivore resistance. Curr. Opin. Plant Biol. 3(4): 309-314.
175. E. Rojo, R. Solano, and J.J. Sánchez-Serrano. **2003**. Interactions between signaling compounds involved in plant defense. 22(1): 82-98.
176. M.J. Pozo, L.C. Van Loon, and C.M.J. Pieterse. **2005**. Jasmonates - signals in plant-microbe interactions. J. Plant Growth Regul. 23(3): 211-222.
177. H.M. Doherty, R.R. Selvendran, and D.J. Bowles. **1988**. The wound response of tomato plants can be inhibited by aspirin and related hydroxy-benzoic acids. Physiol. Mol. Plant Pathol. 33(3): 377-384.
178. H. Peña-Cortés, T. Albrecht, S. Prat, E.W. Weiler, and L. Willmitzer. **1993**. Aspirin prevents wound-induced gene expression in tomato leaves by blocking jasmonic acid biosynthesis. Planta 191(1): 123-128.
179. S.H. Doares, J. Narváez-Vásquez, A. Conconi, and C.A. Ryan. **1995**. Salicylic acid inhibits synthesis of proteinase inhibitors in tomato leaves induced by systemin and jasmonic acid. Plant Physiol. 108(4): 1741-1746.
180. G.W. Felton, K.L. Korth, J.L. Bi, S.V. Wesley, D.V. Huhman, M.C. Mathews, J.B. Murphy, C. Lamb, and R.A. Dixon. **1999**. Inverse relationship between systemic resistance of plants to microorganisms and to insect herbivory. Curr. Biol. 9(6): 317-320.
181. C.A. Preston, C. Lewandowski, A.J. Enyedi, and I.T. Baldwin. **1999**. Tobacco mosaic virus inoculation inhibits wound-induced jasmonic acid-mediated responses within but not between plants. Planta 209(1): 87-95.
182. H.U. Stotz, T. Koch, A. Biedermann, K. Weniger, W. Boland, and T. Mitchell-Olds. **2002**. Evidence for regulation of resistance in *Arabidopsis* to Egyptian cotton worm by salicylic and jasmonic acid signaling pathways. Planta 214(4): 648-652.
183. K. Harms, I. Ramirez, and H. Peña-Cortés. **1998**. Inhibition of wound-induced accumulation of allene oxide synthase transcripts in flax leaves by aspirin and salicylic acid. Plant Physiol. 118(3): 1057-1065.

184. J. Ziegler, M. Hamberg, O. Miersch, and B. Parthier. **1997**. Purification and characterization of allene oxide cyclase from dry corn seeds. Plant Physiol. 114(2): 565-573.
185. D. Laudert and E.W. Weiler. **1998**. Allene oxide synthase - a major control point in *Arabidopsis thaliana* octadecanoid signalling. Plant J. 15(5): 675-684.
186. J. Engelberth, T. Koch, G. Schüler, N. Bachmann, J. Rechtenbach, and W. Boland. **2001**. Ion channel-forming alamethicin is a potent elicitor of volatile biosynthesis and tendril coiling. Cross talk between jasmonate and salicylate signaling in Lima bean. Plant Physiol. 125(1): 369-377.
187. D. Cipollini, S. Enright, M.B. Traw, and J. Bergelson. **2004**. Salicylic acid inhibits jasmonic acid-induced resistance of *Arabidopsis thaliana* to *Spodoptera exigua.* Mol. Ecol. 13(6): 1643-1653.
188. B.N. Kunkel and D.M. Brooks. **2002**. Cross talk between signaling pathways in pathogen defense. Curr. Opin. Plant Biol. 5(4): 325-331.
189. C.M.J. Pieterse, J.A. Van Pelt, S.C.M. Van Wees, J. Ton, K.M. Léon-Kloosterziel, J.J.B. Keurentjes, B.W.M. Verhagen, M. Knoester, I. Van der Sluis, P. Bakker, and L.C. Van Loon. **2001**. Rhizobacteria-mediated induced systemic resistance: Triggering, signalling and expression. Eur. J. Plant Pathol. 107(1): 51-61.
190. C.M.J. Pieterse, J.A. Van Pelt, J. Ton, S. Parchmann, M.J. Mueller, A.J. Buchala, J.P. Métraux, and L.C. Van Loon. **2000**. Rhizobacteria-mediated induced systemic resistance (ISR) in *Arabidopsis* requires sensitivity to jasmonate and ethylene but is not accompanied by an increase in their production. Physiol. Mol. Plant Pathol. 57(3): 123-134.
191. S.C.M. van Wees, E.A.M. de Swart, J.A. van Pelt, L.C. van Loon, and C.M.J. Pieterse. **2000**. Enhancement of induced disease resistance by simultaneous activation of salicylate- and jasmonate-dependent defense pathways in *Arabidopsis thaliana.* Proc. Natl. Acad. Sci. USA 97(15): 8711-8716.
192. T. Niki, I. Mitsuhara, S. Seo, N. Ohtsubo, and Y. Ohashi. **1998**. Antagonistic effect of salicylic acid and jasmonic acid on the expression of pathogenesis-related (PR) protein genes in wounded mature tobacco leaves. Plant Cell Physiol. 39(5): 500-507.
193. B. Thomma, K. Eggermont, W.F. Broekaert, and B.P.A. Cammue. **2000**. Disease development of several fungi on *Arabidopsis* can be reduced by treatment with methyl jasmonate. Plant Physiol. Biochem. 38(5): 421-427.
194. A. Nickstadt, B. Thomma, I. Feussner, J. Kangasjärvi, J. Zeier, C. Loeffler, D. Scheel, and S. Berger. **2004**. The jasmonate-insensitive mutant *jin1* shows increased resistance to biotrophic as well as necrotrophic pathogens. Mol. Plant Pathol. 5(5): 425-434.
195. P. Landgraf, I. Feussner, A. Hunger, D. Scheel, and S. Rosahl. **2002**. Systemic accumulation of 12-oxo-phytodienoic acid in SAR-induced potato plants. Eur. J. Plant Pathol. 108(3): 279-283.
196. E. Rojo, J. Léon, and J.J. Sánchez-Serrano. **1999**. Cross-talk between wound signalling pathways determines local versus systemic gene expression in *Arabidopsis thaliana.* Plant J. 20(2): 135-142.
197. I.A.M.A. Penninckx, B.P.H.J. Thomma, A. Buchala, J.P. Métraux, and W.F. Broekaert. **1998**. Concomitant activation of jasmonate and ethylene response pathways is required for induction of a plant defensin gene in *Arabidopsis.* Plant Cell 10(12): 2103-2113.
198. Y. Xu, P.F.L. Chang, D. Liu, M.L. Narasimhan, K.G. Raghothama, P.M. Hasegawa, and R.A. Bressan. **1994**. Plant defense genes are synergistically induced by ethylene and methyl jasmonate. Plant Cell 6(8): 1077-1085.

199. O. Lorenzo, R. Piqueras, J.J. Sánchez-Serrano, and R. Solano. **2003**. ETHYLENE RESPONSE FACTOR1 integrates signals from ethylene and jasmonate pathways in plant defense. Plant Cell 15(1): 165-178.
200. T. Shoji, K. Nakajima, and T. Hashimoto. **2000**. Ethylene suppresses jasmonate-induced gene expression in nicotine biosynthesis. Plant Cell Physiol. 41(9): 1072-1076.
201. J. Kahl, D.H. Siemens, R.J. Aerts, R. Gäbler, F. Kühnemann, C.A. Preston, and I.T. Baldwin. **2000**. Herbivore-induced ethylene suppresses a direct defense but not a putative indirect defense against an adapted herbivore. Planta 210(2): 336-342.
202. R. Ozawa, G. Arimura, J. Takabayashi, T. Shimoda, and T. Nishioka. **2000**. Involvement of jasmonate- and salicylate-related signaling pathways for the production of specific herbivore-induced volatiles in plants. Plant Cell Physiol. 41(4): 391-398.
203. J. Horiuchi, G. Arimura, R. Ozawa, T. Shimoda, J. Takabayashi, and T. Nishioka. **2001**. Exogenous ACC enhances volatiles production mediated by jasmonic acid in Lima bean leaves. FEBS Lett. 509(2): 332-336.
204. G. Arimura, R. Ozawa, T. Nishioka, W. Boland, T. Koch, F. Kühnemann, and J. Takabayashi. **2002**. Herbivore-induced volatiles induce the emission of ethylene in neighboring Lima bean plants. Plant J. 29(1): 87-98.
205. H. Weichert, I. Stenzel, E. Berndt, C. Wasternack, and I. Feussner. **1999**. Metabolic profiling of oxylipins upon salicylate treatment in barley leaves - preferential induction of the reductase pathway by salicylate. FEBS Lett. 464(3): 133-137.
206. R. Halitschke, J. Ziegler, M. Keinänen, and I.T. Baldwin. **2004**. Silencing of hydroperoxide lyase and allene oxide synthase reveals substrate and defense signaling crosstalk in *Nicotiana attenuata.* Plant J. 40(1): 35-46.
207. A. Mithöfer, B. Schulze, and W. Boland. **2004**. Biotic and heavy metal stress response in plants: evidence for common signals. FEBS Lett. 566(1-3): 1-5.
208. M. Weisser, M. Vieth, M. Stolte, P. Riederer, R. Pfeuffer, F. Leblhuber, and G. Spiteller. **1997**. Dramatic increase of α-hydroxyaldehydes derived from plasmalogens in the aged human brain. Chem. Phys. Lipids 90(1-2): 135-142.
209. G. Spiteller. **2003**. Are lipid peroxidation processes induced by changes in the cell wall structure and how are these processes connected with diseases? Med. Hypotheses 60(1): 69-83.
210. M.J. Mueller and W. Brodschelm. **1994**. Quantification of jasmonic acid by capillary gas chromatography-negative chemical-ionization mass-spectrometry. Anal. Biochem. 218(2): 425-435.
211. B.A. Stelmach, A. Müller, P. Hennig, D. Laudert, L. Andert, and E.W. Weiler. **1998**. Quantitation of the octadecanoid 12-oxo-phytodienoic acid, a signalling compound in plant mechanotransduction. Phytochemistry 47(4): 539-546.
212. C. Rustérucci, J.L. Montillet, J.P. Agnel, C. Battesti, B. Alonso, A. Knoll, J.J. Bessoule, P. Etienne, L. Suty, J.P. Blein, and C. Triantaphylidès. **1999**. Involvement of lipoxygenase-dependent production of fatty acid hydroperoxides in the development of the hypersensitive cell death induced by cryptogein on tobacco leaves. J. Biol. Chem. 274(51): 36446-36455.
213. M.P. Gilabert and F.G. Carmona. **2002**. Chromatographic analysis of lipoxygenase products. Anal. Chim. Acta 465(1-2): 319-335.
214. J.L. Montillet, J.L. Cacas, L. Garnier, M.H. Montané, T. Douki, J.J. Bessoule, L. Polkowska-Kowalczyk, U. Maciejewska, J.P. Agnel, A. Vial, and C. Triantaphylidès. **2004**. The upstream oxylipin profile of *Arabidopsis thaliana*: a tool to scan for oxidative stresses. Plant J. 40(3): 439-451.

215. M. Hamberg and G. Hamberg. **1996**. Peroxygenase-catalyzed fatty acid epoxidation in cereal seeds - Sequential oxidation of linoleic acid into 9(*S*),12(*S*),13(*S*)-trihydroxy-10(*E*)-octadecenoic acid. Plant Physiol. 110(3): 807-815.
216. B. Rehbock, D. Ganßer, and R.C. Berger. **1997**. Analysis of oxylipins by high-performance liquid chromatography with evaporative light-scattering detection and particle beam mass spectrometry. Lipids 32(9): 1003-1010.
217. P.S. Blake, J.M. Taylor, and W.E. Finch-Savage. **2002**. Identification of abscisic acid, indole-3-acetic acid, jasmonic acid, indole-3-acetonitrile, methyl jasmonate and gibberellins in developing, dormant and stratified seeds of ash (*Fraxinus excelsior*). Plant Growth Regul. 37(2): 119-125.
218. E.A. Schmelz, J. Engelberth, H.T. Alborn, P. O'Donnell, M. Sammons, H. Toshima, and J.H. Tumlinson. **2003**. Simultaneous analysis of phytohormones, phytotoxins, and volatile organic compounds in plants. Proc. Natl. Acad. Sci. USA 100(18): 10552-10557.
219. E.A. Schmelz, J. Engelberth, J.H. Tumlinson, A. Block, and H.T. Alborn. **2004**. The use of vapor phase extraction in metabolic profiling of phytohormones and other metabolites. Plant J. 39(5): 790-808.
220. H. Esterbauer, R.J. Schaur, and H. Zollner. **1991**. Chemistry and biochemistry of 4-hydroxynonenal, malonaldehyde and related adehydes. Free Radic. Biol. Med. 11(1): 81-128.
221. V.M. Carvalho, P. Di Mascio, I.P.D. Campos, T. Douki, J. Cadet, and M.H.G. Medeiros. **1998**. Formation of 1,N^6-etheno-2 '-deoxyadenosine adducts by *trans*,*trans*-2,4-decadienal. Chem. Res. Toxicol. 11(9): 1042-1047.
222. S.H. Lee, M.V.S. Elipe, J.S. Arora, and I.A. Blair. **2005**. Dioxododecenoic acid: A lipid hydroperoxide-derived bifunctional electrophile responsible for etheno DNA adduct formation. Chem. Res. Toxicol. 18(3): 566-578.
223. E.G. Bligh and W.J. Dyer. **1959**. A Rapid Method of Total Lipid Extraction and Purification. Can. J. Biochem. Physiol. 37(8): 911-917.
224. S.J. Iverson, S.L.C. Lang, and M.H. Cooper. **2001**. Comparison of the Bligh and Dyer and Folch methods for total lipid determination in a broad range of marine tissue. Lipids 36(11): 1283-1287.
225. I.T. Baldwin, Z.P. Zhang, N. Diab, T.E. Ohnmeiss, E.S. McCloud, G.Y. Lynds, and E.A. Schmelz. **1997**. Quantification, correlations and manipulations of wound-induced changes in jasmonic acid and nicotine in *Nicotiana sylvestris.* Planta 201(4): 397-404.
226. H. Weichert, A. Kolbe, A. Kraus, C. Wasternack, and I. Feussner. **2002**. Metabolic profiling of oxylipins in germinating cucumber seedlings lipoxygenase-dependent degradation of triacylglycerols and biosynthesis of volatile aldehydes. Planta 215(4): 612-619.
227. A.G. Harrison. **1992**. Chemical ionization mass spectrometry. CRC Press, Boca Raton.
228. F.J.G.M. van Kuijk, D.W. Thomas, R.J. Stephens, and E.A. Dratz. **1986**. Occurrence of 4-hydroxyalkenals in rat tissues determined as pentafluorobenzyl oxime derivatives by gas chromatography-mass spectrometry. Biochem. Biophys. Res. Commun. 139(1): 144-149.
229. M.L. Selley, M.R. Bartlett, J.A. McGuiness, A.J. Hapel, N.G. Ardlie, and M.J. Lacey. **1989**. Determination of the lipid peroxidation product *trans*-4-hydroxy-2-nonenal in biological samples by high-performance liquid chromatography and combined capillary column gas chromatography-negative-ion chemical ionization mass spectrometry. J. Chromatogr.-Biomed. Appl. 488(2): 329-340.

230. G.F. Hoffmann and L. Sweetman. **1991**. *O*-(2,3,4,5,6-Pentafluorobenzyl)oxime-trimethylsilyl ester derivatives for sensitive identification and quantitation of aldehydes, ketones, and oxoacids in biological fluids. Clin. Chim. Acta 199(3): 237-242.
231. A. Loidl-Stahlhofen, K. Hannemann, and G. Spiteller. **1995**. Detection of short-chain α-hydroxyaldehydic compounds as pentafluorbenzyloxime derivatives in bovine liver. Chem. Phys. Lipids 77(1): 113-119.
232. M. Kohlmann, A. Bachmann, H. Weichert, A. Kolbe, T. Balkenhohl, C. Wasternack, and I. Feussner. **1999**. Formation of lipoxygenase-pathway-derived aldehydes in barley leaves upon methyl jasmonate treatment. Eur. J. Biochem. 260(3): 885-895.
233. T. Wichard, S.A. Poulet, and G. Pohnert. **2005**. Determination and quantification of α,β,γ,δ-unsaturated aldehydes as pentafluorobenzyl-oxime derivates in diatom cultures and natural phytoplankton populations: application in marine field studies. J. Chromatogr. B 814(1): 155-161.
234. G. Hoffmann and L. Sweetman. **1987**. O-(2,3,4,5,6-Pentafluorobenzyl)oxime-trimethylsilyl ester derivatives for quantitative gas chromatographic and gas chromatographic-mass spectrometric studies of aldehydes, ketones and oxoacids. J. Chromatogr.-Biomed. Appl. 421(2): 336-343.
235. R.S. Spaulding and M.J. Charles. **2002**. Comparison of methods for extraction, storage, and silylation of pentafluorobenzyl derivatives of carbonyl compounds and multi-functional carbonyl compounds. Anal. Bioanal. Chem. 372(7-8): 808-816.
236. M.J. Mueller, W. Brodschelm, E. Spannagl, and M.H. Zenk. **1993**. Signaling in the elicitation process is mediated through the octadecanoid pathway leading to jasmonic acid. Proc. Natl. Acad. Sci. USA 90(16): 7490-7494.
237. B.A.W. Gallasch. **1998**. Untersuchungen pflanzlicher Fettsäureoxidationsprodukte mittels GC/FID/MSD-Kopplung - *Lens culinaris* Medik, ein Modellsystem für LOX Typ-2 *in vitro*? Universität Bayreuth, Bayreuth. Dissertation.
238. B.A.W. Gallasch and G. Spiteller. **2000**. Synthesis of 9,12-dioxo-10(*Z*)-dodecenoic acid, a new fatty acid metabolite derived from 9-hydroperoxy-10,12-octadecadienoic acid in lentil seed (*Lens culinaris* Medik.). Lipids 35(9): 953-960.
239. A. Mlakar and G. Spiteller. **1994**. Reinvestigation of lipid-peroxidation of linolenic acid. Biochim. Biophys. Acta-Lipids Lipid Metab. 1214(2): 209-220.
240. F.F. Hsu, S.L. Hazen, D. Giblin, J. Turk, J.W. Heinecke, and M.L. Gross. **1999**. Mass spectrometric analysis of pentafluorobenzyl oxime derivatives of reactive biological aldehydes. Int. J. Mass Spectrom. 187: 795-812.
241. G. Spiteller, W. Kern, and P. Spiteller. **1999**. Investigation of aldehydic lipid peroxidation products by gas chromatography-mass spectrometry. J. Chromatogr. A 843(1-2): 29-98.
242. M. Hesse, H. Meier, and B. Zeeh. **2002**. Spektroskopische Methoden in der organischen Chemie. Georg Thieme Verlag, Stuttgart.
243. F.W. McLafferty. **1959**. Mass spectrometric analysis - molecular rearrangements. Anal. Chem. 31(1): 82-87.
244. A. Mlakar and G. Spiteller. **1996**. Dihydroxy and hydroxyoxo fatty acids as products of nonenzymic lipid peroxidation of polyunsaturated fatty acids. Chem. Phys. Lipids 82(1): 25-32.
245. M. Leitner, A. Mithöfer, and W. Boland. **2005**. Direct and indirect defences induced by piercing-sucking and chewing herbivores in *Medicago truncatula.* New Phytol. doi: 10.1111/j.1469-8137.2005.01426.x.
246. G. Hoffmann, S. Aramaki, E. Blum-Hoffmann, W.L. Nyhan, and L. Sweetman. **1989**. Quantitative analysis for organic acids in biological samples: batch isolation followed by gas chromatographic-mass spectrometric analysis. Clin. Chem. 35(4): 587-595.

247. T.C.J. Turlings, U.B. Lengwiler, M.L. Bernasconi, and D. Wechsler. **1998**. Timing of induced volatile emissions in maize seedlings. Planta 207(1): 146-152.
248. M. Kunert, A. Biedermann, T. Koch, and W. Boland. **2002**. Ultrafast sampling and analysis of plant volatiles by a hand-held miniaturised GC with pre-concentration unit: Kinetic and quantitative aspects of plant volatile production. J. Sep. Sci. 25(10-11): 677-684.
249. M. Heil. **2002**. Ecological costs of induced resistance. Curr. Opin. Plant Biol. 5(4): 345-350.
250. L. Mattiacci, M. Dicke, and M.A. Posthumus. **1995**. β-Glucosidase - an elicitor of herbivore-induced plant odor that attracts host-searching parasitic wasps. Proc. Natl. Acad. Sci. USA 92(6): 2036-2040.
251. K.A. Shackel, M. de la Paz Celorio-Mancera, H. Ahmadi, L.C. Greve, L.R. Teuber, E.A. Backus, and J.M. Labavitch. **2005**. Micro-injection of Lygus salivary gland proteins to simulate feeding damage in alfalfa and cotton flowers. Arch. Insect Biochem. Physiol. 58(2): 69-83.
252. T. Alborn, T.C.J. Turlings, T.H. Jones, G. Stenhagen, J.H. Loughrin, and J.H. Tumlinson. **1997**. An elicitor of plant volatiles from beet armyworm oral secretion. Science 276(5314): 945-949.
253. C.L. Truitt and P.W. Pare. **2004**. In situ translocation of volicitin by beet armyworm larvae to maize and systemic immobility of the herbivore elicitor in planta. Planta 218(6): 999-1007.
254. G. Pohnert, V. Jung, E. Haukioja, K. Lempa, and W. Boland. **1999**. New fatty acid amides from regurgitant of lepidopteran (Noctuidae, Geometridae) caterpillars. Tetrahedron 55(37): 11275-11280.
255. D. Spiteller, K. Dettner, and W. Boland. **2000**. Gut bacteria may be involved in interactions between plants, herbivores and their predators: Microbial biosynthesis of *N*-acylglutamine surfactants as elicitors of plant volatiles. Biol. Chem. 381(8): 755-762.
256. P.W. Paré, H.T. Alborn, and J.H. Tumlinson. **1998**. Concerted biosynthesis of an insect elicitor of plant volatiles. Proc. Natl. Acad. Sci. USA 95(23): 13971-13975.
257. C.G. Lait, H.T. Alborn, P.E.A. Teal, and J.H. Tumlinson. **2003**. Rapid biosynthesis of *N*-linolenoyl-L-glutamine, an elicitor of plant volatiles, by membrane-associated enzyme(s) in *Manduca sexta*. Proc. Natl. Acad. Sci. USA 100(12): 7027-7032.
258. J.H. Tumlinson and C.G. Lait. **2005**. Biosynthesis of fatty acid amide elicitors of plant volatiles by insect herbivores. Arch. Insect Biochem. Physiol. 58(2): 54-68.
259. L. Ping, D. Spiteller, and W. Boland. **2003**. Plant defense-inducing *N*-acylglutamines from insect guts: structural diversity and microbe-assisted biosynthesis. Pages 1211-1216 *in* The BCPC International Congress - Crop Science & Technology 2003. British Crop Protection Council, Alton.
260. L. Ping. **2005**. Biosynthesis of *N*-acyl glutamines in the insect gut: impact and characterisation of microbial enzymes. Friedrich Schiller Universität, Jena. Dissertation.
261. S.C. Peterson, N.D. Johnson, and J.L. Leguyader. **1987**. Defensive regurgitation of allelochemicals derived from host cyanogenesis by eastern tent caterpillars. Ecology 68(5): 1268-1272.
262. P.A. Blau, P. Feeny, L. Contardo, and D.S. Robson. **1978**. Allylglucosinolate and herbivorous caterpillars: contrast in toxicity and tolerance. Science 200(4347): 1296-1298.
263. A. Giamoustaris and R. Mithen. **1995**. The effect of modifying the glucosinolate content of leaves of oilseed rape (*Brassica napus* ssp. *oleifera*) on its interaction with specialist and generalist pests. Ann. Appl. Biol. 126(2): 347-363.

264. A.M. Bones and J.T. Rossiter. **1996**. The myrosinase-glucosinolate system, its organisation and biochemistry. Physiol. Plant. 97(1): 194-208.
265. L.S. Self, F.E. Guthrie, and E. Hodgson. **1964**. Adaptation of tobacco hornworms to the ingestion of nicotine. J. Insect Physiol. 10(6): 907-914.
266. K. Konno, C. Hirayama, and H. Shinbo. **1996**. Unusually high concentration of free glycine in the midgut content of the silkworm, *Bombyx mori*, and other lepidopteran larvae. Comp. Biochem. Physiol. A-Physiol. 115(3): 229-235.
267. K. Konno, H. Yasui, C. Hirayama, and H. Shinbo. **1998**. Glycine protects against strong protein-denaturing activity of oleuropein. A phenolic compound in privet leaves. J. Chem. Ecol. 24(4): 735-751.
268. W.S. Pierpoint. **1969**. *o*-Quinones formed in plant extracts - their reactions with amino acids and peptides. Biochem. J. 112(5): 609-617.
269. K. Konno, C. Hirayama, and H. Shinbo. **1997**. Glycine in digestive juice: A strategy of herbivorous insects against chemical defense of host plants. J. Insect Physiol. 43(3): 217-224.
270. K. Konno, S. Okada, and C. Hirayama. **2001**. Selective secretion of free glycine, a neutralizer against a plant defense chemical, in the digestive juice of the privet moth larvae. J. Insect Physiol. 47(12): 1451-1457.
271. H. Eichenseer, M.C. Mathews, J.L. Bi, J.B. Murphy, and G.W. Felton. **1999**. Salivary glucose oxidase: Multifunctional roles for *Helicoverpa zea*? Arch. Insect Biochem. Physiol. 42(1): 99-109.
272. R.O. Musser, S.M. Hum-Musser, H. Eichenseer, M. Peiffer, G. Ervin, J.B. Murphy, and G.W. Felton. **2002**. Herbivory: Caterpillar saliva beats plant defences - A new weapon emerges in the evolutionary arms race between plants and herbivores. Nature 416(6881): 599-600.
273. R.O. Musser, D.F. Cipollini, S.M. Hum-Musser, S.A. Williams, J.K. Brown, and G.W. Felton. **2005**. Evidence that the caterpillar salivary enzyme glucose oxidase provides herbivore offense in Solanaceous plants. Arch. Insect Biochem. Physiol. 58(2): 128-137.
274. M. Peiffer and G.W. Felton. **2005**. The host plant as a factor in the synthesis and secretion of salivary glucose oxidase in larval *Helicoverpa zea.* Arch. Insect Biochem. Phys. 58(2): 106-113.
275. L.B. Brattsten. **1988**. Enzymic adaptations in leaf-feeding insects to host-plant allelochemicals. J. Chem. Ecol. 14(10): 1919-1939.
276. X.C. Li, J. Baudry, M.R. Berenbaum, and M.A. Schuler. **2004**. Structural and functional divergence of insect CYP6B proteins: From specialist to generalist cytochrome P450. Proc. Natl. Acad. Sci. USA 101(9): 2939-2944.
277. K.S. Brown. **1987**. Chemistry at the Solanaceae/Ithomiinae interface. Ann. Mo. Bot. Gard. 74(2): 359-397.
278. A.R. Masters. **1990**. Pyrrolizidine alkaloids in artificial nectar protect adult *Ithomiine* butterflies from a spider predator. Biotropica 22(3): 298-304.
279. T. Hartmann. **1999**. Chemical ecology of pyrrolizidine alkaloids. Planta 207(4): 483-495.
280. P. Barbosa, P. Gross, and J. Kemper. **1991**. Influence of plant allelochemicals on the tobacco hornworm and its parasitoid, *Cotesia congregata.* Ecology 72(5): 1567-1575.
281. M.J. Snyder, J.K. Walding, and R. Feyereisen. **1994**. Metabolic fate of the allelochemical nicotine in the tobacco hornworm *Manduca sexta.* Insect Biochem. Mol. Biol. 24(8): 837-846.

282. O. Fietz, K. Dettner, H. Görls, K. Klemm, and W. Boland. **2002**. (*R*)-(+)-Palasonin, a cantharidin-related plant toxin, also occurs in insect hemolymph and tissues. J. Chem. Ecol. 28(7): 1315-1327.
283. M. Berenbaum and P. Feeny. **1981**. Toxicity of angular furanocoumarins to swallowtail butterflies: Escalation in a coevolutionary arms race. Science 212(4497): 927-929.
284. X.C. Li, M.A. Schuler, and M.R. Berenbaum. **2002**. Jasmonate and salicylate induce expression of herbivore cytochrome P450 genes. Nature 419(6908): 712-715.
285. J. Chiu, R. DeSalle, H.M. Lam, L. Meisel, and G. Coruzzi. **1999**. Molecular evolution of glutamate receptors: A primitive signaling mechanism that existed before plants and animals diverged. Mol. Biol. Evol. 16(6): 826-838.
286. H.M. Lam, J. Chiu, M.H. Hsieh, L. Meisel, I.C. Oliveira, M. Shin, and G. Coruzzi. **1998**. Glutamate-receptor genes in plants. Nature 396(6707): 125-126.
287. K. Hori. **1992**. Insect secreations and their effect on plant growth, with special referece to Hemipterans. Pages 157-170 *in* J.D. Shorthouse and O. Rohfritsch, editors. Biology of insect-induced galls. Oxford University Press, Oxford.
288. W. Hovanitz. **1959**. Insects and plant galls. Sci. Am. 201(5): 151-162.
289. G.W. Elzen. **1983**. Cytokinins and insect galls. Comp. Biochem. Physiol. A-Physiol. 76(1): 17-19.
290. V.V. Roshchina. **2001**. Neurotransmitters in plant life. Science Publishers Inc., Enfield.
291. J.C. Schultz. **2002**. Shared signals and the potential for phylogenetic espionage between plants and animals. Integr. Comp. Biol. 42(3): 454-462.
292. M.J. Mueller. **2004**. Archetype signals in plants: the phytoprostanes. Curr. Opin. Plant Biol. 7(4): 441-448.
293. K. Büyükgüzel, H. Tunaz, S.M. Putnam, and D. Stanley. **2002**. Prostaglandin biosynthesis by midgut tissue isolated from the tobacco hornworm, *Manduca sexta.* Insect Biochem. Mol. Biol. 32(4): 435-443.
294. J.C. Schultz and H.M. Appel. **2004**. Cross-kingdom cross-talk: Hormones shared by plants and their insect herbivores. Ecology 85(1): 70-77.
295. D.Q. Yu, Y.D. Liu, B.F. Fan, D.F. Klessig, and Z.X. Chen. **1997**. Is the high basal level of salicylic acid important for disease resistance in potato? Plant Physiol. 115(2): 343-349.
296. A. Mithöfer, G. Wanner, and W. Boland. **2005**. Effects of feeding *Spodoptera littoralis* on Lima bean leaves. II. Continuous mechanical wounding resembling insect feeding is sufficient to elicit herbivory-related volatile emission. Plant Physiol. 137(3): 1160-1168.
297. D. Bowles. **1998**. Signal transduction in the wound response of tomato plants. Philos. Trans. R. Soc. Lond. B 353(1374): 1495-1510.
298. G.L. Gentry and L.A. Dyer. **2002**. On the conditional, nature of neotropical caterpillar defenses against their natural enemies. Ecology 83(11): 3108-3119.
299. G.W. Felton and S.S. Duffey. **1991**. Reassessment of the role of gut alkalinity and detergency in insect herbivory. J. Chem. Ecol. 17(9): 1821-1836.
300. I.A. Butovich and C.C. Reddy. **2001**. Enzyme-catalyzed and enzyme-triggered pathways in dioxygenation of 1-monolinoleoyl-*rac*-glycerol by potato tuber lipoxygenase. Biochim. Biophys. Acta-Protein Struct. Molec. Enzym. 1546(2): 379-398.
301. B.A. Stelmach, A. Müller, P. Hennig, S. Gebhardt, M. Schubert-Zsilavecz, and E.W. Weiler. **2001**. A novel class of oxylipins, *sn*1-*O*-(12-oxophytodienoyl)-*sn*2-*O*-(hexadecatrienoyl)-monogalactosyl diglyceride, from *Arabidopsis thaliana.* J. Biol. Chem. 276(16): 12832-12838.
302. Y. Hisamatsu, N. Goto, K. Hasegawa, and H. Shigemori. **2003**. Arabidopsides A and B, two new oxylipins from *Arabidopsis thaliana.* Tetrahedron Lett. 44(29): 5553-5556.

303. Y. Hisamatsu, N. Goto, M. Sekiguchi, K. Hasegawa, and H. Shigemori. **2005**. Oxylipins arabidopsides C and D from *Arabidopsis thaliana.* J. Nat. Prod. 68(4): 600-603.
304. T. Ohashi, Y. Ito, M. Okada, and Y. Sakagami. **2005**. Isolation and stomatal opening activity of two oxylipins from *Ipomoea tricolor.* Bioorg. Med. Chem. Lett. 15(2): 263-265.
305. R.L. Rana and D.W. Stanley. **1999**. In vitro secretion of digestive phospholipase A_2 by midguts isolated from tobacco hornworms, *Manduca sexta.* Arch. Insect Biochem. Physiol. 42(3): 179-187.
306. P. Sitte, H. Zeigler, F. Ehrendorfer, and A. Bresinsky. **1998**. Strasburger Lehrbuch der Botanik. Gustav Fischer Verlag, Stuttgart.
307. J. Piel, R. Atzorn, R. Gäbler, F. Kühnemann, and W. Boland. **1997**. Cellulysin from the plant parasitic fungus *Trichoderma viride* elicits volatile biosynthesis in higher plants via the octadecanoid signalling cascade. FEBS Lett. 416(2): 143-148.
308. R. Lauchli and W. Boland. **2003**. Indanoyl amino acid conjugates: Tunable elicitors of plant secondary metabolism. Chem. Rec. 3(1): 12-21.
309. A. Mithöfer, M. Maitrejean, and W. Boland. **2004**. Structural and biological diversity of cyclic octadecanoids, jasmonates, and mimetics. J. Plant Growth Regul. 23(3): 170-178.
310. M. Dicke, R. Gols, D. Ludeking, and M.A. Posthumus. **1999**. Jasmonic acid and herbivory differentially induce carnivore- attracting plant volatiles in lima bean plants. J. Chem. Ecol. 25(8): 1907-1922.
311. R. Volinsky, S. Kolusheva, A. Berman, and R. Jelinek. **2004**. Microscopic visualization of alamethicin incorporation into model membrane monolayers. Langmuir 20(25): 11084-11091.
312. D.S. Cafiso. **1994**. Alamethicin: a peptide model for voltage gating and protein membrane interactions. Annu. Rev. Biophys. Biomolec. Struct. 23: 141-165.
313. J. Engelberth, T. Koch, F. Kühnemann, and W. Boland. **2000**. Channel-forming peptaibols are potent elicitors of plant secondary metabolism and tendril coiling. Angew. Chem.-Int. Edit. 39(10): 1860-1862.
314. M.D. Rosenthal, B.S. Vishwanath, and R.C. Franson. **1989**. Effects of aristolochic acid on phospholipase A_2 activity and arachidonate metabolism of human neutrophils. Biochim. Biophys. Acta 1001(1): 1-8.
315. G.F.E. Scherer and B. Arnold. **1997**. Inhibitors of animal phospholipase A_2 enzymes are selective inhibitors of auxin-dependent growth. Implications for auxin- induced signal transduction. Planta 202(4): 462-469.
316. C. Cucurou, J.P. Battioni, D.C. Thang, N.H. Nam, and D. Mansuy. **1991**. Mechanisms of inactivation of lipoxygenases by phenidone and BW755C. Biochemistry 30(37): 8964-8970.
317. S. Berger. **2002**. Jasmonate-related mutants of *Arabidopsis* as tools for studying stress signaling. Planta 214(4): 497-504.
318. H. Cao, S.A. Bowling, A.S. Gordon, and X.N. Dong. **1994**. Characterization of an *Arabidopsis* mutant that is nonresponsive to inducers of systemic acquired-resistance. Plant Cell 6(11): 1583-1592.
319. K. Maleck and R.A. Dietrich. **1999**. Defense on multiple fronts: How do plants cope with diverse enemies? Trends Plant Sci. 4(6): 215-219.
320. J.P. Cui, G. Jander, L.R. Racki, P.D. Kim, N.E. Pierce, and F.M. Ausubel. **2002**. Signals involved in *Arabidopsis* resistance to *Trichoplusia ni* caterpillars induced by virulent and avirulent strains of the phytopathogen *Pseudomonas syringae.* Plant Physiol. 129(2): 551-564.

321. J. Cui, A.K. Bahrami, E.G. Pringle, G. Hernandez-Guzman, C.L. Bender, N.E. Pierce, and F.M. Ausubel. **2005**. *Pseudomonas syringae* manipulates systemic plant defenses against pathogens and herbivores. Proc. Natl. Acad. Sci. USA 102(5): 1791-1796.
322. J.L. Riechmann, J. Heard, G. Martin, L. Reuber, C.Z. Jiang, J. Keddie, L. Adam, O. Pineda, O.J. Ratcliffe, R.R. Samaha, R. Creelman, M. Pilgrim, P. Broun, J.Z. Zhang, D. Ghandehari, B.K. Sherman, and C.L. Yu. **2000**. *Arabidopsis* transcription factors: Genome-wide comparative analysis among eukaryotes. Science 290(5499): 2105-2110.
323. W.Q. Chen, N.J. Provart, J. Glazebrook, F. Katagiri, H.S. Chang, T. Eulgem, F. Mauch, S. Luan, G.Z. Zou, S.A. Whitham, P.R. Budworth, Y. Tao, Z.Y. Xie, X. Chen, S. Lam, J.A. Kreps, J.F. Harper, A. Si-Ammour, B. Mauch-Mani, M. Heinlein, K. Kobayashi, T. Hohn, J.L. Dangl, X. Wang, and T. Zhu. **2002**. Expression profile matrix of *Arabidopsis* transcription factor genes suggests their putative functions in response to environmental stresses. Plant Cell 14(3): 559-574.
324. S. Berger, T. Mitchell-Olds, and H.U. Stotz. **2002**. Local and differential control of vegetative storage protein expression in response to herbivore damage in *Arabidopsis thaliana.* Physiol. Plant. 114(1): 85-91.
325. G.S. Liu, E.B. Holub, J.M. Alonso, J.R. Ecker, and P.R. Fobert. **2005**. An Arabidopsis *NPR1*-like gene, *NPR4*, is required for disease resistance. Plant J. 41(2): 304-318.
326. I. Penninckx, K. Eggermont, F.R.G. Terras, B. Thomma, G.W. Desamblanx, A. Buchala, J.P. Métraux, J.M. Manners, and W.F. Broekaert. **1996**. Pathogen-induced systemic activation of a plant defensin gene in *Arabidopsis* follows a salicylic acid-independent pathway. Plant Cell 8(12): 2309-2323.
327. N.D. LeBrasseur, G.C. MacIntosh, M.A. Pérez-Amador, M. Saitoh, and P.J. Green. **2002**. Local and systemic wound-induction of RNase and nuclease activities in Arabidopsis: RNS1 as a marker for a JA-independent systemic signaling pathway. Plant J. 29(4): 393-403.
328. M. Aida, T. Ishida, H. Fukaki, H. Fujisawa, and M. Tasaka. **1997**. Genes involved in organ separation in *Arabidopsis*: An analysis of the *cup-shaped cotyledon* mutant. Plant Cell 9(6): 841-857.
329. A.N. Olsen, H.A. Ernst, L. Lo Leggio, and K. Skriver. **2005**. NAC transcription factors: structurally distinct, functionally diverse. Trends Plant Sci. 10(2): 79-87.
330. P. Reymond, N. Bodenhausen, R.M.P. Van Poecke, V. Krishnamurthy, M. Dicke, and E.E. Farmer. **2004**. A conserved transcript pattern in response to a specialist and a generalist herbivore. Plant Cell 16(11): 3132-3147.
331. R.M.P. Van Poecke, M.A. Posthumus, and M. Dicke. **2001**. Herbivore-induced volatile production by *Arabidopsis thaliana* leads to attraction of the parasitoid *Cotesia rubecula*: Chemical, behavioral, and gene-expression analysis. J. Chem. Ecol. 27(10): 1911-1928.
332. F. Chen, J.C. D'Auria, D. Tholl, J.R. Ross, J. Gershenzon, J.P. Noel, and E. Pichersky. **2003**. An *Arabidopsis thaliana* gene for methylsalicylate biosynthesis, identified by a biochemical genomics approach, has a role in defense. Plant J. 36(5): 577-588.
333. D. Tholl, F. Chen, J. Gershenson, and E. Pichersky. **2004**. *Arabidopsis thaliana*, a model system for investigating volatile terpene biosynthesis, regulation, and function. Pages 1-18 *in* J.T. Romeo, editor Secondary metabolism in model systems. Elsevier, Amsterdam.
334. J. Ebel and A. Mithöfer. **1998**. Early events in the elicitation of plant defence. Planta 206(3): 335-348.

335. P. Moesta and H. Grisebach. **1981**. Investigation of the mechanism of phytoalexin accumulation in soybean induced by glucan or mercuric chloride. Arch. Biochem. Biophys. 211(1): 39-43.
336. G. Schüler. **2001**. Coronatin-analoga: molekulare Sonden für pflanzliche Signalwege. Friedrich-Schiller-Universität, Jena. Dissertation.
337. V.M. Temperton, R.J. Hobbs, T. Nuttle, and S. Halle. **2004**. Assembly rules and restoration ecology: bridging the gap between theory and practice. Island Press, Washington, DC.
338. W. Heinrich, J. Perner, and R. Marstaller. **2001**. Regeneration und Sekundärsukzession - 10 Jahre Dauerflächenuntersuchungen im Immissionsgebiet eines ehemaligen Düngemittelwerkes. Zeitschr. Ökol. Naturschutz 9: 237-253.
339. K. Metzner, Y. Friedrich, and G. Schäller. **1997**. Bodenparameter eines Immissionsgebietes vor und nach der Schließung eines Düngemittelwerkes (1979-1997). Beitr. Ökol. 3(1): 51-75.
340. T. Koch. **2001**. Analytik pflanzlicher Signalstoffe: Phytohormone und Abwehr. Friedrich Schiller Universität, Jena. Dissertation.
341. T. Fink, S. Büscher, R. Gäbler, Q. Yu, A. Dax, and W. Urban. **1996**. An improved CO_2 laser intracavity photoacoustic spectrometer for trace gas analysis. Rev. Sci. Instrum. 67(11): 4000-4004.
342. M. Held. **2003**. The effect of pollutant emission on the resistance and tolerance of *Artemisia vulgaris* to herbivores. Friedrich Schiller Universität, Jena. Dissertation.
343. A. Chaoui, S. Mazhoudi, M.H. Ghorbal, and E. Elferjani. **1997**. Cadmium and zinc induction of lipid peroxidation and effects on antioxidant enzyme activities in bean (*Phaseolus vulgaris* L.). Plant Sci. 127(2): 139-147.
344. S. Bhattacharjee. **1998**. Membrane lipid peroxidation, free radical scavengers and ethylene evolution in *Amaranthus* as affected by lead and cadmium. Biol. Plant. 40(1): 131-135.
345. B. Halliwell and J.M.C. Gutteridge. **1992**. Biologically relevant metal ion-dependent hydroxyl radical generation - an update. FEBS Lett. 307(1): 108-112.
346. H.W. Gardner. **1989**. Oxygen radical chemistry of polyunsaturated fatty acids. Free Radic. Biol. Med. 7(1): 65-86.
347. P. Spiteller and G. Spiteller. **1998**. Strong dependence of the lipid peroxidation product spectrum whether Fe^{2+}/O^{-2} or Fe^{3+}/O^{-2} is used as oxidant. Biochim. Biophys. Acta-Lipids Lipid Metab. 1392(1): 23-40.
348. R. Imbusch and M.J. Mueller. **2000**. Analysis of oxidative stress and wound-inducible dinor isoprostanes F_1 (phytoprostanes F_1) in plants. Plant Physiol. 124(3): 1293-1303.
349. J. Léon, M.A. Lawton, and I. Raskin. **1995**. Hydrogen peroxide stimulates salicylic acid biosynthesis in tobacco. Plant Physiol. 108(4): 1673-1678.
350. K. Summermatter, L. Sticher, and J.P. Métraux. **1995**. Systemic responses in *Arabidopsis thaliana* infected and challenged with *Pseudomonas syringae* pv *syringae*. Plant Physiol. 108(4): 1379-1385.
351. U. Neuenschwander, B. Vernooij, L. Friedrich, S. Uknes, H. Kessmann, and J. Ryals. **1995**. Is hydrogen peroxide a second messenger of salicylic acid in systemic acquired resistance? Plant J. 8(2): 227-233.
352. K.A. Blee, K.Y. Yang, and A.J. Anderson. **2004**. Activation of defense pathways: synergism between reactive oxygen species and salicylic acid and consideration of field applicability. Eur. J. Plant Pathol. 110(2): 203-212.
353. D.V. Lynch, S. Sridhara, and J.E. Thompson. **1985**. Lipoxygenase-generated hydroperoxides account for the nonphysiological features of ethylene formation from 1-

aminocyclopropane-1-carboxylic acid by microsomal membranes of carnations. Planta 164(1): 121-125.
354. A.J. de Jong, E.T. Yakimova, V.M. Kapchina, and E.J. Woltering. **2002**. A critical role for ethylene in hydrogen peroxide release during programmed cell death in tomato suspension cells. Planta 214(4): 537-545.
355. D.M. Gibeaut, J. Hulett, G.R. Cramer, and J.R. Seemann. **1997**. Maximal biomass of *Arabidopsis thaliana* using a simple, low-maintenance hydroponic method and favorable environmental conditions. Plant Physiol. 115(2): 317-319.
356. R. Bergomaz and M. Boppré. **1986**. A simple insect diet for rearing Arctiidae and other moths. J. Lepidopterist´s Soc. 40: 131-137.
357. M. Veith, N.J. Oldham, K. Dettner, J.M. Pasteels, and W. Boland. **1997**. Biosynthesis of defensive allomones in leaf beatle larvae. J. Chem. Ecol. 23(2): 429-443.
358. R. Lauchli and W. Boland. **2003**. Efficient synthesis of [$^2H_2$]-tetrahydrodicranenone B and a 3-oxa-analogue resistant against β-oxidation. Tetrahedron 59(2): 149-153.
359. C.A. Brown and V.K. Ahuja. **1973**. "P-2 nickel" catalyst with ethylenediamine, a novel system for highly stereospecific reduction of alkynes to *cis*-olefins. J. Chem. Soc.-Chem. Commun. (15): 553-554.
360. S. Adolph, S.A. Poulet, and G. Pohnert. **2003**. Synthesis and biological activity of α,β,γ,δ-unsaturated aldehydes from diatoms. Tetrahedron 59(17): 3003-3008.
361. D. Spiteller. **2002**. Charakterisierung von *N*-Acyl-glutaminkonjugaten aus dem Regurgitat von Lepidoptera Larven. Friedrich Schiller Universität, Jena. Dissertation.
362. J.M. Bobbitt. **1998**. Oxoammonium salts. 6. 4-acetylamino-2,2,6,6-tetramethylpiperidine-1-oxoammonium perchlorate: A stable and convenient reagent for the oxidation of alcohols. Silica gel catalysis. J. Org. Chem. 63(25): 9367-9374.
363. P. Wheelan, R.C. Murphy, and F.R. Simon. **1996**. Gas chromatographic mass spectrometric analysis of oxo and chain-shortened leukotriene B-4 metabolites, leukotriene B-4 metabolism in Ito cells. J. Mass Spectrom. 31(3): 236-246.
364. J. Donath and W. Boland. **1995**. Biosynthesis of acyclic homoterpenes: Enzyme selectivity and absolute configuration of the nerolidol precursor. Phytochemistry 39(4): 785-790.
365. L.A.C.J. Voesenek, F.J.M. Harren, G.M. Bögemann, C.W.P.M. Blom, and J. Reuss. **1990**. Ethylene production and petiole growth in *Rumex* plants induced by soil waterlogging - The application of a continuous flow system and a laser driven intracavity photoacoustic detection system. Plant Physiol. 94(3): 1071-1077.
366. H.G. Zachmann. **1994**. Mathematik für Chemiker. VCH, Weinheim.

11 ACKNOWLEDGEMENTS

In particular I want to express my gratitude to my supervisor **Prof. Wilhelm Boland**, for giving me the opportunity to work on this exciting topic of oxylipins; for his encouragement, stimulating enthusiasm, and unrestricted support, providing me with the freedom to design my project according to my interests.

I want to thank **Prof. Jochen Lehmann** for advising my work from the pharmaceutical aspect and giving me the chance to present thesis at the Faculty for Biology and Pharmacy at the Friedrich-Schiller-University, Jena.

Further, I am grateful to **Prof. Stefan Halle** for consulting this study from the ecological point of view and for the coordination of the Graduate Research School “Analysis of the Functioning and Regeneration of Degraded Ecosystems” (GRK 266).

In addition, I want to thank **Prof. Christiane Gatz** and **Marco Herde** for the opportunity to contribute to the development of a combined chemical and molecular biological analysis matching the oxylipin profiling to defense related gene expression.

I am indebted to **Prof. Claus Wasternack** (IPB, Halle, Germany) for the generous gift of purified 12-oxophytodienoic acid; **Prof. Thierry Durand** for sending samples of type F_1 phytoprostanes and **Dr. Gerd Trautmann** (Bayer AG, Monheim, Germany) for supplying our group with egg clutches of lepidopteran larvae. Moreover, I want to thank to **Prof. Frank Kühnemann** for the ethylene measurements of the heavy metal induced Lima bean plants.

In particular I want express my sincere thanks **Prof. Gerhard Spiteller** for supporting me with his experience in the interpretation of intricate mass spectra.

Financial support by the **Deutsche Forschungsgemeinschaft**, Graduiertenkolleg GRK 266 and by the **Max-Planck-Gesellschaft** is gratefully acknowledged.

All members of the **Max Planck Institute for Chemical Ecology** and **colleagues at the Friedrich-Schiller-University** are thanked for their kind friendship and for creating a motivating and pleasant working atmosphere and supporting me wherever they could.

From my colleagues at the **Bioorganic Chemistry Group** I am especially indebted to:

Georg Pohnert not only for great mental and practical support concerning analytical and laboratory questions, in particular for helping me during serious breakdowns of the mass spectrometer, but also for being a critical reviewer of my texts, posters and oral presentations. Additionally I have to thank him and his family for all the shared hours and

joined activities including gardening, botanical excursions, and cross-country skiing; **Stefan Bartram** for supporting my work with this analytical know-how and for always having time to listen to scientific and private problems; **Anja Biedermann** for introducing me into various laboratory techniques commonly used in our group and for so much of help with extracting thousands of samples; **Angelika Berg** for the intensive care of the caterpillar eggs and larvae, the growth of Lima bean plants, and for raising some extra plants for my window and garden; **Janine Rattke** and **Christoph Beckmann** for supporting me from the very beginning as well as for shared hours including lots of delicious meals and BBQing on their terrace; **Sven Adolph** for the synthesis of 13-oxo-9,11-tridecadienoic acid, improving my script, and for always having the right slogans at hand; **Christian Kost** for patiently teaching me statistics, lots of inspiring conversation and scientific discussions, and for proof reading my texts; **Margit Leitner** for Austrian food and beer specialties, her botanical enthusiasm, and for ameliorating various texts of mine; **Thomas Wichard** for provocative debates on queer topics and inspiring discussions, for his excellent maintenance of the Trace MS instrument, and proof reading my manuscript; **Ryan Lauchli** for the synthesis of [15,16-$^{2}H_2$]-tetrahydrodicranenone B, 11-oxo-9-undecenoic acid, and [9,10-$^{2}H_2$]-11-oxo-9-undecenoic acid, and for being a cheerful office member; **Mesmin Mekem Sonwa** for providing me with oxylipin enriched samples of his linolenic acid autoxidation experiments, for helping me with the tomato-mousse-synthesis, and fruitful debates on the interpretation of mass spectra; **Axel Mithöfer** for supporting my work with his knowledge on biological and biochemical aspects; **Doreen Schachtschabel** for helping me with experiments on the isomerization of jasmonic acid, for our motivating sports sessions, and for being a cheerful office member; **Andreas Habel** for accompanying me during late working times and for sharing his tips and tricks on computer problems and instrumentations; **Lihua Nie** for so many shared hours and late evenings, and introducing me to delicious Chinese tea and food; **Annika Schmidt** for the synthesis of the Phytoprostanes B_1 type I and II and various other phytoprostane derivatives; **Heiko Maischak** for his affable company during weekend working times and for consequently forcing me to interrupt my stressed writing; **Stefan Garms** for lots of fun and queer experiences during the synthesis of 9- or 13-KOTE; **Jian-Wen Tan** for fruitful discussions on the identity of phytoprostanes in Lima bean and other samples; **Maritta Kunert**, **Rita Büchler**, **Antje Burse** and **Sabrina Discher** for the inspiring and cheerful sharing of lab space; **Grit Winnefeld** for coordination and help with all administrative paper-warfare; **Paulina Dąbrowska** for enthusiastically continuing this work on oxylipin analysis.

From my colleagues at the **Molecular Ecology Group** I want to thank **Caroline von Dahl**, **Silvia Schmidt**, **Anke Steppuhn**, and **Anja Paschold** for lots of fun during collaborative lab-experiences, scientific disputations, as well as hours of coffee drinking, and joined tours in and around Jena.

Moreover, I want to thank all members of the institute's service facilities especially **Bernd Schneider** and **Christian Paetz** for instructing me in the usage of the NMR instrument; **Aleš Svatoš** and **Sybille Lorenz** for their efforts in recording high resolution mass spectra; the staff of the greenhouse especially **Tamara Krügel** and **Andreas Weber** for caring for the Lima bean plants; the members of the Haustechnik and workshop, for supplying me with the right tools for repairing several instrument breakdowns, in particular **Christian Gast** for repeatedly replacing burned electrical condensers; the staff of our library **Linda Maack**, **Simone Bieniek** and **Wieland Micheel** for their support, especially for assistance concerning usage and programming of Endnote; the EDV-group in particular **Dieter Ruder** and **Matthias Stoll** for their support concerning computer problems and for giving me the chance to present my orchids-webpage in the internet.

From my colleagues at the **Graduate Research School** I especially want to thank **Verena Blanke** for our "defragmentation" session at the Irish pub and our intense writing of the restoration paper; **Marlene Willkomm** and **Clemens Augspurger** for the inspiring and relaxing after-the-seminar meetings.

From my colleagues of the **Department of Pharmaceutical Chemistry** I especially want to thank **Kathrin Lange**, **Manuela Hammitzsch**, and **Jörg Konter** for our joint mensa eat outs.

I want to thank my former colleagues from the **Max Plank Institute for Biogeochemistry** for their friendship and support. In particular I want to mention **Lina-Maria Mercado**, **Annett Börner**, **Leticia Cotrim da Cunha**, **Ansgar Kahmen**, **Volker Hahn**, and **Dirk Sachse**.

In this place I want to thank **Dieter** for supporting me from the very beginning of my work and encouraging me when struggling with various drawbacks. Without his inspiration and implicit backing this work would not have been possible.

Last but not least I would like to thank my **parents** for supporting me during my studies and during my time as doctoral student.

12 CURRICULUM VITAE

Jena, 7/5/2005

Name Birgit Schulze
Date of birth 10. December 1975, Bayreuth, Germany
Nationality German

Education

Nov. 2000 Staatsexamen and Approbation
1995 - 1999 Study of Pharmacy at the Philipps-University, Marburg
June 1995 Abitur, Markgräfin-Wilhelmine-Gymnasium, Bayreuth

Professional and scientific career

since Doctoral student at the Max Planck Institute for Chemical Ecology, Jena
Sept. 2001 Fellow of the Graduate Research School "Analysis of the Functioning and Regeneration of Degraded Ecosystems" (GRK 226), Friedrich-Schiller-University, Jena
Project: *Oxylipins and their involvement in plant response to biotic and abiotic stress*
2001 Technician at the Max Planck Institute for Biogeochemistry, Jena
Project: *Developing a laser ablation technique coupled with an isotope ratio MS for the online detection of $\delta^{13}C$ variations in tree rings*
June - Oct. 2000 Trainee Pharmacist at the Life Science Center - Natural Products, Bayer AG, Wuppertal
Trainee Pharmacist at the Tannenberg Apotheke, Wuppertal
Nov. 1999 - May 2000 Trainee Pharmacist at the Groß Grönauer Apotheke, Groß Grönau; near Lübeck
1997 - 1998 Student assistant at the Max Planck Institute of Biogeochemistry, Jena
Project: *Forest inventory in Central Siberia*
Student assistant at the Institute of Pharmaceutical Chemistry, Marburg
Projects: *Crystallizing proteins for x-ray spectroscopy*
Investigating the protocol of tropic acid identification
1991 Winner of the German-wide contest, "Jugend forscht"
Project: *"Frische Luft im Klassenzimmer?" - CO_2-measurements in classrooms*

Publications

- G. Arimura, A. Mithöfer, M. Maffei, R. Gäbler, H. Uchtenhagen, S. Bossi, L. Starvaggi-Cucuzza, B. Schulze, M. Leitner, and W. Boland. **2005**. Multi-functional cross-talk among signaling pathways associated with herbivory-induced, indirect defense in a legume*. In preparation*.

- V. Blanke, B. Schulze, U. Gerighausen, S. Küster, R. Rothe, H. Schulze, and M. Siñeriz. **2005**. From regeneration to restoration - Lessons from the Steudnitz field site. *In preparation* for Restoration Ecology.

- B. Schulze, R. Lauchli, M. Mekem Sonwa, A. Schmidt, and W. Boland. **2005**. Profiling of structurally labile oxylipins in plants by *in situ* derivatization with pentafluorobenzyl hydroxylamine (PFBHA). *Submitted* to Analytical Biochemistry.

- A. Mithöfer, B. Schulze, and W. Boland. **2004**. Biotic and heavy metal stress response in plants: evidence for common signals. FEBS Letters 566(1-3): 1-5

- B. Schulze, C. Wirth, P. Linke, W. A. Brand, I. Kuhlmann, V. Horna, and E.-D. Schulze. **2004**. Laser ablation-combustion-GC-IRMS - a new method for online analysis of intra-annual variation of $\delta^{13}C$ in tree rings. Tree Physiology 24(11): 1193-1201.

- C. Wirth, E.-D. Schulze, V. Kusznetova, I. Milyukova, G. Hardes, M. Siry, B. Schulze, and N. N. Vygodskaya. **2002**. Comparing the influence of site quality, stand age, fire and climate on above-ground production in Siberian Scots pine forests. Tree Physiology 22(8): 537-552.

- P. Imming, J. Becker, Ch. Blümer, B. Sauer, B. Schulze, and G. Laufenberg. **1999**. Identification of Tropic Acid in Tropicamide Ph. Eur. 1997. Pharmeuropa 11(2): 313-314.

Conference contributions

- B. Schulze, A. Mithöfer, and W. Boland. **2004**. Biotic and heavy metal stress response in plants: evidence for common signals Present State and Future Perspectives of Restoration Ecology. Jena. (Oral presentation)

- B. Schulze and W. Boland. **2004**. Oxylipin monitoring in attacked Lima bean leaves and the feeding insect's gut. Botanikertagung. Braunschweig. (Poster)

- B. Schulze and W. Boland. **2004**. Oxylipin monitoring in attacked Lima bean leaves and the feeding insect's gut 12th International Symposium on Insect-Plant Relationships. Berlin. (Oral presentation)

- Schulze, B. and W. Boland. **2004**. Neue Signalmoleküle - Oxylipine im verletzten Blatt und im Darm ihrer Herbivoren 27. Fränkisch-Mitteldeutsches Naturstoffchemiker-Treffen. Bayreuth. (Oral presentation)

Erklärung

Jena, den 05.07.2005

Die geltende Promotionsordnung der Biologisch-Pharmazeutischen Fakultät der Friedrich-Schiller-Universität ist mir bekannt. Die vorliegende Dissertation habe ich selbständig verfasst und keine anderen als die von mir angegebenen Quellen, persönlichen Mitteilungen und Hilfsmittel benutzt.

Bei der Auswahl und Auswertung des Materials haben mich die in der Danksagung meiner Dissertation genannten Personen unterstützt.

Ich habe nicht die Hilfe eines Promotionsberaters in Anspruch genommen und Dritte haben weder unmittelbar noch mittelbar geldwerte Leistungen von mir für Arbeiten erhalten, die im Zusammenhang mit dem Inhalt der vorliegenden Dissertation stehen.

Ich habe die Dissertation noch nicht als Prüfungsarbeit für eine staatliche oder andere wissenschaftliche Prüfung eingereicht. Ferner habe ich nicht versucht, diese Arbeit oder eine in wesentlichen Teilen ähnliche oder eine andere Abhandlung bei einer anderen Hochschule als Dissertation einzureichen.

.....

Birgit Schulze

13 SUPPLEMENTARY MATERIAL

13.1 NMR-spectra

(10*E*,12*Z*,15*Z*)-9-Oxo-10,12,15-octadecatrienoic acid (9-KOTE; 71)

^{1}H-NMR (500 MHz, $CDCl_3$)

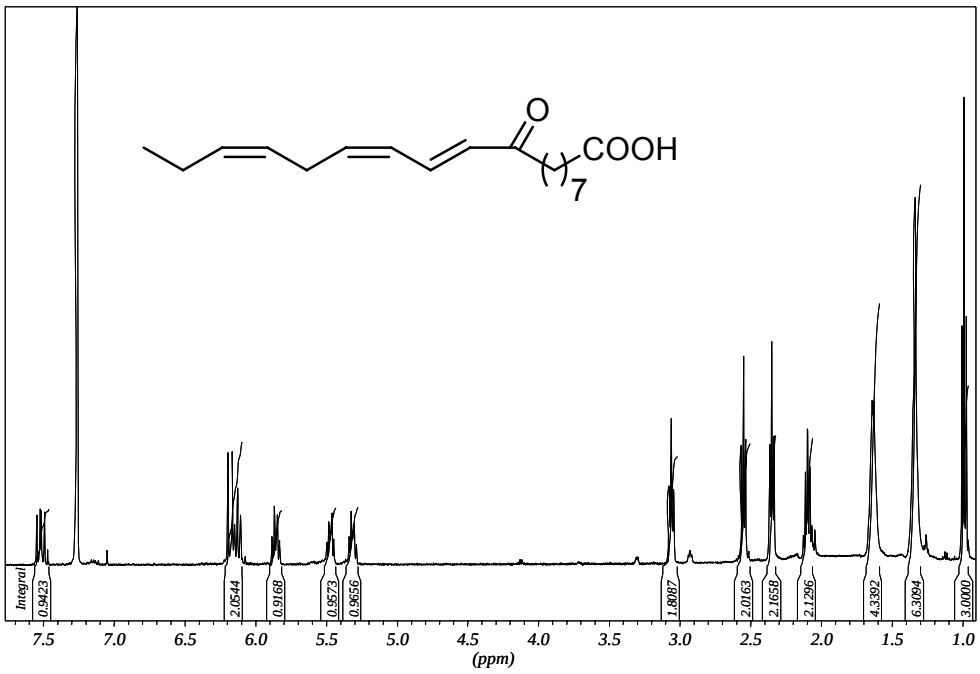

^{13}C-NMR (125 MHz, $CDCl_3$)

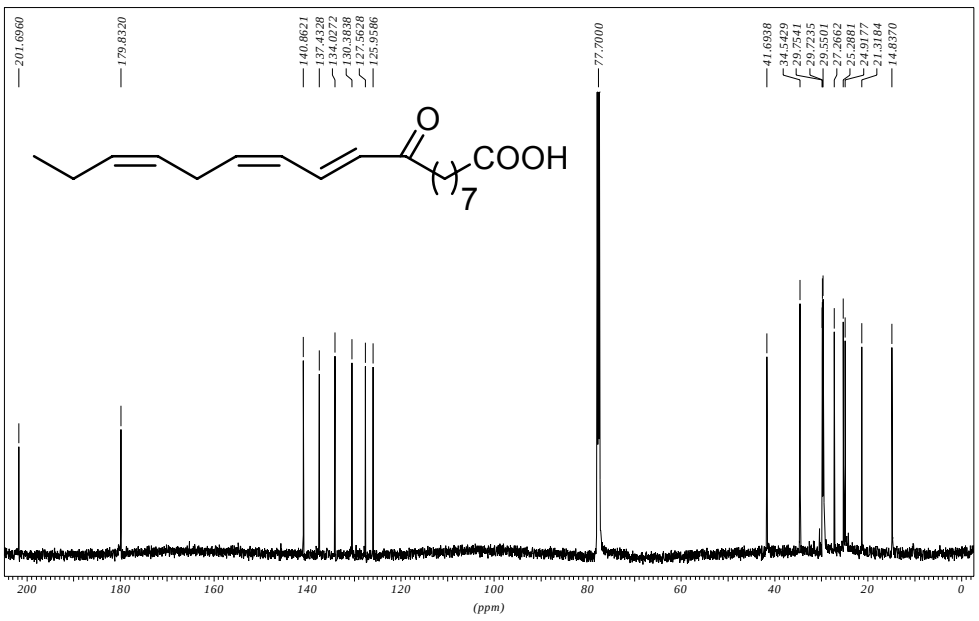

H,H-Cosy-NMR (500 MHz, $CDCl_3$)

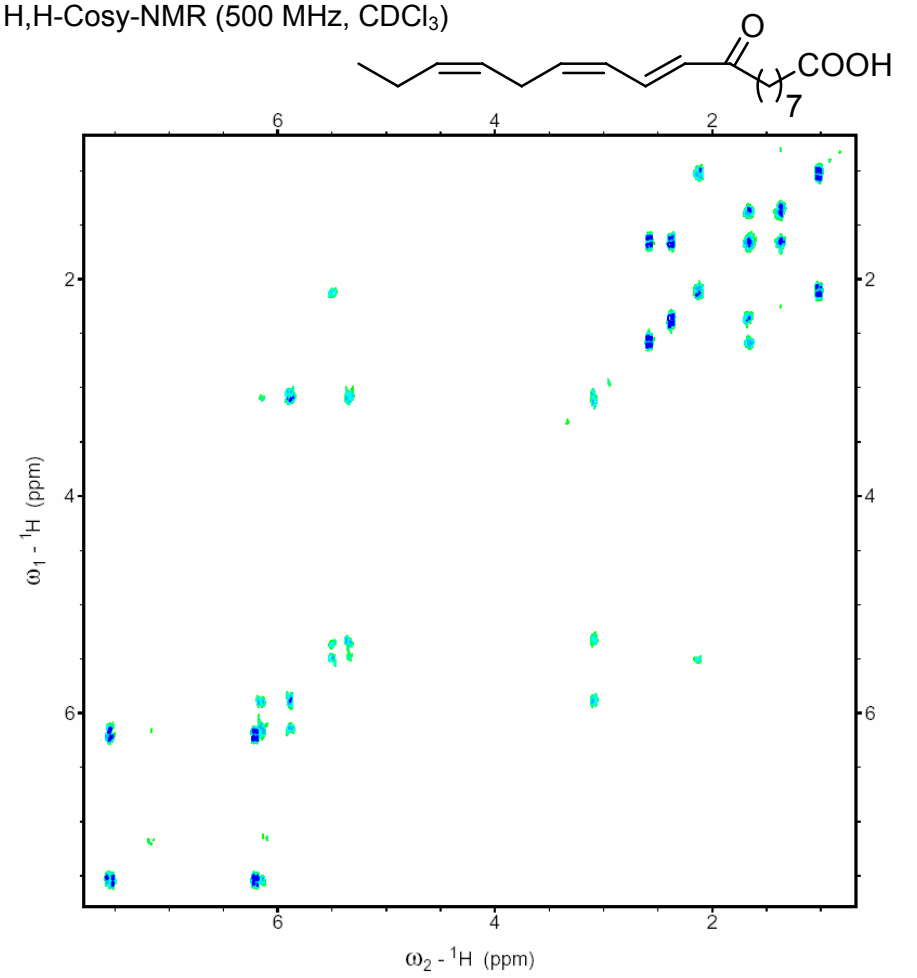

(9*Z*,11*E*,15*Z*)-13-Oxo-9,11,15-octadecatrienoic acid (13-KOTE; 21)

^{1}H-NMR (500 MHz, $CDCl_3$)

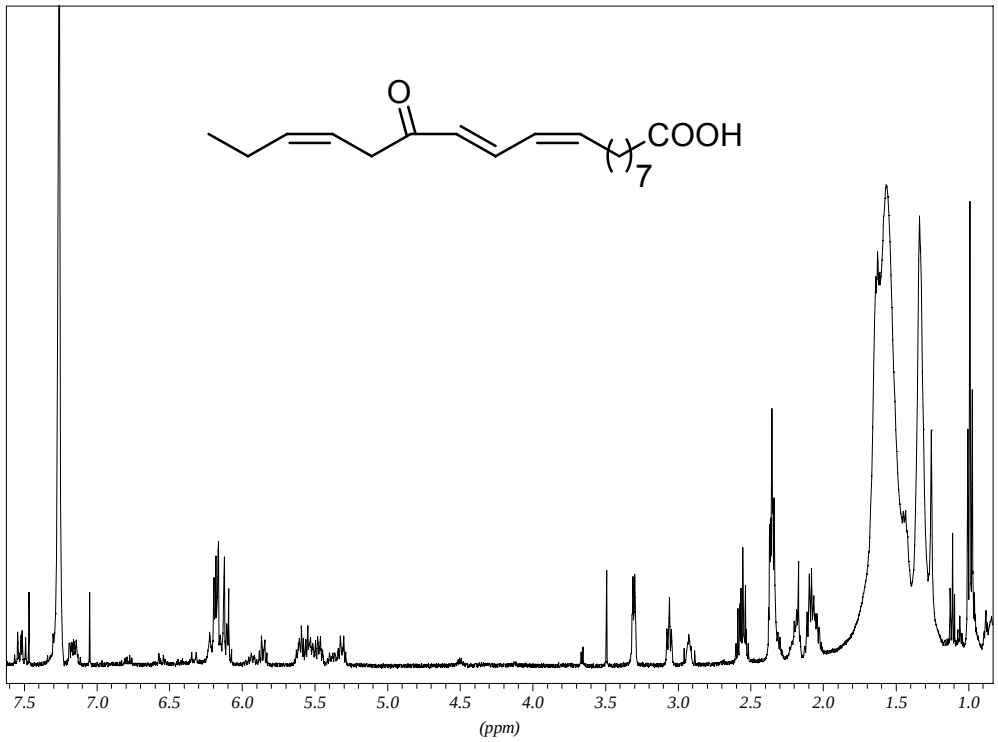

9-Hydroxy-10-oxooctadecanoic acid (76) and 10-hydroxy-9-oxooctadecanoic acid (77)

^{1}H-NMR (500 MHz, $CDCl_3$)

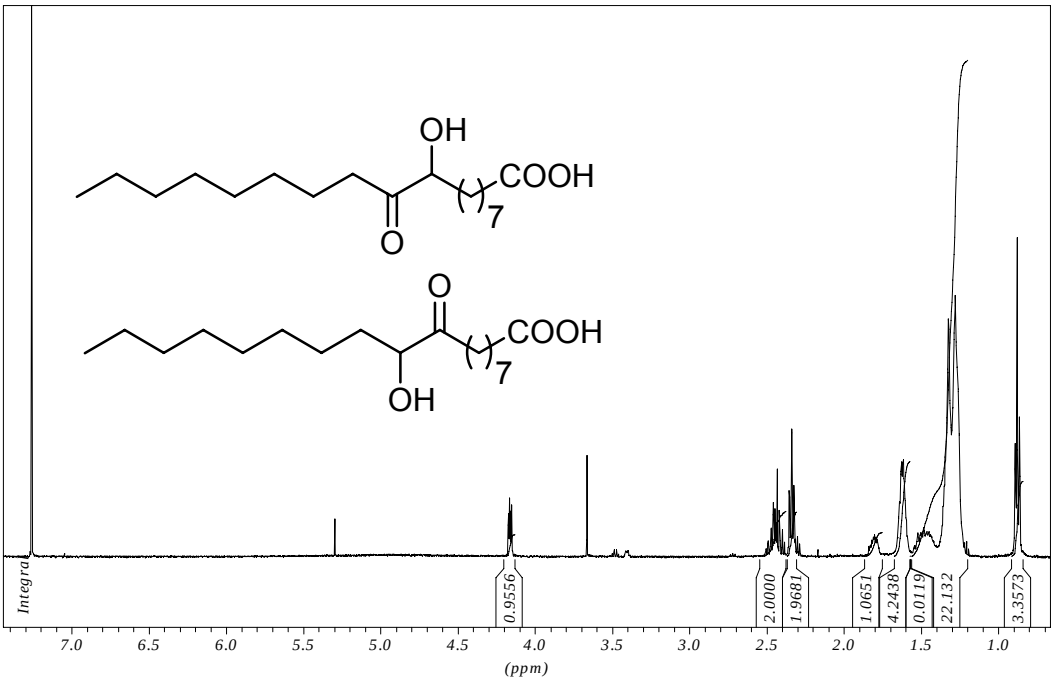

^{13}C-NMR (125 MHz, $CDCl_3$)

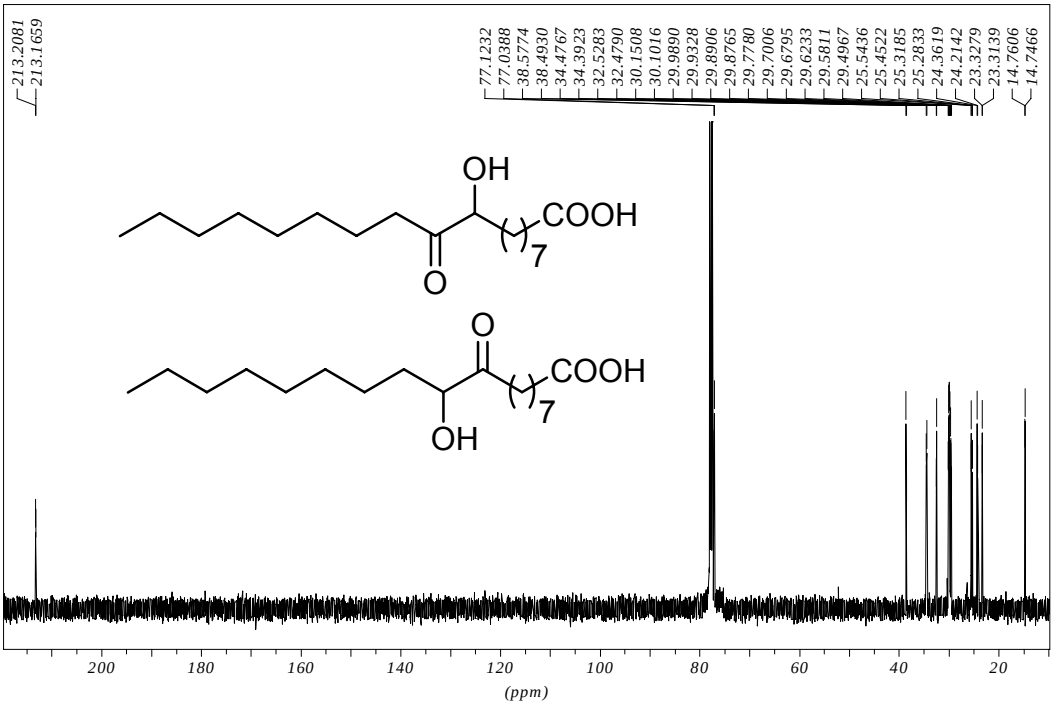

H,H-Cosy-NMR (500 MHz, $CDCl_3$)

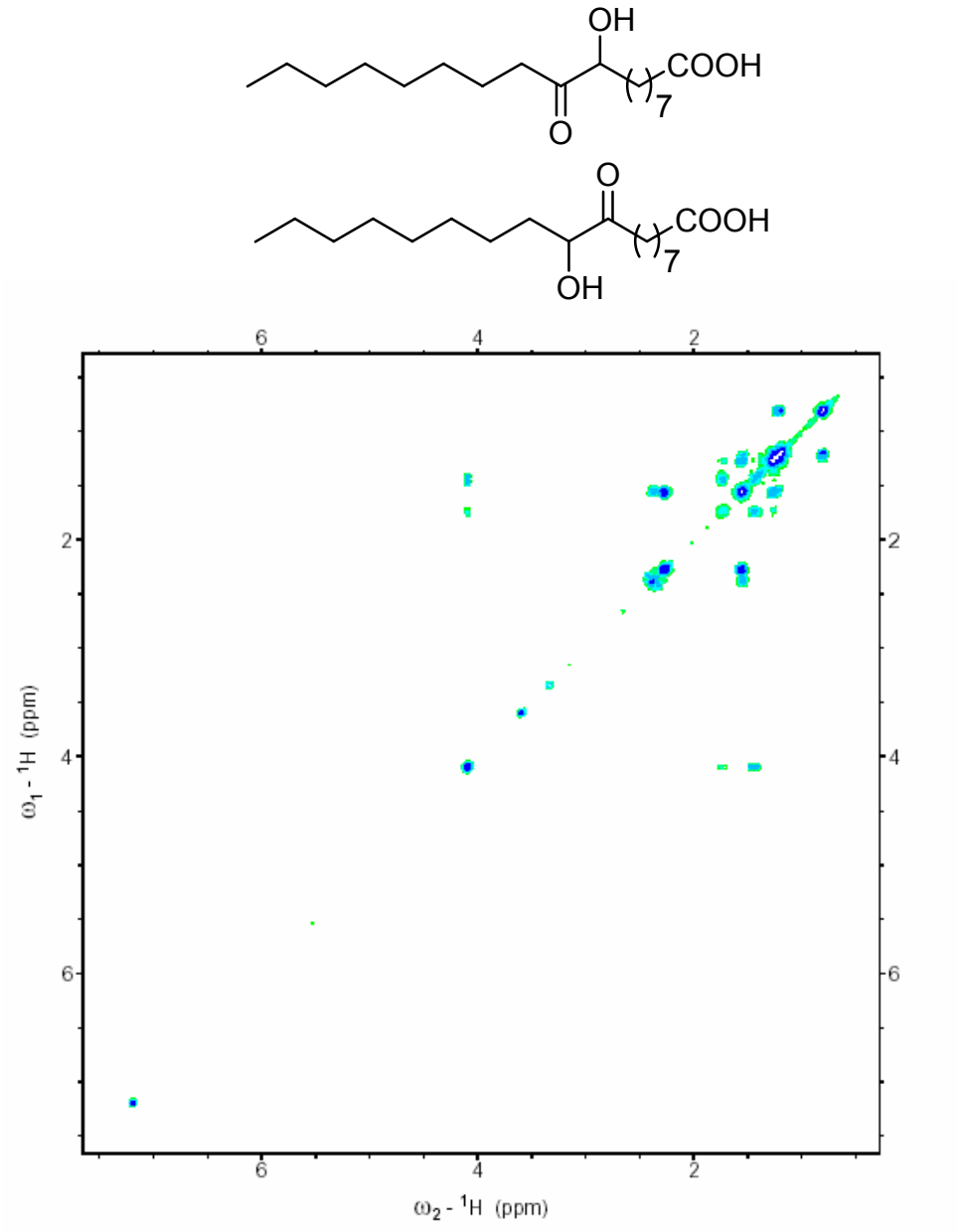

13.2 IR-spectra

(10*E*,12*Z*,15*Z*)-9-Oxo-10,12,15-octadecatrienoic acid (9-KOTE; 71)

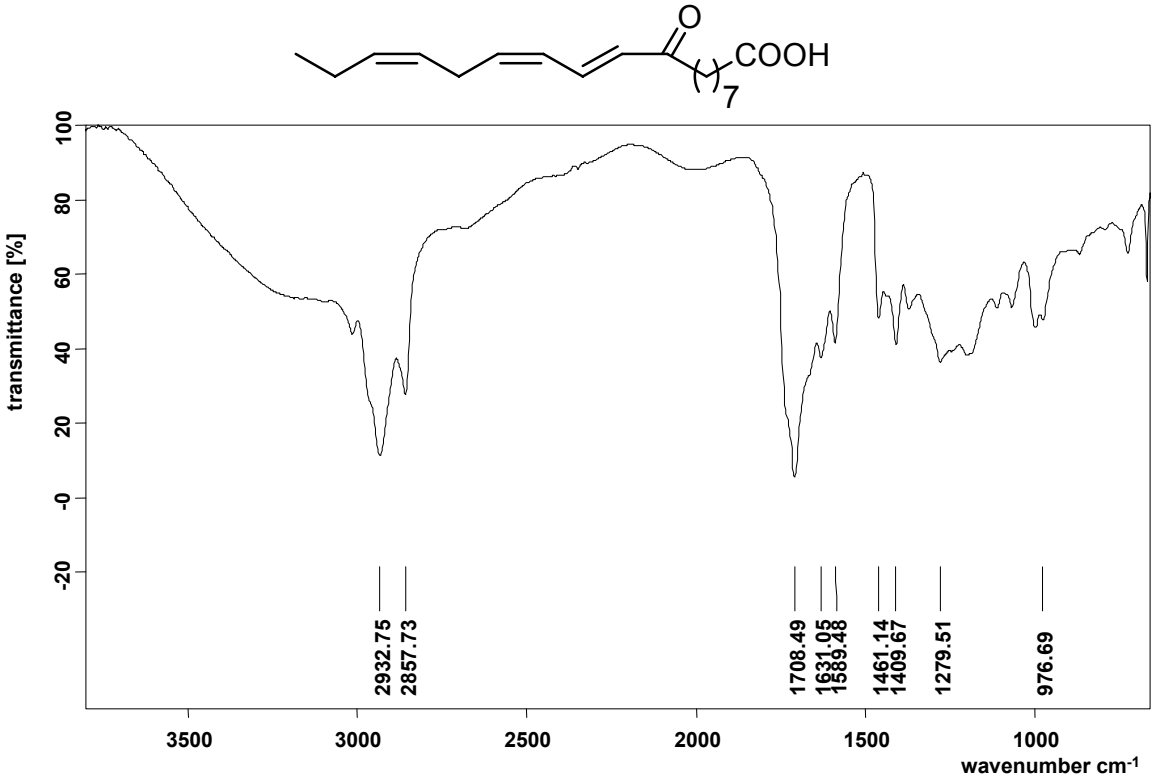

(9*Z*,11*E*,15*Z*)-13-Oxo-9,11,15-octadecatrienoic acid (13-KOTE; 21)

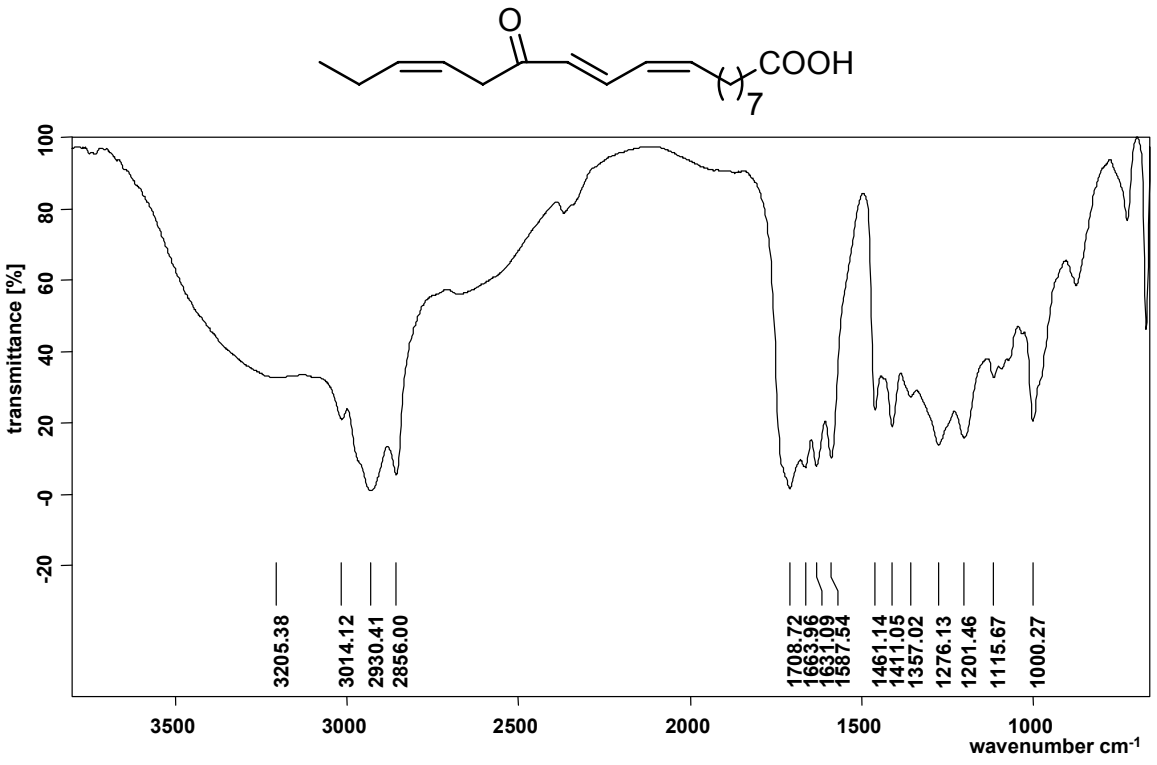

9-Hydroxy-10-oxostearic acid (76) and
10-hydroxy-9-oxostearic acid (77)

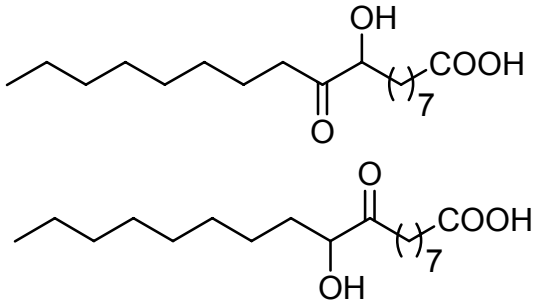

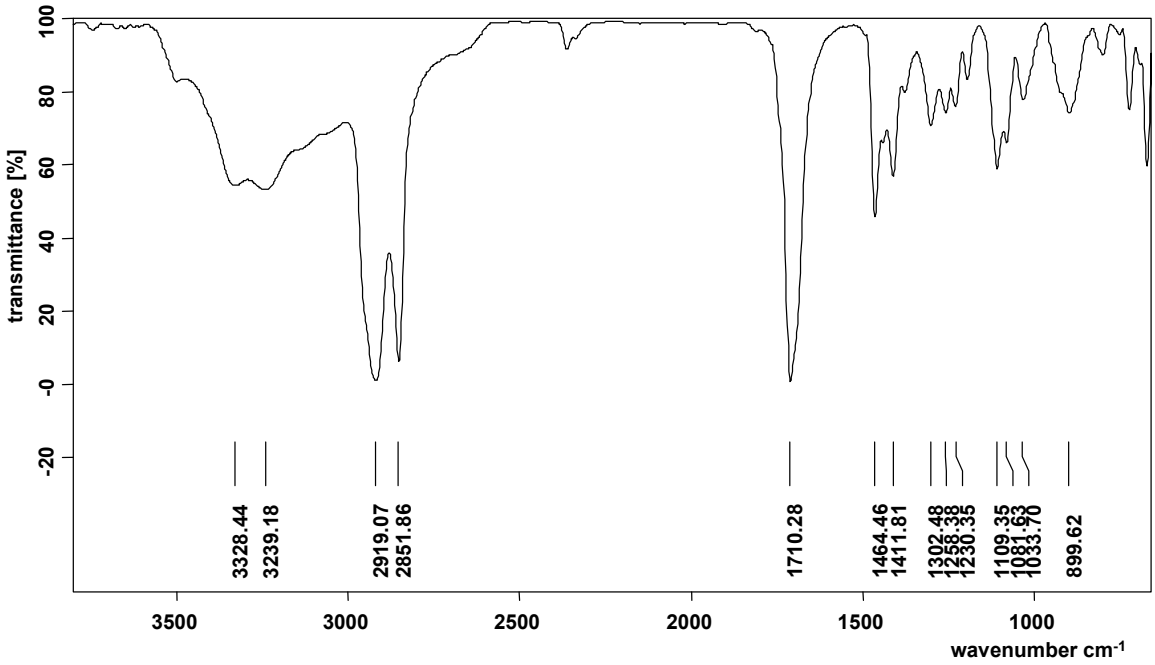

13.3 MS-spectra

Pentafluorobenzyl 2-[3-oxo-2-((*Z*)-pent-2-enyl)cyclopentyl]-acetate (45)

EI postitve MS

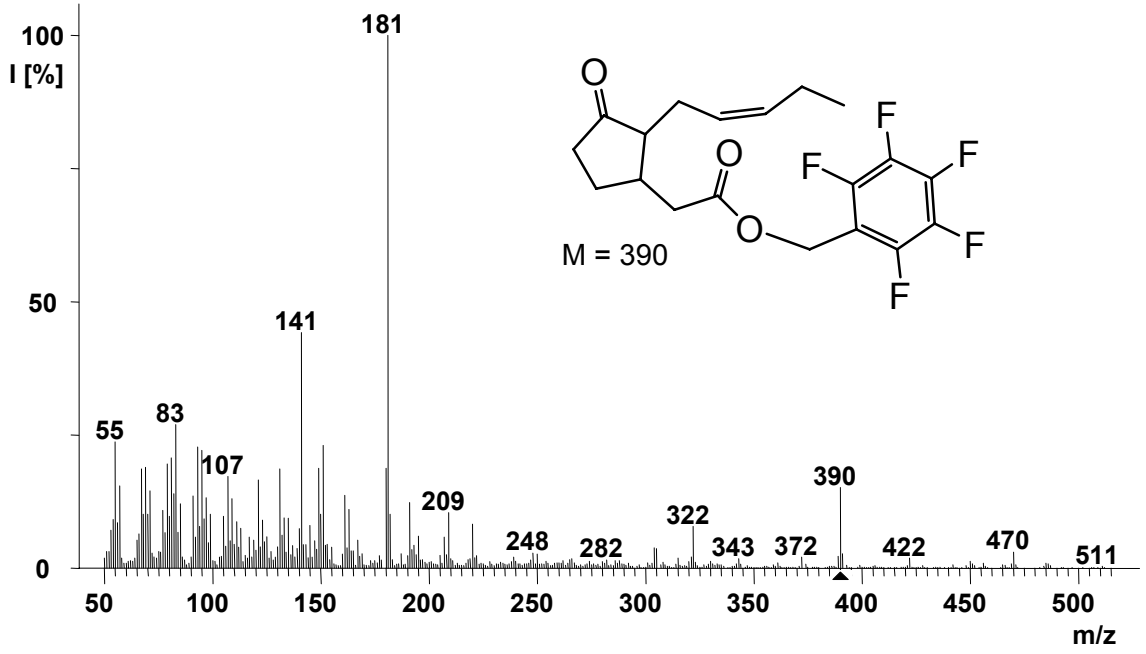

CI negative MS

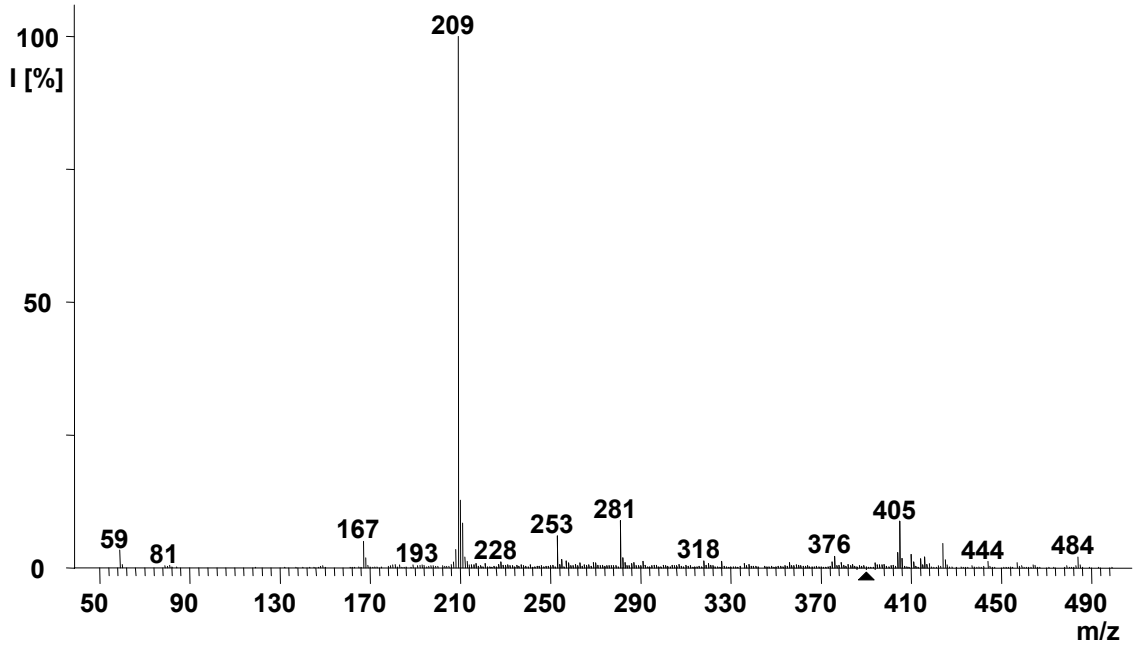

Pentafluorobenzyl 8-[4-oxo-5-((*Z*)-pent-2-enyl)cyclopent-2-enyl]-octanoate (46)

EI postitve MS

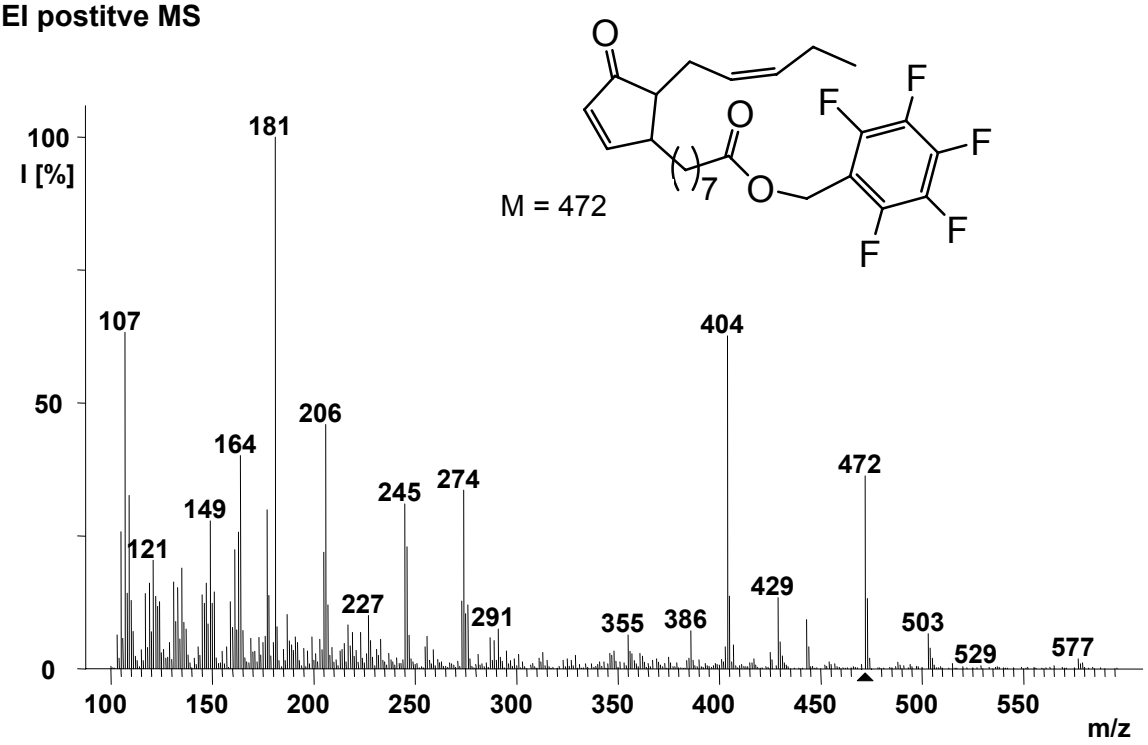

CI negative MS

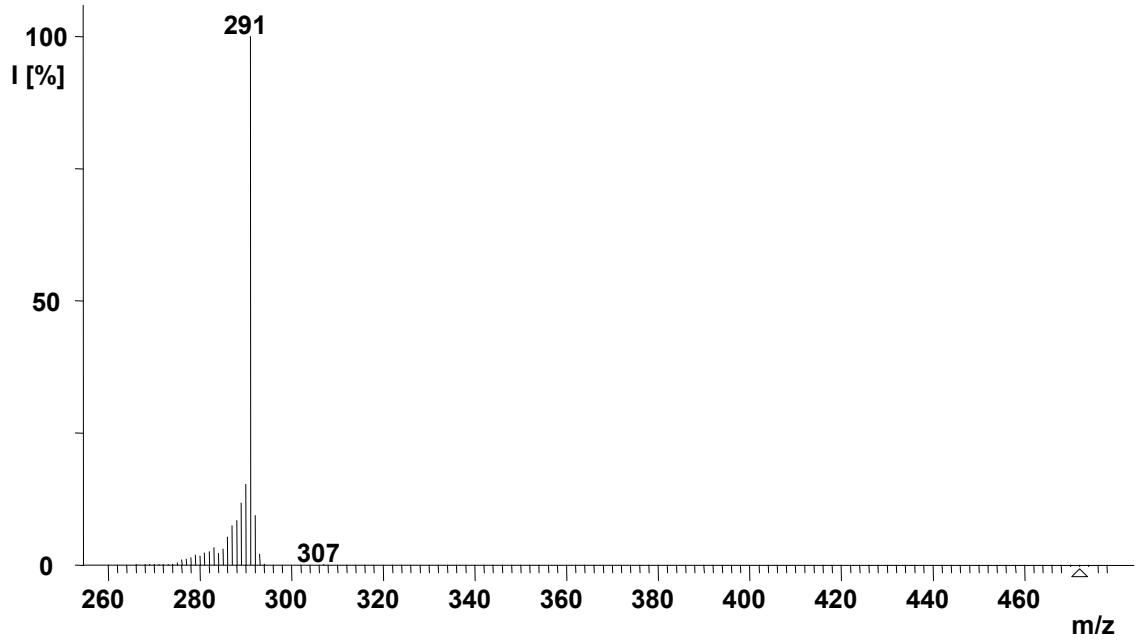

Pentafluorobenzyl 2-hydroxybenzoate (47)

EI postitve MS

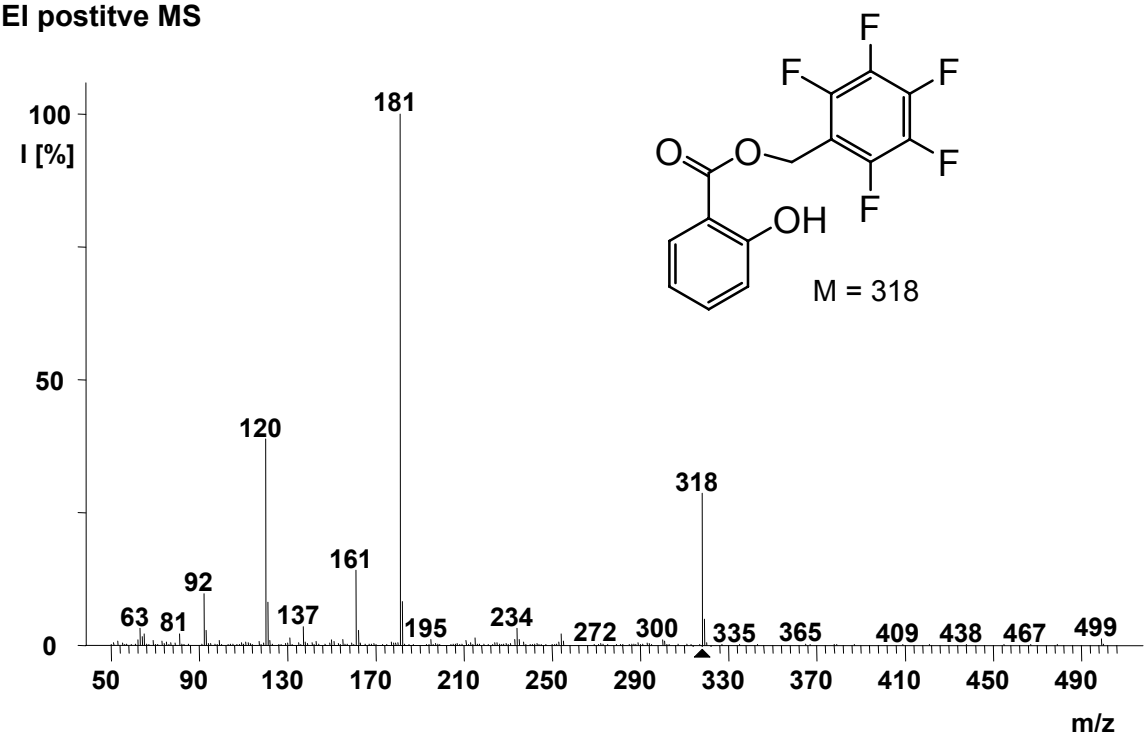

CI negative MS

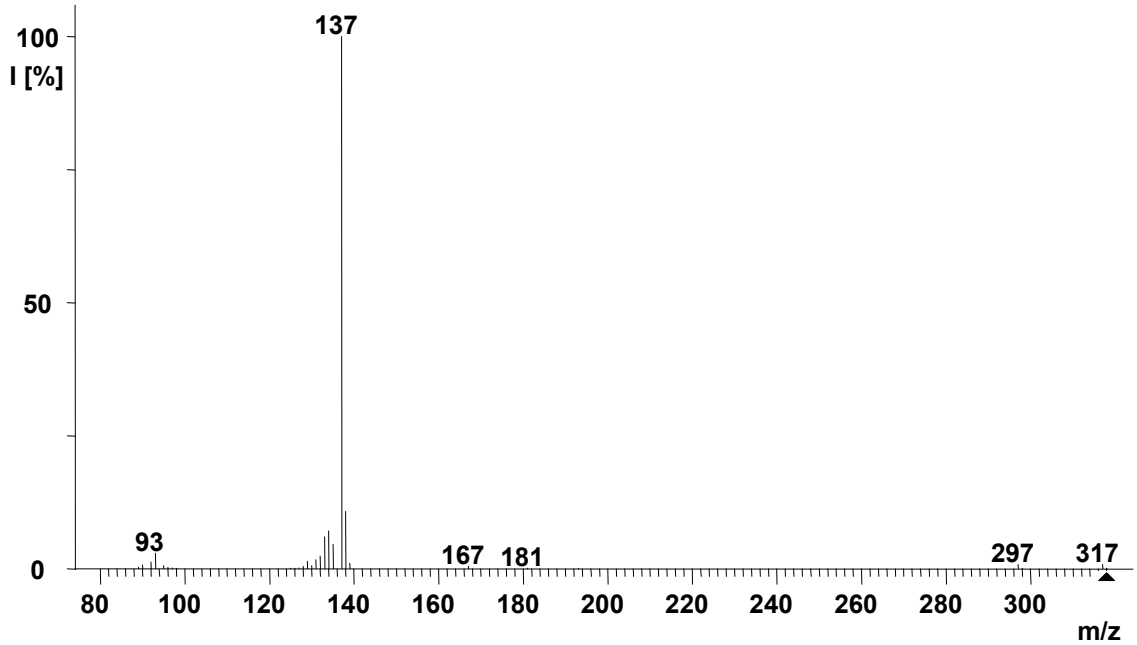

Methyl 2-[2-((*Z*)-pent-2-enyl)-3-pentafluorobenzyloxyimino-cyclopentyl]-acetate (51)

EI positive MS

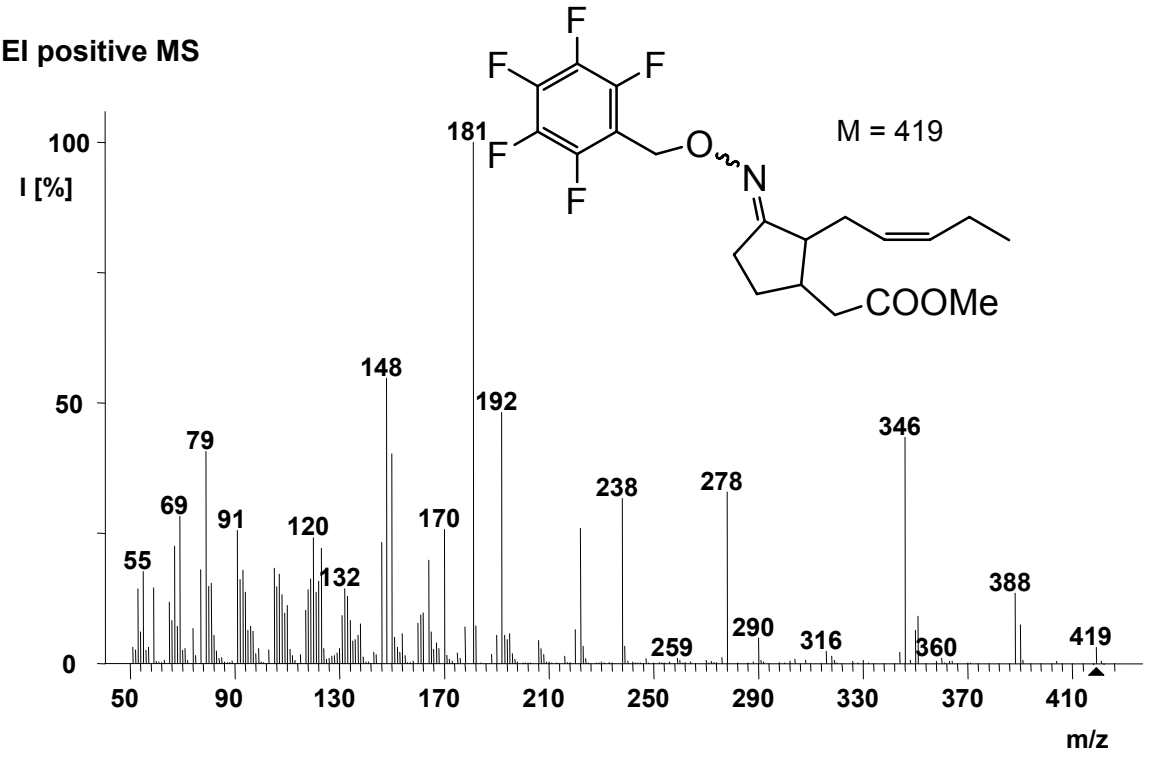

CI negative MS

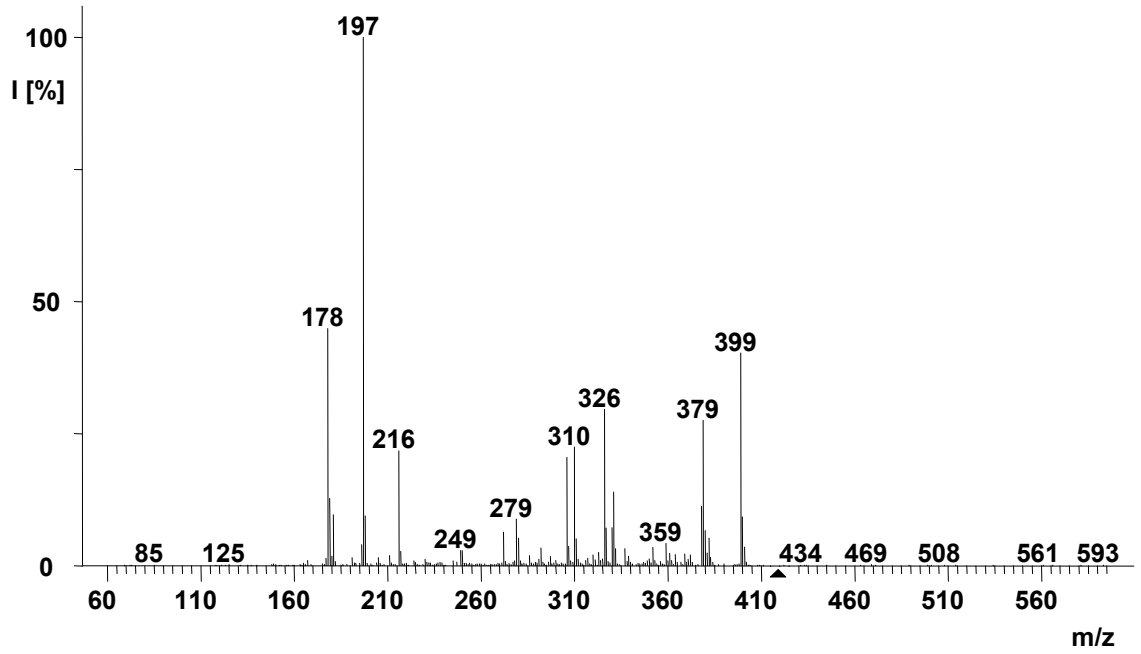

Methyl 2-[2-([2,3-$^2H_2$]-pentyl)-3-pentafluorobenzyloxyimino cyclopentyl]-acetate (52)

EI positive MS

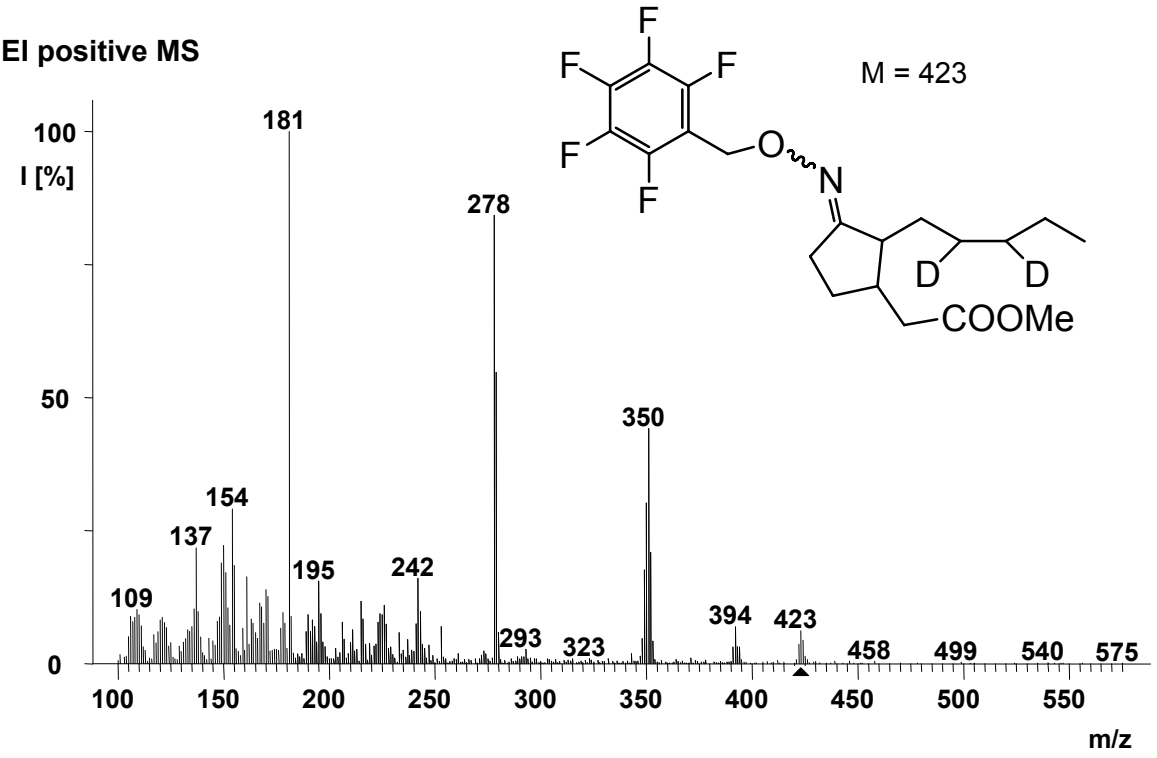

CI negative MS

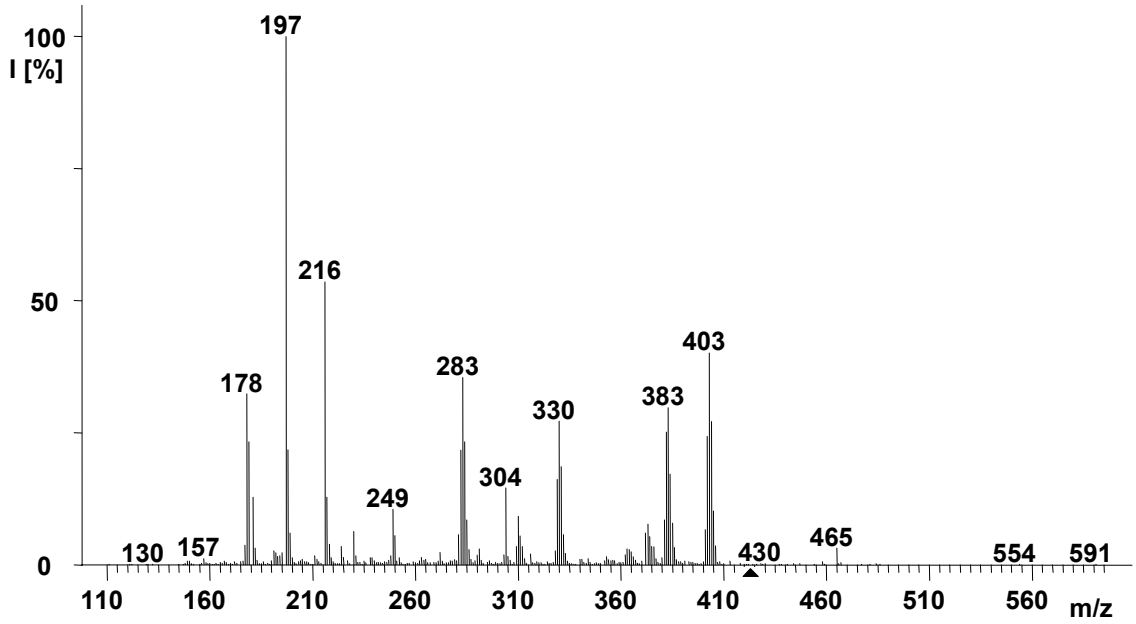

Methyl 8-[5-((*Z*)-pent-2-enyl)-4-pentafluorobenzyloxyiminocyclopent-2-enyl]-octanoate (53)

EI positive MS

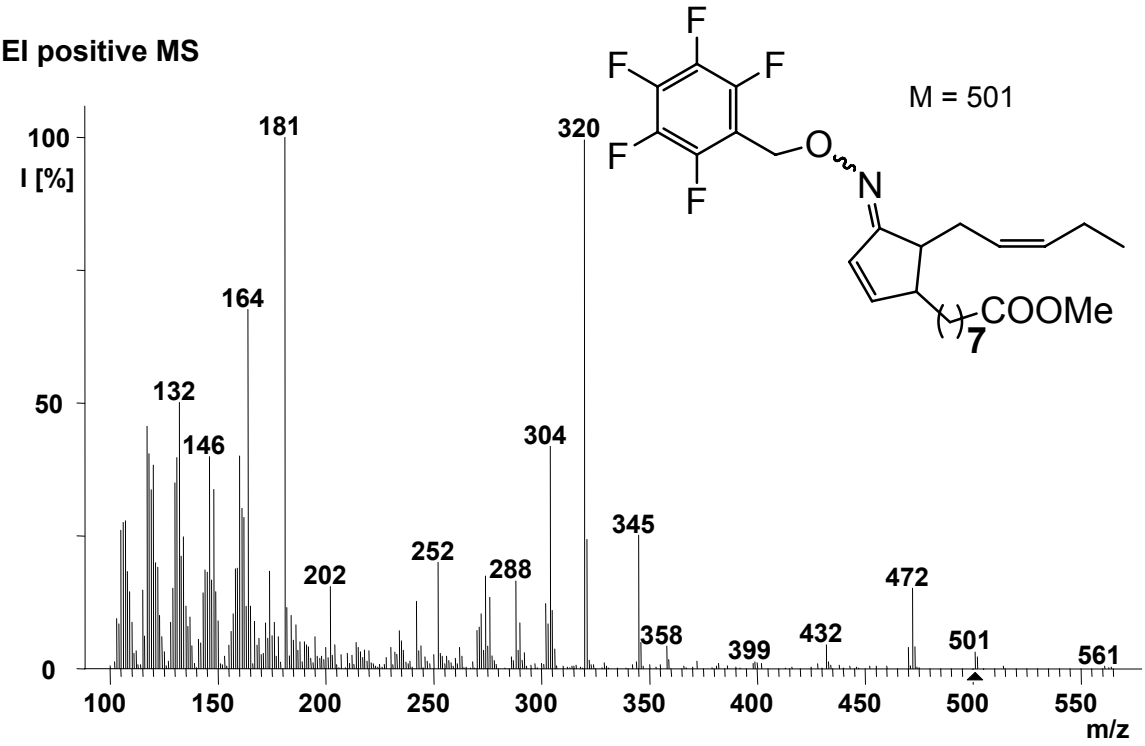

CI negative MS

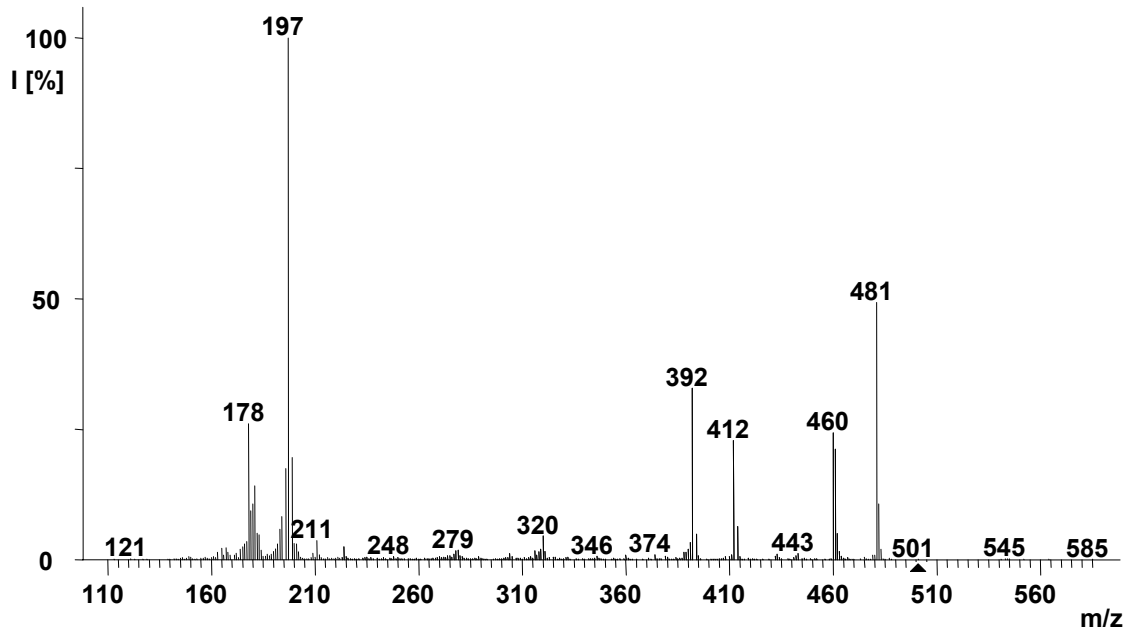

Methyl 8-[2-((*Z*)-2-[2,3-$^2H_2$]-pentenyl)-3-pentafluorobenzyloxyimino-cyclopent-1-enyl]-octanoate (54)

EI positive MS

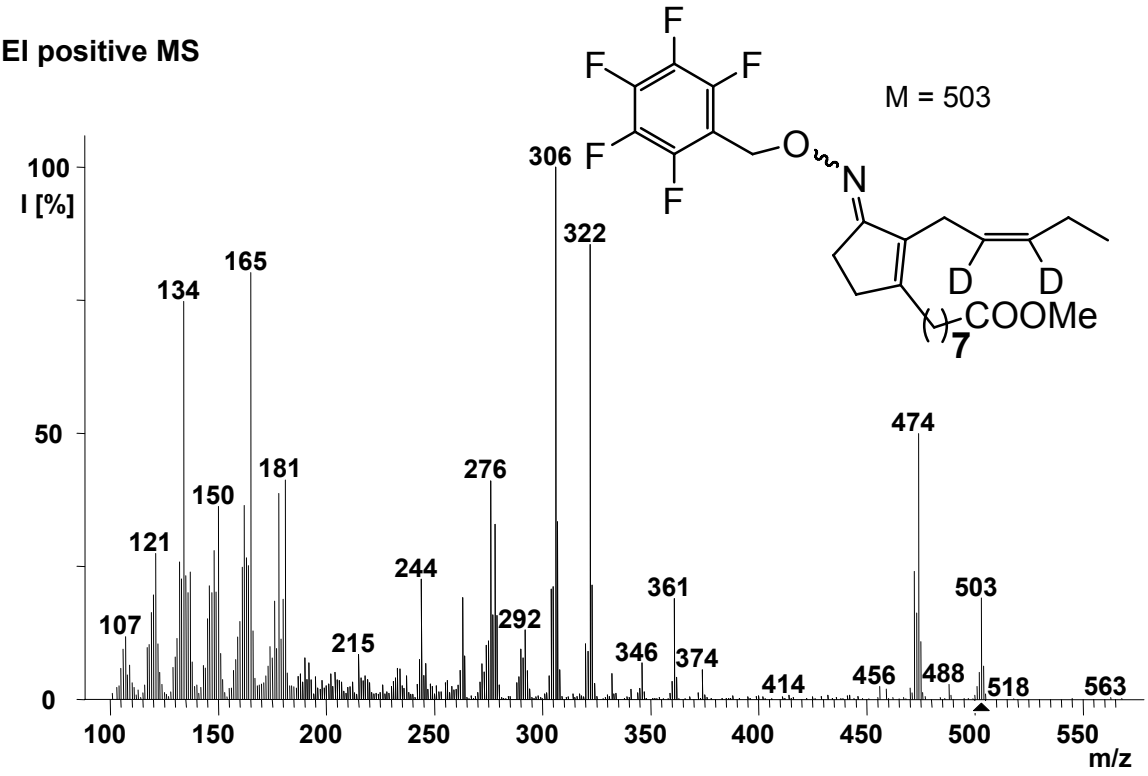

CI negative MS

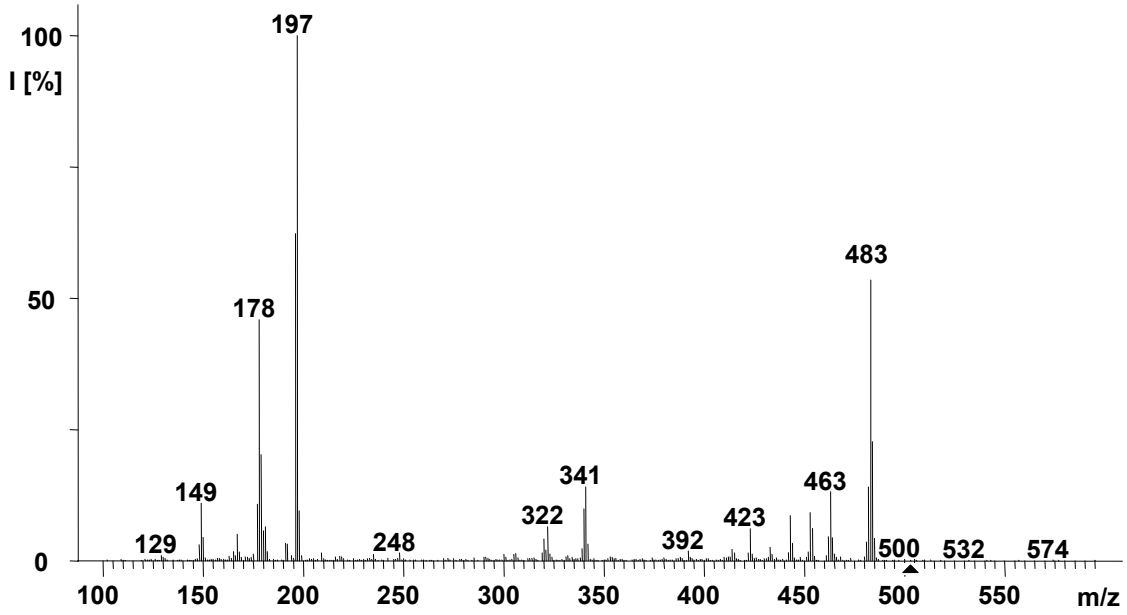

Methyl 8-[2-((*E*)-3-trimethylsilyloxypent-1-enyl)-5-pentafluorobenzyl-oxyiminocyclopent-1-enyl]-octanoate (55)

EI positive MS

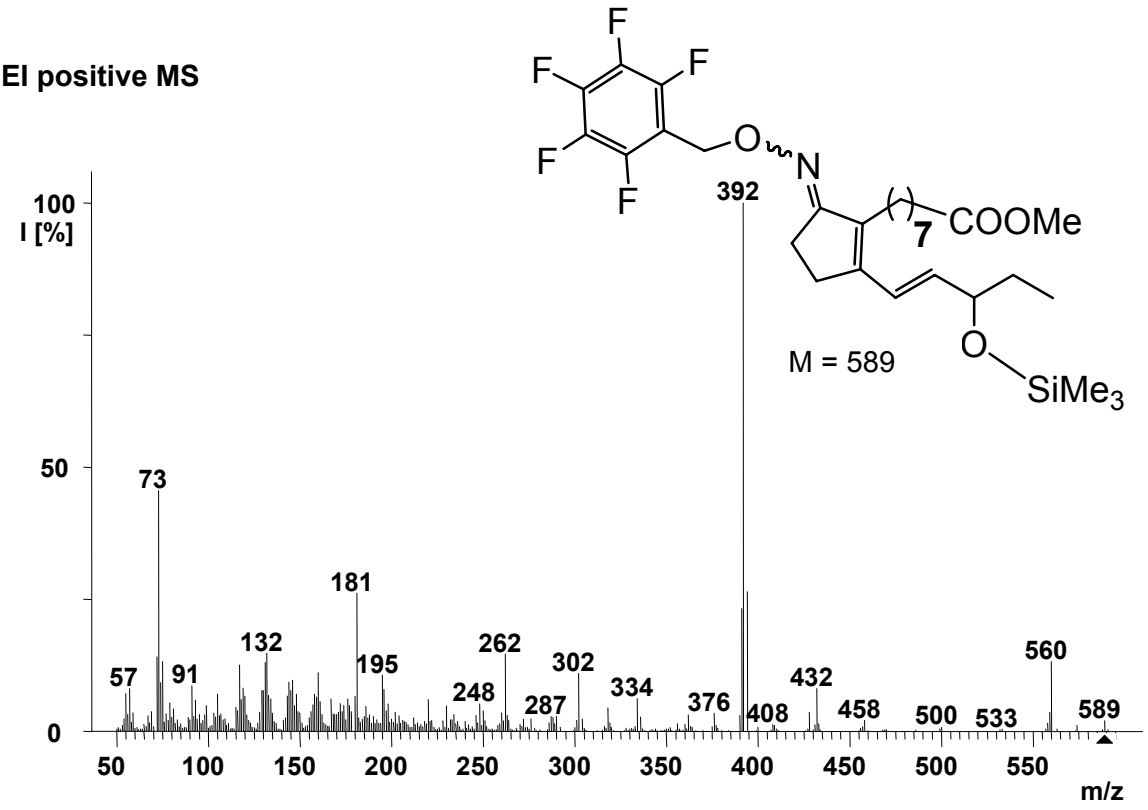

CI negative MS

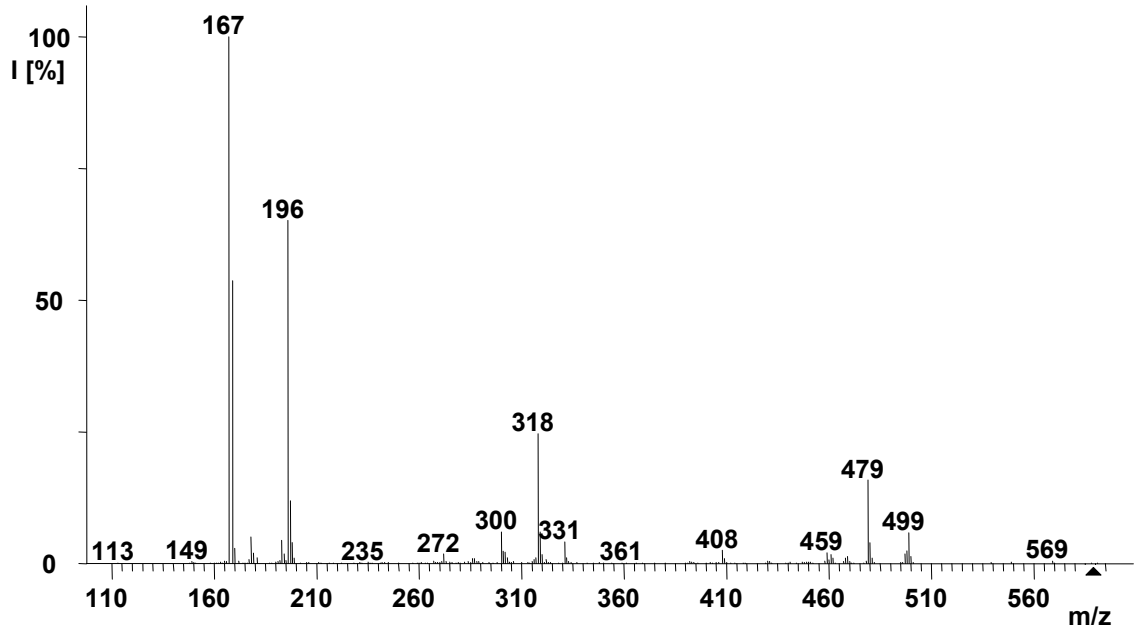

(10*E*)-Methyl 11-[2-ethyl-3-pentafluorobenzyloxyiminocyclopent-1-enyl]-9-trimethylsilyloxy-10-undecenoate (56)

EI positive MS

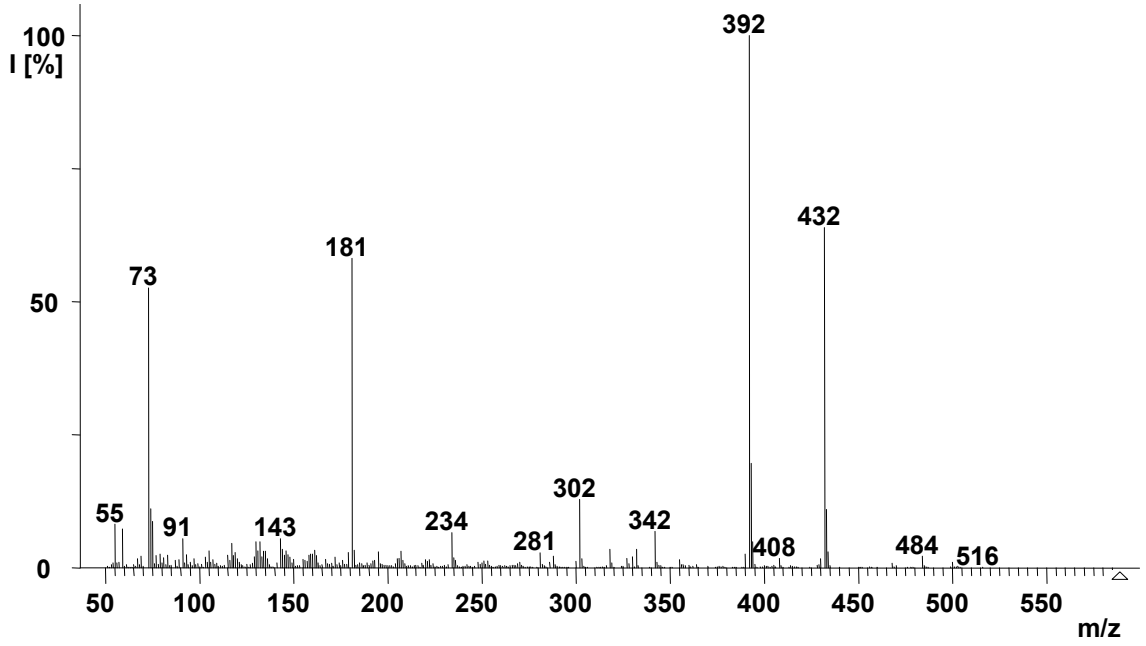

CI negative MS

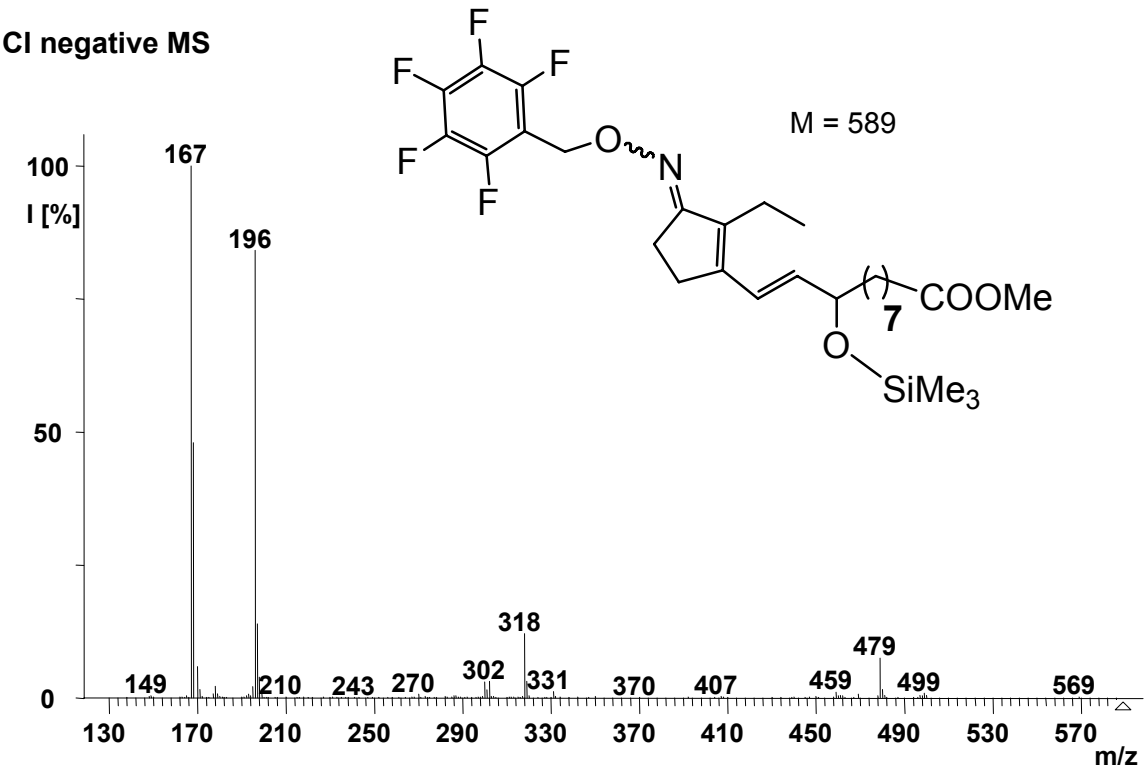

(9*Z*,15*Z*)-Methyl 12-(pentafluorobenzyloxy)imino-13-trimethylsilyloxy-9,15-octadecadienoate (57)

EI positive MS

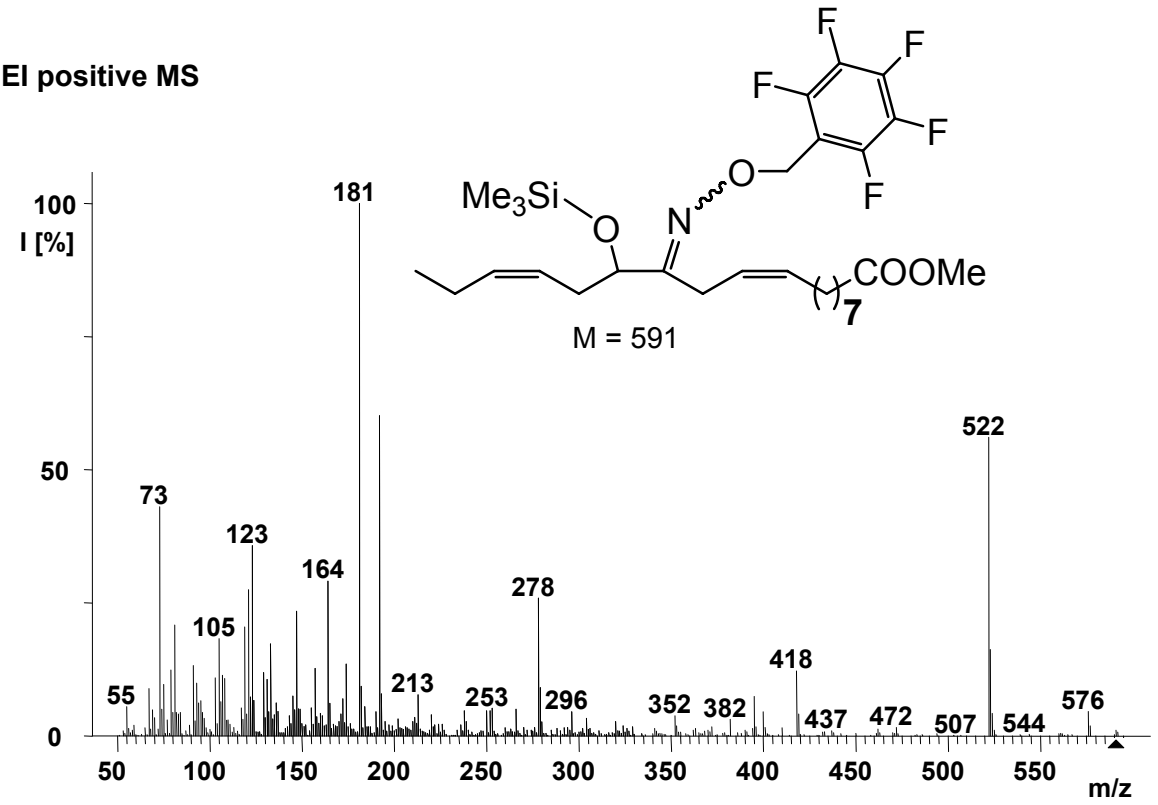

CI negative MS

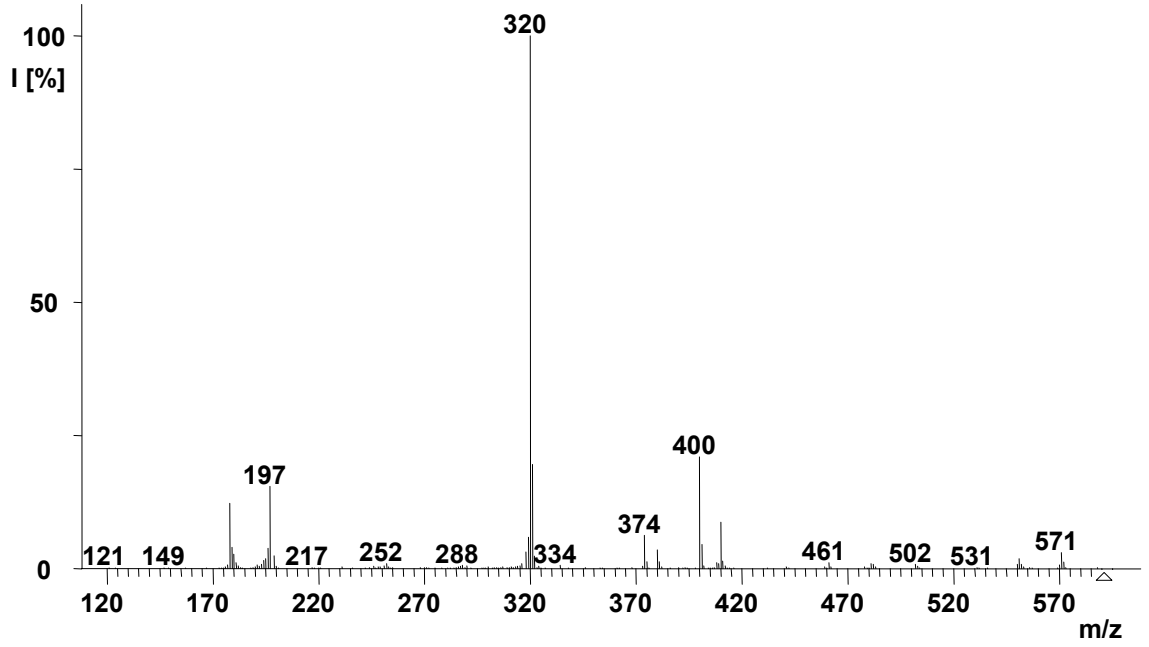

(10*E*,15*Z*)-Methyl 12-(pentafluorobenzyloxy)imino-9-trimethyl-silyloxy-10,15-octadecadienoate (58)

EI positive MS

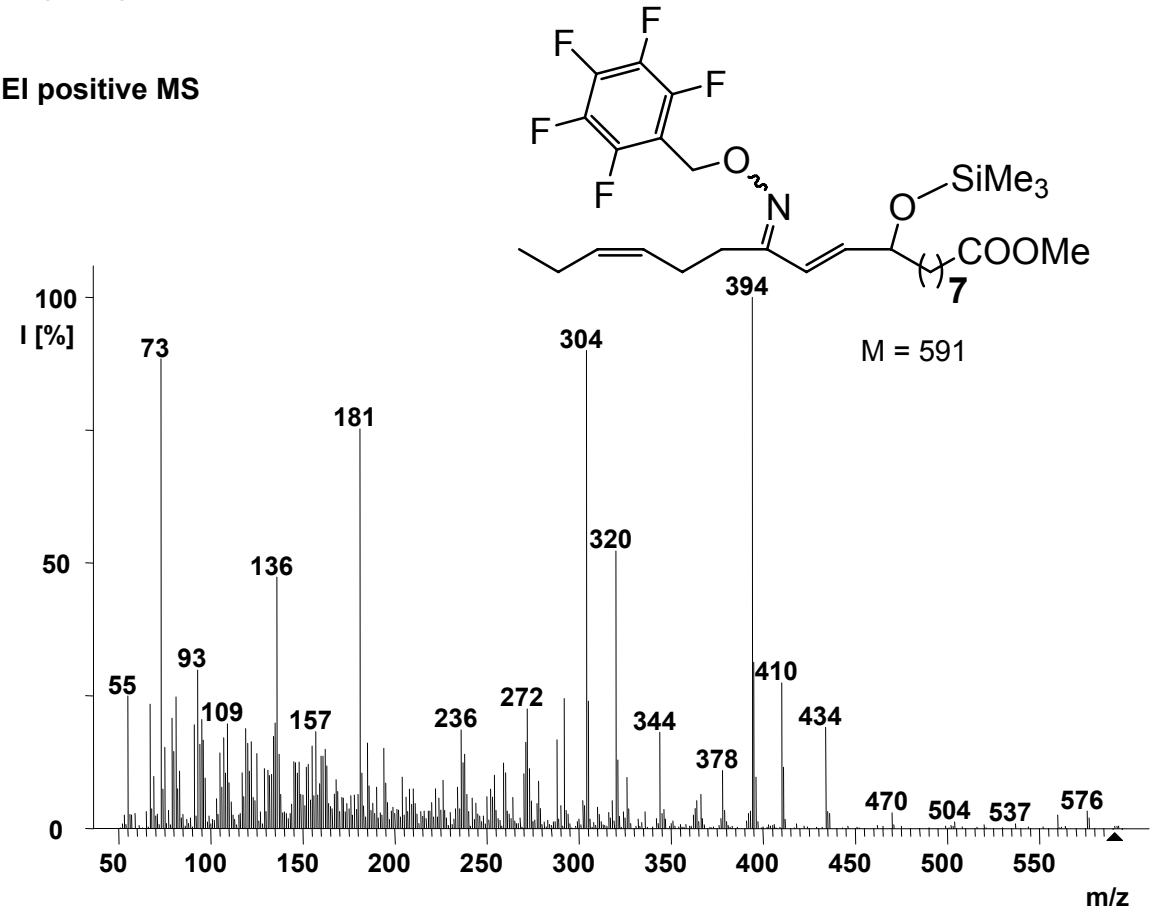

CI negative MS

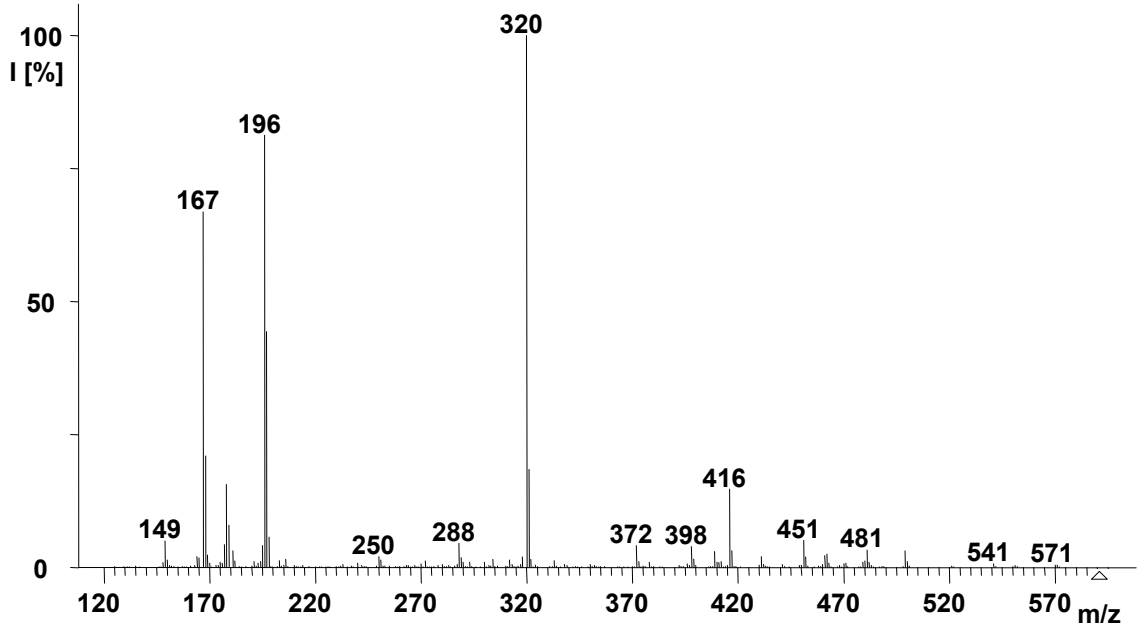

(*Z*)-Methyl 10-(pentafluorobenzyloxy)imino-9-trimethylsilyloxy-octadecanoate ((*Z*)-oxime 68)

EI positive MS

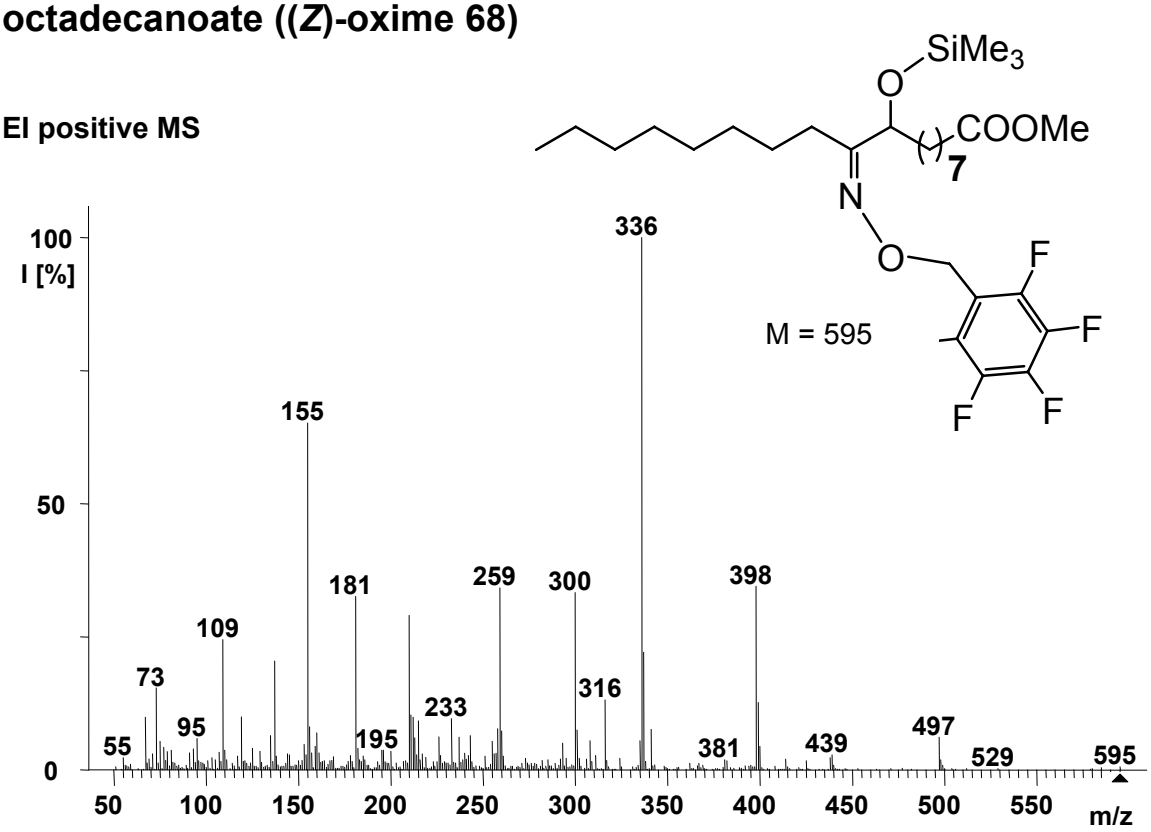

CI negative MS

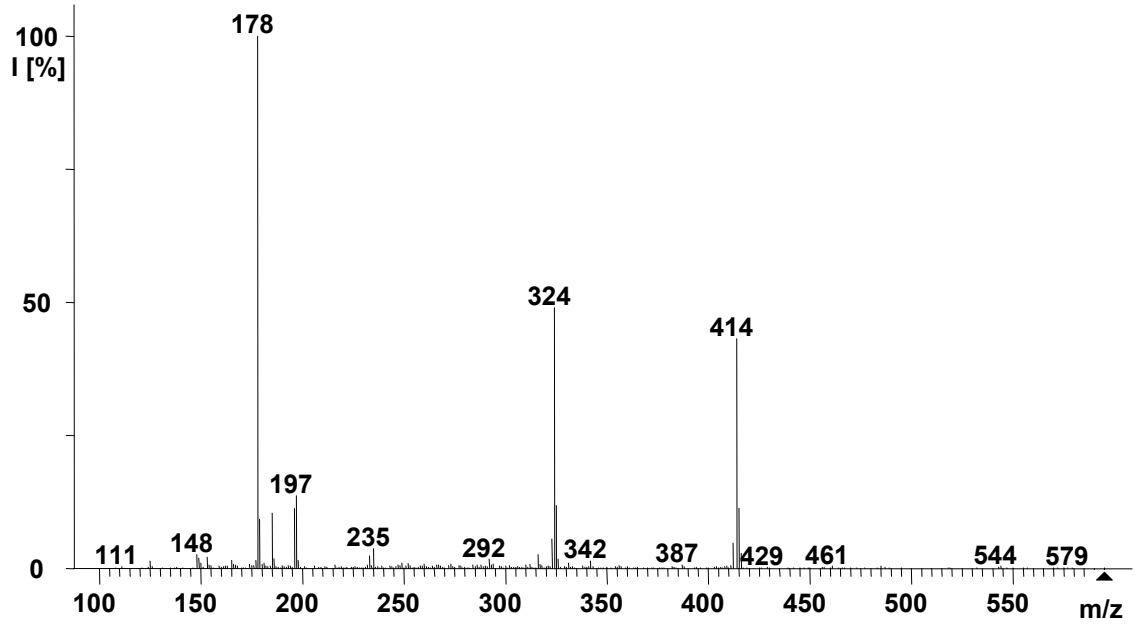

(*E*)-Methyl 10-(pentafluorobenzyloxy)imino-9-trimethylsilyloxy-octadecanoate ((*E*)-oxime 68)

EI positive MS

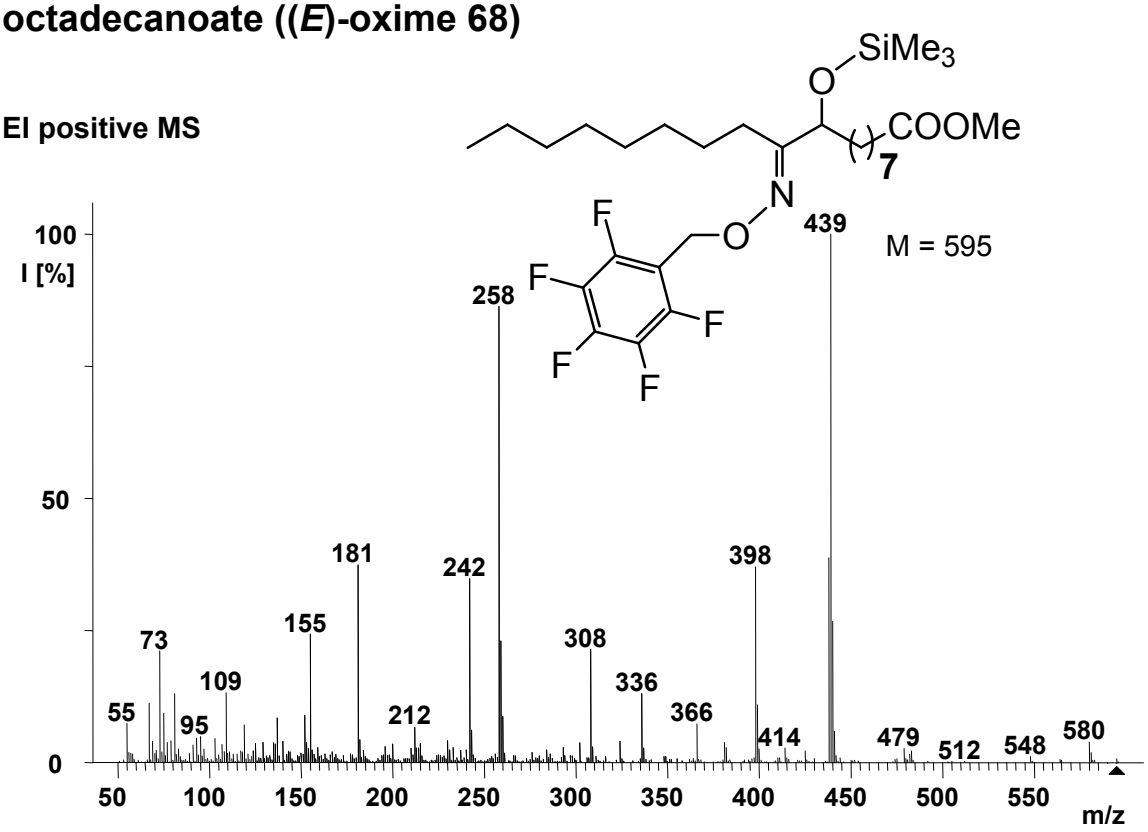

CI negative MS

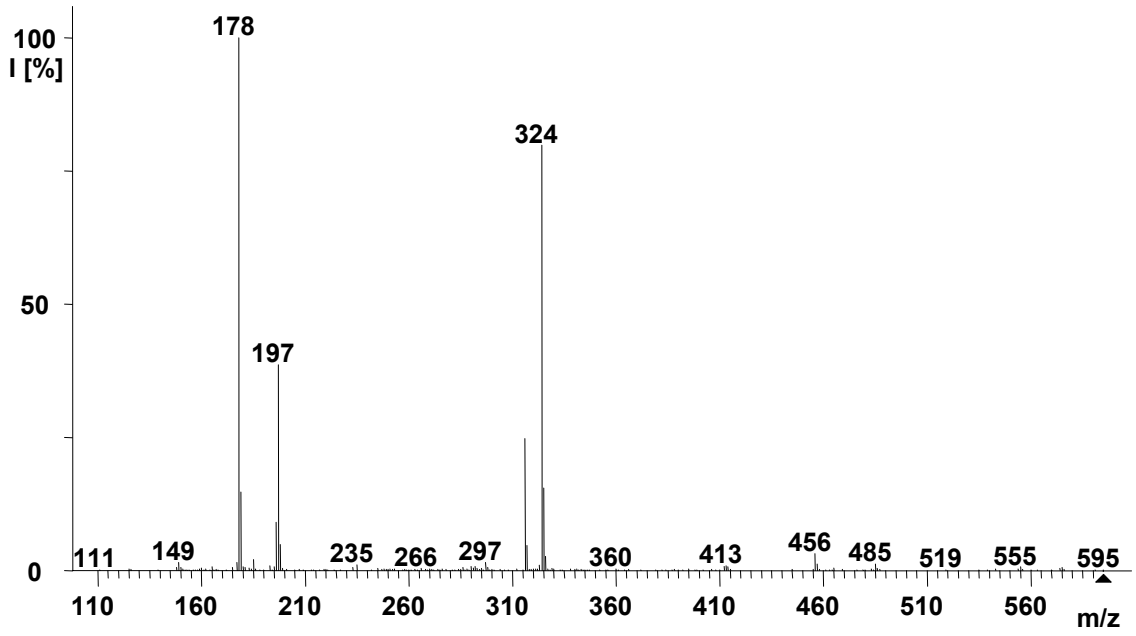

(*Z*)-Methyl 9-(pentafluorobenzyloxy)imino-10-trimethylsilyloxy-octadecanoate ((*Z*)-oxime 69)

EI positive MS

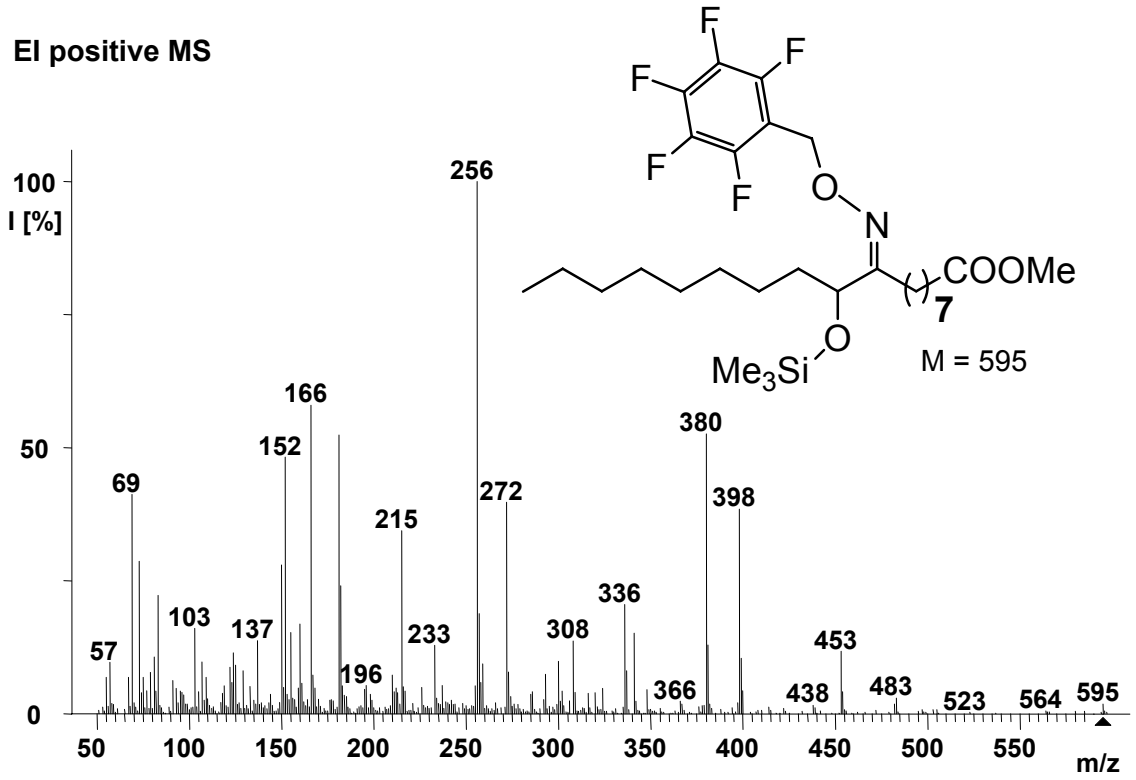

CI negative MS

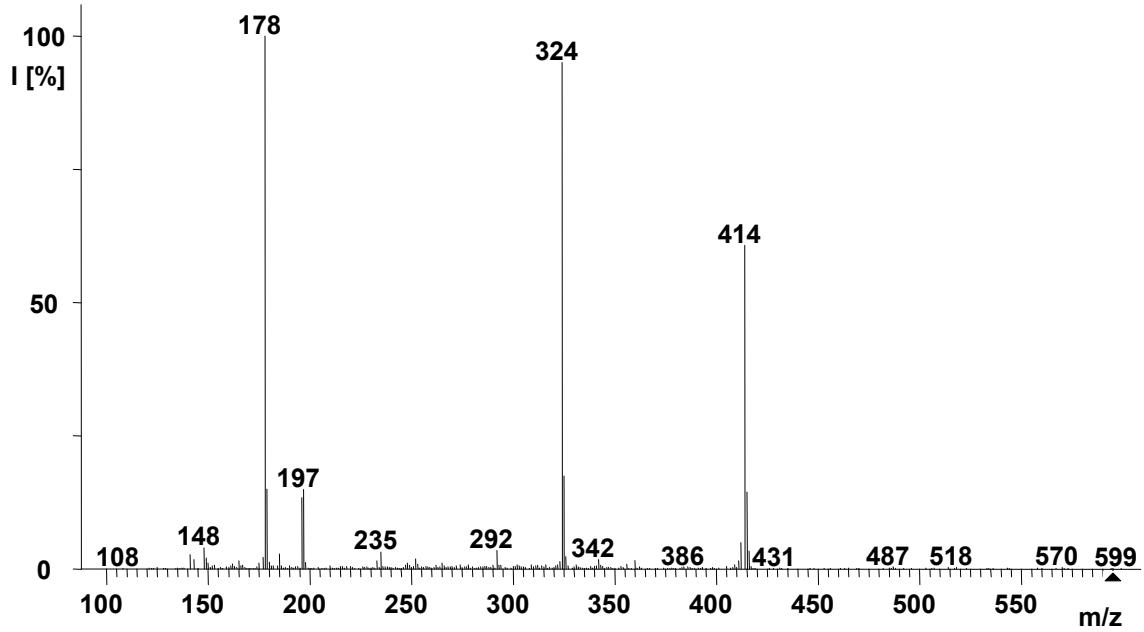

(*E*)-Methyl 9-(pentafluorobenzyloxy)imino-10-trimethylsilyloxy-octadecanoate ((*E*)-oxime 69)

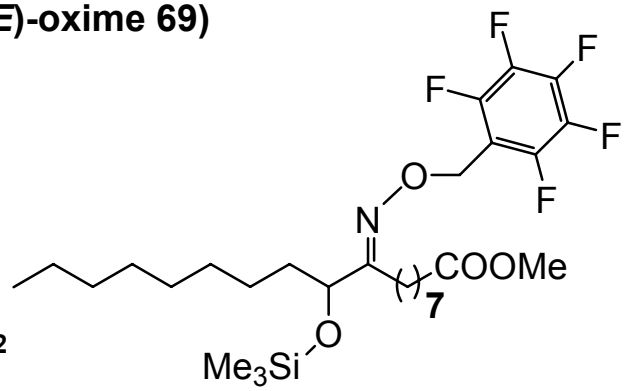

M = 595

EI positive MS

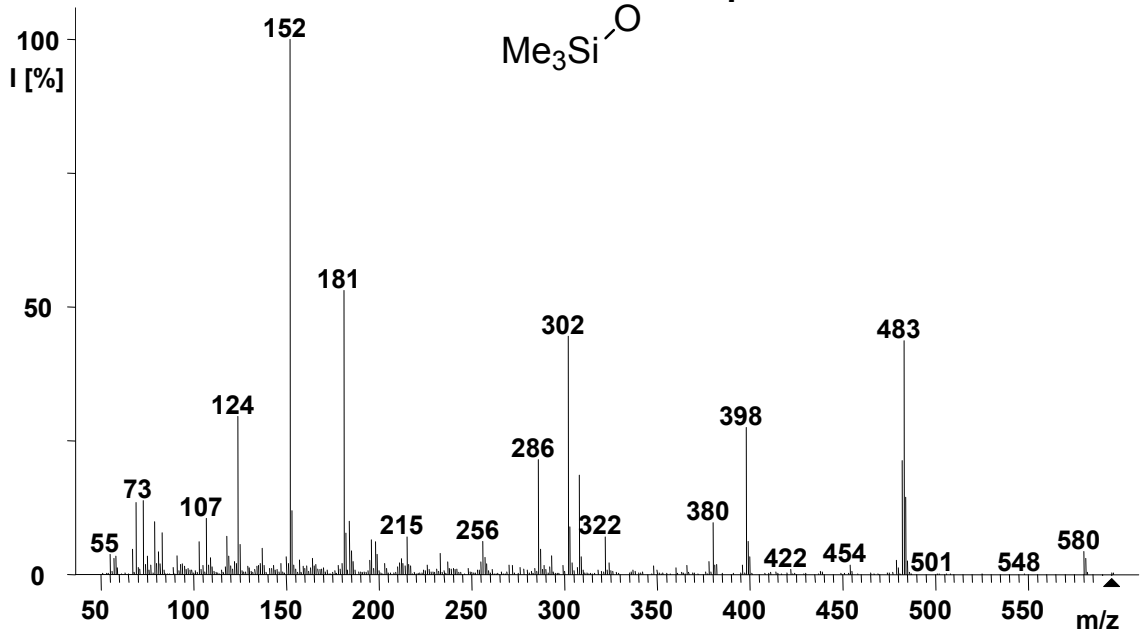

CI negative MS

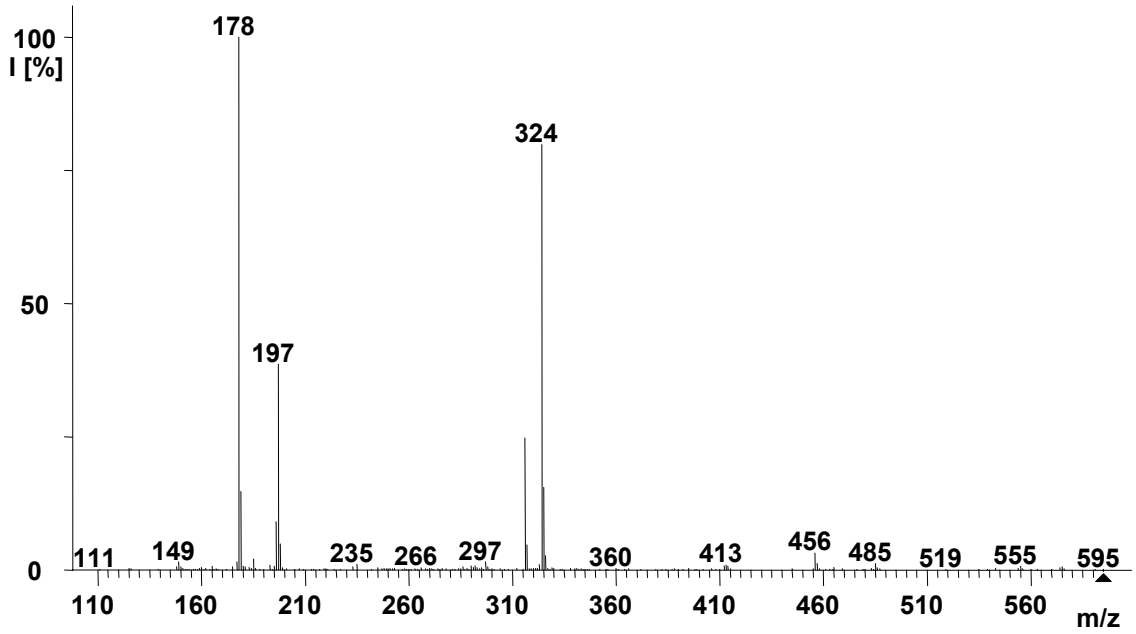

(10*E*,12*Z*,15*Z*)-Methyl 9-(pentafluorobenzyloxy)imino-10,12,15-octadecatrienoate (59)

EI positive MS

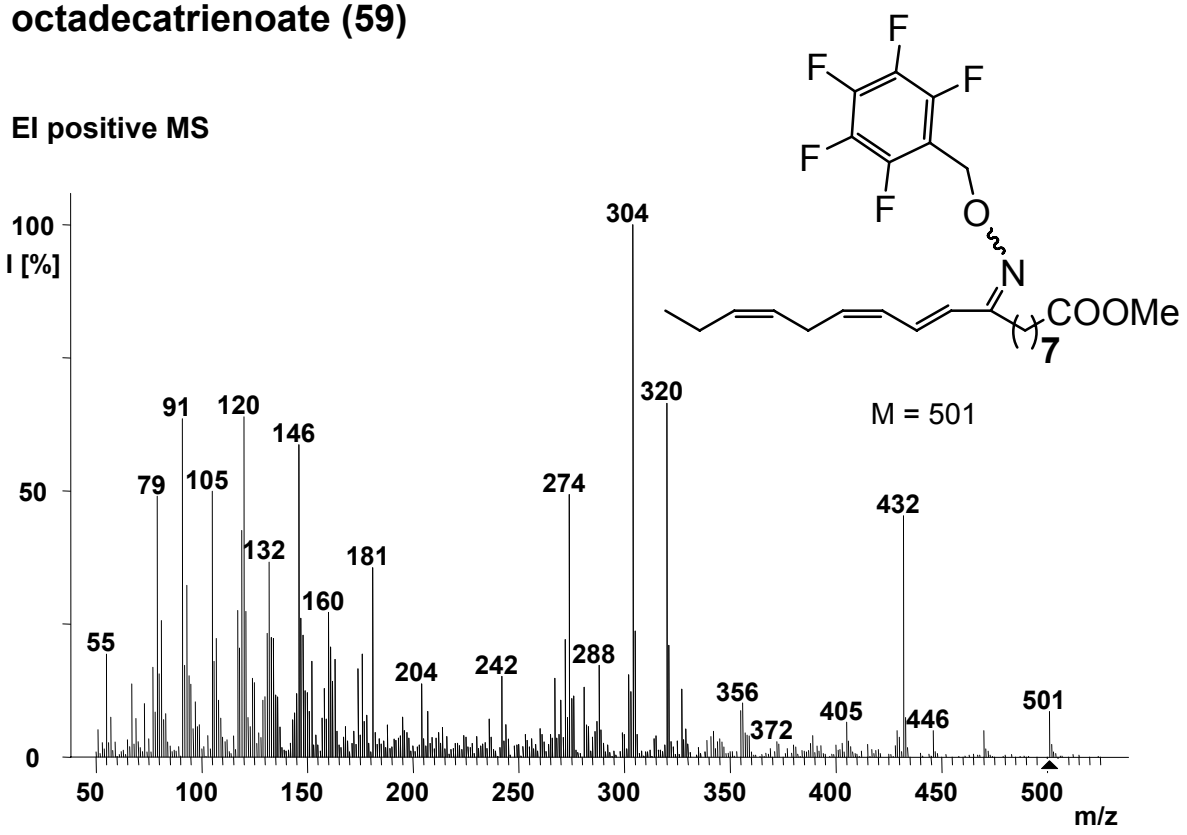

CI negative MS

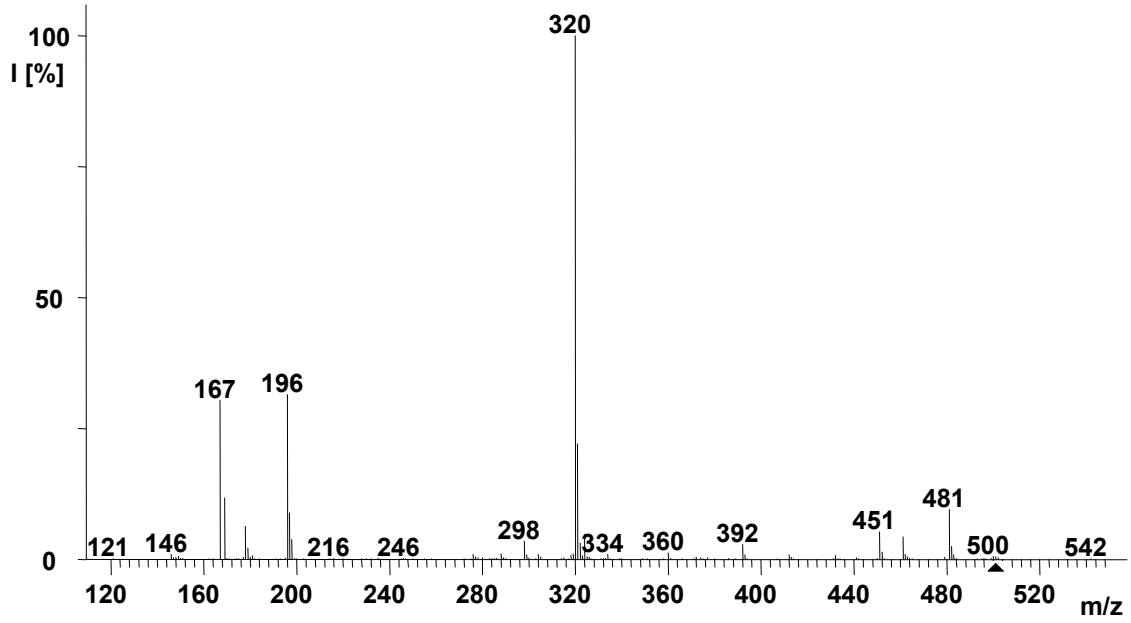

(9*Z*,11*E*,15*Z*)-Methyl 13-(pentafluorobenzyloxy)imino-9,11,15-octadecatrienoate (60)

EI positive MS

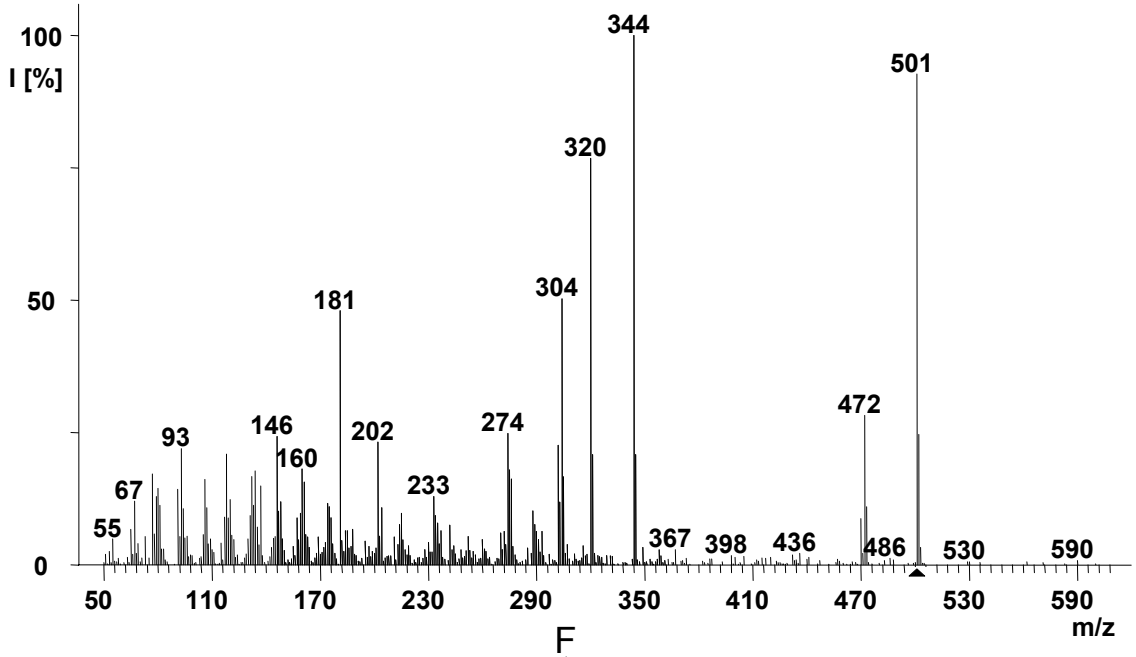

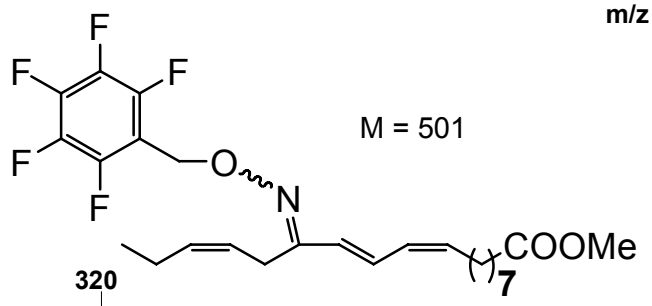

M = 501

CI negative MS

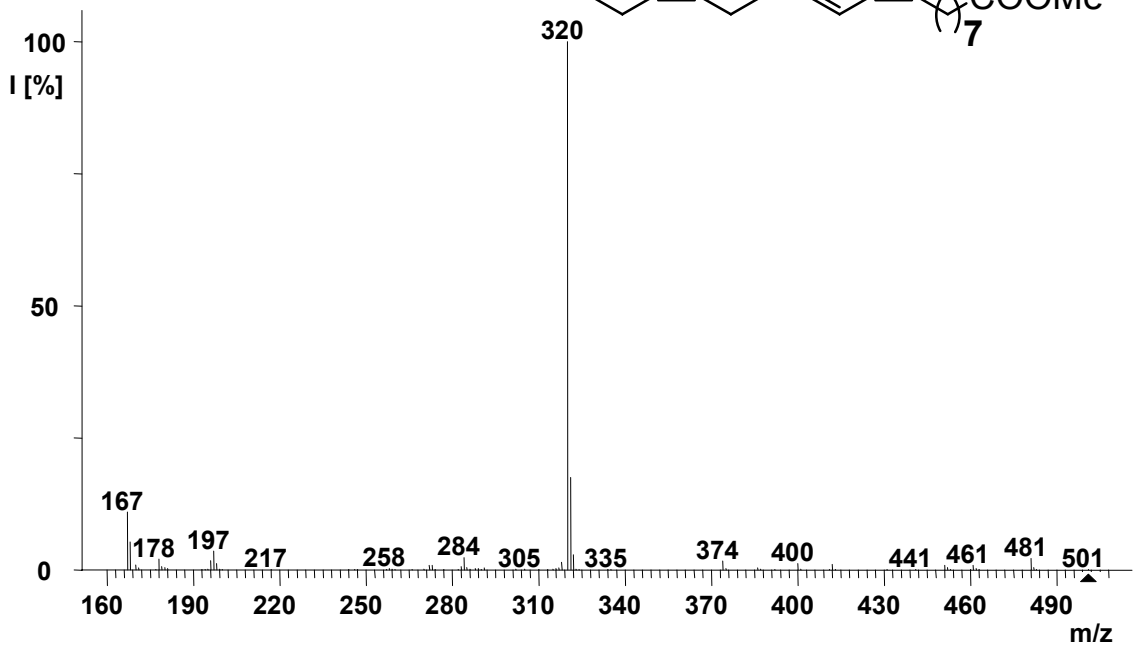

(8*E*,10*E*)-Methyl 12-(pentafluorobenzyloxy)imino-9-trimethylsilyloxy--8,10-dodecadienoate (61)

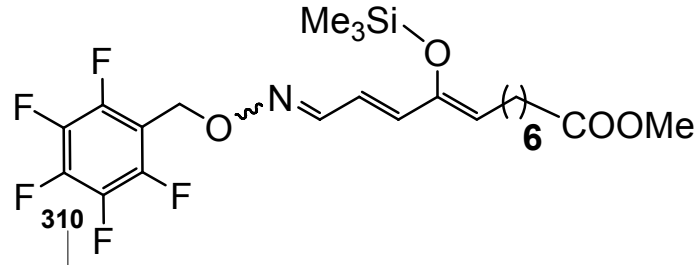

EI positive MS

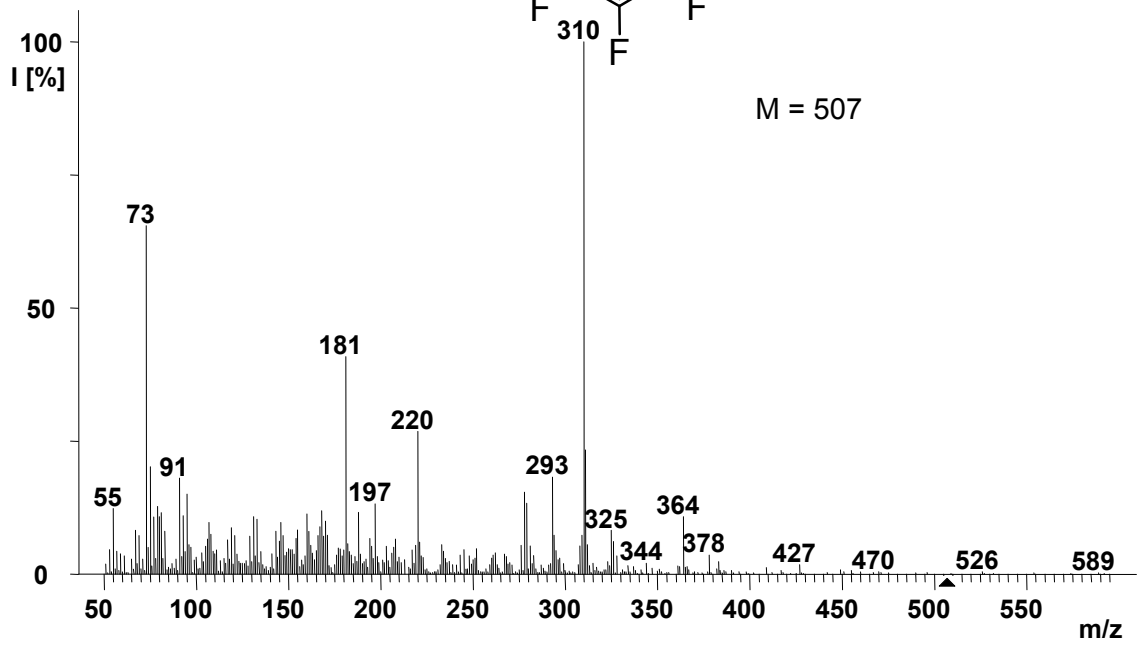

CI negative MS

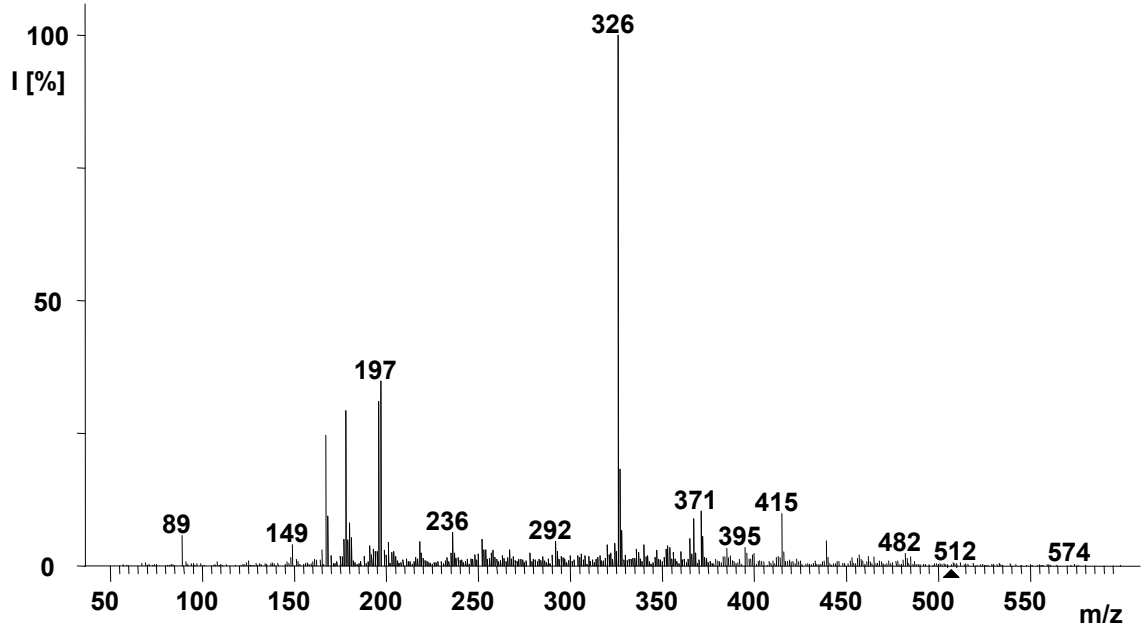

(10*E*)-Methyl 12-(pentafluorobenzyloxy)imino-9-trimethylsilyloxy-10-dodecenoate (62)

EI positive MS

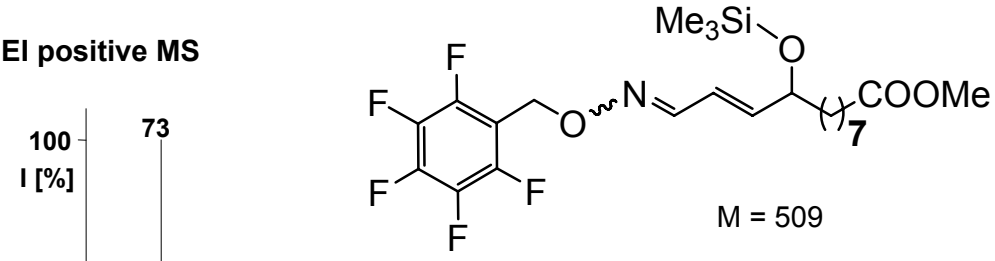

M = 509

CI negative MS

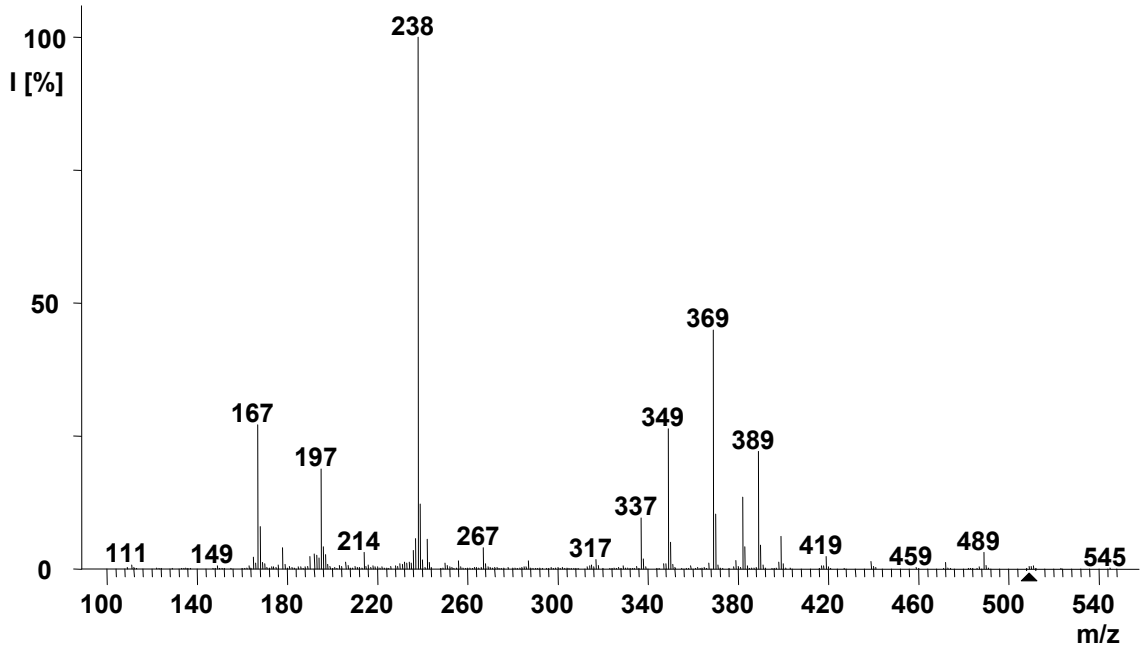

(9*E*,11*Z*)-Methyl 13-(pentafluorobenzyloxy)imino-9,11-tridecadienoate (63)

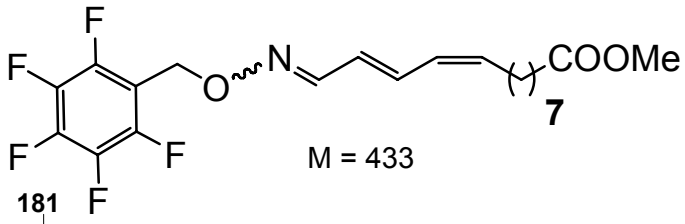

7

M = 433

EI positive MS

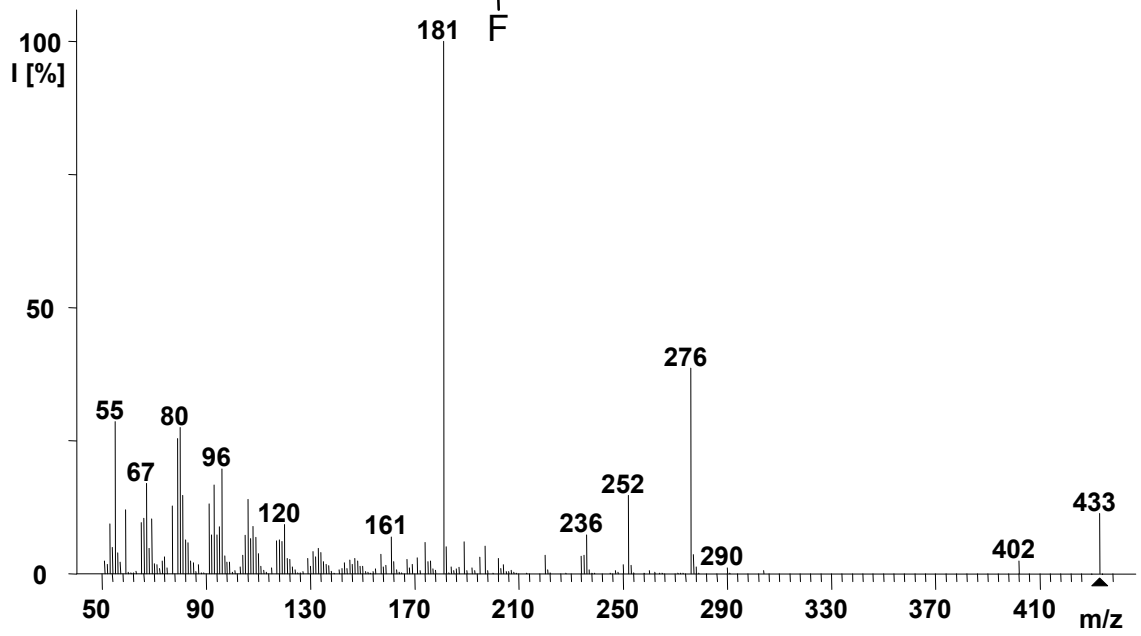

CI negative MS

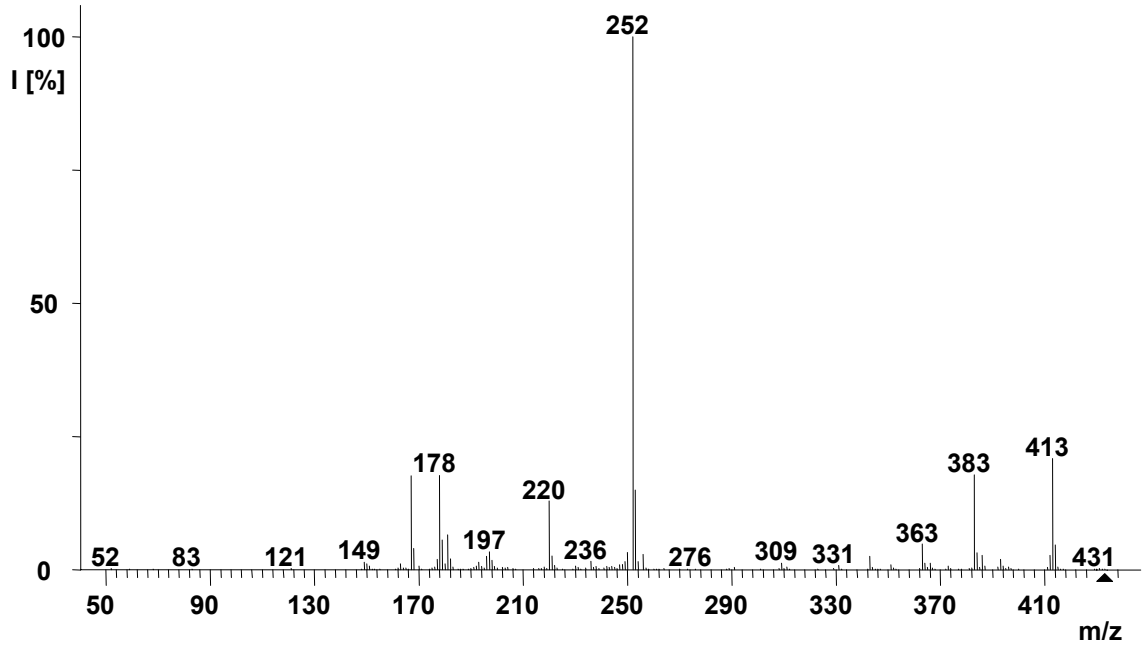

(10*E*)-Methyl 12-(pentafluorobenzyloxy)imino-10-dodecenoate (64)

EI positive MS

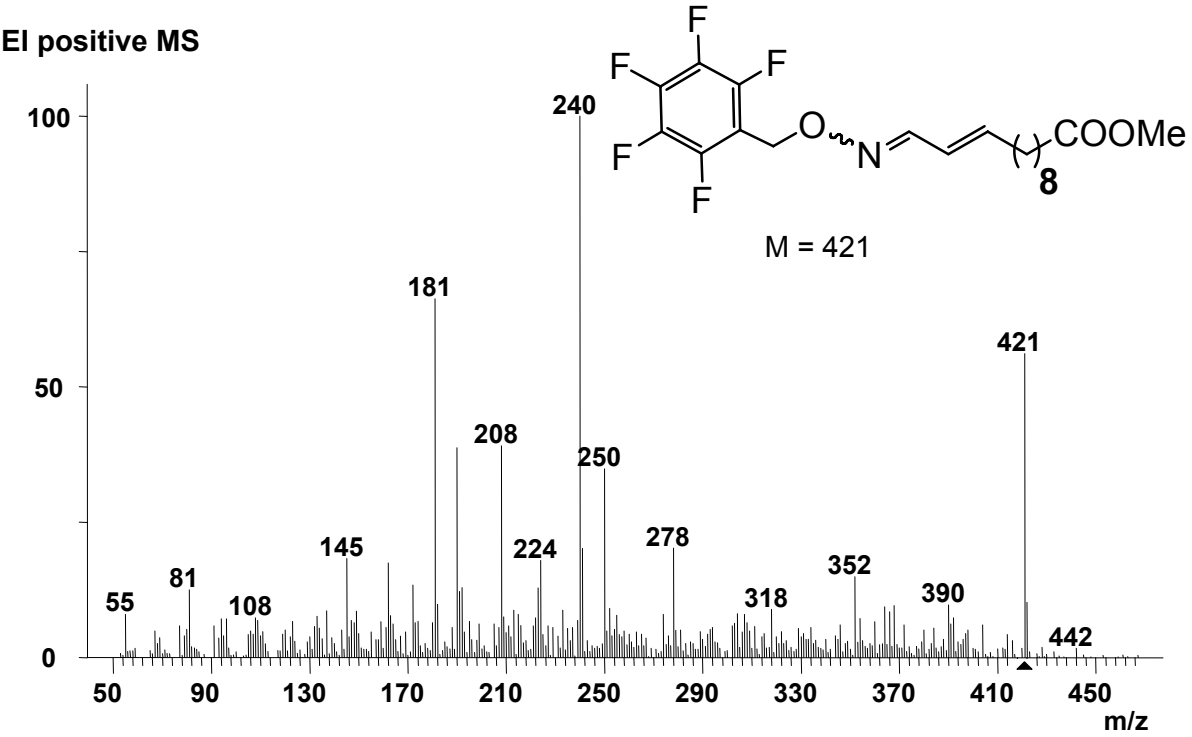

CI negative MS

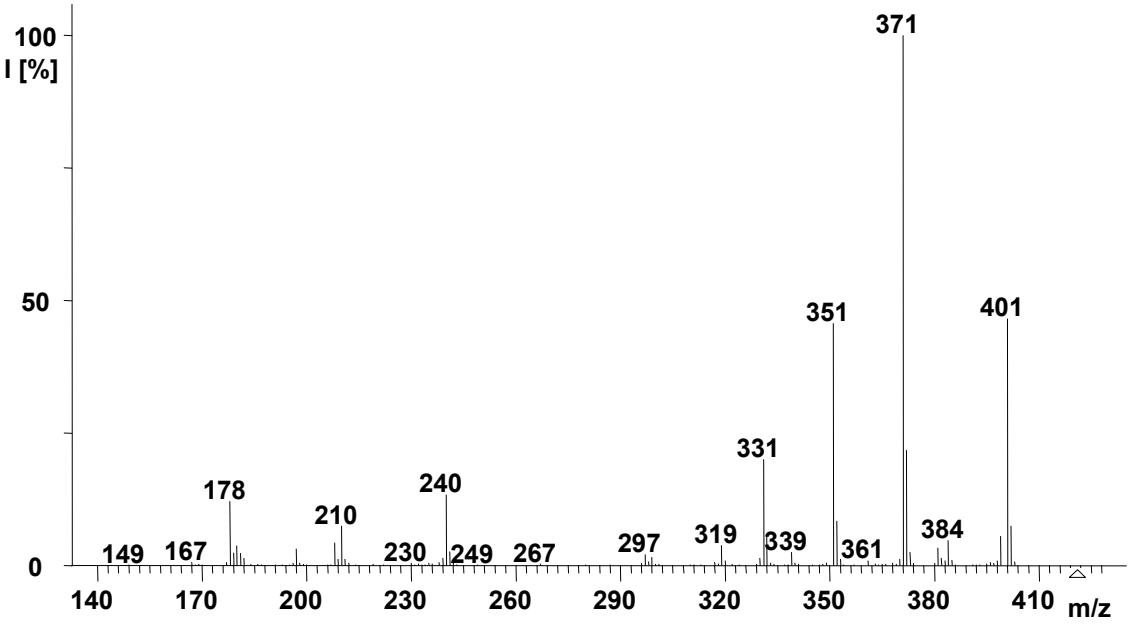

(9*Z*)-Methyl 11-(pentafluorobenzyloxy)imino-9-undecenoate (65)

EI positive MS

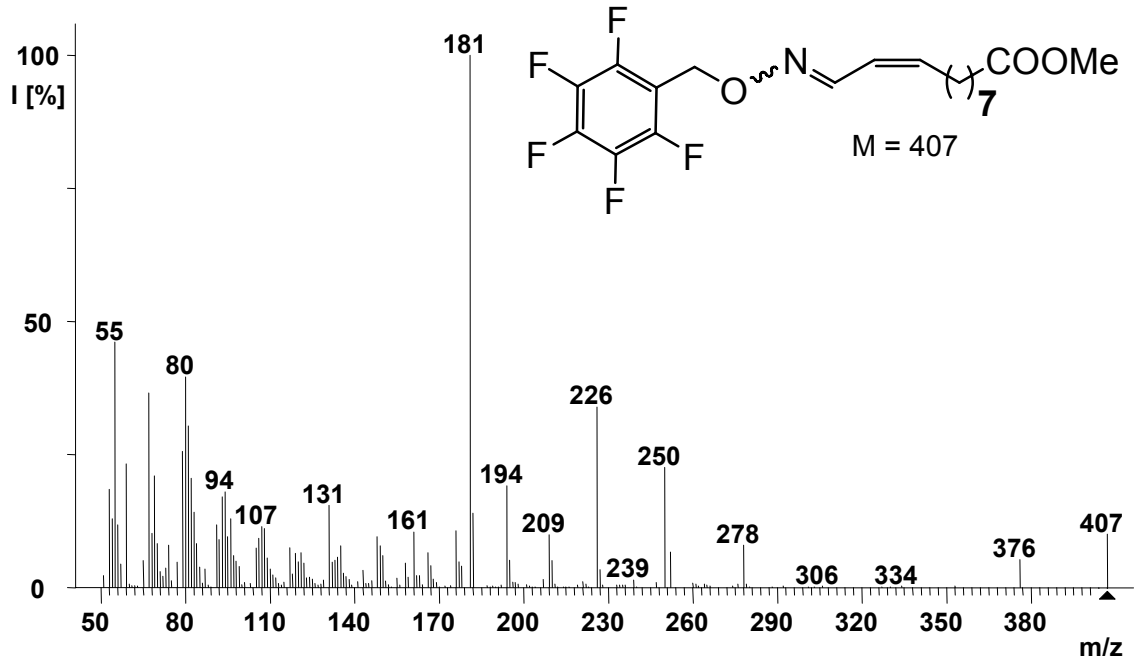

CI negative MS

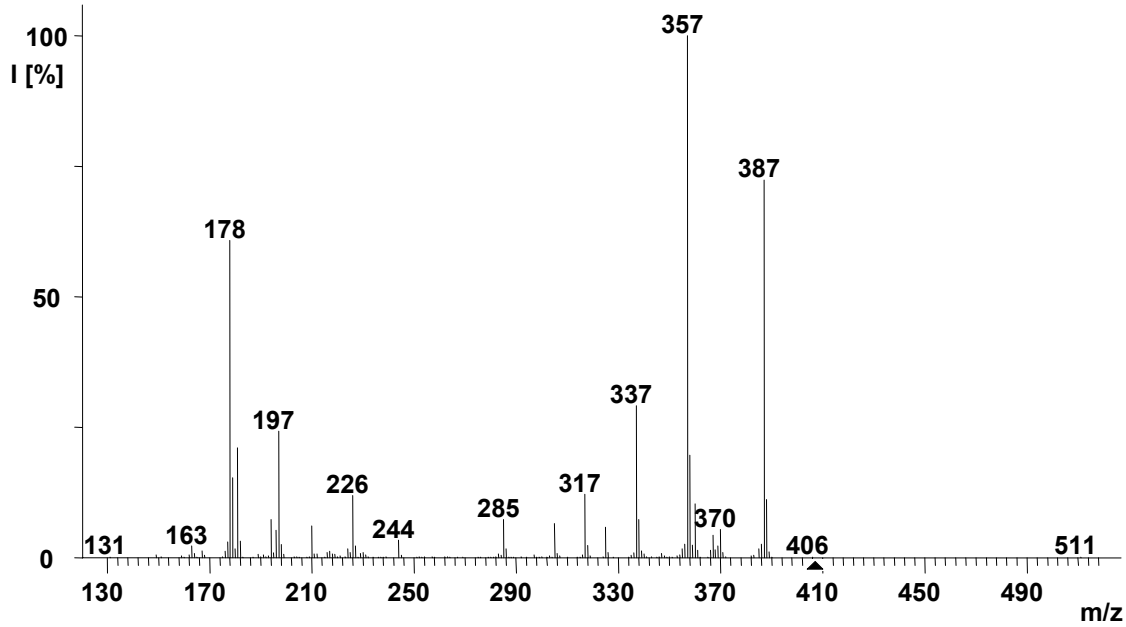

(9*Z*)-Methyl [9,10-$^2H_2$]-11-(pentafluorobenzyloxy)imino-9-undecenoate (66)

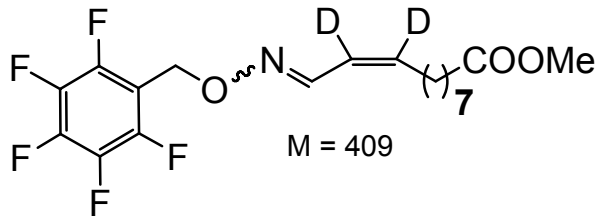

M = 409

EI positive MS

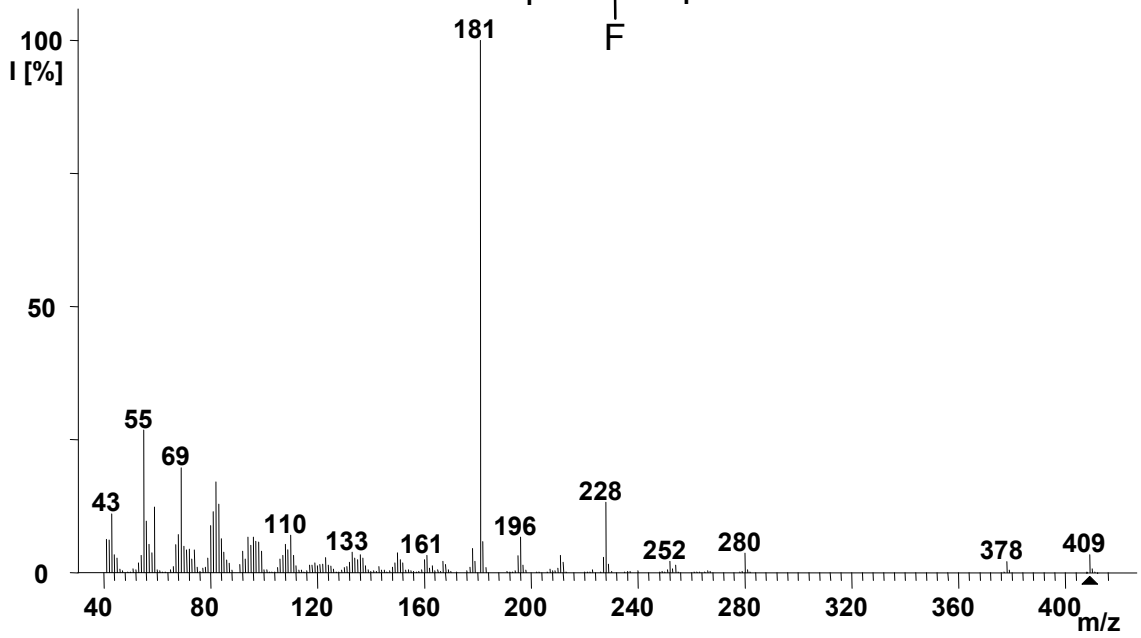

CI negative MS

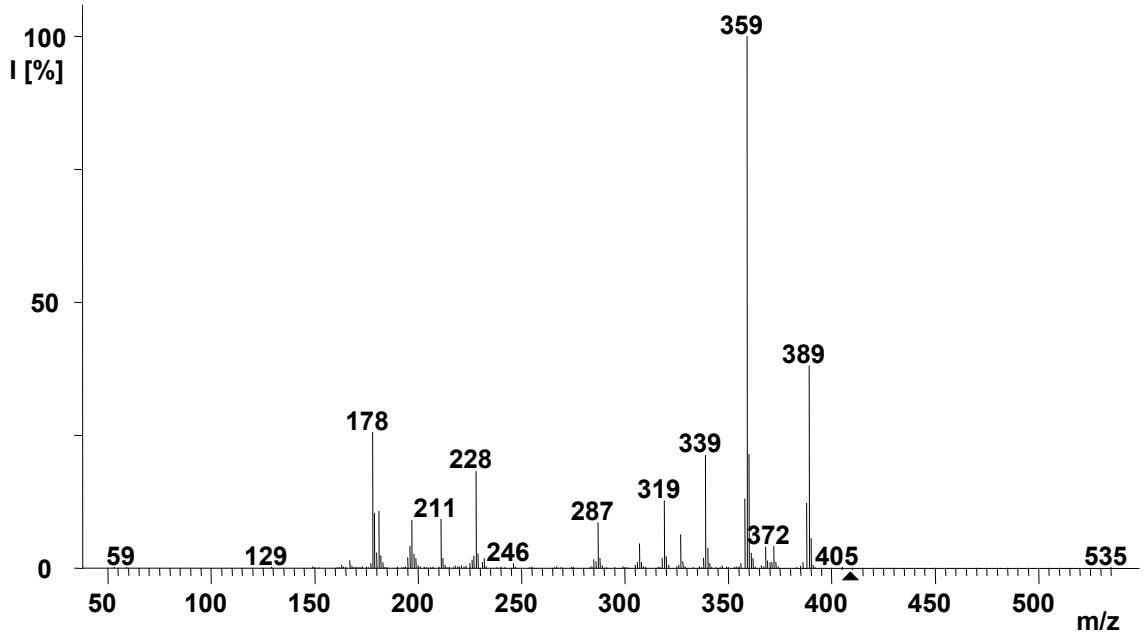

Methyl 9-(pentafluorobenzyloxy)iminononanoate (67)

EI positive MS

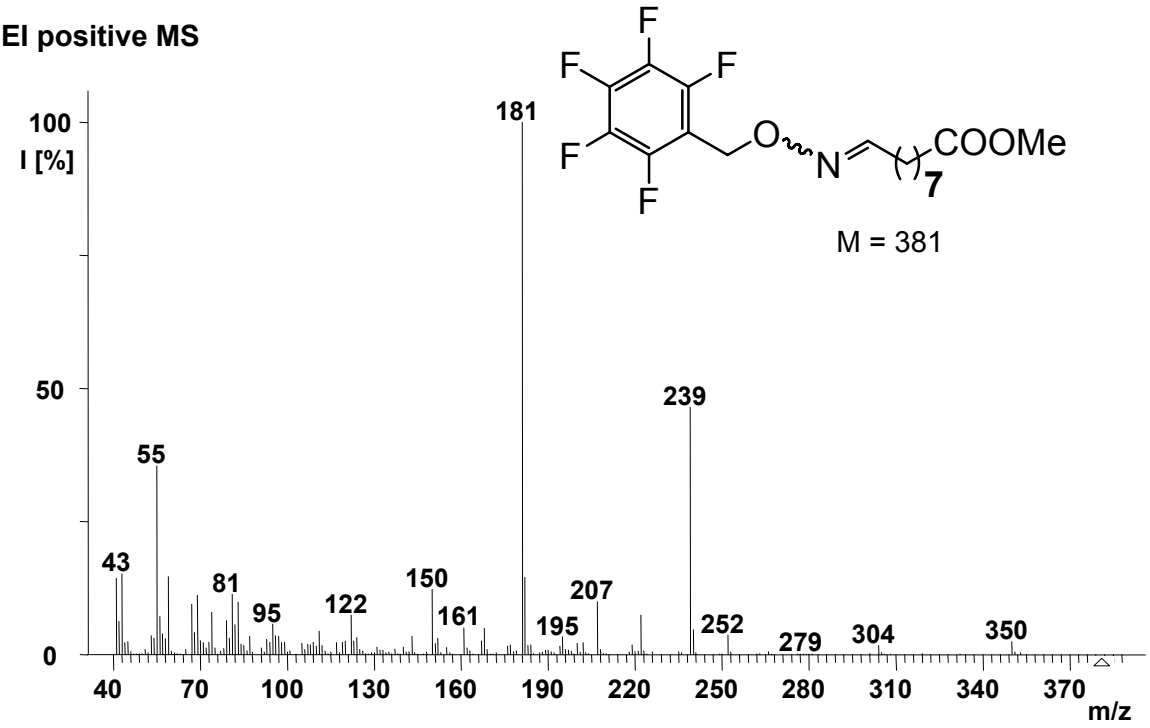

CI negative MS

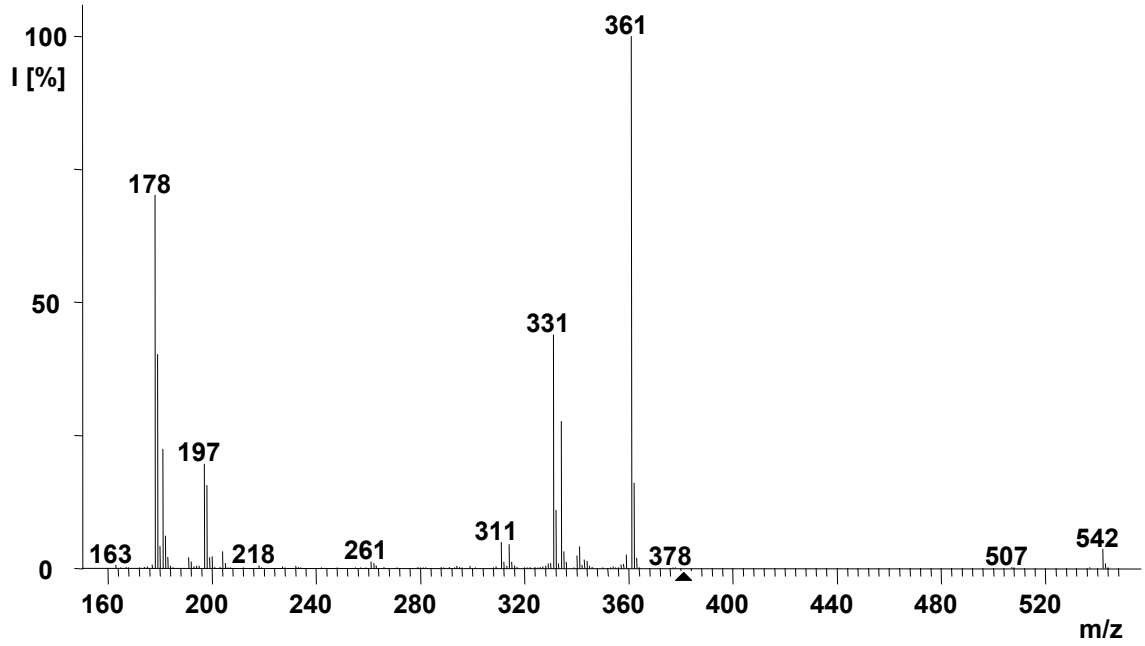

Methyl 8-[2,4-bis(trimethylsilyloxy)-5-((*E*)-3-trimethylsilyloxypent-1-enyl)cyclopentyl]-octanoate (89)

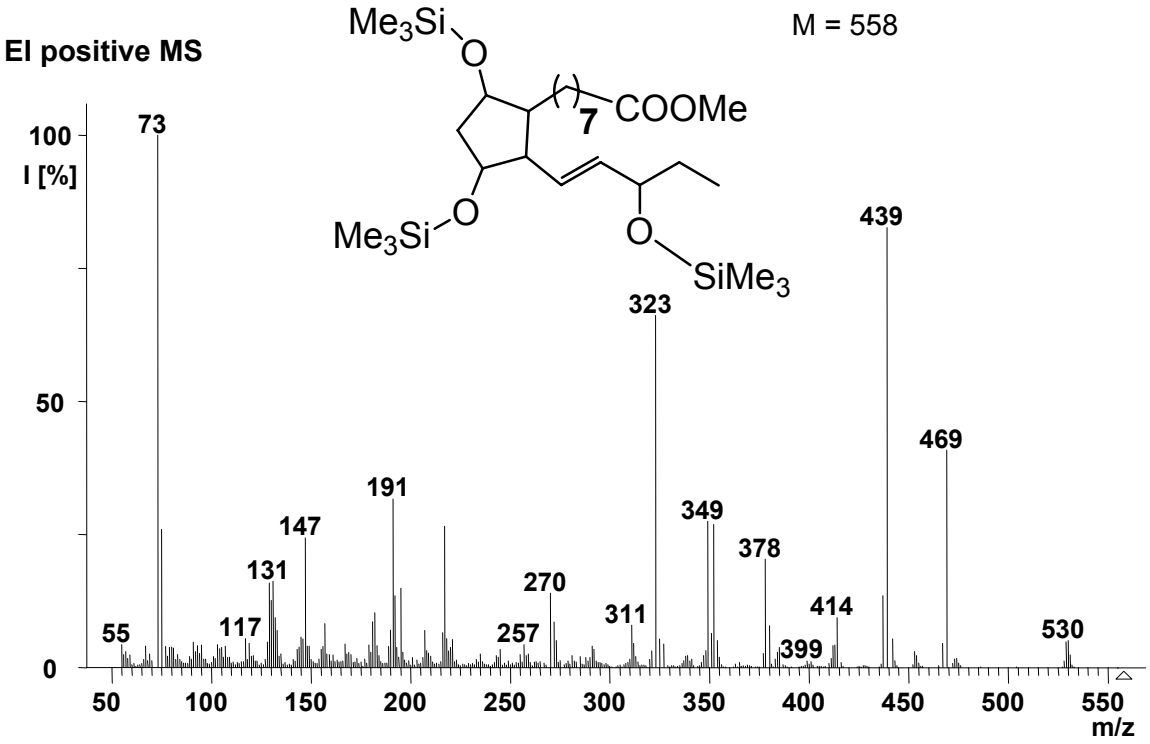

(10*E*)-Methyl 11-[5-ethyl-2,4-bis(trimethylsilyloxy)-cyclopentyl]-9-trimethylsilyloxy-10-undecenoate (90)

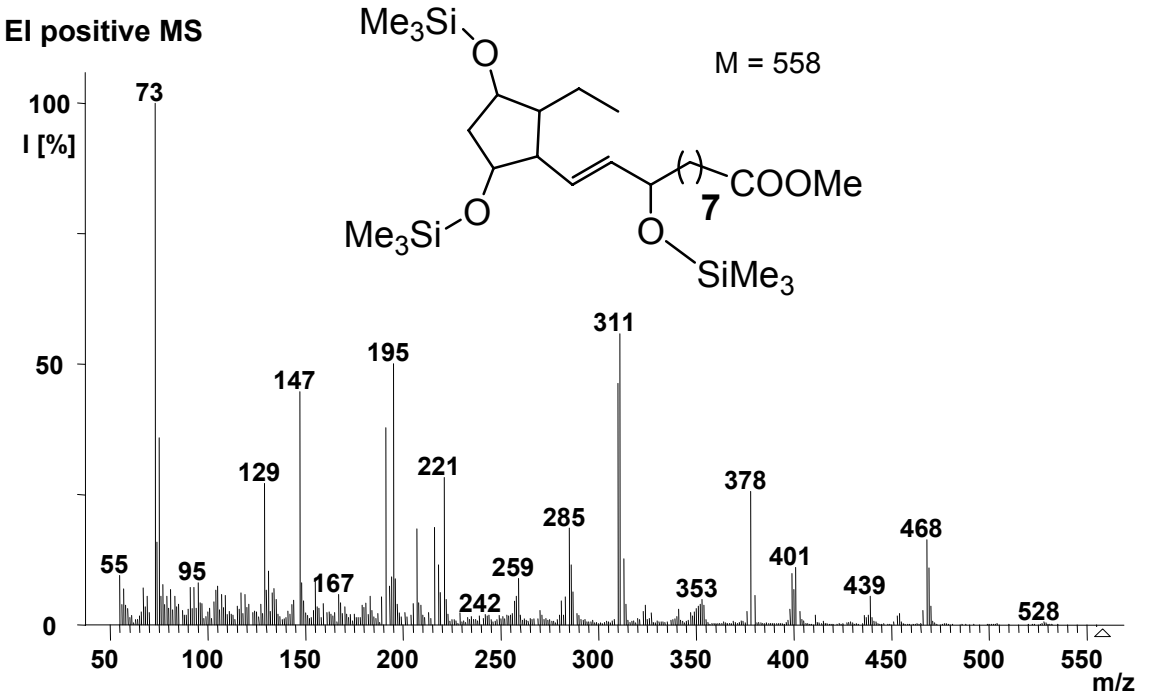

(12*Z*,15*Z*)-Methyl 9,10,11-tris(trimethylsilyloxy)-12,15-octadecadienoate (91)

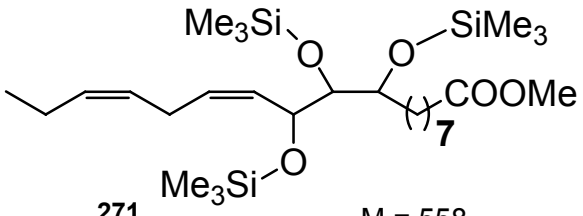

M = 558

EI positive MS

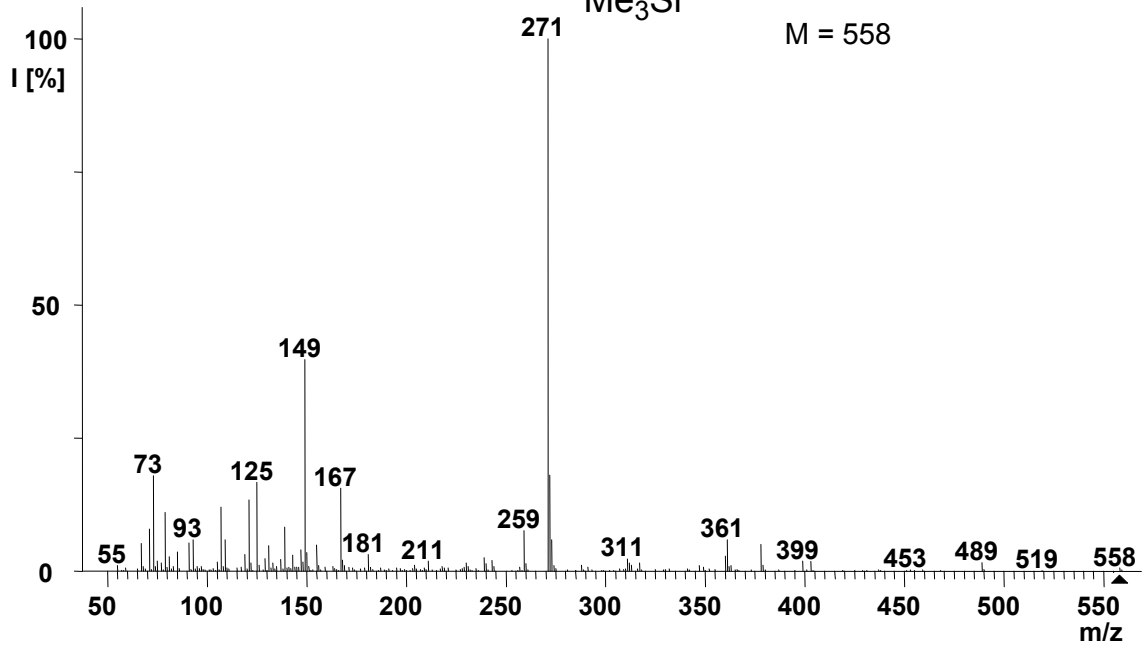

(10*E*,15*Z*)-Methyl 9,12,13-tris(trimethylsilyloxy)-10,15-octadecadienoate (92)

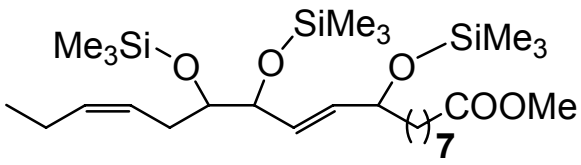

M = 558

EI positive MS

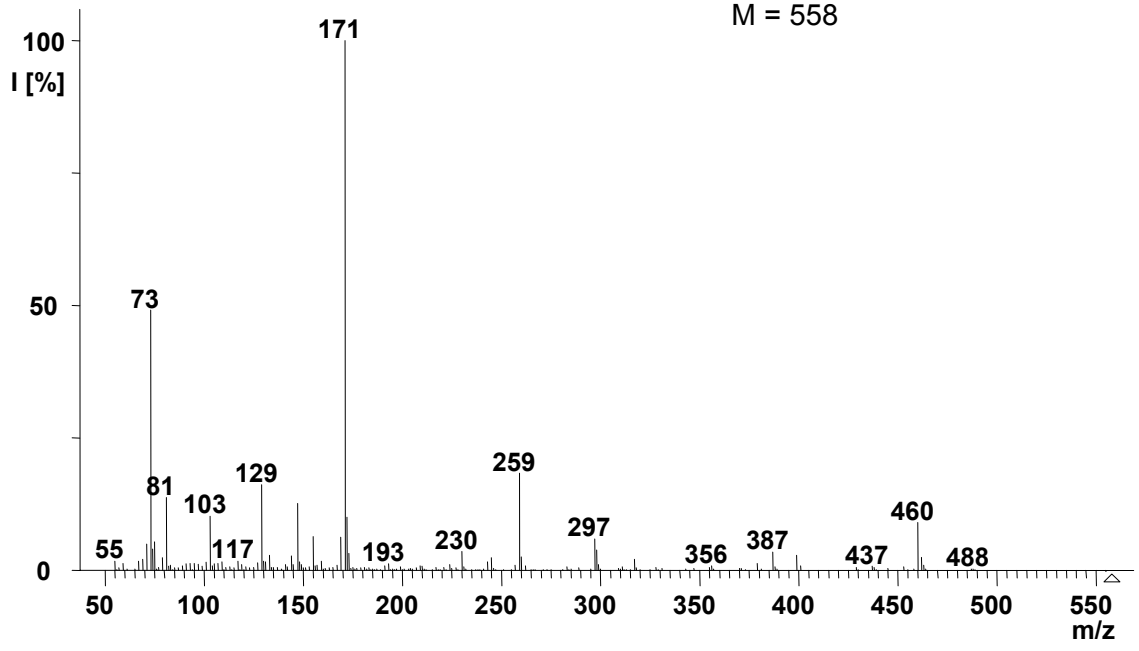

(12*Z*,15*Z*)-Methyl 10,11-epoxy-9-trimethylsilyloxy-12,15-octadecadienoate (93)

EI positive MS

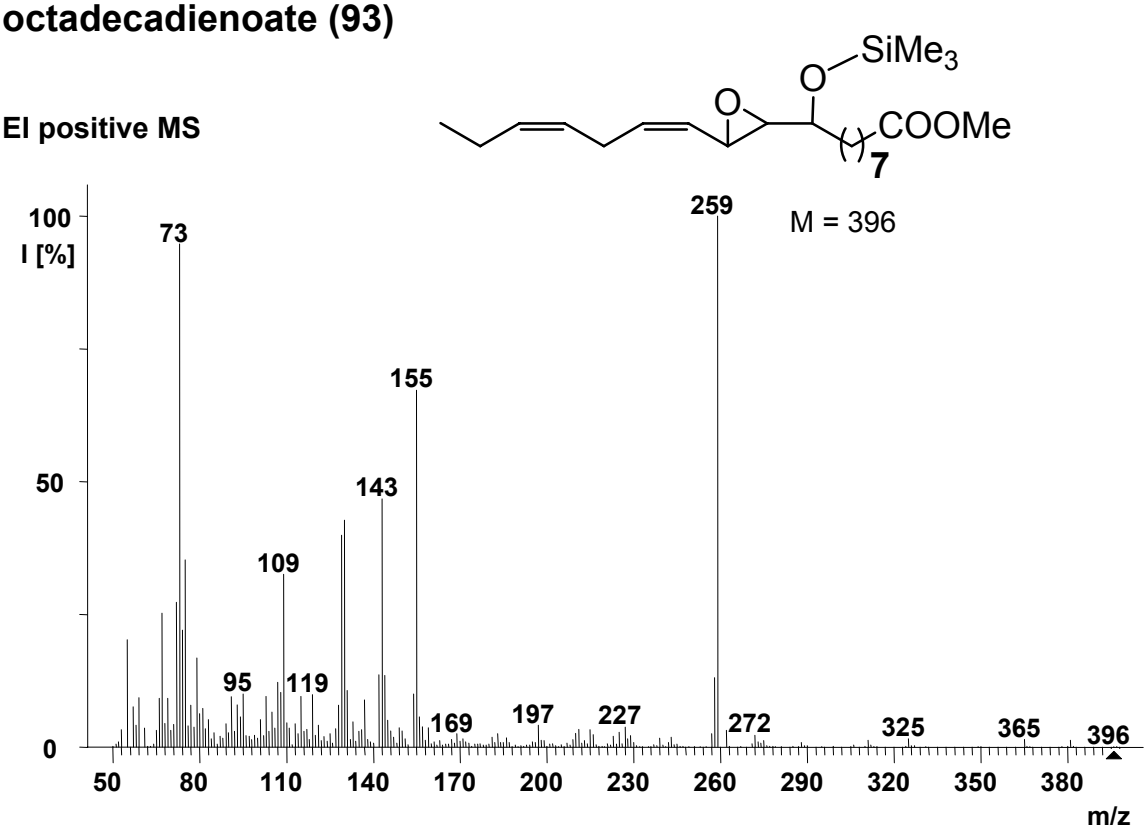

(10*E*,15*Z*)-Methyl 12,13-epoxy-9-trimethylsilyloxy-10,15-octadecadienoate (94)

EI positive MS

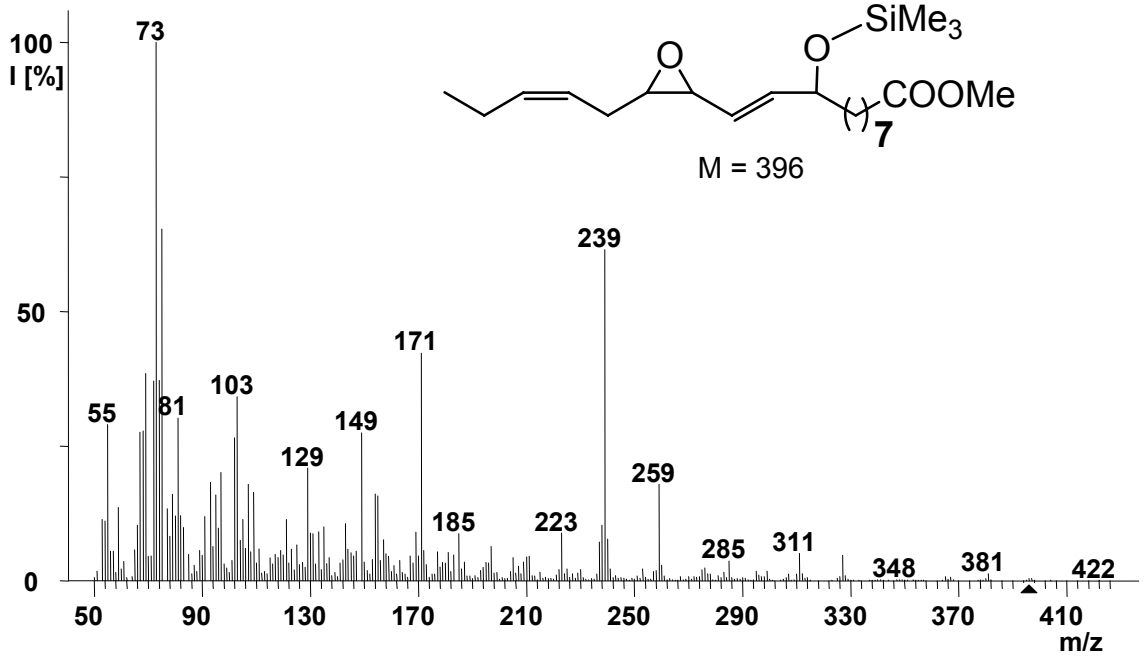

(9*Z*,15*Z*)-Methyl 12,13-epoxy-11-trimethylsilyloxy-9,15-octadecadienoate (95)

EI positive MS

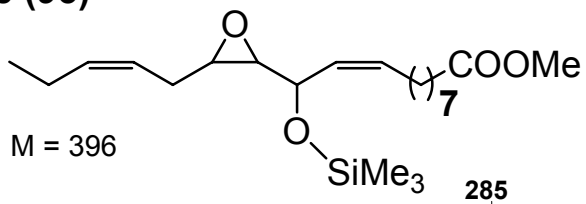

M = 396

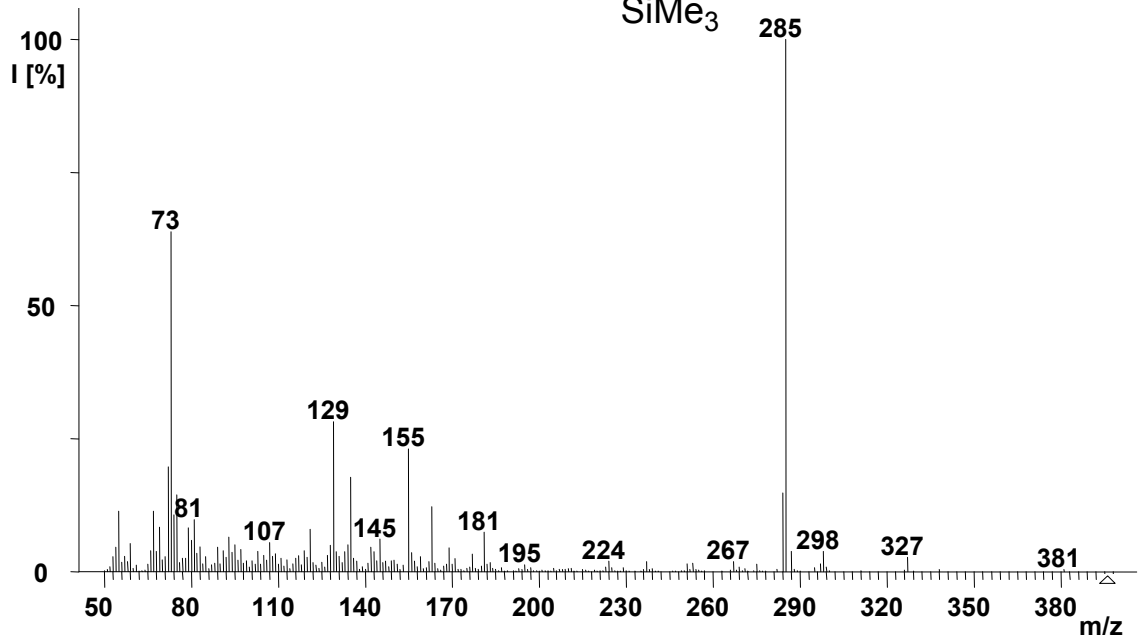

(10*E*,12*Z*,15*Z*)-Methyl 9-trimethylsilyloxy-10,12,15-octadecatrienoate (96)

EI positive

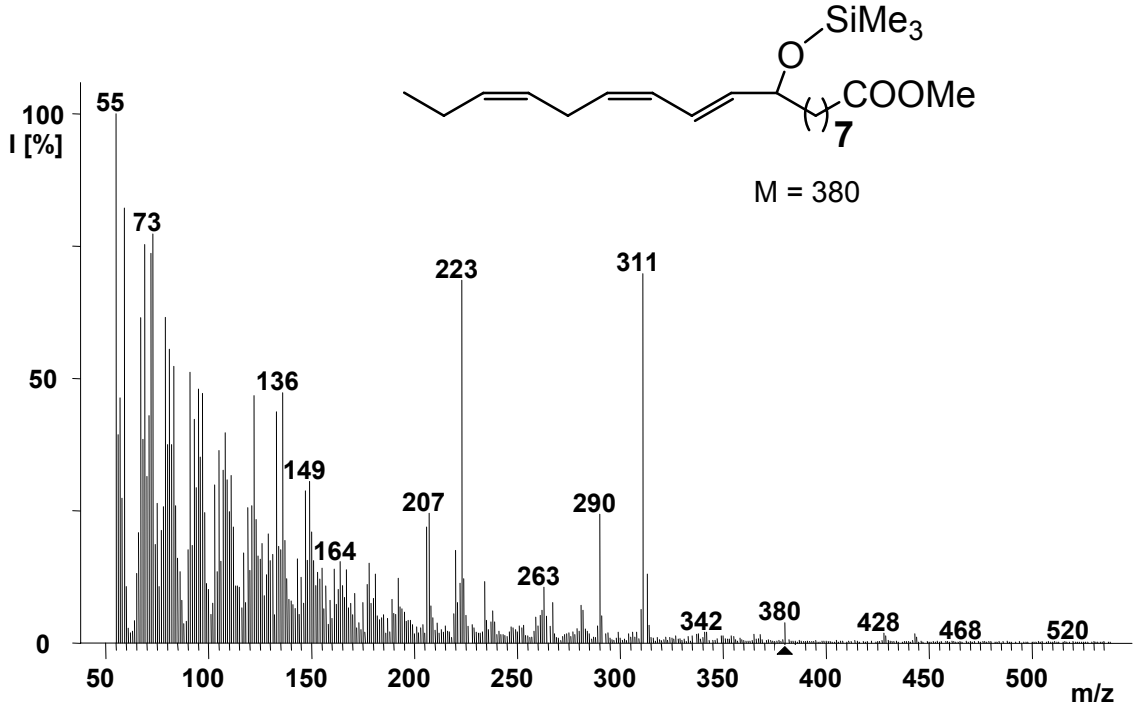

(9*Z*,11*E*,15*Z*)-methyl 13-trimethylsilyloxyoctadeca-9,11,15-trienoate (97)

EI positive

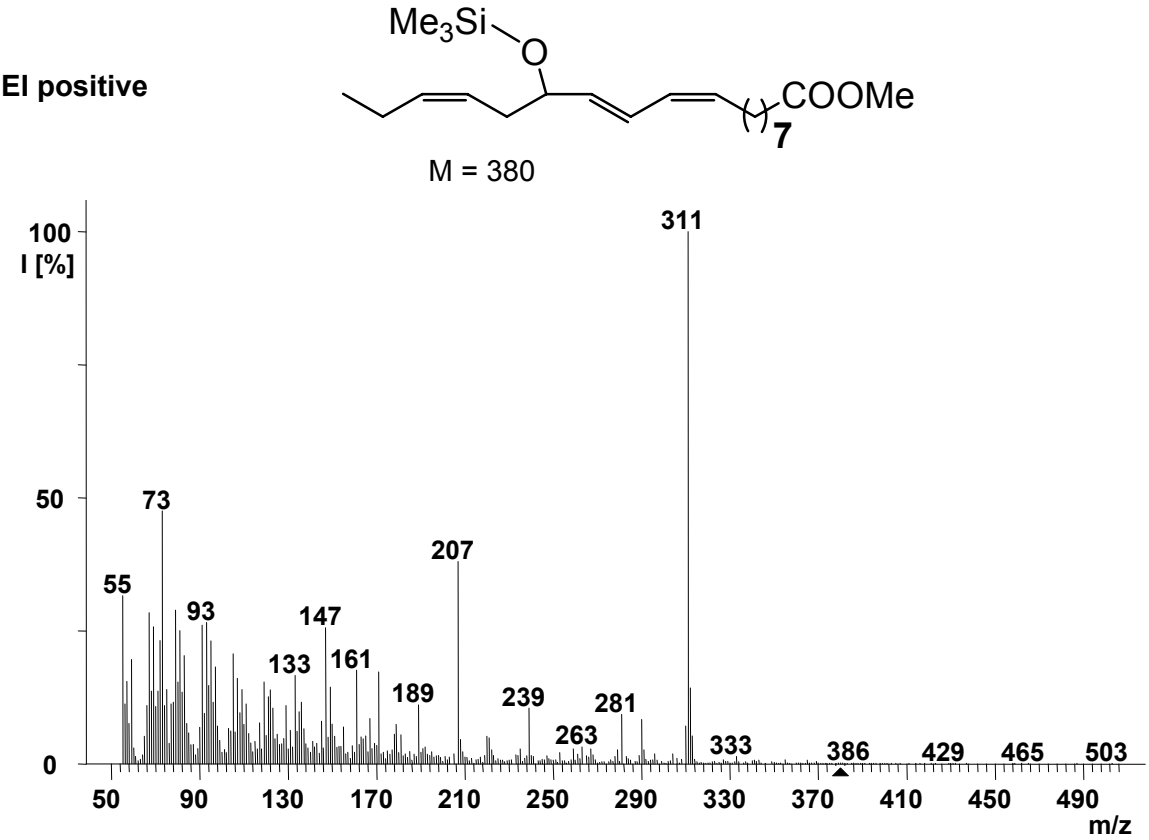

13.4 Data sheets

Calibration curves

Calibration curves for determination of JA (1) (with 0.5 g frw Lima bean leaf)

amount of added **1** [367]	area ratio **1**/std	amount of added **1** [ng]	area ratio **1**/std
0	0,05	300	6,55
0	0,30	300	9,19
0	0,06	300	4,10
0	0,08	300	3,84
0	0,02	300	4,27
20	0,65	600	11,64
20	0,58	600	14,72
20	0,68	600	6,15
20	0,64	600	5,836
20	0,30	600	8,26
50	1,12	1000	13,94
50	0,92	1000	13,98
50	2,29	1000	10,72
50	0,75	1000	11,97
50	0,97	1000	14,42
80	1,56	1000	15,16
80	2,46	1000	12,27
80	1,42	2000	24,63
80	1,60	2000	31,22
150	2,48	2000	24,30
150	3,61		
150	2,32		
150	2,43		
150	2,17		

Calibration curve for determination of OPDA (7)

amount of added **7** [ng]	area ratio **7**/std	amount of added **7** [ng]	area ratio **7**/std
0	1,07	1000	1,273
0	2,38	1000	1,73
0	0,06	1000	1,02
0	0,07	1000	1,60
50	0,60	2000	2,07
50	1,46	2000	2,66
50	0,08	2000	1,64
50	0,12	2000	2,89
100	0,65	3000	3,62
100	1,39	3000	4,07
100	0,076	3000	2,93
100	0,19	3000	4,68
300	0,53	3000	3,59
300	1,88	3000	3,32
300	0,33	3000	3,50
300	0,36	5000	5,92
500	0,72	5000	5,38
500	1,87	5000	6,11
500	0,88	5000	6,03
500	0,60		

Calibration curve for determination of 11-oxo-9-undecenoic acid (48)

amount of added **48** [ng]	area ratio **48**/std	amount of added **48** [ng]	area ratio **48**/std
0	1,74	500	1,63
0	0,95	500	1,17
0	0,15	500	3,22
0	0,17	500	2,18
50	1,21	500	1,17
50	0,99	1000	5,75
50	0,28	1000	2,92
50	0,28	1000	2,61
100	1,72	1000	2,31
100	0,93	1500	7,15
100	0,34	1500	4,32
100	0,37	1500	4,75
300	2,09	1500	4,28
300	1,47	2000	8,8
300	0,89	2000	5,35
300	0,88	2000	6,55
		2000	7,03

Calibration curve for determination of 13-oxo-9,11-tridecadienoic acid (18)

amount of added **18** [ng]	area ratio **18**/std	amount of added **18** [ng]	area ratio **18**/std
0	0,54	1000	1,67
0	0,68	1000	1,20
0	0,22	1000	0,97
0	0,64	1000	0,93
50	0,24	1500	1,75
50	0,78	1500	1,87
50	0,29	1500	1,21
50	0,65	2000	2,41
100	0,89	2000	2,92
100	0,98	2000	3,46
100	0,16	2000	4,04
100	0,63	2000	1,99
300	0,54	2000	3,45
300	1,09	2000	3,30
300	0,33	5000	5,32
300	0,45	5000	4,42
500	0,71	5000	6,03
500	1,80	5000	5,96
500	1,35	10000	10,42
500	0,48	10000	9,75
		10000	9,03
		10000	8,82

Recovery rates

Jasmonic acid (1)

amount of added **1** [ng]	area ratio **1**/std	amount of added **1** [ng]	area ratio **1**/std
0	-18,63	300	227,66
0	-2,04	300	574,88
0	-18,04	300	255,29
0	-16,76	600	734,32
20	20,33	600	356,80
20	22,49	600	934,19
20	15,73	600	377,91
20	-2,11	600	514,44
20	19,88	1000	1240,12
50	51,09	1000	1642,49

50	37,74	1000	674,53
50	127,16	1000	755,35
50	26,80	1000	774,90
50	42,33	1000	883,81
80	79,87	1000	886,30
80	70,53	1000	914,702
80	81,97	1000	963,07
80	54,23	1500	816,26
80	138,16	1500	1130,73
150	136,01	1500	1493,99
150	128,65	1500	1207,71
150	139,32	2000	2006,13
150	118,94	2000	1578,02
150	212,61	2000	1556,32
300	244,85	2000	1546,74
300	403,66		

12-Oxophytodienoic acid (7)

amount of added **7** [ng]	area ratio **7**/std	amount of added **7** [ng]	area ratio **7**/std
0	479,73	1000	1078,04
0	1670,64	1000	661,49
0	-441,98	1000	438,65
0	-427,35	1000	960,20
50	55,81	2000	1387,93
50	-382,09	2000	1926,96
50	836,12	2000	2132,39
50	-420,75	2000	999,21
100	101,78	3000	2795,95
100	-321,81	3000	3209,49
100	770,76	3000	2171,89
100	-423,55	3000	3764,90
300	-12,03	3000	2772,71
300	-167,40	3000	2521,43
300	1215,37	3000	2690,23
300	-188,51	5000	4987,84
500	1204,16	5000	4887,29
500	305,07	5000	4398,90
500	158,18	5000	5066,34
500	50,13		

11-Oxo-9-undecenoic acid (47)

amount of added **48** [ng]	area ratio **48**/std	amount of added **48** [ng]	area ratio **48**/std
0	322,62	500	714,29
0	115,81	500	440,78
0	-93,75	500	296,23
0	-89,34	500	174,08
50	184,65	1000	1380,38
50	125,82	1000	633,43
50	-60,62	1000	552,26
50	-61,48	1000	474,44
100	317,36	1500	1747,58
100	111,98	1500	1001,95
100	-45,49	1500	1117,05
100	-35,80	1500	991,29
300	99,78	2000	1273,35
300	96,72	2000	2181,79
300	417,50	2000	1588,86
300	253,53	2000	1716,03

13-Oxo-9,11-tridecadienoic acid (18)

amount of added **18** [ng]	area ratio **18**/std	amount of added **18** [ng]	area ratio **18**/std
0	121,99	1000	1065,15
0	312,86	1000	669,93
0	-345,42	1000	1736,16
0	255,48	1000	724,79
50	-307,51	1500	2020,97
50	453,73	1500	1081,17
50	-239,54	2000	2781,51
50	280,24	2000	4288,35
100	622,45	2000	3515,63
100	726,70	2000	2184,59
100	238,68	2000	5121,15
100	-422,70	2000	4053,54
300	115,75	2000	4276,01
300	909,06	5000	5652,94
300	-5,90	5000	6944,20
300	-183,48	5000	7952,93
500	354,04	5000	7858,80
500	1916,55	10000	12238,11
500	1267,97	10000	13273,82
500	36,41	10000	11944,40
		10000	14204,72

Oxylipin analysis of mechanically wounded *P. lunatus*

Jasmonic acid (1)

treatment	time [min]	sample weight [g]	area ratio **1**/std	amount **1** [ng/g frw]	*cis*/total **1** [%]
wounded	40	0,5	5,26	674	72,9
wounded	40	0,5	4,23	542	73,3
wounded	40	0,5	2,90	372	88,7
wounded	40	0,5	4,56	584	76,5
wounded	60	0,5	4,35	558	71,2
wounded	60	0,5	2,06	264	68,9
wounded	60	0,5	5,19	665	70,0
wounded	60	0,5	5,06	649	75,4
wounded	90	0,5	5,10	653	40,1
wounded	90	0,5	5,18	664	54,4
wounded	90	0,5	5,36	688	43,5
wounded	90	0,5	3,71	476	62,8
wounded	120	0,5	7,75	993	68,6
wounded	120	0,5	7,73	991	73,0
wounded	120	0,5	2,69	345	63,6
wounded	120	0,5	5,80	744	77,2
wounded	240	0,5	3,24	415	64,9
wounded	240	0,5	0,84	107	54,6
wounded	240	0,5	2,91	373	66,9
wounded	240	0,5	1,57	201	60,7
wounded	600	0,5	2,02	259	12,2
wounded	600	0,5	4,03	517	7,5
wounded	600	0,5	2,40	308	10,5
wounded	600	0,5	0,39	50	37,9
control	40	0,5	0,06	8	30,3
control	40	0,5	0,04	5	0
control	40	0,5	0,05	7	26,8
control	60	0,5	0,13	17	16,8
control	60	0,5	0,02	3	39,7
control	60	0,5	0,06	8	27,6
control	60	0,5	0,02	3	0
control	90	0,5	1,85	237	2,9
control	90	0,5	1,16	149	2,2
control	90	0,5	0,43	55	20,6

control	120	0,5	0,03	4	0
control	120	0,5	0,04	5	22,7
control	120	0,5	0,05	6	26,6
control	120	0,5	0,39	51	10,9
control	240	0,5	0,19	25	6,6
control	240	0,5	0,03	3	40,7
control	240	0,5	0,09	11	18,6
control	240	0,5	0,24	30	10,8
control	600	0,5	1,01	129	7,1
control	600	0,5	1,16	148	5,5
control	600	0,5	1,66	213	5,9
control	600	0,5	0,06	8	20,2

12-Oxophytodienoic acid (7)

treatment	time [min]	sample weight [g]	area ratio **7**/std	amount **7** [µg/g frw]
wounded	40	0,5	1,40	2,54
wounded	40	0,5	0,28	0,50
wounded	40	0,5	2,51	4,57
wounded	60	0,5	1,34	2,43
wounded	60	0,5	0,18	0,32
wounded	60	0,5	3,02	5,49
wounded	90	0,5	1,94	3,53
wounded	90	0,5	1,45	2,63
wounded	90	0,5	1,52	2,76
wounded	120	0,5	1,27	2,30
wounded	120	0,5	0,39	0,71
wounded	120	0,5	3,53	6,41
wounded	120	0,5	1,83	3,33
wounded	240	0,5	1,19	2,16
wounded	240	0,5	0,20	0,36
wounded	240	0,5	3,30	6,00
wounded	600	0,5	4,51	8,21
wounded	600	0,5	7,33	13,33
control	40	0,5	0,14	0,30
control	40	0,5	1,54	3,42
control	40	0,5	1,09	2,43
control	60	0,5	1,84	4,08
control	60	0,5	2,01	4,46
control	60	0,5	1,03	2,29
control	90	0,5	5,46	12,14
control	90	0,5	2,43	5,40
control	90	0,5	4,50	10,00
control	120	0,5	0,17	0,38
control	120	0,5	2,90	6,45
control	120	0,5	4,44	9,88
control	120	0,5	3,24	7,21
control	240	0,5	1,16	2,57
control	240	0,5	2,65	5,89
control	240	0,5	1,77	3,94
control	600	0,5	1,25	2,78
control	600	0,5	0,43	0,95
control	600	0,5	4,06	9,03

11-Oxo-9-undecenoic acid (48)

treatment	time [min]	sample weight [g]	area ratio **48**/std	amount **48** [µg/g frw]
wounded	40	0,5	0,99	0,71
wounded	40	0,5	0,70	0,50
wounded	40	0,5	0,27	0,19
wounded	40	0,5	0,30	0,21
wounded	60	0,5	0,90	0,65
wounded	60	0,5	0,41	0,30
wounded	60	0,5	0,36	0,26
wounded	60	0,5	0,48	0,34
wounded	90	0,5	0,30	0,21

wounded	90	0,5	0,30	0,22
wounded	90	0,5	0,30	0,21
wounded	120	0,5	0,82	0,59
wounded	120	0,5	0,72	0,51
wounded	120	0,5	0,33	0,24
wounded	120	0,5	0,36	0,25
wounded	240	0,5	0,39	0,28
wounded	240	0,5	0,82	0,58
wounded	240	0,5	0,65	0,46
wounded	240	0,5	0,48	0,34
wounded	600	0,5	0,57	0,40
wounded	600	0,5	0,71	0,51
control	40	0,5	0,39	0,28
control	40	0,5	0,28	0,20
control	40	0,5	0,20	0,14
control	60	0,5	0,83	0,59
control	60	0,5	0,15	0,10
control	60	0,5	0,27	0,19
control	60	0,5	0,24	0,17
control	90	0,5	0,45	0,32
control	90	0,5	0,24	0,17
control	90	0,5	0,38	0,27
control	120	0,5	0,39	0,28
control	120	0,5	0,34	0,24
control	120	0,5	0,31	0,22
control	120	0,5	0,23	0,16
control	240	0,5	0,92	0,66
control	240	0,5	0,23	0,16
control	240	0,5	0,22	0,16
control	240	0,5	0,28	0,20
control	600	0,5	0,36	0,25
control	600	0,5	0,30	0,22
control	600	0,5	0,53	0,38

13-Oxo-9,11-tridecadienoic acid (18)

treatment	time [min]	sample weight [g]	area ratio **18**/std	amount **18** [µg/g frw]
wounded	40	0,5	5,37	9,76
wounded	40	0,5	10,29	18,71
wounded	40	0,5	0,24	0,44
wounded	40	0,5	0,13	0,23
wounded	60	0,5	5,06	9,19
wounded	60	0,5	6,65	12,09
wounded	60	0,5	0,46	0,84
wounded	60	0,5	1,48	2,69
wounded	90	0,5	0,68	1,23
wounded	90	0,5	0,84	1,52
wounded	90	0,5	0,97	1,76
wounded	120	0,5	3,27	5,95
wounded	120	0,5	0,77	1,40
wounded	240	0,5	1,52	2,76
wounded	240	0,5	0,41	0,74
wounded	240	0,5	1,51	2,74
wounded	240	0,5	0,81	1,47
wounded	240	0,5	2,08	3,79
wounded	240	0,5	1,37	2,49
control	40	0,5	5,01	9,12
control	40	0,5	0,23	0,42
control	40	0,5	0,21	0,38
control	60	0,5	3,73	6,77
control	60	0,5	0,34	0,62
control	60	0,5	0,35	0,64
control	60	0,5	0,32	0,58
control	90	0,5	1,66	3,01
control	90	0,5	0,36	0,66
control	90	0,5	0,67	1,22

control	120	0,5	4,41	8,02
control	120	0,5	0,64	1,16
control	120	0,5	0,47	0,86
control	120	0,5	0,65	1,17
control	240	0,5	0,33	0,60
control	240	0,5	0,30	0,55
control	240	0,5	0,77	1,40
control	600	0,5	0,31	0,56
control	600	0,5	1,81	3,29
control	600	0,5	0,51	0,93

α-Ketol (9)

treatment	time [min]	sample weight [g]	area ratio **9**/std	amount **9** [µg/g frw]
wounded	40	0,5	39,90	3,99
wounded	40	0,5	16,22	1,62
wounded	40	0,5	5,61	0,56
wounded	60	0,5	24,97	2,50
wounded	60	0,5	4,65	0,46
wounded	60	0,5	2,54	0,25
wounded	120	0,5	21,21	2,12
wounded	120	0,5	43,84	4,38
wounded	120	0,5	5,80	0,58
wounded	240	0,5	32,87	3,29
wounded	240	0,5	6,41	0,64
wounded	240	0,5	20,95	2,10
control	40	0,5	2,95	0,59
control	60	0,5	19,13	3,83
control	120	0,5	3,06	0,61
control	240	0,5	22,83	4,57

γ-Ketol (10)

treatment	time [min]	sample weight [g]	area ratio **10**/std	amount **10** [µg/g frw]
wounded	40	0,5	32,81	8,20
wounded	40	0,5	28,86	7,21
wounded	60	0,5	10,88	2,18
wounded	60	0,5	1,66	0,33
wounded	90	0,5	0,27	0,05
wounded	90	0,5	0,13	0,03
wounded	90	0,5	0,50	0,10
wounded	120	0,5	8,27	1,65
wounded	120	0,5	12,65	2,53
wounded	240	0,5	6,73	1,35
wounded	240	0,5	1,80	0,36
wounded	600	0,5	2,78	0,56
wounded	600	0,5	3,79	0,76
wounded	600	0,5	4,45	0,89
control	40	0,5	0,53	0,11
control	60	0,5	6,18	1,24
control	90	0,5	0,46	0,09
control	90	0,5	0,20	0,04
control	90	0,5	0,28	0,06
control	120	0,5	0,59	0,12
control	240	0,5	5,48	1,10
control	600	0,5	3,56	0,71
control	600	0,5	2,80	0,56
control	600	0,5	2,30	0,46

9-Hydroxy-12-oxo-10-dodecenoic acid (49)

treatment	time [min]	sample weight [g]	area ratio **49**/std	amount **49** [µg/g frw]
wounded	40	0,5	72,27	7,226926912
wounded	40	0,5	71,65	7,165390916
wounded	40	0,5	10,88	1,088168434

wounded	60	0,5	47,04	4,70378862
wounded	60	0,5	48,52	4,851974443
wounded	60	0,5	3,53	0,353371559
wounded	120	0,5	15,21	1,521271078
wounded	120	0,5	52,01	5,201445448
wounded	120	0,5	14,52	1,452398988
wounded	240	0,5	73,19	7,319464521
wounded	240	0,5	20,81	2,081241271
wounded	240	0,5	30,33	3,032900346
control	40	0,5	24,31	2,430868854
control	60	0,5	58,97	5,896853442
control	120	0,5	19,10	1,910345687
control	240	0,5	57,58	5,758243494

12,13-Epoxy-11-HODE (20)

treatment	time [min]	sample weight [g]	area ratio **20**/std	amount **20** [µg/g frw]
wounded	40	0,5	60,57	6,06
wounded	40	0,5	84,20	8,42
wounded	40	0,5	5,40	0,54
wounded	60	0,5	32,00	3,20
wounded	60	0,5	38,53	3,85
wounded	60	0,5	3,16	0,32
wounded	120	0,5	39,21	3,92
wounded	120	0,5	52,02	5,20
wounded	120	0,5	9,83	0,98
wounded	240	0,5	42,33	4,23
wounded	240	0,5	33,42	3,34
wounded	240	0,5	16,26	1,63
control	40	0,5	42,60	4,26
control	60	0,5	46,75	4,67
control	120	0,5	23,55	2,35
control	240	0,5	44,93	4,49

13-KOTE (21)

treatment	time [min]	sample weight [g]	area ratio **21**/std	amount **21** [µg/g frw]
wounded	40	0,5	27,76	5,55
wounded	40	0,5	67,72	13,54
wounded	40	0,5	58,86	11,77
wounded	60	0,5	31,52	6,30
wounded	60	0,5	47,12	9,42
wounded	60	0,5	78,11	15,62
wounded	120	0,5	28,61	5,72
wounded	120	0,5	38,77	7,75
wounded	120	0,5	72,26	14,45
wounded	240	0,5	20,06	4,01
wounded	240	0,5	30,24	6,05
wounded	240	0,5	66,08	13,22
control	40	0,5	55,80	11,16
control	40	0,5	39,58	7,92
control	40	0,5	68,99	13,80
control	60	0,5	18,88	3,78
control	60	0,5	67,88	13,58
control	60	0,5	60,61	12,12
control	120	0,5	38,64	7,73
control	120	0,5	90,62	18,12
control	120	0,5	69,29	13,86
control	240	0,5	22,19	4,44
control	240	0,5	70,47	14,09
control	240	0,5	52,51	10,50

Oxylipin profiling in *S. littoralis* damaged leaves of *P. lunatus*

Jasmonic acid (1)

sample	sample weight [g]	area ratio **1**/std	amount **1** [ng/g frw]
0 – 10 mm	0,46	3,37	523
0 – 10 mm	0,3	4,32	1028
0 – 10 mm	0,3	3,39	808
0 – 10 mm	0,35	3,44	703
0 – 10 mm	0,24	2,23	665
0 – 10 mm	0,27	1,58	418
10 – 20 mm	0,27	3,09	1705
10 – 20 mm	0,24	5,73	751
10 – 20 mm	0,2	2,10	97
10 – 20 mm	0,34	3,08	648
10 – 20 mm	0,24	2,07	617
10 – 20 mm	0,24	1,22	363
neighbor	0,32	0,44	751
neighbor	0,42	0,58	97
neighbor	0,37	0,27	99
systemic	0,3	0,51	120
systemic	0,3	0,37	89
systemic	0,29	0,40	100
control	0,27	0,42	111
control	0,29	0,15	38
control	0,31	0,31	72
control	0,37	0,11	21
control	0,33	0,11	23
control	0,41	0,04	7

12-Oxophytodienoic acid (7)

sample	sample weight [g]	area ratio **7**/std	amount **7** [µg/g frw]
0 – 10 mm	0,46	3,59	8,68
0 – 10 mm	0,3	0,43	1,58
0 – 10 mm	0,3	2,53	9,38
0 – 10 mm	0,35	3,08	9,77
0 – 10 mm	0,24	3,01	13,93
0 – 10 mm	0,27	4,01	16,87
10 – 20 mm	0,27	1,54	6,34
10 – 20 mm	0,24	3,84	17,79
10 – 20 mm	0,2	2,38	13,21
10 – 20 mm	0,34	4,08	13,34
10 – 20 mm	0,24	3,84	17,79
10 – 20 mm	0,24	1,84	8,51
neighbor	0,32	2,32	8,06
neighbor	0,42	1,65	4,38
neighbor	0,37	1,55	4,66
systemic	0,3	0,57	2,11
systemic	0,3	0,69	2,56
systemic	0,29	0,42	1,63
control	0,5	0,14	0,30
control	0,5	1,54	3,42
control	0,5	1,09	2,43
control	0,5	1,84	4,08
control	0,5	2,01	4,46
control	0,5	1,03	2,29

11-Oxo-9-undecenoic acid (48)

sample	sample weight [g]	area ratio **48**/std	amount **48** [µg/g frw]
0 – 10 mm	0,35	0,91	0,92
0 – 10 mm	0,24	0,80	1,20
0 – 10 mm	0,27	0,72	0,95
0 – 10 mm	0,46	0,75	0,58

0 – 10 mm	0,3	0,56	0,67
0 – 10 mm	0,3	0,36	0,43
10 – 20 mm	0,34	1,41	1,48
10 – 20 mm	0,24	1,16	1,73
10 – 20 mm	0,24	0,85	1,27
10 – 20 mm	0,27	0,50	0,66
10 – 20 mm	0,24	0,44	0,65
10 – 20 mm	0,2	0,37	0,66
neighbor	0,32	0,35	0,39
neighbor	0,42	0,23	0,19
neighbor	0,37	0,21	0,20
systemic	0,3	0,91	1,09
systemic	0,3	0,72	0,85
systemic	0,29	0,57	0,70
control	0,32	0,35	0,39
control	0,42	0,23	0,19
control	0,37	0,21	0,20
control	0,37	0,54	0,52
control	0,27	0,72	0,77
control	0,29	1,28	1,12

13-Oxo-9,11-tridecadienoic acid (18)

sample	sample weight [g]	area ratio **18**/std	amount **18** [µg/g frw]
0 – 10 mm	0,35	9,08	23,60
0 – 10 mm	0,24	7,40	28,02
0 – 10 mm	0,27	7,06	23,76
0 – 10 mm	0,46	3,43	6,78
0 – 10 mm	0,3	3,56	10,79
0 – 10 mm	0,3	5,87	17,77
10 – 20 mm	0,34	6,27	16,75
10 – 20 mm	0,24	7,29	27,61
10 – 20 mm	0,24	4,85	18,36
10 – 20 mm	0,27	2,09	7,03
10 – 20 mm	0,24	6,57	24,87
10 – 20 mm	0,2	8,33	37,88
neighbor	0,32	1,76	5,00
neighbor	0,42	4,97	10,76
neighbor	0,37	6,19	15,20
systemic	0,3	7,04	21,32
systemic	0,3	10,83	32,83
systemic	0,29	3,68	11,53
control	0,32	1,76	5,00
control	0,42	4,97	10,76
control	0,37	6,19	15,20
control	0,37	3,20	7,86
control	0,27	5,08	14,01
control	0,29	8,97	19,90

α-Ketol (9)

sample	sample weight [g]	area ratio **9**/std	amount **9** [µg/g frw]
0 – 10 mm	0,46	2,3	1,0
0 – 10 mm	0,3	4,3	2,8
0 – 10 mm	0,3	2,6	1,8
0 – 10 mm	0,35	9,3	2,7
0 – 10 mm	0,24	3,9	1,6
0 – 10 mm	0,27	2,4	0,9
10 – 20 mm	0,27	3,2	2,4
10 – 20 mm	0,24	3,9	3,2
10 – 20 mm	0,2	1,8	1,8
10 – 20 mm	0,34	7,9	2,3
10 – 20 mm	0,24	6,3	2,6
10 – 20 mm	0,24	4,1	1,7
neighbor	0,32	2,2	1,4
neighbor	0,42	2,4	1,1

neighbor	0,37	1,4	0,8
systemic	0,3	0,6	0,2
systemic	0,3	0,7	0,2
systemic	0,29	0,2	0,1
control	0,29	4,5	1,5
control	0,37	3,6	1,0
control	0,33	6,5	2,0

γ-Ketol (10)

sample	sample weight [g]	area ratio **10**/std	amount **10** [µg/g frw]
0 – 10 mm	0,35	1,64	1,17
0 – 10 mm	0,24	0,96	1,00
0 – 10 mm	0,27	0,78	0,72
0 – 10 mm	0,46	0,48	0,52
0 – 10 mm	0,3	0,51	0,85
0 – 10 mm	0,3	0,48	0,80
10 – 20 mm	0,24	1,61	1,68
10 – 20 mm	0,24	0,74	0,78
10 – 20 mm	0,27	0,60	1,11
10 – 20 mm	0,24	0,59	1,23
10 – 20 mm	0,2	0,25	0,62
neighbor	0,32	0,37	0,59
neighbor	0,42	0,36	0,43
neighbor	0,37	0,16	0,22
systemic	0,3	0,24	0,20
systemic	0,3	0,16	0,13
systemic	0,29	0,04	0,04
control	0,37	0,74	0,50
control	0,27	0,21	0,39
control	0,29	0,54	0,46

9-Hydroxy-12-oxo-10-dodecenoic acid (49)

sample	sample weight [g]	area ratio **49**/std	amount **49** [µg/g frw]
0 – 10 mm	0,35	18,4	5,2
0 – 10 mm	0,24	11,3	4,7
0 – 10 mm	0,27	12,4	4,6
0 – 10 mm	0,46	8,3	3,6
0 – 10 mm	0,3	12,5	8,3
0 – 10 mm	0,3	7,5	5,0
10 – 20 mm	0,34	18,2	5,3
10 – 20 mm	0,24	14,6	6,1
10 – 20 mm	0,24	9,4	3,9
10 – 20 mm	0,27	9,5	7,0
10 – 20 mm	0,24	8,1	6,7
10 – 20 mm	0,2	4,5	4,5
neighbor	0,32	5,7	3,5
neighbor	0,42	4,8	2,3
neighbor	0,37	2,4	1,3
systemic	0,3	13,6	4,5
systemic	0,3	9,3	3,1
systemic	0,29	6,6	2,3
control	0,27	4,2	3,1
control	0,37	9,2	2,5
control	0,33	12,5	3,8

13-KOTE (21)

sample	sample weight [g]	area ratio **21**/std	amount **21** [µg/g frw]
0 – 10 mm	0,35	36,3	10,37
0 – 10 mm	0,24	20,4	8,48
0 – 10 mm	0,27	15,4	5,71
0 – 10 mm	0,46	30,6	6,65
0 – 10 mm	0,3	6,5	2,17

0 – 10 mm	0,3	40,2	13,40
10 – 20 mm	0,34	35,8	10,54
10 – 20 mm	0,24	6,7	2,78
10 – 20 mm	0,24	11,0	4,57
10 – 20 mm	0,27	8,8	3,25
10 – 20 mm	0,24	51,2	21,31
10 – 20 mm	0,2	42,1	21,06
neighbor	0,32	14,8	4,63
neighbor	0,42	38,9	9,27
neighbor	0,37	34,7	9,39
systemic	0,3	14,2	4,73
systemic	0,3	16,0	5,34
systemic	0,29	18,8	6,48
control	0,32	18,8	5,09
control	0,42	11,7	3,53
control	0,37	37,6	9,16
control	0,37	13,1	4,85
control	0,27	43,9	15,13
control	0,29	22,2	7,17

12,13-Epoxy-11-HODE (20)

sample	sample weight [g]	area ratio **20**/std	amount **20** [µg/g frw]
0 – 10 mm	0,35	9,03	2,58
0 – 10 mm	0,24	5,19	2,16
0 – 10 mm	0,27	12,18	4,51
0 – 10 mm	0,46	4,94	2,15
0 – 10 mm	0,3	3,56	2,37
0 – 10 mm	0,3	5,75	3,84
10 – 20 mm	0,34	9,82	2,89
10 – 20 mm	0,24	12,33	5,14
10 – 20 mm	0,24	5,54	2,31
10 – 20 mm	0,27	3,82	2,83
10 – 20 mm	0,24	6,24	5,20
10 – 20 mm	0,2	0,98	0,98
neighbor	0,32	3,42	2,14
neighbor	0,42	3,79	1,81
neighbor	0,37	2,96	1,60
systemic	0,3	7,70	2,57
systemic	0,3	7,52	2,51
systemic	0,29	11,61	4,00
control	0,37	3,22	0,87
control	0,33	15,15	4,59
control	0,41	7,16	1,75
control	0,27	2,52	1,86
control	0,29	6,18	4,27

Phytohormone analysis of alamethicin treated *A. thaliana*

Calibration curves

Calibration curve for determination of JA (1)

amount of added **1** [367]	area ratio **1**/std	amount of added **1** [ng]	area ratio **1**/std
0	0,36	100	1,42
0	0,33	100	1,60
50	0,95	150	2,01
50	0,83	150	2,02
		200	2,58

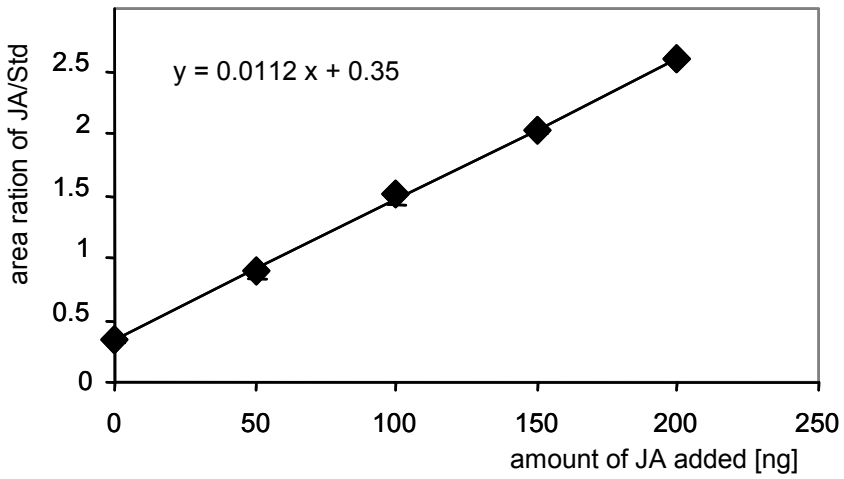

Calibration curve for determination of OPDA (7)

amount of added **7** [ng]	area ratio **7**/std	amount of added **7** [ng]	area ratio **7**/std
0	0,93	1500	4,12
0	1,26	1500	3,53
500	2,51	2000	5,72
500	1,72	2000	4,82
1000	4,00	5000	10,36
1000	2,58	5000	12,76

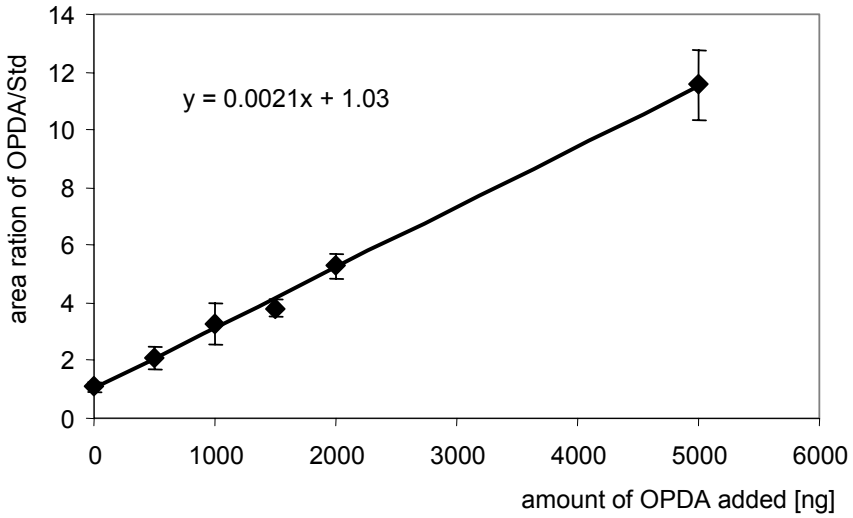

Phytohormone determination

Salicylic acid (2)

treatment	time [min]	sample weight [g]	area ratio **2**/std	amount **2** [ng/g frw]
alamethicin	30	1,12	0,30	127
alamethicin	30	1,2	0,37	145
alamethicin	30	1,17	0,27	109
alamethicin	30	1,06	0,26	114
alamethicin	30	0,99	0,39	181
alamethicin	60	1	0,38	180
alamethicin	60	0,73	0,30	193
alamethicin	60	0,59	0,16	128
alamethicin	60	0,5	0,14	129
alamethicin	60	0,71	0,23	149
alamethicin	90	0,86	0,30	162
alamethicin	90	1,07	0,41	185

alamethicin	90	0,9	0,35	182
alamethicin	90	1,25	0,40	150
alamethicin	90	0,75	0,27	168
alamethicin	120	0,5	0,41	381
alamethicin	120	0,6	0,79	612
alamethicin	120	0,4	0,55	643
alamethicin	120	0,5	0,33	312
alamethicin	120	0,49	0,17	161
alamethicin	180	0,8	0,81	475
alamethicin	180	0,75	0,72	448
alamethicin	180	0,7	1,18	789
alamethicin	180	0,46	0,22	220
alamethicin	180	0,75	1,48	922
alamethicin	240	1	0,32	149
alamethicin	240	0,85	2,42	1329
alamethicin	240	1,16	4,60	1851
alamethicin	240	1,02	3,21	1470
alamethicin	240	0,44	1,00	467
alamethicin	360	0,88	5,52	2931
alamethicin	360	0,73	3,84	2458
alamethicin	360	0,96	0,29	143
alamethicin	360	1,4	4,97	1659
alamethicin	360	0,6	1,86	1449
alamethicin	480	1,1	6,64	2819
alamethicin	480	1,1	6,52	2770
alamethicin	480	1,2	4,84	1885
alamethicin	480	1,1	4,71	2001
alamethicin	480	1,1	5,26	2234
alamethicin	720	1,07	2,42	1057
alamethicin	720	1,1	2,30	977
alamethicin	720	1,1	2,85	1211
alamethicin	720	1,04	2,07	931
alamethicin	720	1,09	2,71	1162
control	0	1,7	0,25	68
control	0	1,1	0,61	258
control	0	1,8	0,40	103
control	60	0,8	0,36	207
control	60	0,5	0,22	206
control	60	0,5	0,24	220
control	60	0,53	0,23	201
control	60	0,43	0,31	342
control	180	0,71	0,19	126
control	180	0,33	0,15	217
control	180	0,38	0,12	145
control	180	0,39	0,15	179
control	180	1,1	0,23	99
control	360	0,5	0,14	131
control	360	1,1	0,31	132
control	360	0,6	0,16	125
control	360	0,9	0,25	130
control	360	0,61	0,26	199
control	720	1,25	0,28	105
control	720	1	0,39	182
control	720	1,1	0,30	128
control	720	1,12	0,20	85
control	720	1,11	0,31	132

Jasmonic acid (1)

treatment	time [min]	sample weight [g]	area ratio **1**/std	amount **1** [ng/g frw]	*cis*/total **1** [%]
alamethicin	15	1,1	0,79	64	53
alamethicin	15	1	0,97	86	72
alamethicin	15	1	0,08	7	54
alamethicin	30	0,93	0,77	74	56
alamethicin	30	0,98	0,97	89	55
alamethicin	30	0,77	1,03	119	47
alamethicin	45	0,97	0,96	89	55
alamethicin	45	0,74	0,41	50	48
alamethicin	45	0,93	0,50	48	56
alamethicin	60	1,04	1,09	94	58
alamethicin	60	0,95	1,57	148	43
alamethicin	60	1,07	0,43	36	55
alamethicin	90	0,93	2,60	249	43
alamethicin	90	0,99	1,64	148	52
alamethicin	90	1,18	1,81	137	48
alamethicin	90	0,95	0,49	46	60
alamethicin	120	0,89	0,78	86	60
alamethicin	120	0,9	1,34	149	51
alamethicin	125	1,08	2,41	362	44
alamethicin	180	1,08	1,43	118	41
alamethicin	180	1,09	1,10	90	31
alamethicin	180	0,93	2,32	223	39
alamethicin	240	1,02	2,65	232	29
alamethicin	240	1,14	1,95	153	30
alamethicin	240	0,89	0,96	97	24
alamethicin	360	1,04	2,00	172	27
alamethicin	360	0,94	1,91	181	24
alamethicin	360	1,27	2,33	164	22
alamethicin	600	0,93	0,89	86	28
alamethicin	600	0,51	0,64	111	36
alamethicin	600	1,04	1,20	103	21
control	0	1	1,45	129	31
control	0	1	0,59	52	60
control	15	1,06	0,82	69	47
control	15	1,22	2,01	147	56
control	15	1,04	1,16	100	56
control	30	1	0,99	88	44
control	30	1,04	0,64	55	57
control	30	1,04	0,35	30	46
control	45	0,74	0,66	80	53
control	45	1,18	1,21	91	62
control	45	0,71	0,30	38	49
control	60	0,97	0,67	62	54
control	60	1,08	0,80	66	63
control	60	1,07	0,51	42	56
control	90	0,93	0,59	57	50
control	90	1,03	0,78	67	66
control	90	1,03	0,53	46	61
control	120	0,98	1,08	99	57
control	120	0,92	0,64	62	44
control	120	1	0,44	39	56
control	180	0,97	0,90	83	52
control	180	1,01	0,42	37	63
control	180	1,11	0,55	44	54
control	240	1,08	0,57	47	62
control	240	1,03	0,50	43	41
control	240	1,02	0,35	31	61
control	360	1,08	0,41	34	59
control	360	1,02	0,24	21	67
control	360	0,94	0,28	27	60
control	600	1,11	0,59	47	68
control	600	1,06	0,29	25	65
control	600	0,9	0,28	27	62

12-Oxophytodienoic acid (7)

treatment	time [min]	sample weight [g]	area ratio **7**/std	amount **7** [ng/g frw]
alamethicin	15	1,1	0,75	327
alamethicin	15	1	0,38	181
alamethicin	15	1	0,29	137
alamethicin	30	0,93	0,53	272
alamethicin	30	0,98	0,68	332
alamethicin	30	0,77	0,48	297
alamethicin	45	0,97	0,41	203
alamethicin	45	0,74	0,69	444
alamethicin	45	0,93	0,43	222
alamethicin	60	1,04	0,77	354
alamethicin	60	0,95	0,83	418
alamethicin	60	1,07	0,58	258
alamethicin	90	0,93	1,27	648
alamethicin	90	0,99	1,88	905
alamethicin	90	0,95	1,01	508
alamethicin	90	1,18	1,47	594
alamethicin	120	0,89	1,01	540
alamethicin	120	0,9	0,63	332
alamethicin	120	1,08	0,71	314
alamethicin	180	1,08	0,95	420
alamethicin	180	1,09	1,62	707
alamethicin	180	0,93	0,89	455
alamethicin	240	1,02	0,97	452
alamethicin	240	1,14	1,47	616
alamethicin	240	0,89	0,54	287
alamethicin	360	1,04	0,92	423
alamethicin	360	0,94	1,30	659
alamethicin	360	1,27	1,76	658
alamethicin	600	0,93	0,52	268
alamethicin	600	0,51	0,51	475
alamethicin	600	1,04	0,85	391
control	0	1	1,15	549
control	0	1	0,76	362
control	15	1,06	0,54	242
control	15	1,22	1,03	402
control	15	1,04	0,41	188
control	30	1	0,71	340
control	30	1,04	1,15	525
control	30	1,04	0,36	164
control	45	0,74	0,60	386
control	45	1,18	0,87	351
control	45	0,71	0,33	222
control	60	0,97	0,69	341
control	60	1,08	1,09	481
control	60	1,07	0,78	349
control	90	0,93	0,91	468
control	90	1,03	1,00	464
control	90	1,03	0,66	307
control	120	0,98	1,06	517
control	120	0,92	0,97	502
control	120	1	1,34	638
control	180	0,97	0,93	455
control	180	1,01	1,15	542
control	180	1,11	1,34	573
control	240	1,08	0,57	251
control	240	1,03	0,62	287
control	240	1,02	1,26	590
control	360	1,08	0,53	236
control	360	1,02	0,81	379
control	360	0,94	0,91	459
control	600	1,11	0,49	212
control	600	1,06	0,62	278
control	600	0,9	0,89	471

Phytohormone and oxylipin analysis of $CuSO_4$ treated *P. lunatus*

Salicylic acid (2)

sample	time [min]	sample weight [g]	area ratio **2**/std	amount **2** [ng/g frw]
$CuSO_4$	120	1,02	0,87	284,87
$CuSO_4$	120	1	1,48	492,86
$CuSO_4$	120	1,12	0,78	234,18
$CuSO_4$	120	1,11	1,35	405,86
$CuSO_4$	200	1,39	7,24	1735,66
$CuSO_4$	200	1,25	3,72	991,226
$CuSO_4$	200	1,02	0,17	56,91
$CuSO_4$	200	1,3	1,45	370,82
$CuSO_4$	300	1,33	10,578	2649,60
$CuSO_4$	300	1,29	6,91	1785,83
$CuSO_4$	300	1,03	6,75	2184,24
$CuSO_4$	300	1,17	7,55	2152,20
$CuSO_4$	500	1,13	7,21	2127,33
$CuSO_4$	500	1,19	4,07	1140,38
$CuSO_4$	500	1,19	11,95	3348,13
$CuSO_4$	500	0,83	10,95	4399,19
$CuSO_4$	800	1,09	15,87	4853,02
$CuSO_4$	800	1,32	22,94	5793,37
$CuSO_4$	800	1,1	22,82	6916,91
$CuSO_4$	800	1,41	18,32	4330,29
control	120	1,29	0,93	241,24
control	120	1,22	2,26	616,33
control	120	1,15	5,75	1666,28
control	120	1,12	1,07	318,27
control	200	1,37	2,11	512,53
control	200	1,24	0,79	213,42
control	200	1,21	1,04	285,61
control	200	1,11	0,56	168,15
control	300	1,22	2,34	638,65
control	300	1,31	3,00	763,77
control	300	1,31	1,41	358,04
control	300	1,15	1,55	449,20
control	500	1,24	8,37	2250,67
control	500	1,3	2,82	723,21
control	500	1,11	1,79	536,71
control	800	1,45	3,01	693,11
control	800	1,11	1,74	523,33
control	800	1,14	1,71	499,20

Salicylic acid (2)

sample	concentration	sample weight [g]	area ratio **2**/std	amount **2** [ng/g frw]
$CuSO_4$	50 µM	1,0	0,73	0,39
$CuSO_4$	50 µM	1,0	0,66	0,36
$CuSO_4$	50 µM	1,0	0,46	0,26
$CuSO_4$	300 µM	1,0	4,06	1,98
$CuSO_4$	300 µM	1,0	4,37	2,13
$CuSO_4$	300 µM	1,0	3,12	1,53
$CuSO_4$	500 µM	1,0	6,29	3,04
$CuSO_4$	500 µM	1,0	4,86	2,36
$CuSO_4$	500 µM	1,0	5,57	2,70
$CuSO_4$	800 µM	1,0	10,14	4,88
$CuSO_4$	800 µM	1,0	2,39	1,18
$CuSO_4$	800 µM	1,0	8,70	4,20
$CuSO_4$	1000 µM	1,0	4,35	2,12
$CuSO_4$	1000 µM	1,0	7,23	3,49
$CuSO_4$	1000 µM	1,0	10,52	5,06
alamethicin	10 µg /ml	1,0	6,09	2,95
alamethicin	10 µg /ml	1,0	12,38	5,95
alamethicin	10 µg /ml	1,0	4,38	2,13
control		1,0	0,18	0,13

control	1,0	0,84	0,44
control	1,0	0,48	0,27

Jasmonic acid (1)

sample	time [min]	sample weight [g]	area ratio **1**/std	amount **1** [ng/g frw]
$CuSO_4$	40	0,5	0,07	10,47
$CuSO_4$	40	0,5	0,08	11,08
$CuSO_4$	40	0,5	0,17	24,00
$CuSO_4$	40	0,5	0,50	71,52
$CuSO_4$	80	0,5	0,05	7,78
$CuSO_4$	80	0,5	0,04	6,02
$CuSO_4$	80	0,5	0,25	35,74
$CuSO_4$	80	0,5	0,57	80,81
$CuSO_4$	430	0,5	0,19	27,31
$CuSO_4$	430	0,5	0,06	8,03
$CuSO_4$	430	0,5	0,72	103,00
$CuSO_4$	430	0,5	0,38	54,45
$CuSO_4$	585	0,5	0,05	6,58
$CuSO_4$	585	0,5	0,04	5,25
$CuSO_4$	585	0,5	0,07	9,90
$CuSO_4$	585	0,5	0,40	56,65
control	40	0,5	0,30	42,64
control	40	0,5	0,18	26,31
control	40	0,5	0,19	26,70
control	40	0,5	0,24	34,85
control	80	0,5	0,12	17,00
control	80	0,5	0,19	27,61
control	80	0,5	0,14	20,51
control	80	0,5	0,36	51,26
control	430	0,5	0,17	24,81
control	430	0,5	0,30	42,25
control	430	0,5	0,27	37,98
control	430	0,5	0,28	39,72
control	585	0,5	0,14	20,08
control	585	0,5	0,31	44,29
control	585	0,5	0,16	22,53
control	585	0,5	0,42	59,72

12-Oxophytodienoic acid (7)

sample	time [min]	sample weight [g]	area ratio **7**/std	amount **7** [ng/g frw]
$CuSO_4$	40	0,5	7,63	15,27
$CuSO_4$	40	0,5	12,44	24,89
$CuSO_4$	40	0,5	15,18	30,36
$CuSO_4$	80	0,5	12,08	24,16
$CuSO_4$	80	0,5	13,73	27,47
$CuSO_4$	80	0,5	14,85	29,71
$CuSO_4$	430	0,5	5,66	11,33
$CuSO_4$	430	0,5	5,08	10,15
$CuSO_4$	430	0,5	1,55	3,09
$CuSO_4$	430	0,5	1,67	3,34
$CuSO_4$	585	0,5	8,48	16,95
$CuSO_4$	585	0,5	7,40	14,80
$CuSO_4$	585	0,5	3,43	6,87
$CuSO_4$	585	0,5	3,47	6,94
control	40	0,5	2,83	5,65
control	40	0,5	1,24	2,48
control	40	0,5	6,53	13,06
control	40	0,5	3,03	6,06
control	80	0,5	1,40	2,80
control	80	0,5	1,65	3,29
control	80	0,5	7,71	15,41
control	80	0,5	1,18	2,36
control	430	0,5	1,24	2,47
control	430	0,5	3,91	7,83

control	430	0,5	5,03	10,07
control	430	0,5	2,48	4,97
control	585	0,5	1,10	2,20
control	585	0,5	5,66	11,32
control	585	0,5	13,08	26,16
control	585	0,5	4,30	8,61

11-Oxo-9-undecenoic acid (48)

sample	time [min]	sample weight [g]	area ratio **48**/std	amount **48** [ng/g frw]
$CuSO_4$	40	0,5	0,55	351,69
$CuSO_4$	40	0,5	0,86	558,02
$CuSO_4$	40	0,5	0,21	136,19
$CuSO_4$	40	0,5	0,89	567,72
$CuSO_4$	80	0,5	0,82	527,76
$CuSO_4$	80	0,5	0,85	550,86
$CuSO_4$	80	0,5	0,18	117,74
$CuSO_4$	80	0,5	1,01	648,69
$CuSO_4$	430	0,5	0,61	395,97
$CuSO_4$	430	0,5	0,43	275,99
$CuSO_4$	430	0,5	0,18	119,34
$CuSO_4$	430	0,5	0,16	106,94
$CuSO_4$	585	0,5	0,58	375,85
$CuSO_4$	585	0,5	0,74	477,37
$CuSO_4$	585	0,5	0,30	193,56
$CuSO_4$	585	0,5	0,30	196,36
control	40	0,5	0,19	122,36
control	40	0,5	0,21	138,20
control	40	0,5	0,40	259,08
control	40	0,5	0,17	111,07
control	80	0,5	0,18	118,85
control	80	0,5	0,17	111,73
control	80	0,5	0,39	256,86
control	80	0,5	0,12	80,81
control	430	0,5	0,20	129,08
control	430	0,5	0,46	300,33
control	430	0,5	0,21	137,59
control	585	0,5	0,89	572,48
control	585	0,5	0,96	622,12
control	585	0,5	0,88	568,47
control	585	0,5	0,23	150,97

13-Oxo-9,11-tridecadienoic acid (18)

sample	time [min]	sample weight [g]	area ratio **18**/std	amount **18** [ng/g frw]
$CuSO_4$	40	0,5	6,35	14103,93
$CuSO_4$	40	0,5	9,32	20721,09
$CuSO_4$	40	0,5	0,45	1003,23
$CuSO_4$	40	0,5	5,29	11755,48
$CuSO_4$	80	0,5	10,22	22705,60
$CuSO_4$	80	0,5	8,45	18767,08
$CuSO_4$	80	0,5	0,24	541,84
$CuSO_4$	80	0,5	6,67	14813,42
$CuSO_4$	430	0,5	5,67	12602,33
$CuSO_4$	430	0,5	4,45	9897,35
$CuSO_4$	430	0,5	0,51	1134,59
$CuSO_4$	430	0,5	0,39	883,07
$CuSO_4$	585	0,5	6,66	14805,05
$CuSO_4$	585	0,5	8,66	19256,78
$CuSO_4$	585	0,5	0,65	1440,46
$CuSO_4$	585	0,5	0,94	2086,43
control	40	0,5	1,70	3779,05
control	40	0,5	0,37	829,00
control	40	0,5	4,74	10531,89
control	40	0,5	0,71	1582,00
control	80	0,5	0,51	1142,46

control	80	0,5	0,41	916,69
control	80	0,5	3,51	7796,91
control	80	0,5	0,32	714,98
control	430	0,5	0,32	704,22
control	430	0,5	1,84	4100,50
control	430	0,5	5,83	12948,71
control	430	0,5	0,57	1263,17
control	585	0,5	0,33	735,46
control	585	0,5	6,83	15184,20
control	585	0,5	8,37	18607,70
control	585	0,5	1,01	2246,78

α-Ketol (9)

sample	time [min]	sample weight [g]	area ratio **9**/std	amount **9** [ng/g frw]
$CuSO_4$	40	0,5	10,32	3,87
$CuSO_4$	40	0,5	10,18	3,82
$CuSO_4$	40	0,5	25,16	9,44
$CuSO_4$	40	0,5	7,87	2,95
$CuSO_4$	80	0,5	9,24	3,46
$CuSO_4$	80	0,5	9,55	3,58
$CuSO_4$	80	0,5	13,57	5,09
$CuSO_4$	80	0,5	7,73	2,90
$CuSO_4$	430	0,5	3,73	1,40
$CuSO_4$	430	0,5	5,23	1,96
$CuSO_4$	430	0,5	11,02	4,13
$CuSO_4$	430	0,5	3,91	1,47
$CuSO_4$	585	0,5	7,84	2,94
$CuSO_4$	585	0,5	11,34	4,25
$CuSO_4$	585	0,5	2,74	1,03
$CuSO_4$	585	0,5	8,19	3,07
control	40	0,5	7,93	2,97
control	40	0,5	2,77	1,04
control	40	0,5	3,67	1,37
control	40	0,5	0,35	0,13
control	80	0,5	2,92	1,09
control	80	0,5	4,17	1,57
control	80	0,5	5,49	2,06
control	80	0,5	4,41	1,65
control	430	0,5	2,13	0,80
control	430	0,5	7,94	2,98
control	430	0,5	2,50	0,94
control	430	0,5	2,94	1,10
control	585	0,5	1,00	0,38
control	585	0,5	7,21	2,70
control	585	0,5	8,62	3,23
control	585	0,5	0,03	0,01

γ-Ketol (10)

sample	time [min]	sample weight [g]	area ratio **10**/std	amount **10** [ng/g frw]
$CuSO_4$	40	0,5	1,44	0,54
$CuSO_4$	40	0,5	3,08	1,15
$CuSO_4$	40	0,5	7,52	2,82
$CuSO_4$	40	0,5	0,98	0,37
$CuSO_4$	80	0,5	1,19	0,45
$CuSO_4$	80	0,5	3,65	1,37
$CuSO_4$	80	0,5	2,06	0,77
$CuSO_4$	80	0,5	0,84	0,32
$CuSO_4$	430	0,5	0,42	0,16
$CuSO_4$	430	0,5	0,45	0,17
$CuSO_4$	430	0,5	1,62	0,61
$CuSO_4$	430	0,5	0,16	0,06
$CuSO_4$	585	0,5	1,02	0,38
$CuSO_4$	585	0,5	0,52	0,20
$CuSO_4$	585	0,5	0,57	0,21

$CuSO_4$	585	0,5	1,94	0,73
control	40	0,5	0,93	0,35
control	40	0,5	0,25	0,09
control	40	0,5	0,21	0,08
control	40	0,5	0,03	0,01
control	80	0,5	0,37	0,14
control	80	0,5	0,45	0,17
control	80	0,5	0,60	0,22
control	80	0,5	0,13	0,05
control	430	0,5	0,18	0,07
control	430	0,5	0,75	0,28
control	430	0,5	0,21	0,08
control	430	0,5	0,09	0,04
control	585	0,5	0,07	0,03
control	585	0,5	0,53	0,20
control	585	0,5	1,65	0,62
control	585	0,5	0,00	0,00

9-Hydroxy-12-oxo-10-dodecenoic acid (49)

sample	time [min]	sample weight [g]	area ratio **49**/std	amount **49** [ng/g frw]
$CuSO_4$	40	0,5	11,89	4,46
$CuSO_4$	40	0,5	16,31	6,12
$CuSO_4$	40	0,5	26,39	9,90
$CuSO_4$	40	0,5	29,21	10,95
$CuSO_4$	80	0,5	22,00	8,25
$CuSO_4$	80	0,5	24,95	9,36
$CuSO_4$	80	0,5	22,72	8,52
$CuSO_4$	80	0,5	24,94	9,35
$CuSO_4$	430	0,5	17,87	6,70
$CuSO_4$	430	0,5	20,58	7,72
$CuSO_4$	430	0,5	24,62	9,23
$CuSO_4$	430	0,5	2,14	0,80
$CuSO_4$	585	0,5	5,01	1,88
$CuSO_4$	585	0,5	29,10	10,91
$CuSO_4$	585	0,5	29,92	11,22
$CuSO_4$	585	0,5	20,66	7,75
control	40	0,5	26,42	9,91
control	40	0,5	13,02	4,88
control	40	0,5	18,17	6,82
control	40	0,5	10,83	3,09
control	80	0,5	11,25	4,22
control	80	0,5	16,22	6,08
control	80	0,5	20,80	7,80
control	80	0,5	13,32	4,99
control	430	0,5	11,44	4,29
control	430	0,5	20,44	7,67
control	430	0,5	12,80	4,80
control	430	0,5	9,95	3,73
control	585	0,5	8,36	3,13
control	585	0,5	15,99	6,00
control	585	0,5	25,94	9,73
control	585	0,5	1,71	0,64

13-KOTE (21)

sample	time [min]	sample weight [g]	area ratio **21**/std	amount **21** [ng/g frw]
$CuSO_4$	40	0,5	284,47	28,45
$CuSO_4$	40	0,5	278,67	27,87
$CuSO_4$	40	0,5	103,62	10,36
$CuSO_4$	80	0,5	274,47	27,45
$CuSO_4$	80	0,5	281,74	28,17
$CuSO_4$	80	0,5	53,26	5,33
$CuSO_4$	430	0,5	198,34	19,83
$CuSO_4$	430	0,5	179,22	17,92
$CuSO_4$	430	0,5	62,29	6,23

$CuSO_4$	430	0,5	277,20	27,72
$CuSO_4$	585	0,5	223,75	22,37
$CuSO_4$	585	0,5	274,77	27,48
$CuSO_4$	585	0,5	89,83	8,98
$CuSO_4$	585	0,5	422,79	42,28
control	40	0,5	344,41	34,44
control	40	0,5	86,06	8,61
control	40	0,5	377,88	37,79
control	80	0,5	81,34	8,13
control	80	0,5	105,71	10,57
control	80	0,5	548,51	54,85
control	80	0,5	137,76	13,78
control	430	0,5	120,53	12,05
control	430	0,5	376,27	37,63
control	430	0,5	629,22	62,92
control	430	0,5	240,04	24,00
control	585	0,5	527,72	52,77
control	585	0,5	626,85	62,69
control	585	0,5	177,62	17,76